NOAA Technical Report NESDIS 53

NOAA-9 SOLAR BACKSCATTER ULTRAVIOLET (SBUV/2) INSTRUMENT AND DERIVED OZONE DATA: A STATUS REPORT BASED ON A REVIEW ON JANUARY 29, 1990

Washington, D.C.
June 1990

U.S. DEPARTMENT OF COMMERCE
National Oceanic and Atmospheric Administration
National Environmental Satellite, Data, and Information Service

NOAA TECHNICAL REPORTS

National Environmental Satellite, Data, and Information Service

The National Environmental Satellite, Data, and Information Service (NESDIS) manages the Nation's civil Earth-observing satellite systems, as well as global national data bases for meteorology, oceanography, geophysics, and solar-terrestrial sciences. From these sources, it develops and disseminates environmental data and information products critical to the protection of life and property, national defense, the national economy, energy development and distribution, global food supplies, and the development of natural resources.

Publication in the NOAA Technical Report series does not preclude later publication in scientific journals in expanded or modified form. The NESDIS series of NOAA Technical Reports is a continuation of the former NESS and EDIS series of NOAA Technical Reports and the NESC and EDS series of Environmental Science Services Administration (ESSA) Technical Reports.

A limited number of copies are available by contacting Nancy Everson, NOAA/NESDIS, E/RA22, 5200 Auth Road, Washington, DC, 20233. Copies can also be ordered from the National Technical Information Service (NTIS), U.S. Department of Commerce, Sills Bldg., 5285 Port Royal Road, Springfield, VA. 22161, (703) 487-4650 (prices on request for paper copies or microfiche, please refer to PB number when ordering). A partial listing of more recent reports appear below:

NESDIS 1 Satellite Observations on Variations in Southern Hemisphere Snow Cover. Kenneth F Dewey and Richard Heim, Jr., June 1983. (PB83 252908)

NESDIS 2 NODC 1 An Environmental Guide to Ocean Thermal Energy Conversion (OTEC) Operations in the Gulf of Mexico. National Oceanographic Data Center, June 1983. (PB84 115146)

NESDIS 3 Determination of the Planetary Radiation Budget from TIROS-N Satellites. Arnold Gruber, Irwin Ruff and Charles Earnest, August 1983. (PB84 106916)

NESDIS 4 Some Applications of Satellite Radiation Observations to Climate Studies. T.S. Chen, George Ohring and Haim Ganot, September 1983. (PB84 108109)

NESDIS 5 A Statistical Technique for Forecasting Severe Weather from Vertical Soundings by Satellite and Radiosonde. David L. Keller and William L. Smith, June 1983. (PB84 114099)

NESDIS 6 Spatial and Temporal Distribution of Northern Hemisphere Snow Cover. Burt J. Morse and Chester F. Ropelewski (NWS), October 1983. (PB84 118348)

NESDIS 7 Fire Detection Using the NOAA--Series Satellites. Michael Matson, Stanley R. Schneider, Billie Aldridge and Barry Satchwell (NWS), January 1984. (PB84 176890)

NESDIS 8 Monitoring of Long Waves in the Eastern Equatorial Pacific 1981-83 Using Satellite Multi-Channel Sea Surface Temperature Charts. Richard Legeckis and William Pichel, April 1984. (PB84 190487)

NESDIS 9 The NESDIS-SEL Lear Aircraft Instruments and Data Recording System. Gilbert R. Smith, Kenneth O. Hayes, John S. Knoll and Robert S. Koyanagi, June 1984. (PB84 219674)

NESDIS 10 Atlas of Reflectance Patterns for Uniform Earth and Cloud Surfaces (NIMBUS-7 ERB--61 Days). V.R. Taylor and L.L. Stowe, July 1984. (PB85 12440)

NESDIS 11 Tropical Cyclone Intensity Analysis Using Satellite Data. Vernon F. Dvorak, September 1984. (PB85 112951)

NESDIS 12 Utilization of the Polar Platform of NASA's Space Station Program for Operational Earth Observations. John H. McElroy and Stanley R. Schneider, September 1984. (PB85 1525027AS)

NESDIS 13 Summary and Analyses of the NOAA N-ROSS/ERS-1 Environmental Data Development Activity. John W. Sherman III, February 1984. (PB85 222743/43)

NESDIS 14 NOAA N-ROSS/ERS-1 Environmental Data Development (NNEEDD) Activity. John W. Sherman III, February 1985. (PB86 139284 A/S)

NESDIS 15 NOAA N-ROSS/ERS-1 Environmental Data Development (NNEEDD) Products and Services. Franklin E. Kniskern, February 1985, (PB86 213527/AS)

NESDIS 16 Temporal and Spatial Analyses of Civil Marine Satellite Requirements. Nancy J. Hooper and John W. Sherman III, February 1985. (PB86 212123/AS)

NESDIS 17 reserved

NOAA Technical Report NESDIS 53

NOAA-9 SOLAR BACKSCATTER ULTRAVIOLET (SBUV/2) INSTRUMENT AND DERIVED OZONE DATA: A STATUS REPORT BASED ON A REVIEW ON JANUARY 29, 1990

Edited by:
Walter G. Planet

Office of Research and Applications
Satellite Research Laboratory

Washington, D.C.
June 1990

U.S. DEPARTMENT OF COMMERCE
Robert A. Mosbacher, Secretary

National Oceanic and Atmospheric Administration
John A. Knauss, Under Secretary

National Environmental Satellite, Data, and Information Service
Thomas N. Pyke, Jr. , Assistant Administrator

Table of Contents

* Did not attend meeting.

Introduction

The NOAA satellite ozone monitoring program was initiated by the National Environmental Satellite Data and Information Service (NESDIS) in December 1984 with the launch of the NOAA-9 operational satellite carrying the first operational Solar Backscatter Ultraviolet (SBUV/2) spectrometer. The instrument and its derived data products have been undergoing extensive characterization and validation studies since launch. Much has been learned, pro and con. A review of the status of our knowledge of the system was held on January 29, 1990, at the NOAA facility in Camp Springs, Maryland. The review covered the efforts of the various NOAA, NASA, and contractor scientists who have been engaged in several aspects of the SBUV/2 program.

A data set for the period May 1985 - October 1989 has been assembled and is the base of the evaluation. The evaluation to date has arrived at certain technical conclusions, some firm, and some preliminary or conjectural. The primary conclusions include the following:

1. The NOAA-9 equator crossing time is continually later in the day due to the precession of the orbit. This results in an ever-increasing angle of solar incidence on the diffuser plate, approaching values beyond those used in pre-launch radiometric calibration and testing.

2. The increasing equator crossing times also result in observations at greater solar zenith angles at the observed scenes introducing an uncertain zenith-angle dependency on the retrieved ozone values.

3. Compared to other sources of data (SBUV and TOMS on Nimbus 7 and the ground-based Dobson network), the total ozone amount derived from the SBUV/2 shows an increasing greater difference with the SBUV/2 values being higher. Compared to selected subsets of Dobson values, the SBUV/2 - Dobson differences are diverging about 0.3 - 0.5% per year.

4. Short-term variations in total ozone derived from SBUV/2 measurements show excellent correlation with SBUV and TOMS data with respect to day-to-day, seasonal and latitudinal variabilities.

This report contains the materials presented at, and constitutes an official record of, the review. The individual reports contained herein were provided by the speakers.

NOAA-9 SBUV/2 Summary Meeting
January 29, 1990
World Weather Building
8:30 a.m. - Rm. 707

Agenda

1.	Introductory Remarks	- W. Planet - NESDIS/ORA
2.	Data Status/Availability	- D. Bowman - NESDIS/OSDPD
3.	Pre-launch Calibration/Testing	- D. Heath - NASA/GSFC
4.	Post-launch Performance	- J. Lienesch - NESDIS/ORA - R. Cebula - STX - H Weiss - STX - R. McPeters - NASA/GSFC
	Lunch	- ALL
5.	Ground-truth Data/Comparisons	- A.J. Miller - NWS/NMC - J. DeLuisi - NOAA/ERL-CMDL - C. Wellemeyer - STX - E. Hilsenrath - NASA/GSFC - W. Komhyr - NOAA/ERL-CMDL
6.	Data Uses	- R. Donnelly - NOAA/ERL-CMDL - S. Chandra - NASA/GSFC
7.	Recommendations	open

Attendees for SBUV/2 Workshop Seminar, 1/29/90

	P.K. Bhartia	Interferometrics, Inc.	(301) 794-9016
*	Dudley Bowman	NOAA/PSB	(301) 763-4310
*	Richard P. Cebula	STX	(301) 306-1108
*	Sushil Chandra	NASA/GSFC	(301) 286-8743
	Matthew DeLand	STX	(301) 286-4611
*	John DeLuisi	NOAA/OAR	(303) 497-6824
	Andrew Eckewrode	NOAA/SOCC	(301) 763-7577
*	Donald F. Heath	STX	(303) 939-5125
*	Ernest Hilsenrath	NASA/GSFC	(301) 286-6051
	Mary Hollinger	NESDIS/NCDC/SDSD	(301) 763-8402
	Andy Horvitz	NESDIS/NCDC/SDSD	(301) 763-8402
	Robert D. Hudson	NASA/GSFC	(301) 286-5485
	Ed Hurley	Research & Data Systems	(301) 982-3700
	Russell Koffler	NOAA/NESDIS	(301) 763-7190
*	Walter Komhyr	NOAA/OAR	(301) 497-6331
	Jack Koeppen	NOAA/NESDIS	(301) 763-1564
*	Jim Lienesch	NOAA/NESDIS	(301) 763-8136
*	Richard McPeters	NASA/GSFC	(301) 286-3832
*	Alvin J. Miller	NOAA/NWS/CAC	(301) 763-8071
	Wayne Nelson	Ball Aerospace	(303) 939-4271
	Ron Nagatani	NOAA/NWS/CAC	(301) 763-8071
	Walter Planet	NOAA/NESDIS	(301) 763-8136
	William Ramsey	NOAA/NESDIS	(301) 763-8136
	P. Krishna Rao	NOAA/NESDIS	(301) 763-8127
	Jim Shepherd	NOAA/SOCC/PSEG	(301) 763-7577
	James Silva	NOAA/SSD	(301) 763-3216
	Charlie Springer	Ball Aerospace	(303) 939-5225
	Joan Stokes	STX	(301) 286-3029
	Steve Taylor	STX	
*	Howard Weiss	STX	(301) 306-1125
*	Charles Wellemeyer	STX	(301) 306-103
	Tom Wrublewski	NOAA/SSD	(301) 763-3216

* Presented material

Attachment 1
Data Status and Availability
H. D. Bowman II
NOAA/NESDIS

Data Status and Availability

OPERATIONAL NOAA-9

Table (1) contains a list of significant dates related to the NOAA-9 SBUV/2 instrument data.

The first SBUV/2 instrument was launched on the National Environmental Satellite and Data Information Service (NESDIS) NOAA-9 spacecraft in December 1984. At that time the ground based SBUV/2 software processing system (Figure -1) was only partially completed due to the one-year earlier than expected launch of the instrument. The OOPS was able to capture all the SBUV/2, Ancillary, and Meteorological data needed to produce ozone products. This first system was called the 1B Capture System (SASC 1986). This data was stored on the 1B Capture File (Table 2).

The Analysis and Evaluation (A&E) period after every launch is a time when the status of all instruments are studied. The SBUV/2 was the last instrument to be "opened" in an attempt to expose it to the cleanest environment possible. The A&E period for the SBUV/2 was extended through February 1985.

March 1985 is the official start of the SBUV/2 data set. The instrument was in the operational mode (looking at the earth most of the time and at the sun twice a week). The 1B Capture file became the first product to be produced.

In October 1985 Ancillary data (such as absorption coefficients, Rayleigh scattering coefficients, multiple scattering coefficients, total ozone tables, etc.) appropriate for the NOAA-9 SBUV/2 instrument was installed into the OOPS. Previous to this date, Ancillary data for the SBUV on NIMBUS-7 was adapted for the NOAA instrument. A waiting period of about one year after launch of NOAA-9 was required to process the prelaunch ground and A&E period post-launch space data into the needed Ancillary coefficients.

In December 1985 the product processing software was installed into operations. At this time we began producing total, layer, and level ozone products. These products are contained in the Product Master File (PMF) and the Product User File (PUF). These data records are briefly described in Table 2.

TOVS cloud and temperature data are sources of ancillary data for producing the ozone from the instrument data. In April 1986 the TOVS product was changed to the "Enhanced TOVS". This new TOVS provided a finer resolution for the soundings. The OOPS was also changed to use this new product at this time.

In December 1986, the OOPS was upgraded to include the Instrument Support System. This system does automatic calculations of calibration information such as zero offsets, albedo correction factors (ACF), interrange ratios (IRR) etc.

The TOVS data used by the OOPS ended due to TOVS instrument failure in March 1987.

Do to the precession of the NOAA-9 spacecraft, the orbital equator crossing time had moved from its original 2:30 pm local time to 4:00 pm local time by September 1988. At that time this orbital change stopped our automatic offset calculation. The offset calculation requires a period of complete darkness beneath the satellite. The precessed orbit did not provide that period so no "dark" offsets could be calculated. Also the spacecrafts solar array was moved to a new position about this same time and blocked the SBUV/2's view of the Sun. This disabled the Albedo Correction Factor calculation. These two problems were resolved in December of 1988 with the repositioning of the solar array and the beginning of a new SBUV/2 instrument mode. The mercury lamp door was closed over the instrument aperture without being illuminated. This provided a dark target for the offset calculations.

In May of 1989 software was delivered to process the "dark mercury lamp view" data.

REPROCESSED NOAA-9

The reprocessing of SBUV/2 ozone data is the processing again of all data to provide; corrected earth location (during the first 5 months), corrected ancillary data (NIMBUS-7 SBUV ancillary data was used for the first 8 months of initial data processing), improved calibration (with the use of the new Instrument Support Subsystem), replacement of missing days where possible, correction for instrument non-linearity, and corrections and improvements developed by NASA/GSFC, NMC/CAC, and NESDIS (see Table 3).

The reprocessing system (Figure 2) uses an operational 1B Capture File as input, corrects earth location, replaces missing days and corrects the recommended range of the data. The data is then run through an ISS (Figure 1) which has been corrected and updated. A reprocessed HIF and 1B are produced. The reprocessed 1B is input to a corrected and updated product processor which produces a reprocessed PMF and PUF.

Figure 3 schematically illustrates the reprocessing to be a multi-agency effort. NESDIS Office of Operations processes operational 1B data through the Reprocessing System and provides the reprocessed products, to NESDIS Office of Research and Applications who validates the data using ground truth (Dobson, Umkehr, Balloon-sonde, etc.); to the National Meteorological Center / Climate Analysis Center (NMC/CAC) for comparison with other satellite borne ozone sensors, and to the National Aeronautics and Space Administration / Goddard Space Flight Center (NASA/GSFC) who analyzes the data. Each step leads to the development of corrections that are installed into the Reprocessing System.

After almost a year of system testing and improvement, the NOAA-9 SBUV/2 data reprocessing began in May of 1988.

We have completed the first reprocessing of NOAA-9 SBUV/2 data. It covers March 1985 through October 1989. The choice of October 1989 as the ending point of was due to the following reasons; the precessing of the NOAA-9 orbit is increasing the error in the data, the Space Shuttle SBUV (SSBUV) instrument was in orbit during October 1989 and a major solar flare was also observed during October 1989. The reprocessing will be extended beyond October 1989 when orbital factors allow for automatic calibrations to begin again (estimated to occur in May of 1990). Subsequent reprocessing will also expand the data set beyond October 1989.

Copies of the data from the first reprocessing can be ordered from NOAA/NESDIS with the following disclaimer;

> "Currently, from the NOAA-9 PMF data, only the total ozone product has been authorized for distribution. The data products are under technical evaluation by a NOAA/NASA science team, which has identified some deficiencies in the derived ozone data. Based on comparisons with other sources of the ozone data products, namely the NIMBUS-7 SBUV and the ground-based Dobson spectrophotometer, time-dependent differences of about 0.7% per year occurred in the NOAA-9 SBUV/2 that are not understood at this time. Short-term changes, as well as the general ozone patterns, however, have been noted to correlate very well. Therefore, for those interested in examining short time scale features of ozone variability , as well as the general synoptic structure, these data are eminently suitable. The user is strongly cautioned that these data are not to be utilized, at this time, for long-term trend determination within the error limits cited above. Further, data products with solar zenith angles greater than about 65 degrees are in question."

FUTURE CONCERNS

NESDIS is required to continue producing NOAA-9 SBUV/2 data until such time as the satellite and/or instrument can no longer perform its function. This requirement will put severe requirements on the NESDIS Satellite Operational Control Center (SOCC) in that it cannot control 4 active polar orbiting satellites concurrently. NESDIS would be in a 4 active polar orbiting satellite situation with the launch of NOAA-D (scheduled for late June 1990). Arrangements have been made with NASA/GSFC in order to insure that no SBUV/2 data is lost. Starting one month before NOAA-D launch (late May 1990), NASA/Wallops ground station will acquire a majority of the NOAA-9 TIROS Information Processor (TIP) data (NESDIS/Gilmore will bring in the rest). All data will be transmitted to NASA/GSFC on a "when time permits" basis. The data will be processed in a parallel "OOPS" at NASA. NASA will provide NESDIS with a copy of the SBUV/2 data to be used in the NESDIS OOPS to produce 1b Capture data just as we do now. Two months after launch of the NOAA-D (late August 1990), the acquisition and processing of the NOAA-9 SBUV/2 data will again revert back to NESDIS.

Plans for the second reprocessing of NOAA-9 SBUV/2 data include (Table 5.);

- Corrected A, B, C coefficients.

  A pair, B pair and C pair weighting coefficients are used to determine the "Best Ozone". In the operational processing of NOAA-9 data, these coefficients were set to 1, 1, 1. For the first reprocessing, they were to have been set to 1, 0.985, 1.072. However this update did not get into the reprocessing system. This change will be made for the second reprocessing.

- Elimination of Calibration effects.

  The extrapolation for tomorrow's value of the Albedo Correction Factor using the previous four days does not seen to be working correctly. This and other extrapolated quantities need to be investigated and corrected if necessary.

- Correction of Dark Mercury Lamp.

  The software developed to process Dark View Mercury Lamp data did not work after being installed into the reprocessing system. This problem must be corrected.

- Correction for modeling of SBUV/2 vs Ground Truth divergence.

  No answer has yet been offered to explain the drift of the SBUV/2 data from the NIMBUS 7 SBUV and Ground Truth data. More investigation is needed to determine the cause and to propose a correction. It is likely that the second reprocessing will wait until this problem is solved.

List of Tables

List of Figures

REFERENCES

SASC Technologies, Inc., 1986: Solar Backscattered Ultraviolet Radiometer Version 2 (SBUV/2), User's Guide Revision 2

TABLE 1. NOAA-9 SBUV/2 DATA

JANUARY	1983	LAUNCH OF FIRST SBUV/2 RESCHEDULED FOR NOAA-F.
		BREAK SYSTEM INTO 2 PARTS: 1B CAPTURE (TO GATHER DATA), PHASE 2 (PRODUCE OZONE PRODUCTS).
FEBRUARY	1983	CONTRACT WITH STX FOR OPERATIONAL OZONE PRODUCT SYSTEM (OOPS) SIGNED.
MARCH	1983	WORK ON OOPS BEGINS.
		DECISION TO USE ENHANCED TOVS DATA AS INPUT TO OOPS.
DECEMBER	1984	LAUNCH OF NOAA-9 CARRYING FIRST SBUV/2.
		OOPS BEGINS STORING SBUV/2 DATA USING THE 1B CAPTURE SYSTEM.
MARCH	1985	POST LAUNCH INSTRUMENT A&E TESTS FINISHED. BEGIN SBUV/2 DATA SET.
JULY	1985	CORRECT ERROR IN S/C CENTERED SOLAR AZIMUTH & ELEVATION ANGLES (CORRECTED BY REPROCESSING).
OCTOBER	1985	ANCILLARY DATA APPROPRIATE FOR NOAA-9 SBUV/2 INSTALLED IN OOPS.

TABLE 1. (continued) NOAA-9 SBUV/2 DATA

DECEMBER	1985	BEGIN OZONE PRODUCT PROCESSING WITH INSTALLATION OF OOPS PHASE 2.
APRIL	1986	ENHANCED TOVS DATA IN INPUT INTO OOPS.
DECEMBER	1986	UPGRADE TO THE INSTRUMENT SUPPORT SYSTEM IMPLEMENTED.
MARCH	1987	NOAA-9 TOVS INSTRUMENT FAILURE - METEOROLOGICAL DATA STOPPED.
MAY	1988	BEGIN REPROCESSING OF NOAA-9 DATA.
SEPTEMBER	1988	NOAA-9 ORBIT DRIFT CAUSES OFFSETS & ACF PROBLEMS.
		LAUNCH OF NOAA-11 AND NEXT SBUV/2 INSTRUMENT.
DECEMBER	1988	SOCC REPOSITIONED SOLAR ARRAY SO SBUV/2 CAN SEE THE SUN. BEGIN LOOKING AT DARK MERCURY LAMP FOR OFFSET CALCULATIONS.

TABLE 1. (continued) NOAA-9 SBUV/2 DATA

APRIL	1989	SEASONAL CHANGE ALLOWS ACF'S TO BE AUTOMATICALLY CALCULATED AGAIN.
MAY	1989	DARK MERCURY LAMP DATA PROCESSING SOFTWARE DELIVERED.
DECEMBER	1989	DECISION WAS MADE TO REPROCESS NOAA-9 DATA THROUGH OCTOBER 1989 BECAUSE PRECESSION OF ORBIT REQUIRES EXCESSIVE EXTRAPOLATION OF ACF VALUES. OCTOBER 1989 SSBUV FLIGHT AND OCTOBER 1989 SOLAR FLARES.

TABLE 2. SBUV/2 OZONE PRODUCTS DESCRIPTION

The 1B Data Set contains all SBUV/2 sensor data and support data necessary for the derivation of atmospheric ozone and solar flux.

The Historical Instrument File (HIF) contains the data necessary to characterize the instrument performance and albedo correction over time.

The Product Master File (PMF) contains the ozone information derived by the ozone algorithm, located in space and time, other meteorological information developed in support of the ozone computations, parameters indicating the validity of the individual ozone retrievals and the radiance information derived from the SBUV/2 measurements.

The Product User File (PUF) contains a subset of the information contained on the PMF.

Table 3

CHANGES INCLUDED IN THE 1ST REPROCESSING

- *REPLACE MISSING EARTH LOCATION.*
- *REPLACE MISSING DAYS.*
- *UPDATE ANCILLARY DATA.*
- *INSTRUMENT NON-LINEARITY CORRECTION.*
- *ZERO OFFSET ADJUSTMENT.*
- *SUN REFLECTIVITY ANGLE CORRECTION.*
- *WAVELENGTH CALIBRATION CORRECTION.*
- *INTER-RANGE RATIO EXTRAPOLATION CORRECTION.*
- *TIME DEPENDENT IRR CORRECTION.*
- *CORRECT PROGRAM ERRORS.*
- *INCLUDE 3 WAVELENGTHS NOT USED PREVIOUSLY.*
- *CORRECT DAY 1 COEFFICIENTS.*
- *CORRECT DATA RANGE.*
- *REMOVE ONE WAVELENGTH FROM CALCULATION.*
- *SET ERROR FLAGS WHEN CERTAIN APPROXIMATIONS ARE USED.*

Table 4. OZONE PRODUCT AVAILABILITY 7/7/88

The 1B Data Set,
Historical Instrument File Data (HIF),
Product Master File Data (PMF),
and Product User File Data (PUF),
are Produced daily and archived monthly onto separate magnetic tape volumes

These data may be ordered from:

National Oceanic & Atmospheric Administration
National Environmental Satellite & Data Information Service
National Climate Data Center
Satellite Data Services Division
Princeton Executive Square, Room 100
Washington D.C. 20233

Commercial = (301) 763-8400
FTS = 763-8400
FAX = (301) 763-8443

Electronic Mail addressed for SDSD
TELEMAIL: [AHORVITZ/NESDIS] TM44/USA
[SDSDDSB/NESDIS] TM44/USA
OMNET: [A.HORVITZ/OMNET] MAIL/USA

TABLE 5. SECOND REPROCESSING.

- *Corrected A pair, B pair, C pair coefficients*
- *Elimination of Calibration effects.*
- *Correct Dark View Mercury Lamp Processing.*
- *Correction or modeling of SBUV/2 vs. Ground Truth divergence.*

FIGURE 1.

OPERATIONAL OZONE PRODUCT SYSTEM

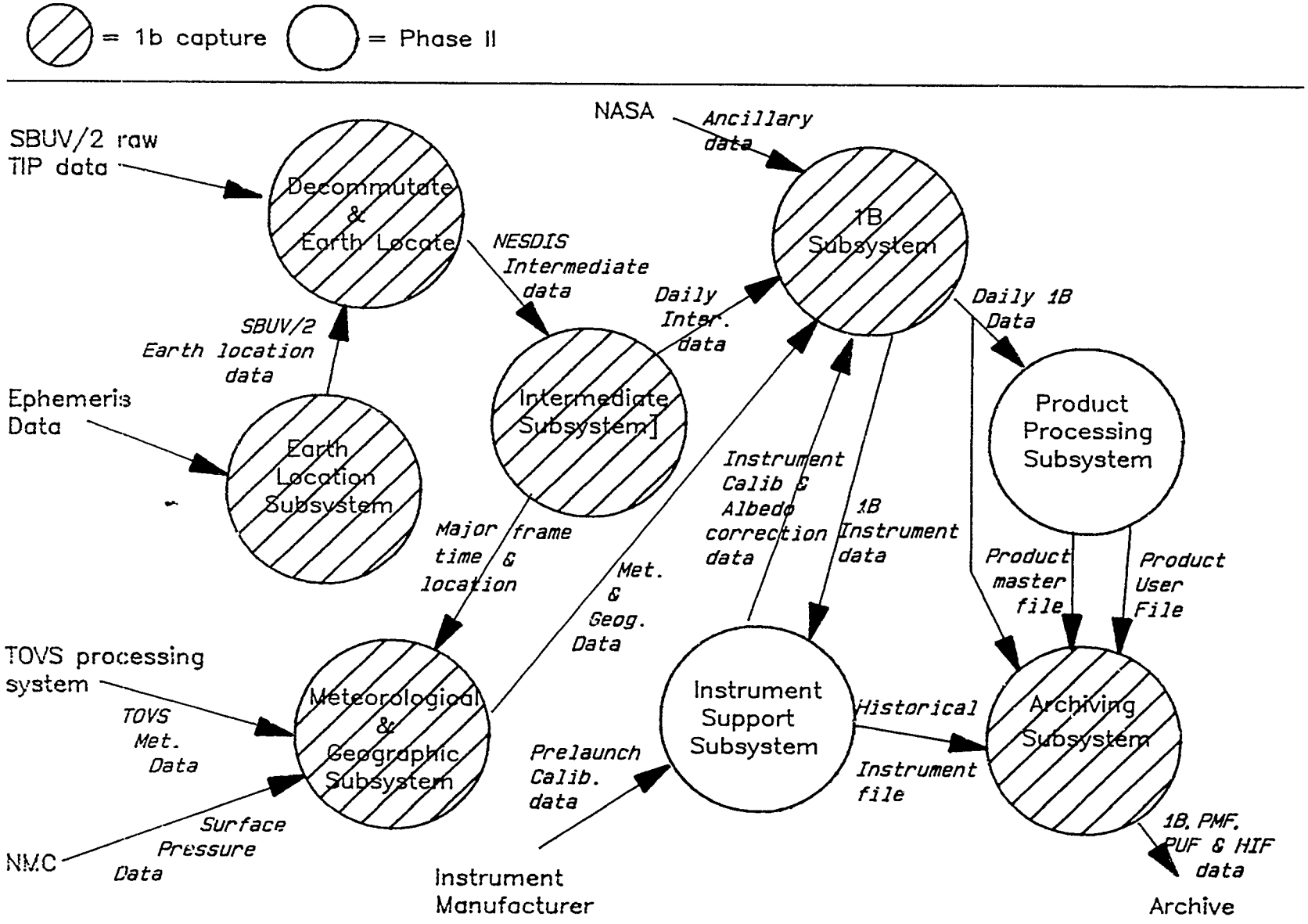

FIGURE 3. REPROCESSING OF SBUV/2 OZONE DATA

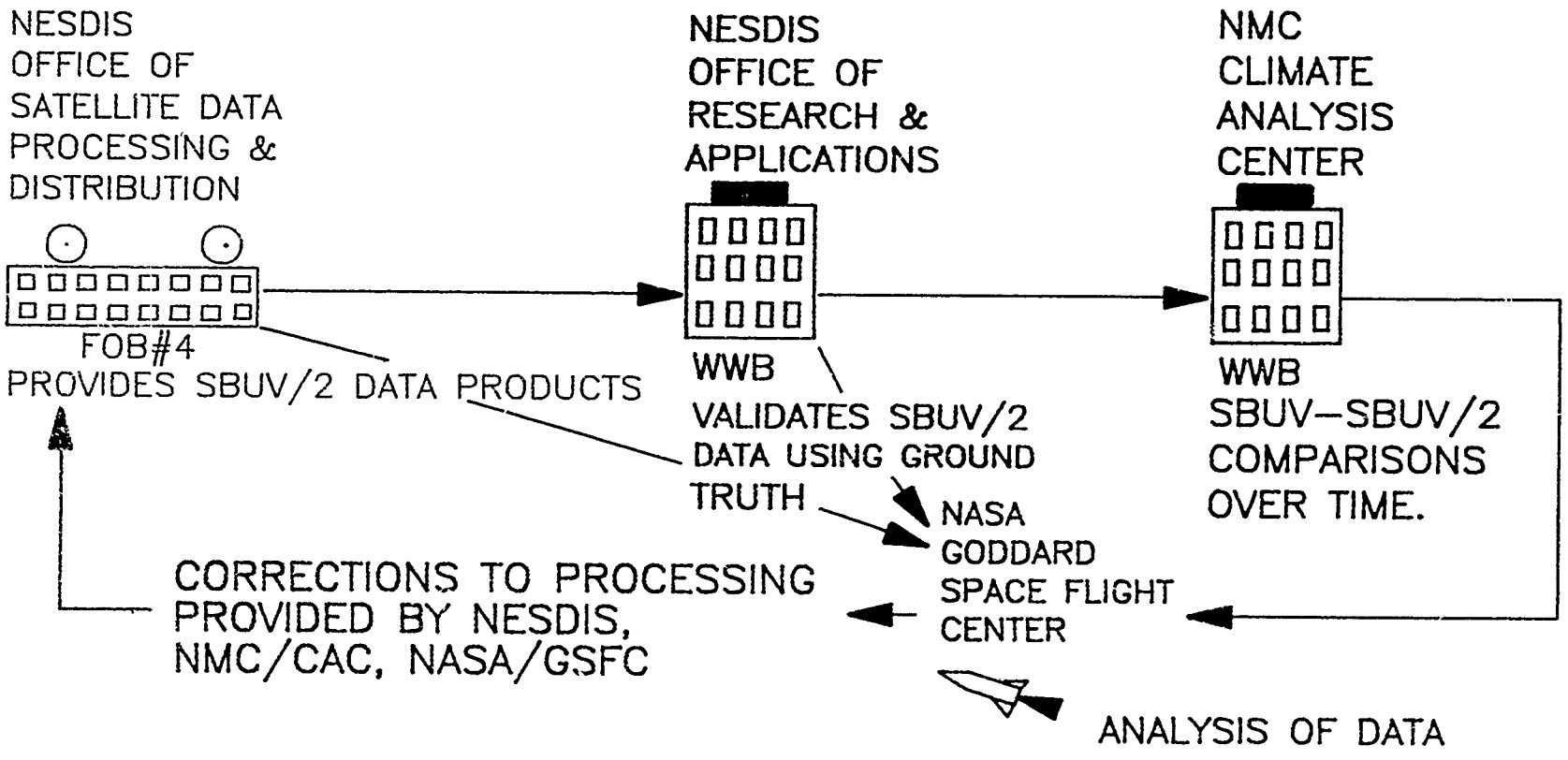

Attachment 2
An Assessment of Instrument Performance
D.F. Heath
ST Systems Corporation

An Assessment of Instrument Performance

for the NOAA-9 SBUV/2

Summary Meeting

29 January 1990

Donald F. Heath

ST Systems Corporation

The requirements for the accuracy of ozone monitoring are given in the National Plan for Stratospheric Monitoring, 1988-1997, FCM-P17-1989. These requirements, 3% per decade at the 95% confidence level at 40 km or approximately 2% per decade in the albedo calibration of the instrument, are more stringent than those contained in the TIROS-N SBUV/2 instrument specification which requires an uncertainty of 1.53% at 250 nm and 1.57% at 300 nm. This is assumed to be at the 95% confidence for an end-to-end spectral bi-directional reflectance instrument calibration for both the instrument pre-flight calibration and its changes throughout its operating lifetime in space.

The purpose of the NOAA-9 SBUV/2 summary meeting was to evaluate the overall performance of this instrument. This report attempts to do this by evaluating the calibration accuracy for all previously flown SBUV type instruments and intercomparing the solar spectral irradiance measurements during the initial period of the instruments observations in space when the effects of instrument degradation is likely to be smallest. A copy of the OSA symposium presentation was the basis for the report made to the NOAA-9 SBUV/2 summary meeting. This is included in Section I of the material presented at the January 29, 1990 summary meeting.

The OSA symposium presentation did not consider an assessment of the accuracy of determining long term drifts in the diffuser reflectance properties of the instrument diffuser plate, which is limited by the precision of the measurements of relative changes in the instrument diffuser reflectivity made with the instrument Hg lamp. This assessment is contained in Section II.

Section I An Assessment of Calibration Errors of SBUV Type Instruments for Measurements of Stratospheric Ozone and UV Solar Spectral Irradiance: 1970-1989

Donald F. Heath
Laboratory for Atmospheres
Goddard Space Flight Center
Greenbelt, Maryland 20771

ABSTRACT

Techniques and uncertainties in the calibrations of SBUV type instruments from 1970-1989 for the determination of stratospheric ozone and UV solar flux are evaluated.

Summary

A continuing series of measurements of atmospheric radiances in the Hartley-Huggins bands of ozone absorption and corresponding solar irradiance measurements have been made since 1970 by a series of 0.25 meter focal length tandem Ebert-Fastie double monochromators. An ozone inversion algorithm yields profiles and total column amounts from the ratio of atmospheric radiances/solar irradiances at 12 wavelengths in the region 250-340 nm. This work discusses major sources of uncertainties in the atmospheric reflectances which are used in the ozone inversion algorithm. A summary of SBUV type instrument calibration parameters are given in Table 1.

TABLE 1

Summary of SBUV Type Instrument Calibration Parameters

	N-4 BUV	AE-5 BUV	N-7 SBUV	NOAA-9 & 11 SBUV/2
Instrument Diffuser	Al	Transmission, S_iO_2	Al	Al
Angle of rays to diffuser normal				
Solar rays at terminator	55°	0°	50°	62°
Irradiance Calibration	55° Uncollimated	0° Uncollimated	50° Uncollimated	71° Collimated
Radiance Calibration	55° Uncollimated	0° Uncollimated	0° Uncollimated	0° Uncollimated
Radiance Standard (diffuser) Reflectance Source of Calib.	$BaSO_4$ Hemispheric Beckman	$BaSO_4$ Hemispheric NIST	$BaSO_4$ Hemispheric NIST	$BaSO_4$ Hemispheric/BRDF NIST

The calibration constants for irradiance, radiance, and albedo are the following:

Irradiance: $$K_E(\lambda) = \frac{E_\lambda \, \overline{g}_E \, \overline{e}_m(\lambda) \, \overline{r}_E}{S_E} \quad (1)$$

Radiance: $$K_L(\lambda) = \frac{E_\lambda \, \overline{g}_L \, \overline{e}_m(\lambda) \, \overline{r}_L \, \overline{BRDF}(\lambda) \cos i_L}{S_L} \quad (2)$$

Albedo:[1] $$A(\lambda) = \frac{K_L(\lambda) = \overline{g}_L \, \overline{e}_m(\lambda) \, \overline{r}_L \, \overline{BRDF}(\lambda) \cos i_E \, S_E}{K_E(\lambda) \quad g_E \, \overline{e}_m(\lambda) \, r_E \quad S_L} \quad (3)$$

[1]The albedo calibration constants, A(λ), which are really BRDF calibration constants, are defined as the ratio of the radiance, $K_L(\lambda)$/irradiance, $K_E(\lambda)$ calibration constants.

Where: E_λ, standard of spectral irradiance; $\overline{g}$, averaged angular variation of source; $\overline{c}_m(\lambda)$, collimator mirror transfer function, f, averaged $1/r^2$ variation of diffuser illumination; $\overline{BRDF}(\lambda)$, average of Bi-directional Reflectance Distribution Function over angles of diffuser and instrument illumination; S, signal output; i, angle of illumination to diffuser normal. The subscripts, L and E, refer to radiance and irradiance calibration modes, respectively.

If the radiance and irradiance calibrations are derived under the same conditions, with the same $\overline{g}$, $\overline{e}_m(\lambda)$, f, then,

$$A(\lambda) = \overline{BRDF(\lambda)_{Al}} \cos i_L = \frac{S_E}{S_L} \overline{BRDF(\lambda)_{BaSO_4}} \cos i_L \qquad (4)$$

Summaries of major sources of uncertainties in the albedo calibrations of the SBUV type instruments flown in polar orbits (N-4, N-7, NOAA-9 and 11) are given in the following sections.

Nimbus-4 BUV: Since the radiance and irradiance calibrations were made at the same angle of incidence, equation (4) gives the albedo calibration constants. The quantity BRDF for the $BaSO_4$ diffuser plate was computed from measurements of hemispheric reflectances at Beckman Instruments Inc. and it was assumed the $BaSO_4$ was Lambertian. Measurements of both BRDF and hemispheric reflectances at NIST of $BaSO_4$ indicate that the assumption of a Lambertian diffuser yields a value of BRDF which is 2-3% too low. The accuracy of the hemispheric reflectances is unknown. At 340 nm, the Beckman value of 0.952 agrees well with NIST measurements of 0.946 for plates used to calibrate the Nimbus-7 SBUV instruments and 0.958 for the NOAA SBUV/2 instruments. At 250 nm, the corresponding reflectances were 0.936, 0.905, and 0.917. A preliminary estimate of the one-sigma BUV prelaunch calibration is that it is greater than 2.4%, which does not include the effects of the assumption of a Lambertian diffuser.

Nimbus-7 SBUV: The principal sources of uncertainty in the calibration of the SBUV instrument are the result of using a large area $BaSO_4$ plate illuminated at normal incidence to establish the radiance calibration instead of at the angle and position of the instrument diffuser. The BRDF was derived from measurements by NIST of hemispheric reflectance of the $BaSO_4$ plate, which was assumed to be Lambertian. No correction was made for angular variations of the 1000 watt quartz halogen FEL lamp illuminating the diffuser. Calibrations of the SBUV/2 instruments indicate that the assumption of a Lambertian surface yields a BRDF for normal incidence illumination, which is 8.4% less than measured. The measured off-axis variations of lamp output reduce the flux entering the instrument by 2.3%. The former error increases the flux into the instrument while the latter decreases it which gives a net error in flux entering the instrument of +6.1%. A preliminary estimate of the one-sigma uncertainty in the SBUV albedo calibration is 1.7% and does not include the bias associated with the $BaSO_4$ being Lambertian.

NOAA-9 AND 11 SBUV/2: The SBUV/2 instruments, while having the best calibrations of all of the SBUV type instruments, unfortunately, have the most sources of calibration uncertainties. In addition to the terms in Equation (3) for the albedo calibration factors, additional sources of significant errors are the angular calibration of the instrument response at the large angles of incidence and the use of two anode current and one cathode current signal ranges to cover the needed dynamic range of the photomultiplier. The two-sigma repeatability is 71° and the irradiance calibration angle is 0.5% and increases at the rate of 0.08%/degree. Similarly, a wavelength dependence in the angular response becomes significant at 71° (the irradiance calibration angle) where the response at 400 nm is 1.0% less than at 270 nm. The wavelength dependence of the correction has not been determined with sufficient accuracy over the range of wavelengths used in the ozone inversion algorithm. The gains of both the ITT and the Hamamatsu photomultipliers have been found to be wavelength dependent and to vary from tube to tube.

The Hamamatsu tube in the instrument flown on NOAA-11 shows a 9% decrease in gain with decreasing wavelengths from 340 to 250 nm whereas a similar tube in the next instrument to be launched shows a decrease in gain of 2% from a flat maximum at 290-340 nm to a minimum at 250 nm. This effect, if not properly calibrated, could lead to significant errors in the measured BRDF of the atmosphere. A major source of uncertainty in the SBUV/2 instrument calibrations are associated with the stability of the $BaSO_4$ diffusers used to determine the radiance calibrations and the inability of NIST to measure the BRDF of the large 30 X 30 cm plate used in the normal incidence calibration. The BRDF of the large plate is inferred from measurements of the BRDF and hemispheric reflectance of a small diffuser and assuming the BRDF is proportional to the hemispheric reflectance of the large plate. This is a significant source of error. A series of nine measurements of BRDF of three $BaSO_4$ plates illuminated at normal incidence and averaged over the field of the instrument, gave a one-sigma uncertainty of 1.2% and a correlation of 0.98 for a linear regression of BRDF against hemispheric reflectances at 292 nm. An estimate of the one-sigma uncertainty of the inferred BRDF at the radiance calibration diffuser is 1.7%. The three-sigma uncertainties given by NIST are 1.7% for BRDF and 0.6% for hemispheric reflectances at 292 nm. An estimate of the uncertainty in the collimator mirror transfer function, $e_m(\lambda)$, is 1.0% based upon a comparison of measured values and those computed from spatially averaged mirror reflectances. A preliminary estimate of the one-sigma uncertainty in the albedo calibration is 2.2%. This does not include a bias associated with a wavelength dependent degradation of the $BaSO_4$ diffusers.

Assessment of the Accuracy of Albedo Calibrations: Equation (4) states that the albedo calibration of SBUV type instruments using an Al diffuser for solar irradiance measurements is given by the BRDF of that diffuser. Unfortunately, it has not been possible to measure the BRDF of the instrument diffuser as a part of the calibration sequence in the past. Another problem is that a ground Al diffuser has poor Lambertian characteristics at angles of illumination of the instrument diffusers given in Table 1. Nevertheless, the relative shape of the reflectance curve can be used to estimate the quality of the albedo calibration of SBUV type instruments. Results of this type of analysis indicate that the quality of the albedo calibration of the Nimbus-7 SBUV instrument was highest and the Nimbus-4 BUV instrument was the lowest.

Solar Irradiance Measurements: The major uncertainties in the spectral irradiance calibrations were the uncertainties in the absolute calibration of the 1000 watt tungsten filament quartz halogen lamps. These were:

N-4 BUV	7% at 250 nm - 3% at 340 nm
AE-5 BUV	5% at 250 nm - 2% at 340 nm
N-7 SBUV	2.6% at 250 nm - 1.7% at 340 nm
NOAA-9 & 11 SBUV/2	2.2% at 250 nm - 1.4% at 340 nm

An additional source of error is introduced into the solar irradiance by the use of a collimator mirror. Measurements of the collimator mirror transfer function were estimated by comparing measured values with those calculated from measured reflectances at ten areas on the mirror. From the measurements of the transfer function it is estimated that this uncertainty is about 1.0%. The root sum square (RSS) of these uncertainties is 9.3% at 250 nm and 4.3% at 340 nm.

The solar spectral irradiances (W cm^{-3}) measured with each of the four instruments before significant degradation occurred are given in Table 2. Column 6 gives the standard deviation divided by the mean of the four series of flux measurements. Column 7 gives relative values of the solar plage contrast function (SPC), which were derived from N-7 SBUV continuous scan solar flux modulation associated with solar rotation of active regions. A linear regression of the SD/Mean Flux against the solar plage contrast function yields SD/Mean Flux = 0.047 + 0.45 SPC with a correlation of 0.89. A comparison of the calculated SD/Mean Flux derived from the regression against the solar plage contrast function (+) against the observed SD/Mean Flux (solid line) is shown in Figure 1. This indicates a bias of 4.7% in the region of negligible solar flux changes associated with solar plages. This bias is similar to the RSS of the lamp

calibration uncertainties (4.3%) at the larger wavelengths. A discussion as to whether the measured solar flux changes are real at the shorter wavelengths is beyond the scope of this paper, especially as they do not appear to be related to the monthly F10.7 cm radio flux.

Section J)

The development of the SBUV/2 instrument included a means for measuring long term drifts or changes in the SBUV/2 diffuser plate reflectivity after the prelaunch spectroradiometric calibrations and throughout its lifetime in space. Changes in the bi-directional reflectance properties of the atmosphere, which are used in the algorithm to derive changes in the ozone profiles and total column amounts, are related to changes in the bi-directional reflectance properties of the instrument diffuser (Section I). Consequently, measurements of long term drifts in the BRDF properties of the instrument diffuser can be used to correct drifts in the inferred ozone time series.

Examples of the measurement stability of the mercury lamp system used to determine changes in the relative diffuser plate reflectivity are given in Table 1 and Figure 9 for Flight Model 4 (FM 4) and Figure 10 for Flight Model 3. These tests indicate that the standard errors of changes in the instrument diffuser reflectivity data for FM 3 and 4 are much better than the system used with FM 1 on NOAA-9. For example, the standard error of eight measurements of instrument diffuser relative BRDF in the vicinity of ozone sounding wavelengths, 250-340 nm, is less than 0.1%. To the best of the author's knowledge, a comparable or greater precision has not been shown for Flight Model #1 on NOAA-9 either during measurements on the ground or in space. Examples of the repeatability of the relative bi-directional reflectance properties of the FM#1 instrument diffuser have been given in reports by R.P. Cebula (refs?)

STX
ST SYSTEMS CORPORATION

GRAND MEAN ALBEDO RATIOS
(Average of all 8 Trials)

	184.9nm	253.7nm	296.7nm	313.2nm	365.4nm	404.7nm
MEAN	.00526	.01548	.01656	.01687	.01756	.01799

STANDARD DEVIATION

	184.9nm	253.7nm	296.7nm	313.2nm	365.4nm	404.7nm
STD. DEV.	6.0×10^{-5}	1.5×10^{-5}	2.0×10^{-5}	4.9×10^{-5}	5.3×10^{-5}	1.5×10^{-5}

STANDARD ERROR (PERCENT)

	184.9nm (REF.)	253.7nm 0.5%	296.7nm 0.5%	313.2nm 0.5%	365.4nm 0.5%	404.7nm 0.5%
STD. ERR.	.40	.03	.04	.10	.11	.03

FIGURE 9
(Continued)

STX
ST SYSTEMS CORPORATION

FM #4 MEAN ALBEDO RATIOS

	184.9nm	253.7nm	296.7nm	313.2nm	365.4nm	404.7nm
RUN#1	.00524	.01549	.01656	.01685	.01759	.01799
RUN#2	.00519	.01547	.01657	.01689	.01757	.01800
RUN#3	.00528	.01548	.01653	.01683	.01752	.01798
RUN#4	.00536	.01547	.01656	.01684	.01752	.01796
RUN#5	.00530	.01549	.01657	.01697	.01755	.01800
RUN#6	.00523	.01549	.01654	.01683	.01762	.01797
RUN#7	.00518	.01549	.01659	.01691	.01747	.01799
RUN#8	.00532	.01545	.01654	.01685	.01762	.01800

FIGURE 9

STX
ST SYSTEMS CORPORATION

FM #3 MEAN ALBEDO RATIOS

	184.9nm	253.7nm	296.7nm	313.2nm	365.4nm	404.7nm
RUN#1	.00563	.01577	.01656	.01749	.01860	.01938
RUN#2	.00565	.01577	.01656	.01744	.01856	.01933
RUN#3	.00571	.01579	.01699	.01743	.01857	.01938
RUN#4	.00574	.01577	.01654	.01744	.01860	.01940
RUN#5	.00561	.01577	.01657	.01739	.01859	.01937
RUN#6	.00558	.01577	.01656	.01743	.01857	.01936
RUN#7	.00565	.01576	.01655	.01742	.01855	.01940
RUN#8	.00561	.01580	.01657	.01740	.01853	.01936

FIGURE 10

TABLE 2

UV Solar Spectral Irradiance (Wcm^{-3})

Wavelength (nm)	N-4 4-70	AE-5 12-75	N-7 11-78	NOAA-9 3-85	SD Mean Flux	Solar Plage Contrast	
255.7	107	96		75	84	0.154	0.270
273.7	235	236		176	205	0.134	0.144
283.1	391	365		303	342	0.107	0.101
287.7	390	373		321	355	0.100	0.082
292.3	639	586		521	566	0.085	0.019
297.6	619	548		501	547	0.080	0.050
302.0	490	446		432	477	0.058	0.084
305.9	632	590		557	603	0.052	0.040
312.6	710	662		660	712	0.042	0.031
317.6	823	785		752	822	0.043	0.013
331.3	946	923		969	1006	0.037	0.000
339.9	972	934		1020	1034	0.046	-0.001
MO F10.7	163	72		148	72		

STX
ST SYSTEMS CORPORATION

GRAND MEAN ALBEDO RATIOS
(Average of All 8 Trials)

	184.9nm	253.7nm	296.7nm	313.2nm	365.4nm	404.7nm
MEAN	.00565	.01578	.01656	.01743	.01857	.01937

STANDARD DEVIATION

	184.9nm	253.7nm	296.7nm	313.2nm	365.4nm	404.7nm
STD. DEV.	5.4×10^{-5}	1.3×10^{-5}	2.3×10^{-5}	3.0×10^{-5}	2.5×10^{-5}	2.3×10^{-5}

STANDARD ERROR (PERCENT)

	184.9nm (REF.)	253.7nm 0.5%	296.7nm 0.5%	313.2nm 0.5%	365.4nm 0.5%	404.7nm 0.5%
STD. ERR.	.34	0.03	0.001	0.06	0.05	0.04

FIGURE 10
(Continued)

Attachment 3

SBUV/2 In-orbit Performance

J.H. Lienesch
NOAA/NESDIS

SBUV/2 IN-ORBIT PERFORMANCE

James H. Lienesch
NOAA/NESDIS

At the time of launch the NOAA-9 spacecraft was placed in orbit with an ascending node equitorial crossing time near 1420Z. A precession in the spacecraft orbit has resulted in the progression of the ascending node time to later in the afternoon. Table 1 shows the change of the ascending node time over the lifetime of NOAA-9. Note that by the end of December 1989 the ascending node time had migrated to 1717Z, about three hours later than at launch. There are several major consequences of this orbital change that relate to the SBUV/2 ozone data by way of the solar zenith angle of the SBUV/2 measurements and the angle of the sun with respect to the spacecraft.

Figure 1 shows the spacecraft sun angle as a function of time. This is the angle between the sun and the spacecraft Z axis which, in practice, is the angle between the sun and the normal to the orbital plane. There appear both annual and semi-annual cycles imposed on a long term decrease in the value of the spacecraft solar angle. The long term decrease is a consequence of the drift in the spacecraft orbit. On the ascending node of the orbit the solar zenith angle of the SBUV/2 measurements increases as the spacecraft sun angle decreases. The algorithm for processing the SBUV/2 data is designed to account for the effects of the changing solar zenith angle.

Fig 2 is a plot of the solar zenith angle of the SBUV/2 measurements versus latitude for July 1985. The data show the zenith angle on the daylit portion of the orbit. Sunrise occurs near 50S and the zenith angle progresses to a minimum value of 30 degrees near 30N. The values rise as the spacecraft passes over the northern polar region until sunset is reached near 60N on the descending part of the orbit. Note that the zenith angle at the equator is above 40 degrees in July 1985. Figure 3 shows similar data for July 1989, four years later than Fig. 2. Here the minimum zenith angle during the orbit has increased to 53 degrees and occurs at approximately 55N. At the equator the zenith angle has increased to about 70 degrees, an increase of 30 degrees over the value in July 1985. The latitudes of sunrise (30S) and sunset (40N) have migrated from those of 1985. A comparison with Fig. 2 shows that the zenith angle has increased at all latitudes over the ascending node of the orbit. Fig. 4 shows a comparable plot of the zenith angles during January 1988. The pattern of latitude vs. zenith angle, seen in Figs. 2 and 3, is reversed during the northern hemisphere winter with sunrise on the descending node and the minimum zenith angle occurring near 30S. Two years later, in January 1990, the minimum solar zenith over the entire daylit part of the orbit was above 70 degrees.

The SBUV/2 processing algorithm accounts for the effects of the changing zenith angle in the calculation of the ozone. This is accomplished by computing different values of ozone from several pairs of measurements (A-pair, B-pair and C-pair) and applying zenith angle dependent weights to the several values to arrive at a best ozone value. Also, the algorithm is designed to apply empirically-derived adjustments to the individual values of ozone in the generation of the best ozone value. Because of a software problem these adjustments were not applied to the reprocessed ozone data. The effect of not applying these adjustments has been assessed at several latitude bands for July 1988. Fig. 5 shows the difference between the corrected total ozone values (with the proper adjustments applied to the A-, B- and C-pair values) and the reprocessed values (with the incorrect adjustments) for the data of July 1988. Shown are the average differences for each day of the month in 2 latitude bands, 5S to 5N and 45N to 55N. The data in these bands were acquired at solar zenith angles of approximately 60° and 45°,respectively. The differences are found to be small (approximately 1-2 Dobson Units) at all but the most extreme zenith angles. From other data (not shown) at zenith angles greater than approximately 80 degrees, we found that the differences may exceed 10 D.U.

The changing spacecraft solar angle has also impacted the instrument through the computation of the instrument calibration. The calibration occurs on one orbit per week, when the instrument's diffuser is exposed to the sun as the spacecraft approaches sunset. The measurements obtained at that time are normally combined with the pre-flight calibration constants, corrections made for sun-earth distance, the angular reflectance characteristics of the instrument diffuser and the diffuser degradation to determine values of solar irradiance. However, for NOAA 9, the effects of diffuser degradation have not been included in the reprocessing because the in-orbit instability of the mercury lamp source rendered the diffuser degradation measurements invalid. The derived values of adjusted irradiance are divided by the "day-1" solar irradiances to arrive at a value of the albedo correction factor (ACF), the calibration term used in the processing of the SBUV/2 data.

A plot of the ACF for channel 12 (339.8 nanometers) is shown in Fig. 6. Plots for the other channels used in the derivation of the total ozone are similar. The values decrease in a time-dependent fashion with the greatest changes occurring in the earliest years. ACF values could not be computed by the processing system during the periods of September 1988 to May 1989 and July 1989 through the end of the data record. Values for these periods were not derived by the instrument support subsystem because the azimuth angles of the sun on the diffuser fell below 30 degrees, the lowest angle for which the diffuser reflectivity was characterized in the software. For those months when the calibration data are missing, interpolated ACF values were manually derived from the periods when the sun's angle on the diffuser was within limits. The annual pattern observed

during previous years was imposed upon the interpolated data. These values were then used in the derivation of the SBUV/2 products.

The spacecraft solar angle should again exceed the threshold value for several months during the summer of 1990. At that time an interpolation between the ACF values of the summers of 1989 and 1990 will be possible. After that period, about 10 months will elapse before the calibration computations will again be provided by the instrument support substation.

The ACF data in Fig.6 appear to define two envelopes, one containing most of the data and another with far fewer data appearing about 1% above the majority. It is believed that this effect is caused by the existence of two positions in which the diffuser may settle when commanded into the sun-viewing mode. In the processing of the SBUV/2 data there has been no attempt to exclude ACF values from the less populated envelope. However, monitoring of the total ozone values has been carried out on a continuing basis and has not revealed any evidence that the data are impacted by these 1% variations in the ACF values.

As each month of SBUV/2 data was reprocessed, plots of the daily values were constructed to monitor the output of the ozone product processor. Fig. 7 shows the daily average value of ozone in July 1988 for the latitude bands of 5S to 5N and 45N to 55N. This month contains a calibration point (see Fig.6) that is clearly in error. An examination of the historical record of the Albedo Correction Factors showed that 2 of the 4 channels used in deriving total ozone exhibited a large increase in the ACF value at that time and the other two showed a modest decrease. The result was an increase in the total ozone for a one-week period in the middle of the month, as shown in Fig. 7. In the whole data record this is the only example of a variation in the ACF correlated with an observable change in the derived ozone.

More typical is the data in Fig. 8 for July 1986. Here, plots of the daily values of ozone are reasonably smooth, although the ACFs for this month include a change as large as 3% (see fig. 6). The calibration changes in the four channels used to derive total ozone were similar in size and direction, in contrast to those of July 1988 (discussed above) where the changes among the channels were in different directions. The variablilty that does exist in the ozone values in Fig. 8 may be attributed to variations in the number of data from which the averages were computed.

A merging of the 12 monthly plots for the year 1986 is shown in Fig. 9 for the latitude bands 55S to 45S, 5S to 5N and 45N to 55N. This figure clearly shows the annual variations in the total ozone for the three latitude bands. The data record, particularly for the tropics, is relatively smooth. Figs. 7, 8, and 9 are examples of data displays used to monitor the output of the Operational Ozone Processing System for instrument-induced discontinuities in the derived values of ozone.

Table 1 The equatorial crossing time of the ascending node for NOAA 9.

31	*DECEMBER*	*1984* *1420Z*
31	*DECEMBER*	*1985* *1436Z*
31	*DECEMBER*	*1986* *1501Z*
31	*DECEMBER*	*1987* *1535Z*
31	*DECEMBER*	*1988* *1617Z*
31	*DECEMBER*	*1989* *1717Z*

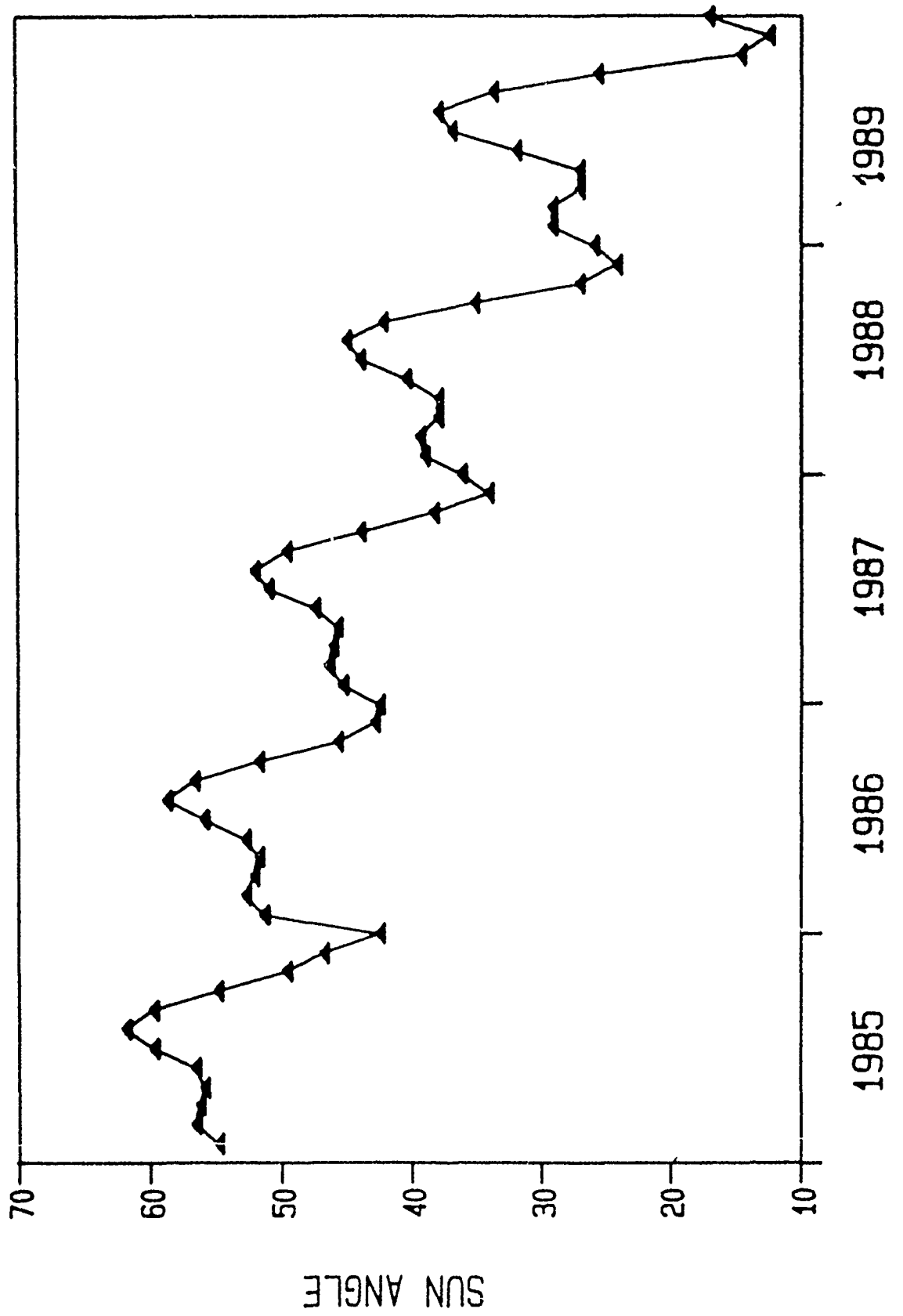

Fig. 1 The spacecraft sun angle for NOAA 9 as a function of time.

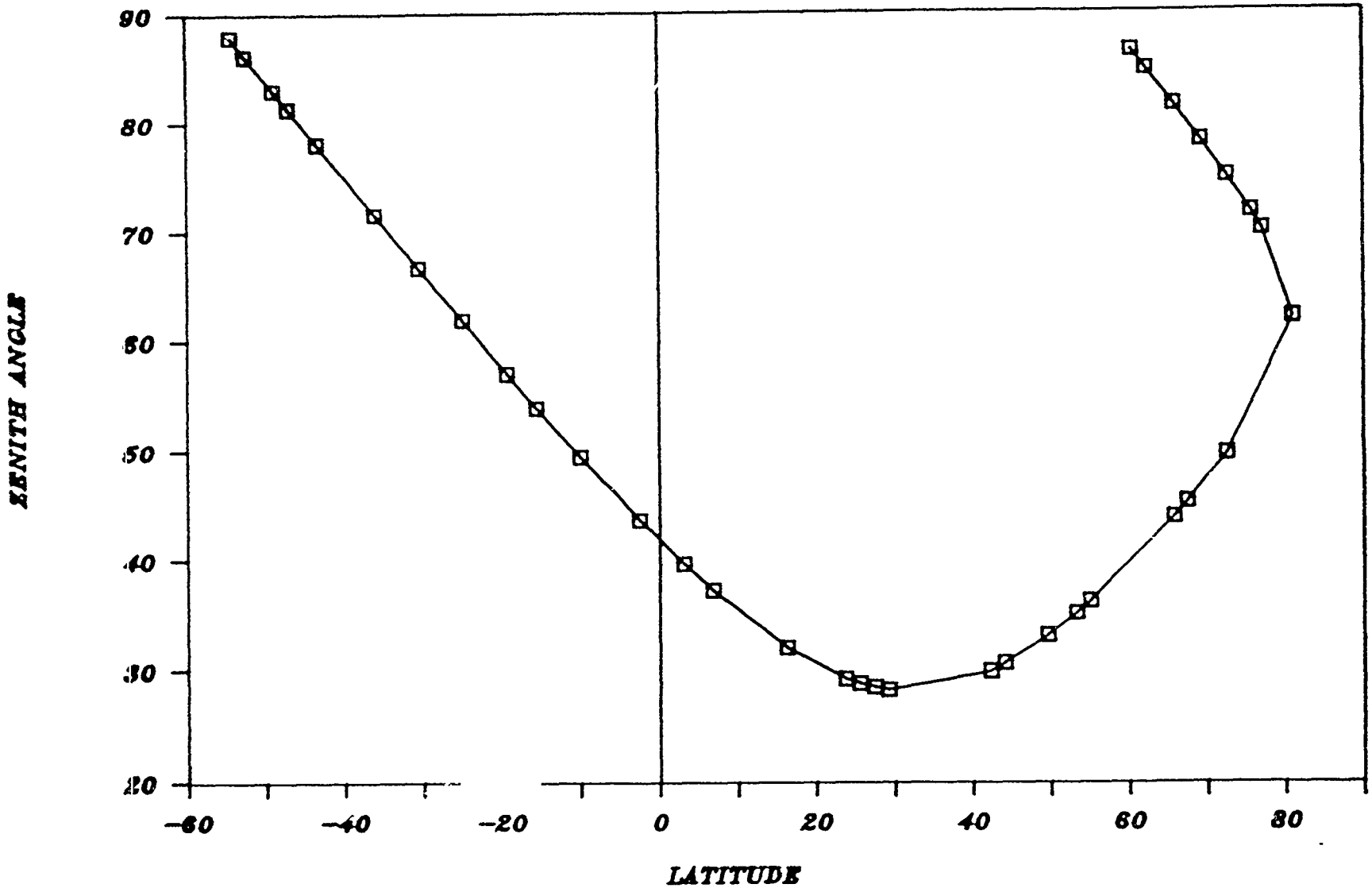

Fig. 2 The solar zenith angle vs. latitude for one orbit in July 1985. Sunrise occurs at the upper left and sunset in the upper right.

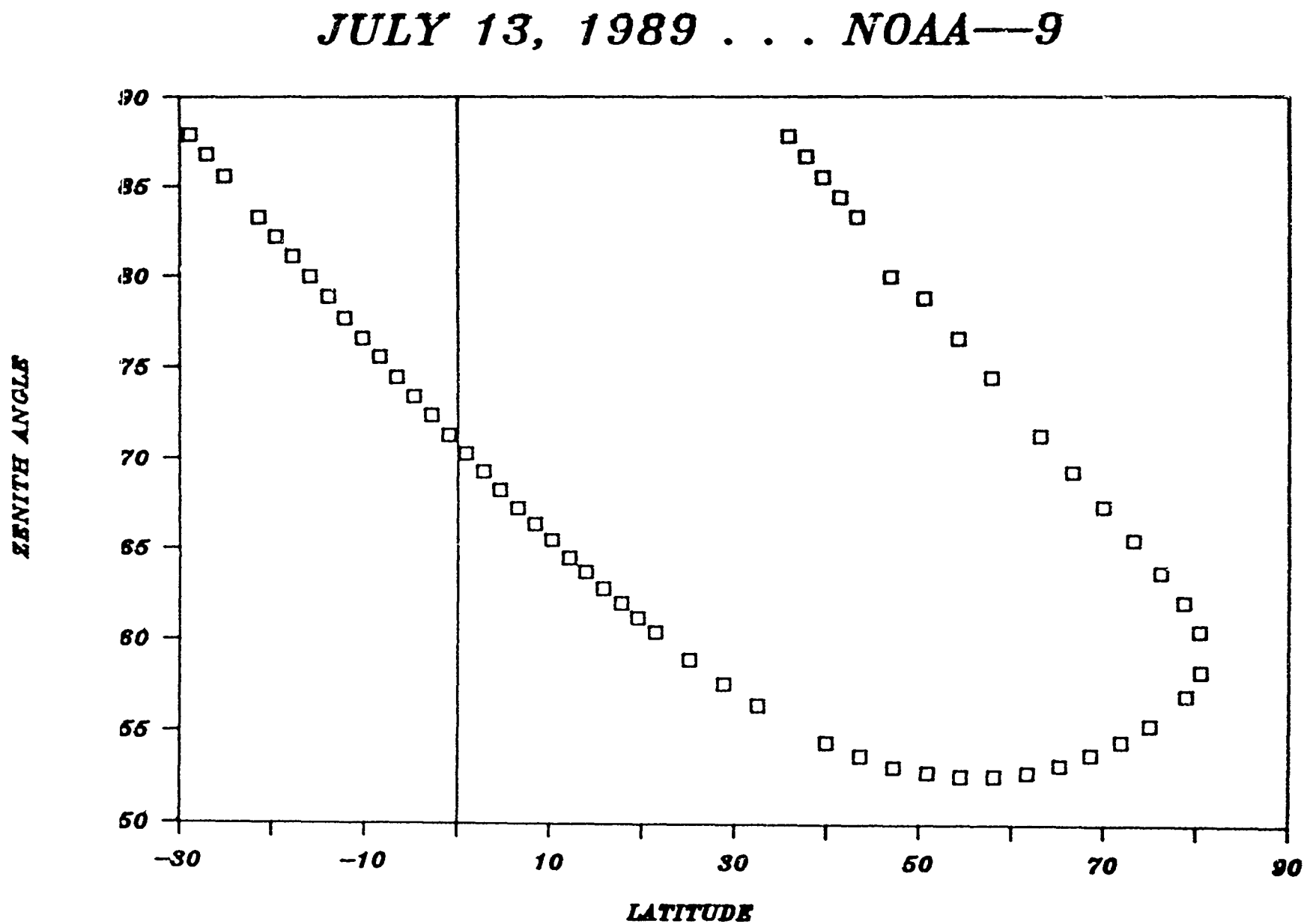

Fig. 3 As in Fig. 2 but for July 13, 1989.

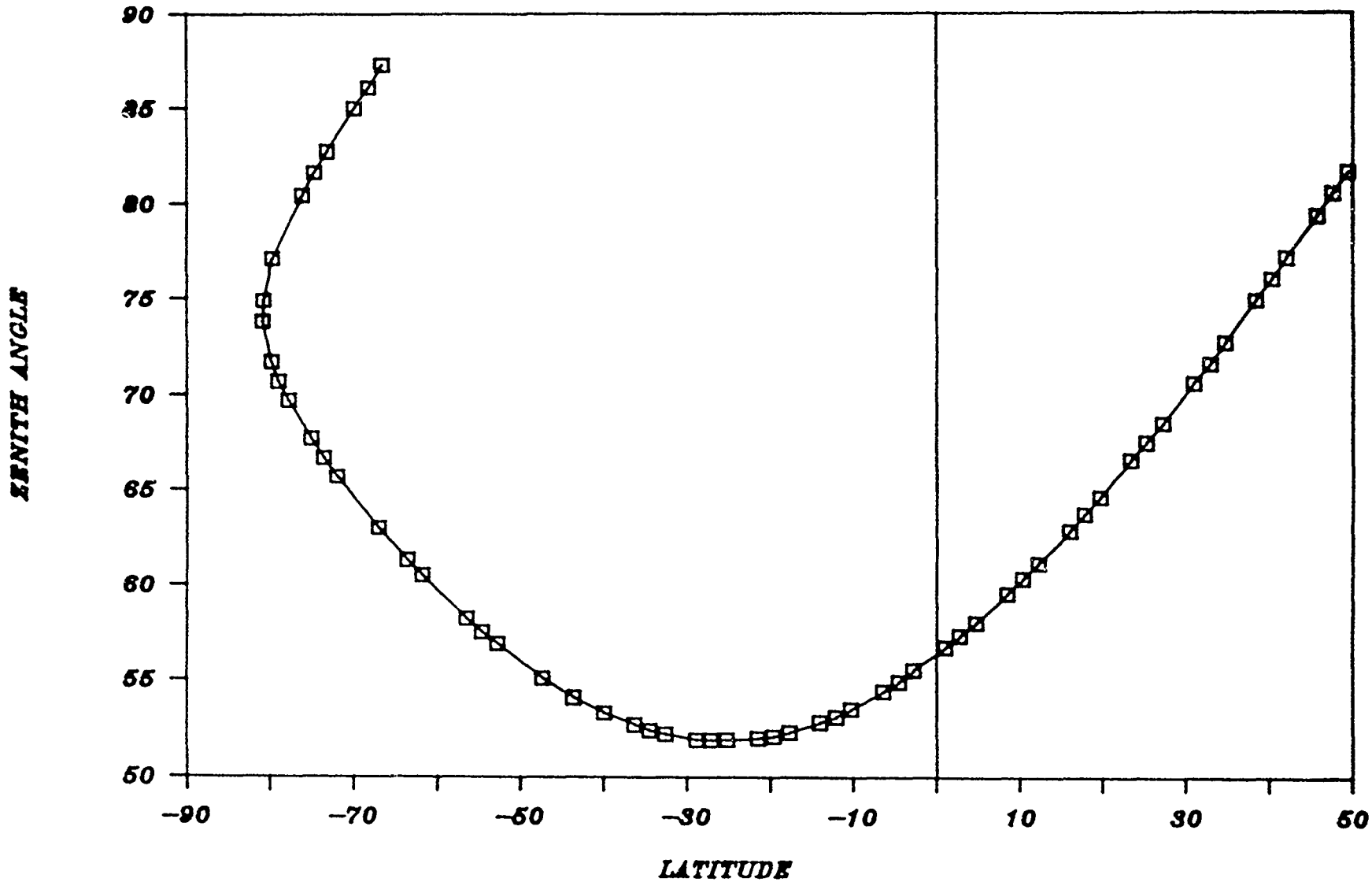

Fig. 4 As in Fig. 2 but for January 1988.

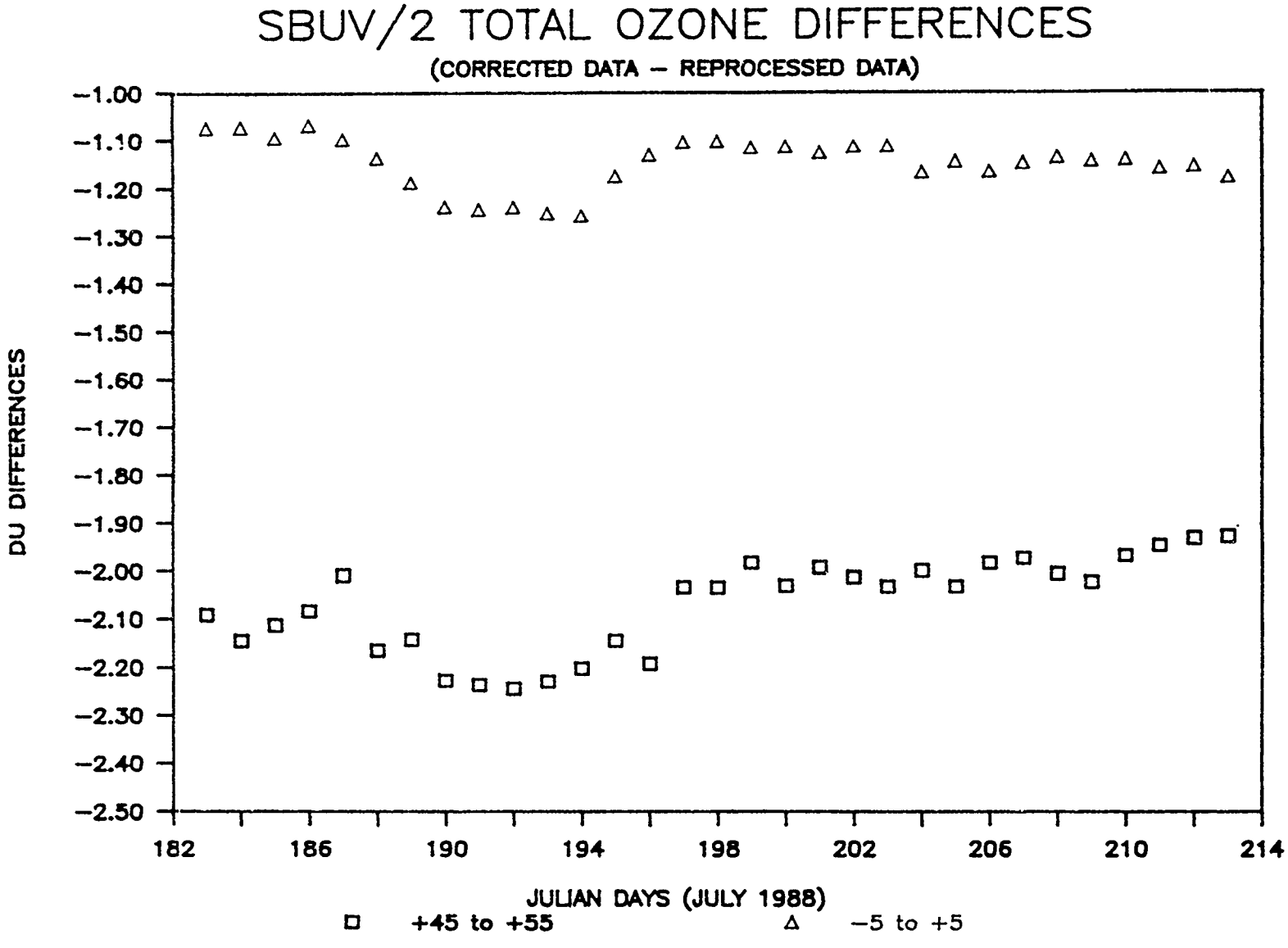

Fig. 5 The differences between the total ozone computed with the correct adjustment factors and that computed with all factors set to 1.0 vs. latitude. Daily values are shown for latitude bands of 45N to 55N and 5S to 5N.

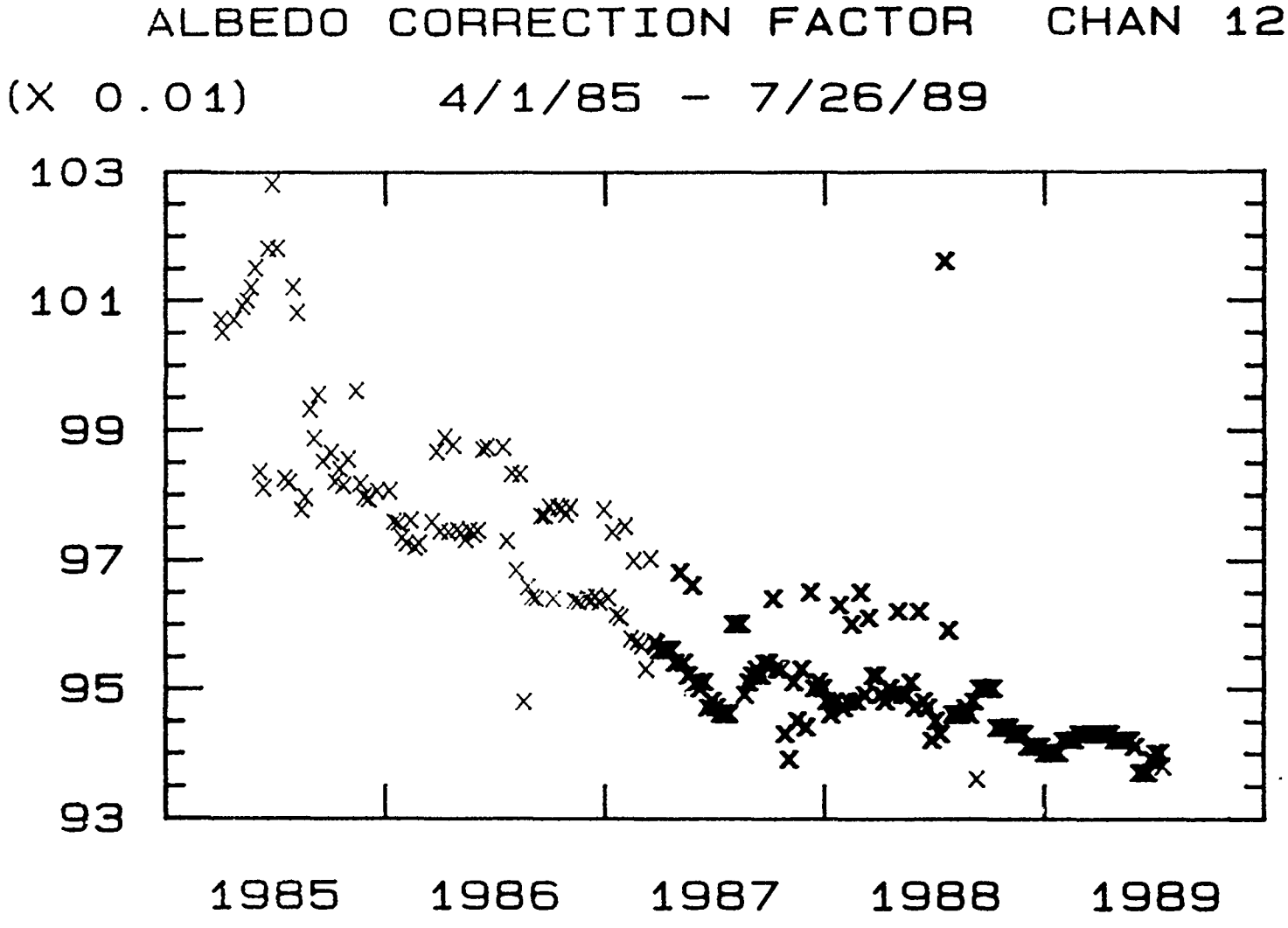

Fig. 6 The albedo correction factors for channel 12 (339 nm.) for the years 1985 to 1989.

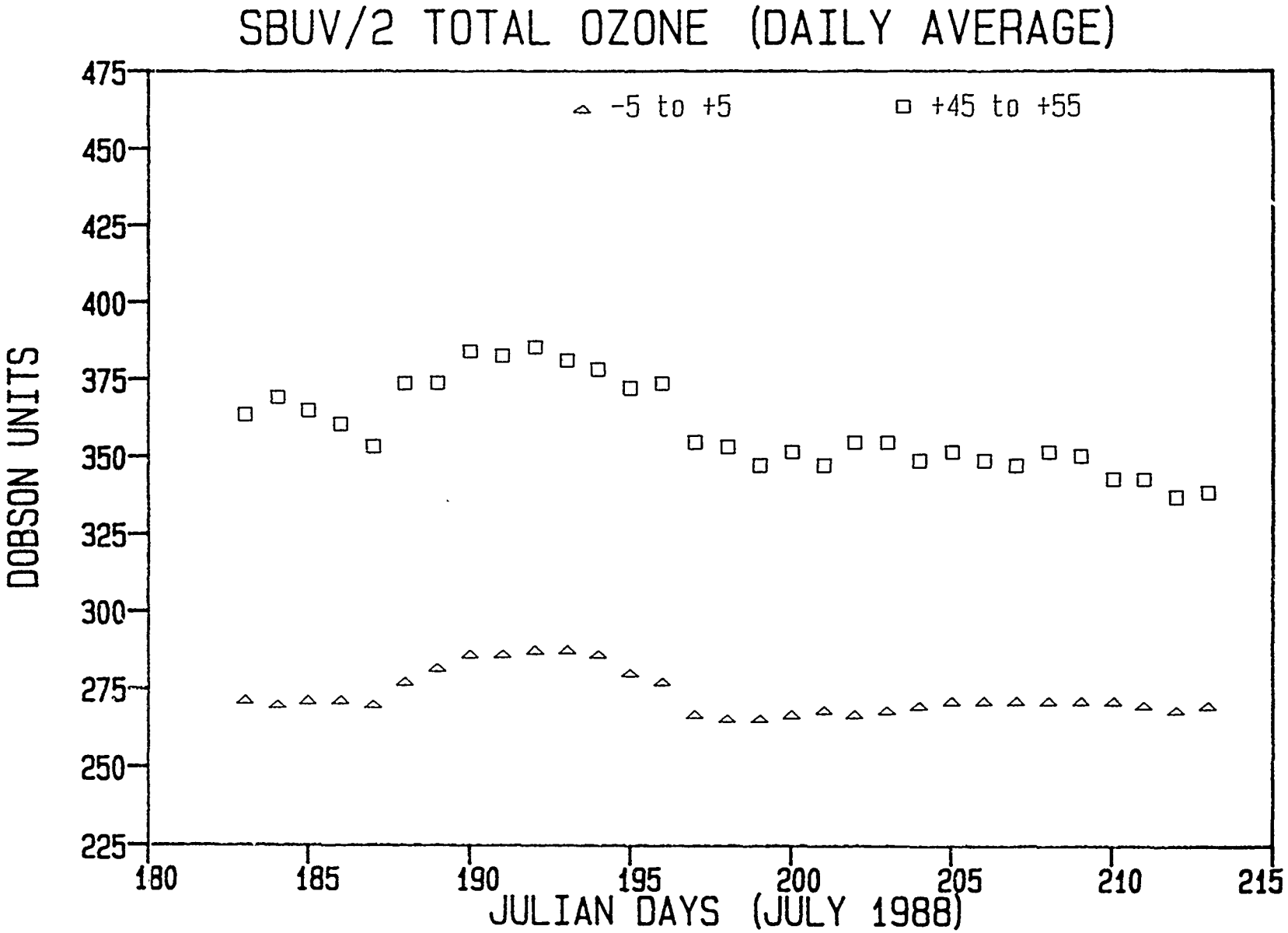

Fig. 7 The daily average of the total ozone for July 1988. Values are shown for 45N to 55N and 5S to 5N.

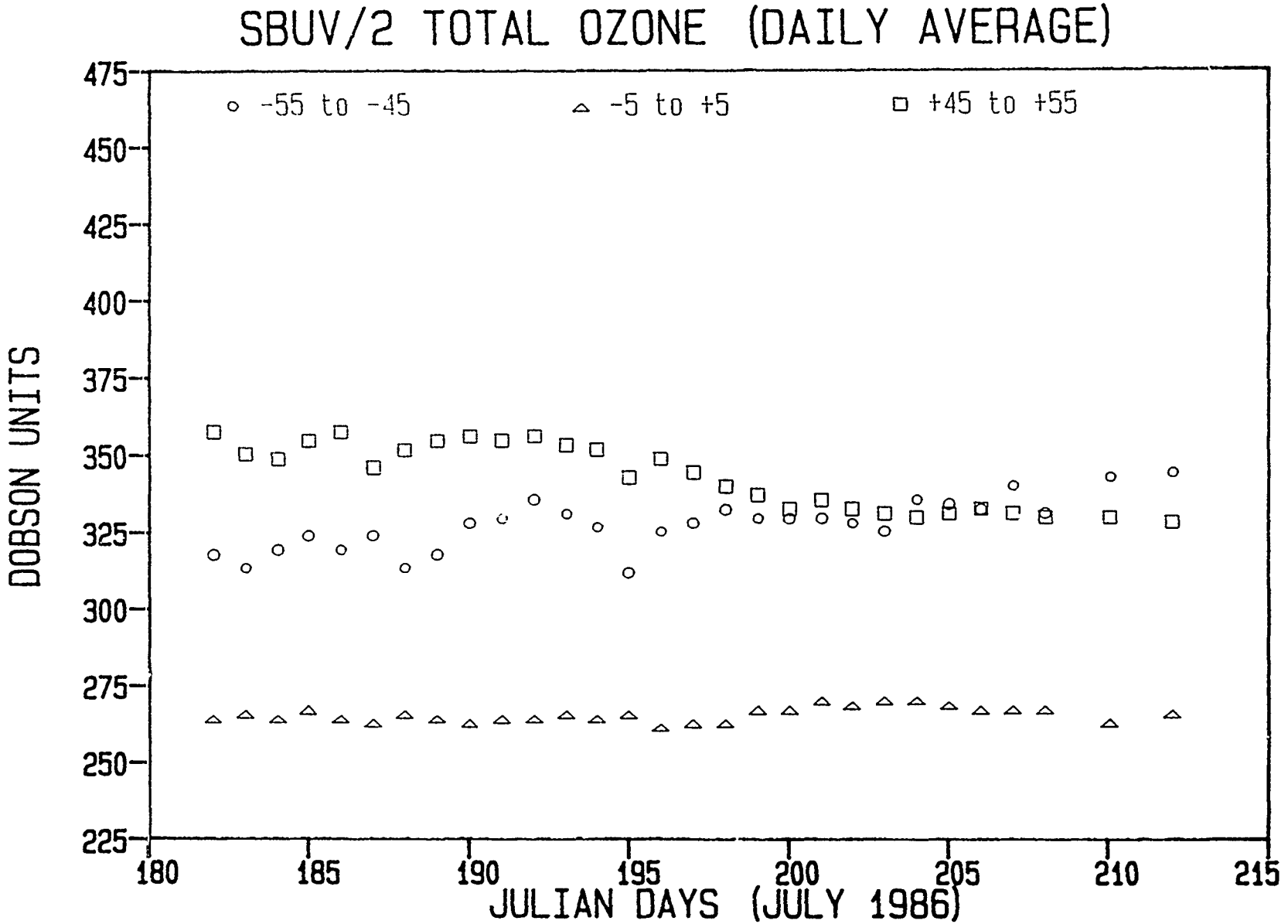

Fig. 8 As in Fig. 7 but for July 1986. Values for 45S to 55S are added.

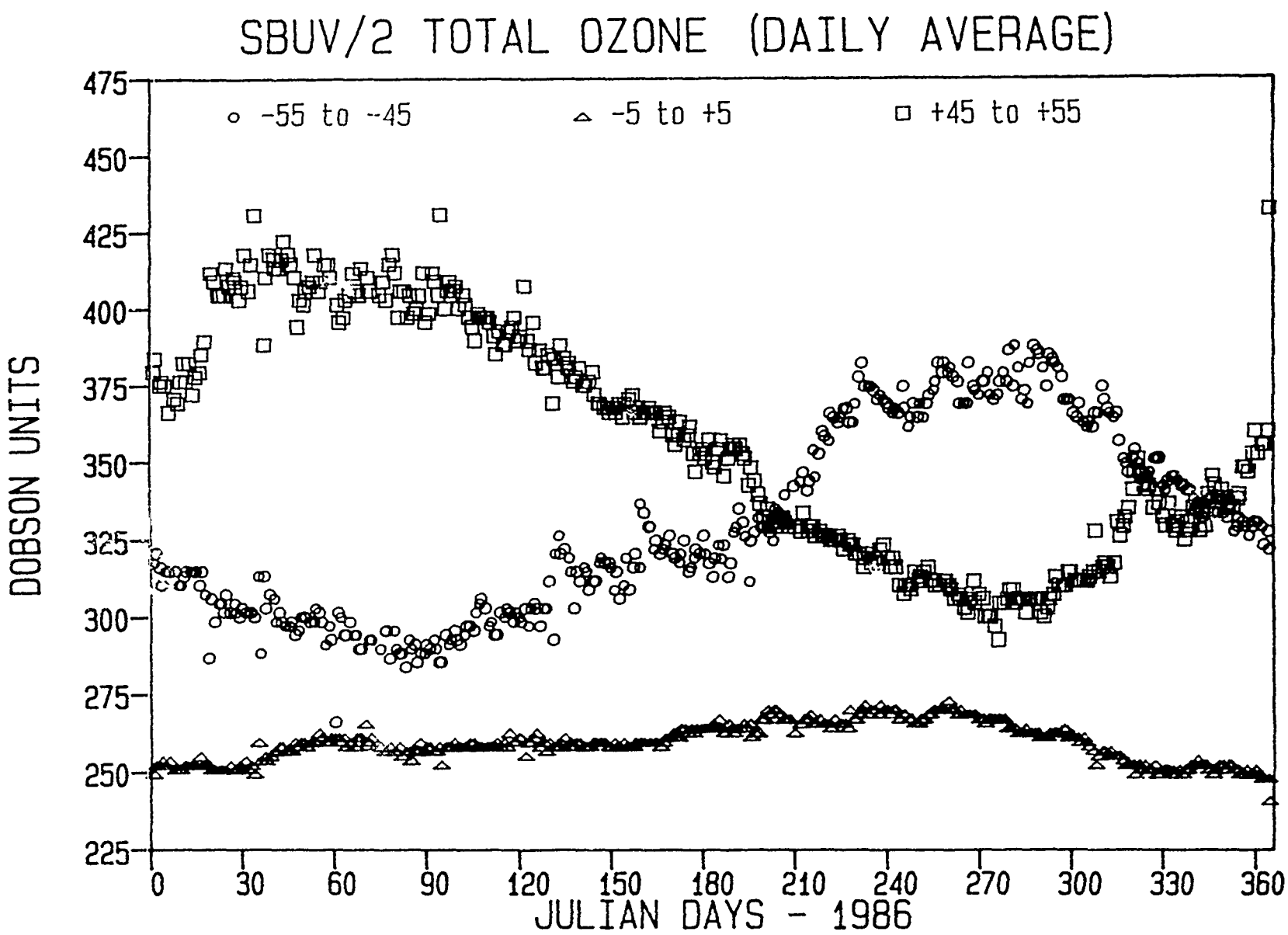

Fig. 9 As in Fig. 8 but for the year 1986.

Attachment 4

A Status Report on the Analysis of the NOAA-9 SBUV/2 Sweep Mode Solar Irradiance Data

R.P. Cebula, M.T. Deland, and B.M. Schlesinger
ST Systems Corporation
R.D. Hudson
NASA/GSFC

A STATUS REPORT ON THE ANALYSIS OF THE NOAA-9 SBUV/2 SWEEP MODE SOLAR IRRADIANCE DATA

R. P. Cebula, M. T. DeLand, and B. M. Schlesinger
ST Systems Corporation, Lanham, Maryland 20706

R. D. Hudson
NASA Goddard Space Flight Center, Greenbelt, Maryland 20771

INTRODUCTION

Monitoring of the near ultraviolet (UV) solar irradiance is important because the solar UV radiation is the primary energy source in the upper atmosphere. The solar irradiance at wavelengths shortward of roughly 300 nm heats the stratosphere via photodissociation of ozone in the Hartley bands. Shortward of 242 nm the solar UV flux photodissociates O_2, which is then available for ozone formation. Upper stratospheric ozone variations coincident with UV solar rotational modulation have been previously reported (Gille et al., 1984). Clearly, short and long-term solar irradiance observations are necessary to separate solar-forced ozone variations from anthropogenic changes.

The SBUV/2 instrument onboard the NOAA-9 spacecraft has made daily measurements of the solar spectral irradiance at approximately 0.15 nm intervals in the wavelength region 160-405 nm at 1 nm resolution since March 1985. These data are not needed to determine the terrestrial ozone overburden or altitude profile, and hence are not utilized in the NOAA Operational Ozone Product System (OOPS). Therefore, assisted by ST Systems Corporation, NASA has developed a scientific software system to process the solar sweep mode data from the NOAA-9 instrument. This software will also be used to process the sweep mode solar irradiance data from the NOAA-11 and later SBUV/2 instruments.

The purpose of this status report is to provide an overview of the software system and a brief discussion of analysis findings to date. Several outstanding concerns/problems will also be presented.

SOFTWARE OVERVIEW

The TIROS SBUV/2 sweep mode solar flux generation software system is based on the Nimbus-7 SBUV Continuous Scan and Solar Flux (CSSF) Products Generation Software (Schlesinger et al., 1988). The TIROS software itself was developed independently, with no adaptation of the Nimbus software. The SBUV/2 software system, shown schematically in Figure 1, consists of 1) a Stripping Program, "SUN1B", which extracts all data other than discrete earth view data (which comprises approximately 90% of the SBUV/2 data) from the monthly SBUV/2 1b data tapes and writes these data to monthly "disk 1b" datasets, where one dataset member is written for each day of the month, and 2) a Sweep Mode Program, "SUNSWP", which uses the "disk 1b" datasets and produces calibrated sweep mode solar irradiance disk datasets. We have also developed additional programs to extract, display, and analyze the solar products. In addition to scan-by-scan solar irradiance values, the Sweep Mode Program writes three separate temporal averages: orbital average, daily average, and Bartel's period (27-day solar rotation period) average; and 5 nm spectral averages (computed using the daily averaged data, with the $\pm$2.5 nm spectral averages reported every 2.5 nm) onto the disk datasets. Two of these datasets are written per calendar year, with one Bartel's period per dataset member. The orbital average is computed and reported only on those days for which solar measurements are made on more than one orbit. Under normal operation, where one solar measurement is made per day, the orbital average equals the daily average, and only the daily average is reported.

Results from the SBUV/2 instrument characterization effort are used as external input to the software (in fact there is much synergism because the sweep mode solar data constitutes a substantial portion of the data used to

characterize the SBUV/2 instrument's in-orbit change). Evolution of the instrument characterization has already and will continue to led to refinements in the Sweep Mode Program and reprocessing of the solar irradiance data. The software is therefore constructed of modules structured so as to minimize the impact of changes in the instrument characterization and facilitate future upgrades. SUN1B is constructed of 8 modules with a total of approximately 600 lines of source code, excluding comment lines. SUNSWP contains 39 modules with a total of over 3300 lines of source code, excluding comment lines. All software is developed in FORTRAN 77 and operates on the NASA/GSFC IBM 3081 under MVS.

STATUS

The Stripping and Sweep Mode Programs are fully developed, tested, and functional. Refinements to the latter software continue as more is learned about the NOAA-9 instrument. To date all solar flux (here and henceforth we use solar flux or solar irradiance to mean sweep mode solar irradiance) data from the commencement of the measurement on 12 March 1985 through 10 July 1988 have been processed.

Over the past five years much has been learned regarding the behavior of the NOAA-9 SBUV/2 instrument. Several important instrument characteristics, specifically the linearity correction, the wavelength dependence of the photomultiplier tube (PMT) gain, and the time dependence of the PMT gain, have been incorporated into the software. However, much remains to be learned. Corrections for time dependent changes in the instrument optics throughput and/or diffuser absolute reflectance and goniometric characteristic are not yet included. Additionally, the goniometric correction is based on the nominal, predictive orbit/attitude information available on the 1b tapes; no corrections for spacecraft departures from the predictive ephemeris, spacecraft departures from nominal attitude, or the small SBUV/2-to-spacecraft mounting angle misalignment are made. Finally, we have recently learned that there are periods during which the solar location data are based on the yaw axis gyrocompass output rather than on the spacecraft solar sensor (F. G. Cunningham, private communication). If a bias exists between the two types of solar location determinations, then there will be an impact on the derived NOAA-9 irradiances. We are presently investigating this potential problem.

MAJOR FINDINGS

The NOAA-9 SBUV/2 "day 1" solar irradiance is presented in Figure 2 as is the Nimbus-7 SBUV "day 1" solar spectra. In this rather insensitive semi-log presentation, agreement between the two instruments is quite good. However, upon closer inspection, significant differences are observed. The ratio of the NOAA-9 SBUV/2 to Nimbus-7 SBUV "day 1" irradiances is shown in Figure 3. The Nimbus data have been corrected for solar change occurring over the intervening period (roughly 6.5 years) using an empirical estimate based on the Mg II core-to-wing index (Heath and Schlesinger, 1986). The correction for solar variability is roughly 7% at 200 nm. The adopted solar variability correction is approximately 3% at 250 nm and decreases to less than 1% longward of 275 nm. The solar variability correction used here compares favorably with independent measurements of long-term solar change (Lean, 1987).

Four significant aspects of the comparison between the NOAA-9 SBUV/2 and Nimbus-7 SBUV "day 1" spectra are noted. These features are present in all comparisons made to date, including comparisons of data taken on the same day, and therefore indicate absolute calibration biases between the two instruments. First, the NOAA-9 solar flux is approximately 10% larger than the Nimbus-7 flux. Second, this bias is wavelength dependent, decreasing from 14% at 200 nm to 6% at 350 nm, then increasing again to about 13% at 400 nm. The significant wavelength-dependent bias between two instruments, particularly in the wavelength region used for ozone determination (250-340 nm) and longward, is rather surprising. Longward of approximately 250 nm quartz halogen lamps are used as the primary light source during the radiometric calibration. The National Institute for Standards and Technology, which provides the calibration of these lamps, estimates that the three sigma uncertainty of the lamp calibrations ranges from 2.2% at 250 nm to 1.4% at 350 nm (Walker, et al., 1987). Even with additional uncertainties entering into the measurement from other sources of error in the prelaunch radiometric calibrations, a 10% relative accuracy with a 10% wavelength dependence is outside the expected error range.

A third aspect of Figure 3 is the spectral feature centered on 232 nm. Both deuterium and argon arc lamps were used to calibrate SBUV/2 shortward of approximately 250 nm. Near 230 nm the instrument's radiometric response changes by approximately 15% over a rather narrow spectral region. Comparisons of the deuterium lamp-based and argon lamp-based radiometric sensitivity curves show a feature similar to the SBUV/2 to SBUV bias in this region. Hence, this feature is probably due to a small error in the NOAA-9 radiometric calibration. Preliminary intercomparisons of the solar data from the first Shuttle SBUV (SSBUV) mission (STS-34) with the NOAA-9 SBUV/2 and the Nimbus-7 SBUV data support the hypothesis that the spectral feature seen in Figure 3 at 232 nm arises from an error in the SBUV/2 calibration. Further work needs to be done in this area, however it is probable that the NOAA-9 SBUV/2 sweep mode irradiance radiometric calibration will need to be revised, at least in the region shortward of approximately 240 nm. This problem has no impact on the NOAA-9 ozone data.

A final aspect of Figure 3 is the increase in the noise level of the comparison in the region 270 to 290 nm. In this region, the SBUV/2 data are output in the lower portion of gain Range 3 and count rates as low as 59 counts (after removal of the electronic offset) are experienced. The standard deviation of the Range 3 electronic offset is approximately 4 counts, thus these data have a one sigma noise of approximately 7% due to the sample-to-sample variation in the offset. Unfortunately, this spectral region contains the Mg II doublet, which is very useful for monitoring short and long-term solar variability. As will be seen, the large noise in the SBUV/2 solar data in this region masks the short-term variability. It is for this reason that the instrument makes daily discrete mode measurements about the 280 nm Mg II doublet.

Figures 4 and 5 present a preliminary intercomparison of the NOAA-9 SBUV/2 solar irradiances with data from Dr. James Mentall's rocket-borne instrument. The relatively large noise level of the comparison shown in Figure 5 arises in part from uncertainty entering into the comparison during the interpolation from the wavelength scale of the rocket instrument to the wavelength scale of SBUV/2. This uncertainty is especially apparent at the Ca II h and k solar absorption lines at 396.8 and 393.3 nm. The two solar measurements agree to within approximately 10%, however there exists a 20% wavelength dependence in the 300 to 370 nm region. The shape of the SBUV/2-to-rocket bias is distinct from the shape of SBUV/2-to-SBUV bias, suggesting that wavelength dependent calibration errors exist in at least two of the three instruments. While the SBUV/2-to-rocket comparison shown in Figure 5 is too noisy to be used to accurately assess possible calibration errors over a narrow wavelength region, we note a slight change in the noise level of the comparison near 230 nm. The SBUV/2 irradiances are higher than both the SBUV and rocket irradiances.

As might be expected from the experience of previous BUV-type instruments, the radiometric sensitivity of the NOAA-9 SBUV/2 instrument has not remained constant. Figure 6 presents the ratio of NOAA-9 SBUV/2 solar irradiance outputs taken one, two, and three years after the start of the solar measurement (roughly 14 March 1986, 1987, and 1988, respectively) to the initial solar irradiance measurement. These data have not been corrected for solar irradiance changes, however March 1985 through March 1987 was a period of low solar activity. During late 1987 solar activity began to increase, and by mid-1988 the Mg II solar activity index had increased by roughly 3.5% relative to the index in 1986 (Donnelly, 1988). Using the NOAA-9 Mg II index and the Nimbus-7 scaling factors, we estimate true solar change over the first three years of the SBUV/2 operation to range from approximately 3-4% at 200 nm, to 1% or less at and longward of 265 nm. Thus, in the first approximation, the changes shown in Figure 6 can be attributed to instrument radiometric sensitivity drift. The instrument solar output is seen to have decreased by between approximately 1% at 400 nm to 5% at 200 nm over the first year of data. The output decrease during second year of operation roughly equaled that observed during the first year of operation, and at the end of two years, the output decreased by approximately 2% at 400 nm to nearly 10% at 200 nm relative to the initial output. As seen in Figure 6 and the time series plots that follow, the instrument sensitivity decrease apparently flattened out during the third year of operation. However, shortward of 250 nm some of this apparent decline in the instrument sensitivity degradation rate is due to an increase in the solar irradiance offsetting the instrument throughput decrease. Based on the Mg II index, shortward of about 250 nm the solar irradiance in mid-1988 was anywhere from approximately 1% to 4% higher than the irradiance in early 1987. After correction for an estimated 3-4% solar flux increase at 200 nm, we estimate roughly a 4-5% instrument sensitivity decrease at 200 nm during the third year of operation. It is interesting to note that longward of 240 nm the spectral shape of the sensitivity

change is similar to the shape of the SBUV/2-to-SBUV bias. We plan to investigate whether or not this is coincidental.

The time series of the SBUV/2 391.3 nm output is presented in Figure 7. The most striking aspect of this figure is the approximate 1.3% day-to-day fluctuation in the irradiance output. This same fluctuation is also clearly seen in the 202.2 nm time series presented in Figure 8. Laboratory tests on later flight units indicate that this fluctuation is likely due to a 0.25^{o} day-to-day variation in the NOAA-9 SBUV/2 solar diffuser deployment angle. At the approximate 70^{o} angle of incidence of the solar ray with respect to the diffuser normal at which the SBUV/2 instruments obtain solar measurements, a 0.25^{o} variation in the diffuser deployment angle translates into roughly a 1.2% error in the derived irradiance. The solar diffuser mechanisms on the NOAA-11 and later SBUV/2 instruments have been modified to correct this problem. Preliminary analysis confirms that the NOAA-11 SBUV/2 solar data is free of this error (H. Weiss, private communication).

The error caused by the day-to-day fluctuation in the diffuser deployment angle is wavelength independent in first order, hence ratios of solar irradiance time series such as that shown in Figure 9 are nearly free of this error. However, because the error in the derived irradiance is given by $\cos(\Theta + \Delta\Theta)/\cos(\Theta)$ where Θ is about 70^{o}, and because this angle increases with time as the spacecraft continues in its orbit, the error increases at the shorter wavelengths (in the sweep scan mode the SBUV/2 instruments scan from long to short wavelengths). Hence there exists a small wavelength dependence to the error. Since the exact time the solar measurement commences varies from day-to-day, there is also a variability in the exact magnitude of the induced error at given wavelength; this effect can be seen in both Figures 7 and 8. Proper correction for errors induced by the day-to-day fluctuation in the diffuser deployment angle is therefore not straightforward. We are continuing to evaluate this problem at present. Since a given scan of the discrete mode wavelengths is completed in 24 seconds, the discrete mode solar irradiance data are less susceptible to these second order effects, and the day-to-day fluctuation in the discrete mode irradiance should approximately cancel out when wavelength pairs are used for total ozone determination. The effect on the profile wavelengths needs further investigation.

A second aspect noted in Figure 7 is the much larger day-to-day variation in the instrument solar output prior to October 1985. This variation seems to occur only at wavelengths longward of approximately 300 nm. We are still investigating the cause of this fluctuation. A similar fluctuation is observed at all wavelengths in discrete mode solar data during the first few months in orbit.

During July and August of 1986 the solar irradiance measurement was made once per orbit (there are 13 or 14 orbits per day) rather than once per day as is done operationally. This period is visible in both Figures 7 and 8 as a period of reduced day-to-day fluctuation. The diffuser plate was stowed after each orbit's solar measurement in order to obtain the operational ozone data and to protect the diffuser plate from contaminants. The reduced noise results from the square root of N reduction achieved as the number of deployments was increased from 1/day to 14/day. Note too that the average daily irradiance during this period is biased with respect to the surrounding data. This is due to the fact that with multiple deployments within a single day, the diffuser will on some fraction of orbits deploy to the normal angle and on some orbits will deploy to the alternate angle.

Over the declining portion of solar cycle 21 the solar irradiance near 400 nm has been estimated to vary by on the order of 0.2% or less (Schlesinger et al., 1988), and during the solar minimum period 1985-1988 the 391.3 nm irradiance measured should be essentially constant. Assuming the solar output to have remained constant at 391.3 nm, we estimate that the NOAA-9 SBUV/2 sensitivity degraded by 1.4% at this wavelength over the first three years of operation.

Figure 9 presents the ratio of the time series at 202.2 nm to that at 391.3 nm. The near removal of the 1.3% day-to-day fluctuation in the instrument output is immediately apparent. Note however the day-to-day fluctuation in the time series ratio during the early part of the data record. Again, this error is manifest only in the longer wavelength data and is introduced into the ratio by the 391.3 nm data. With the removal of the day-to-day fluctuation (except for the mid 1985 problem), 27-day solar rotational modulation is easily observed at 202.2 nm. In 1988 the strength of the rotational modulation increased and the modulation changes from a predominant 27-day periodicity to a predominant 13-day periodicity. Figures 10 and 11, respectively, present the Nimbus-7 SBUV

and NOAA-9 SBUV/2 discrete mode Mg II core-to-wing indices. Note the excellent qualitative agreement amongst these three distinct measurements. Due to slightly different wavelengths and, when comparing SBUV with SBUV/2, slightly different bandpasses, the three Mg II indices (SBUV, SBUV/2 discrete mode, and SBUV/2 sweep mode) are not identical. We plan to perform quantitative comparisons of the strengths of the solar rotational variability as determined from the NOAA-9 SBUV/2 and Nimbus-7 SBUV instruments during the next few months. This comparison has yet to be done, therefore the estimates of solar activity used in this paper are rather rough because we are using the Mg II index from one instrument and the scaling factors from another instrument.

Also seen in Figure 9 is an approximate 8% decrease in the relative 202.2 nm to 391.3 nm output during the period from March 1985 through December 1987, then roughly a 2% increase between December 1987 and July 1988. Note too the change in slope corresponding to the every orbit solar measurement period in the summer of 1986. Long-term solar changes must be considered when using the 202.2 nm data to assess instrument sensitivity change. However, as seen in Figures 10 and 11, from March 1985 through February 1987 solar activity was low. Except for a 1-1.5% rotational modulation, we estimate that the 202.2 nm irradiance was constant to within 1% during this period. Therefore, the 8% decrease in relative instrument output during this period provides a good first order measurement of true instrument sensitivity change. Adding this change to an estimated 1% decrease in the 391.3 nm sensitivity, we estimate that the NOAA-9 SBUV/2 202.2 nm sensitivity decreased by between 8.5 and 9.5% from March 1985 through February 1987.

As shown in Figure 11, the Mg II core-to-wing index increased by approximately 4% from January 1987 through June 1988. The SBUV-based scaling index is nearly unity at 202.2 nm (Heath and Schlesinger, 1986). Thus, in the absence of a wavelength dependent instrument sensitivity change, we would expect to observe roughly a 4% increase in the ratio of the 202.2 nm to 391.3 nm SBUV/2 irradiances. A somewhat smaller increase, about 2%, is actually observed during the latter half of 1987 and the first half of 1988 because of ongoing wavelength dependent degradation. Using the slope of the 202.2nm/391.3nm output ratio determined from September 1986 through February 1987, and assuming this rate to have remained constant through July 1988, we estimate the relative uncorrected instrument drift for the period January 1987 through June 1988 to be about 2%. This simplified analysis suggests good consistency between the empirical model of the rotational and long-term solar change developed for SBUV on Nimbus-7 and the NOAA-9 SBUV/2 data, at least at 202.2 nm. Clearly, we have just begun the analysis in this area.

Figures 12 and 13 present the time series of the sweep mode solar irradiance data obtained near the discrete mode wavelengths 252 and 340 nm, respectively. The irradiances shown here are the average of the 13 individual irradiance values spanning the SBUV/2 slit width. In addition, we have manually reduced the irradiances obtained on days when the diffuser deployment angle was shifted by 0.25^{o} with respect to the nominal deployment angle downward by 1.3%. The most significant aspect of these two figures is the rapid decrease in the instrument solar output coincident with the frequent solar measurement period in mid-1986. These figures present the first clear evidence that the NOAA-9 SBUV/2 instrument, similar to the Nimbus-7 SBUV instrument, degrades as a result of solar exposure. As seen in Figure 9, the effects of the frequent solar measurement are less visible when the ratio of time series at two wavelengths is constructed. This suggests that the SBUV/2 solar degradation rate may not be strongly wavelength dependent. Figures 12 and 13 indicate that the sweep mode solar irradiance data can be very useful for assessing long-term instrument sensitivity change. This is particularly important for the NOAA-9 instrument because of the failure of the onboard calibration system shortly after launch (Frederick et al., 1986).

As previously discussed, due to the noise in the Range 3 low count data, the NOAA-9 SBUV/2 now makes daily discrete mode measurements about the 280 nm Mg II solar absorption line. Shown in Figure 14 is the NOAA-9 Mg II core-to-wing ratio determined from the sweep mode data (the wavelengths 279.79, 279.94, and 280.09 nm were used for the core and the wavelengths 276.54, 276.69, 283.19, and 283.34 nm were used for the wing). Compare this figure to the index determined using the discrete mode data, Figure 11. Except during the frequent measurement period in the summer of 1986, the high noise level of the sweep mode Mg II index masks out the 27-day rotational modulation. However, the long-term behavior of the sweep mode index, in particular the 4% increase observed between 1985 and mid-1988, agrees favorably with the discrete mode index. Therefore, the sweep mode index can be used to assess long-term, if not short term, variability. We are beginning to work with the sweep mode index to see if filtering and/or smoothing may be used to reduce the noise level and assess short term variability.

The preflight goniometric calibration of the NOAA-9 SBUV/2 covered the range of spacecraft centered solar elevation (0^{o} to 20^{o}) and spacecraft centered solar azimuth (30^{o} to 65^{o}) angles expected in orbit. However, as shown in Figure 15, the large drift in spacecraft local time from launch through the present (an ascending node of roughly 1:30 PM to roughly 5:30 PM local time) has resulted in a significant decrease in the spacecraft centered solar azimuth angle. This angle is now less than 30^{o}, and the prelaunch goniometric calibration data no longer spans the needed region. Quarterly tests of the goniometric calibration via position mode solar data have been advocated by STX personnel since the launch of the NOAA-9 spacecraft. Similar tests are now commencing, and analysis of the resulting data as well as the existing sweep mode solar data will be used to derive an extended goniometric calibration.

Commencing with the 16 September 1987 data we began to notice that on some days the sweep mode data acquired at the beginning of the solar measurement was orders of magnitude too low. It appears that once the spacecraft centered solar azimuth angle falls below approximately 40^{o} that data acquired at negative spacecraft centered solar elevation angles is partially or totally occulted. We have developed a simplified algorithm which uses the Cloud Cover Radiometer (CCR) data to identify and exclude the affected monochromator data. The algorithm successfully removed affected sweep mode data during the 1987-1988 shadowing period, which ended in March 1988 when the solar azimuth angle increased to greater than 40^{o}. Although the solar data for late 1988 and 1989 have not been processed yet, examination of the raw data from 1b tape dumps shows a much earlier start for the shadowing effect (approximately August 9), precisely when the azimuth angle again fell below 40^{o} (Figure 15). This effect can be distinguished from the solar array shadowing problem which affected the SBUV/2 solar data during late 1988. A preliminary look at the October 1989 raw data, when the solar azimuth angle was less than 15^{o}, shows additional problems which may invalidate the present correction algorithm. We will continue to investigate these problems.

ONGOING WORK

This status report is intended to provide an overview of the work that has been done to date to process and analyze the NOAA-9 SBUV/2 sweep mode solar irradiance data. This is a work in progress, and much remains to be done. Major lines of current investigation include:

Assessment of the ongoing 1.3% day-to-day fluctuation, with the hope of developing a reasonably straightforward correction. This correction may or may not be wavelength dependent.

Assessment of the day-to-day fluctuation observed only at the longer wavelengths during the first few months of solar observation. At present we do not have a good hypothesis as to the source of this problem.

Assess the impact, if any, of the periodic switch from solar location angles determined using the spacecraft solar sensor to angles determined using the yaw axis gyrocompass.

Quantitative evaluation of the scaling factors between the discrete mode Mg II core-to-wing ratio and rotational modulation at selected sweep mode wavelengths.

Intercomparison of the NOAA-9 and Nimbus-7 scaling factors.

Investigation of the sweep mode Mg II core-to-wing index, including attempts to filter and/or smooth the index to facilitate using the index to evaluate short-term rotational modulation. Quantitative intercomparisons of the SBUV/2 sweep mode Mg II index with the SBUV/2 discrete mode and SBUV indices.

Evaluation of long-term instrument sensitivity change including analysis of the effects of the every orbit solar measurement.

Extension of the goniometric calibration to a wider range of spacecraft centered solar azimuth angles.

Further assessment of the "shadowing" effects.

ACKNOWLEDGEMENTS

We would like to thank Dr. R. F. Donnelly of NOAA/ERL/ARL for supplying the NOAA-9 SBUV/2 Mg II data, Dr. D. F. Heath of ST Systems Corporation for supplying the Nimbus 7 SBUV Mg II data and scaling factors, and Dr. J. E. Mentall of NASA/GSFC for supplying the rocket irradiances. This research was done under contract at the NASA Goddard Space Flight Center, Greenbelt, Maryland.

REFERENCES

Donnelly, R. F., "The Solar UV Mg II Core-to-Wing Ratio from the NOAA9 Satellite During the Rise of Solar Cycle 22," Adv. Space Res., 8, (7)77, 1988.

Frederick, J. E., R. P. Cebula, and D. F. Heath, "Instrument Characterization for the Detection of Long-term Changes in Stratospheric Ozone: An Analysis of the SBUV/2 Radiometer," J. Atm. Oceanic Tech., 3, 472, 1986.

Gille, J. C., C. M. Smythe, and D. F. Heath, "Observed Ozone Response to Variations in Solar Ultraviolet Radiation," Science, 225, 315, 1984.

Heath, D. F., and B. M. Schlesinger, "The Mg 280-nm Doublet As A monitor of Changes in the Solar Ultraviolet Irradiance," J. Geophys. Res., 91, 8672, 1986.

Lean, J., "Solar Ultraviolet Irradiance Variations: A Review,", J. Geophys. Res., 92, 839, 1987.

Schlesinger, B. M., R. P. Cebula, D. F. Heath, and A. J. Fleig, Nimbus 7 Solar Backscatter Ultraviolet (SBUV) Spectral Scan Solar Irradiance and Earth Radiance Product User's Guide, NASA Reference Publication 1199, NASA Goddard Space Flight Center, Greenbelt, MD, February 1988.

Walker. J. H., R. D. Saunders, J. K. Jackson, and D. A McSparron, "Spectral Irradiance Calibrations", NBS Special Publication 250-20, National Bureau of Standards, Gaithersburg, MD, September 1987.

SBUV/2 SWEEP MODE SOLAR FLUX
PRODUCTION FLOW CHART

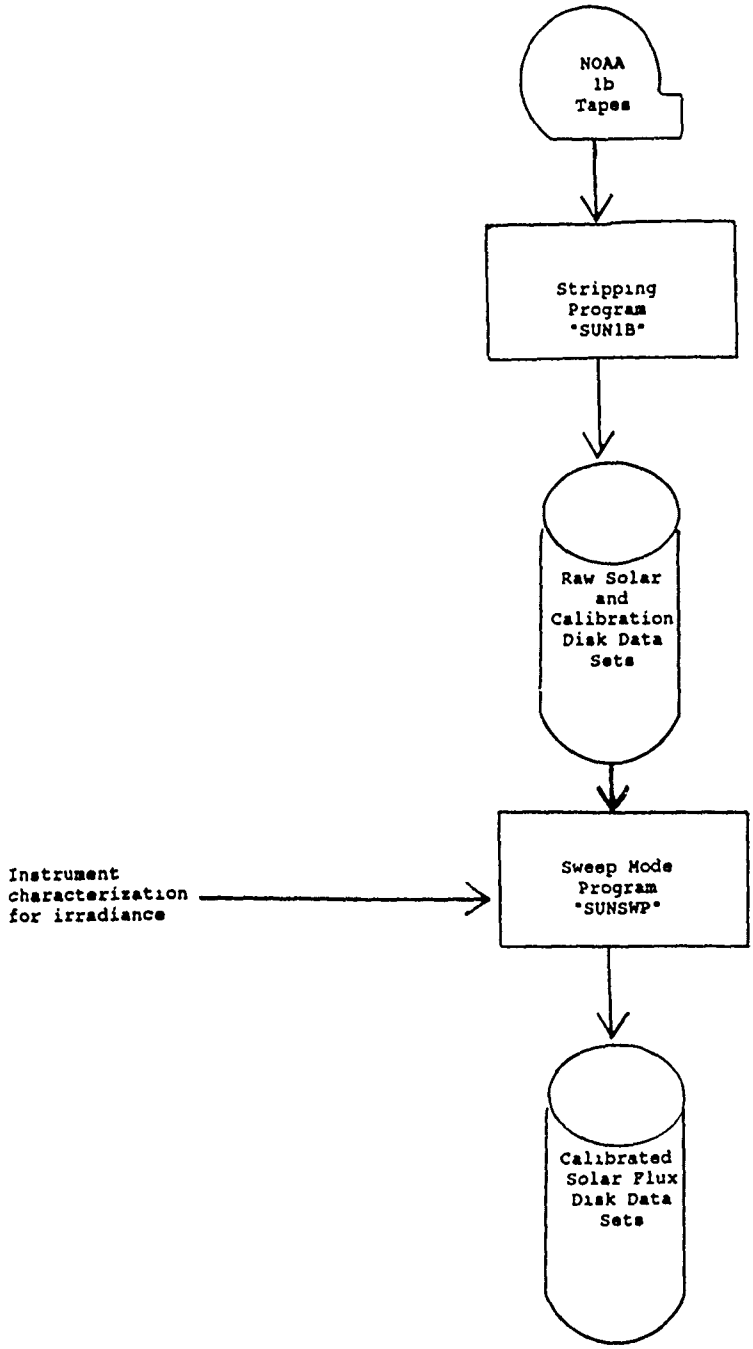

FIGURE 1

FIGURE 2

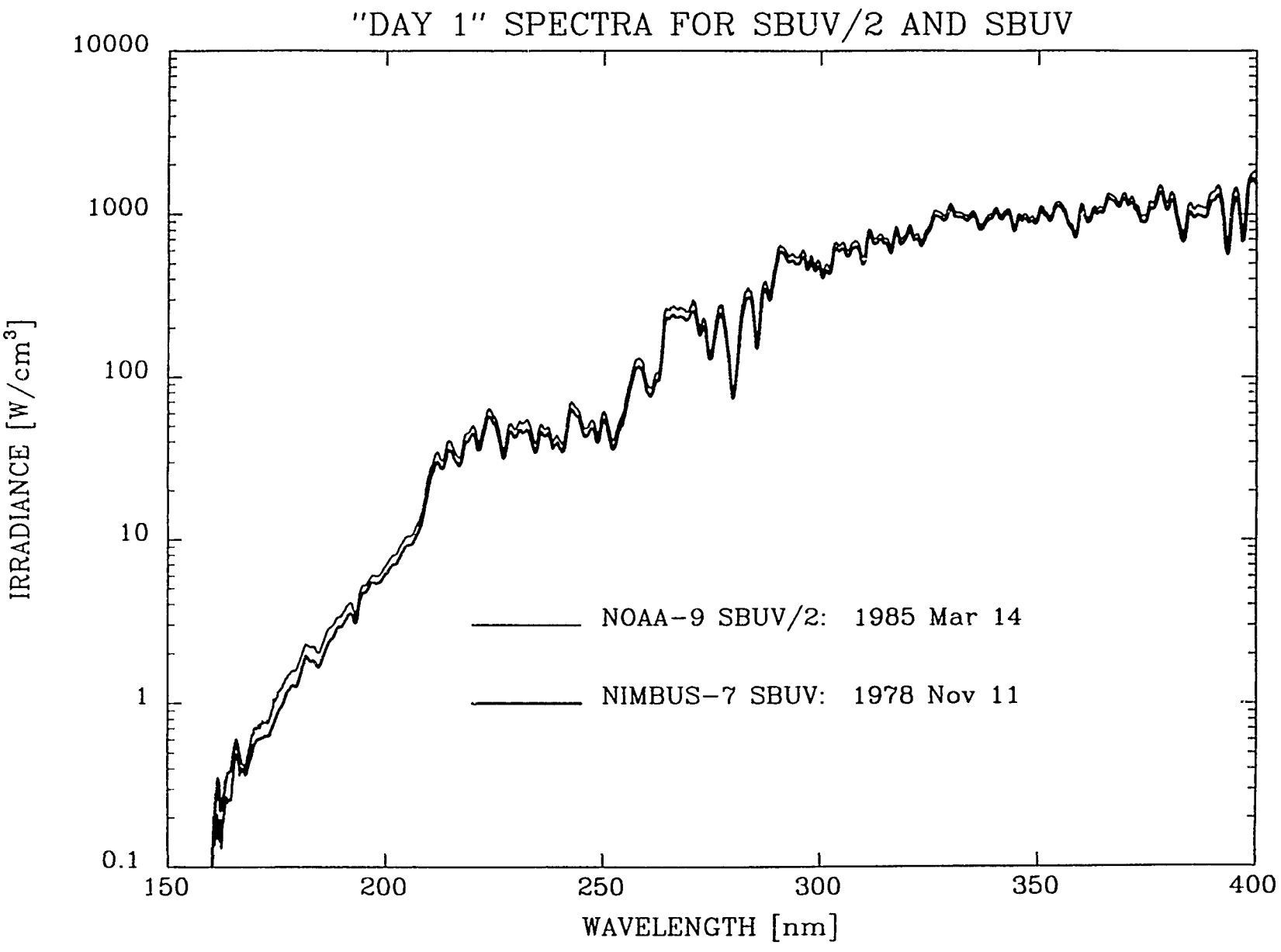
"DAY 1" SPECTRA FOR SBUV/2 AND SBUV
10000
1000
100
10
1
0.1
IRRADIANCE [W/cm^3]
150
200
250
300
350
400
WAVELENGTH [nm]
NOAA-9 SBUV/2: 1985 Mar 14
NIMBUS-7 SBUV: 1978 Nov 11

FIGURE 3

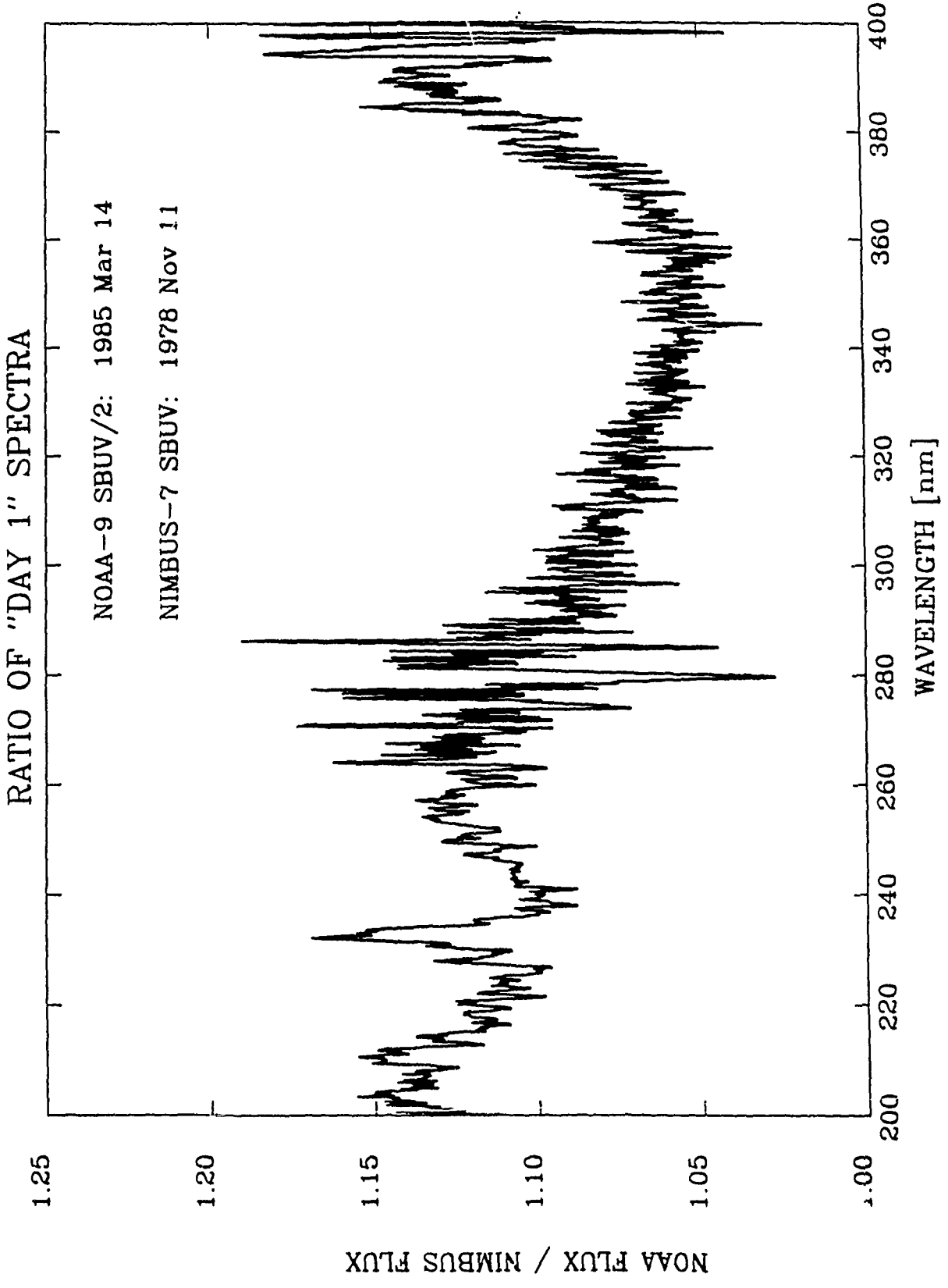
RATIO OF "DAY 1" SPECTRA
NOAA-9 SBUV/2: 1985 Mar 14
NIMBUS-7 SBUV: 1978 Nov 11
NOAA FLUX / NIMBUS FLUX
WAVELENGTH [nm]
1.25
1.20
1.15
1.10
1.05
1.00
200
220
240
260
280
300
320
340
360
380
400

FIGURE 4

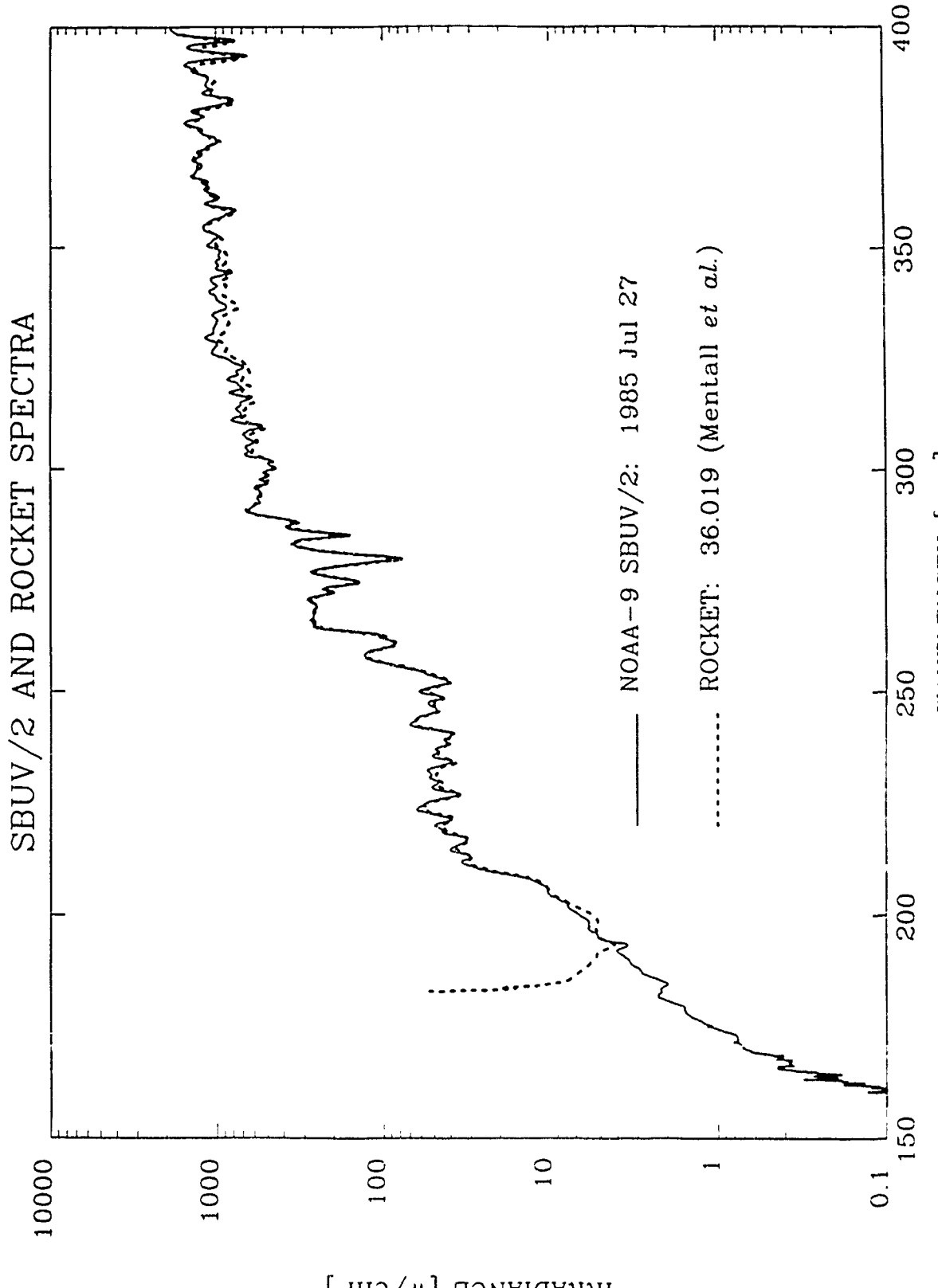
SBUV/2 AND ROCKET SPECTRA
NOAA-9 SBUV/2: 1985 Jul 27
ROCKET: 36.019 (Mentall et al.)
IRRADIANCE [W/cm³]
WAVELENGTH [nm]
10000
1000
100
10
1
0.1
150
200
250
300
350
400

FIGURE 5

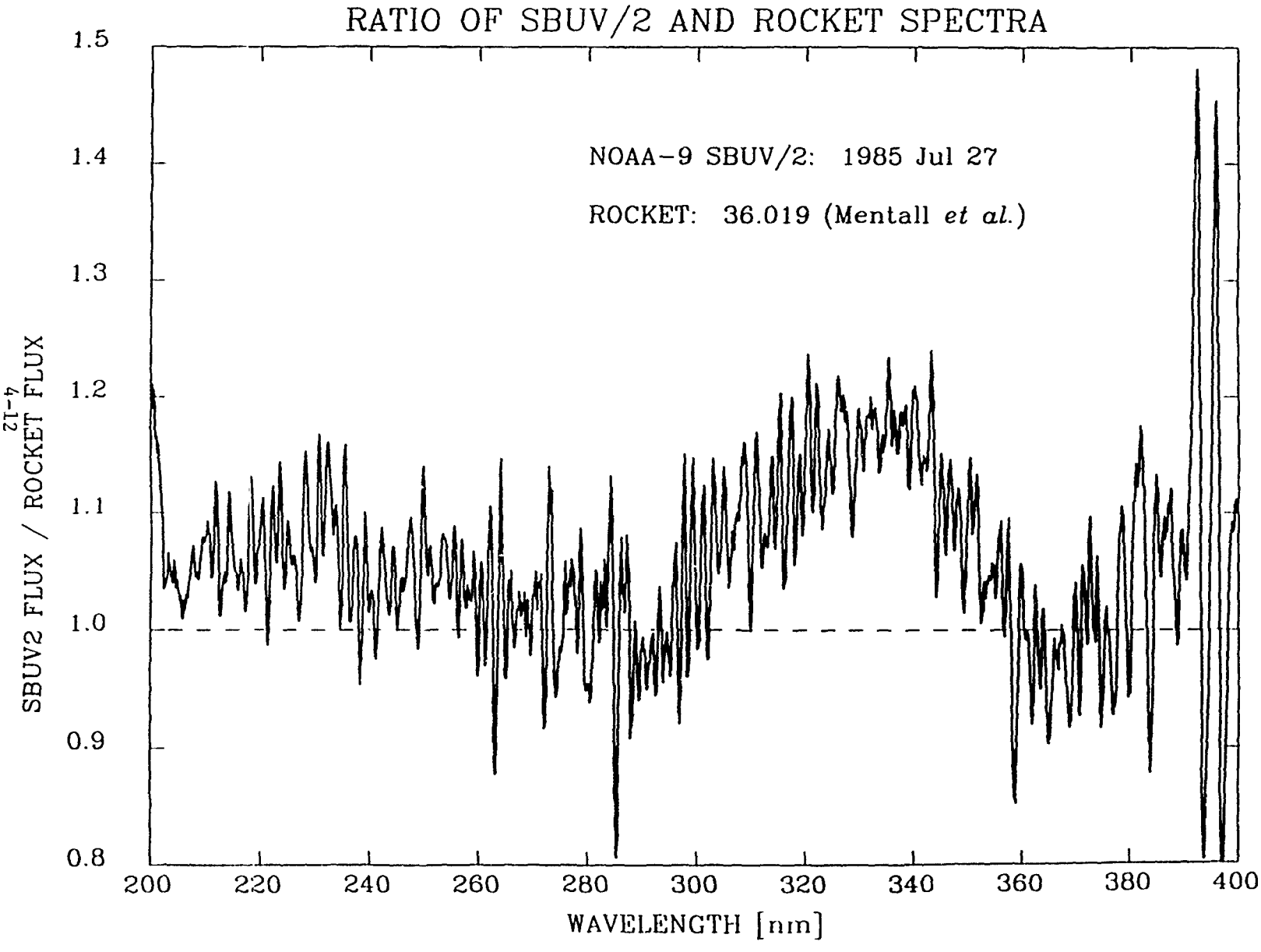
RATIO OF SBUV/2 AND ROCKET SPECTRA
NOAA-9 SBUV/2: 1985 Jul 27
ROCKET: 36.019 (Mentall et al.)
SBUV2 FLUX / ROCKET FLUX
4-12
1.5
1.4
1.3
1.2
1.1
1.0
0.9
0.8
200
220
240
260
280
300
320
340
360
380
400
WAVELENGTH [nm]

FIGURE 6

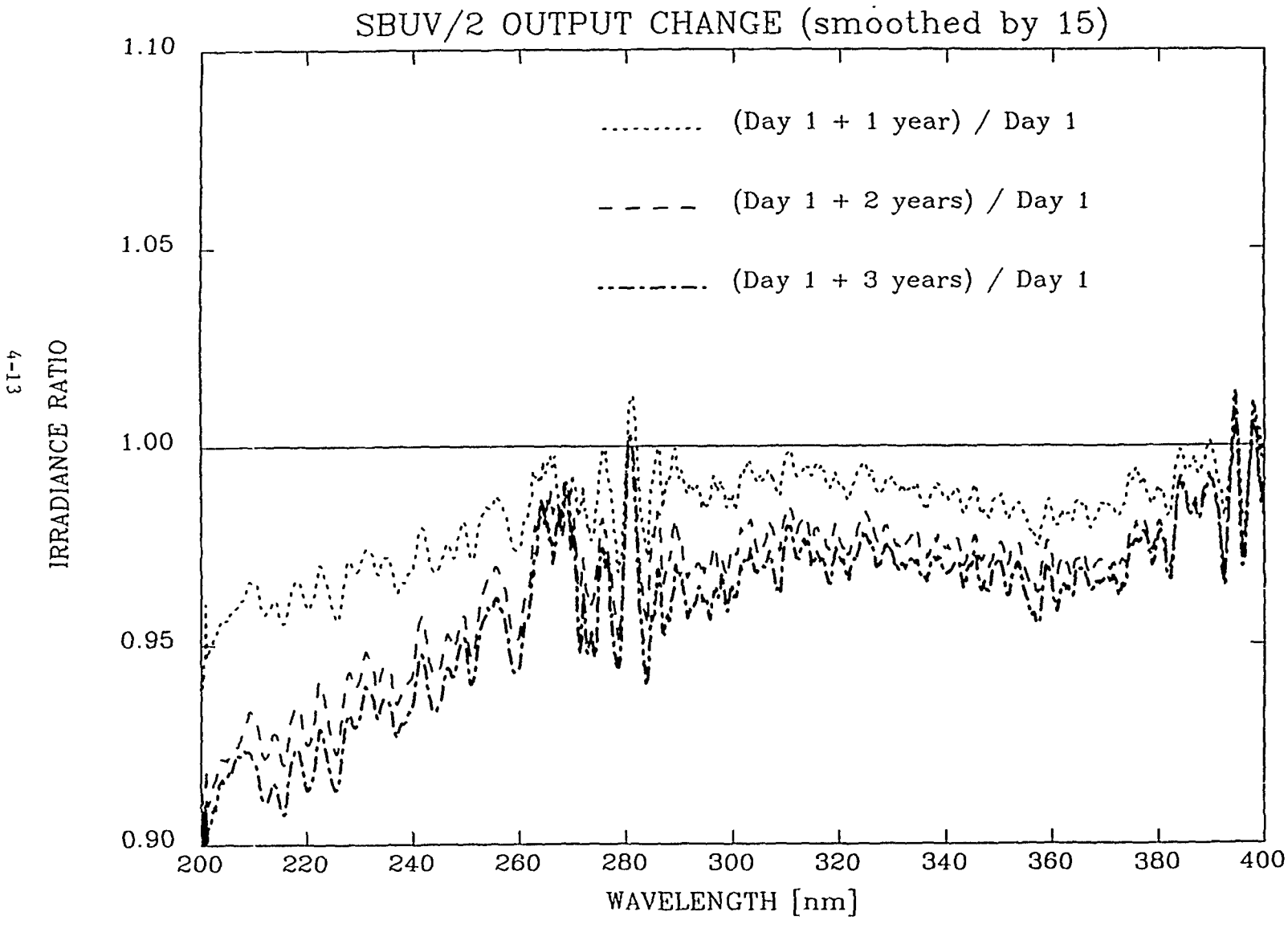
SBUV/2 OUTPUT CHANGE (smoothed by 15)
(Day 1 + 1 year) / Day 1
(Day 1 + 2 years) / Day 1
(Day 1 + 3 years) / Day 1
IRRADIANCE RATIO
1.10
1.05
1.00
0.95
0.90
200
220
240
260
280
300
320
340
360
380
400
WAVELENGTH [nm]

FIGURE 7

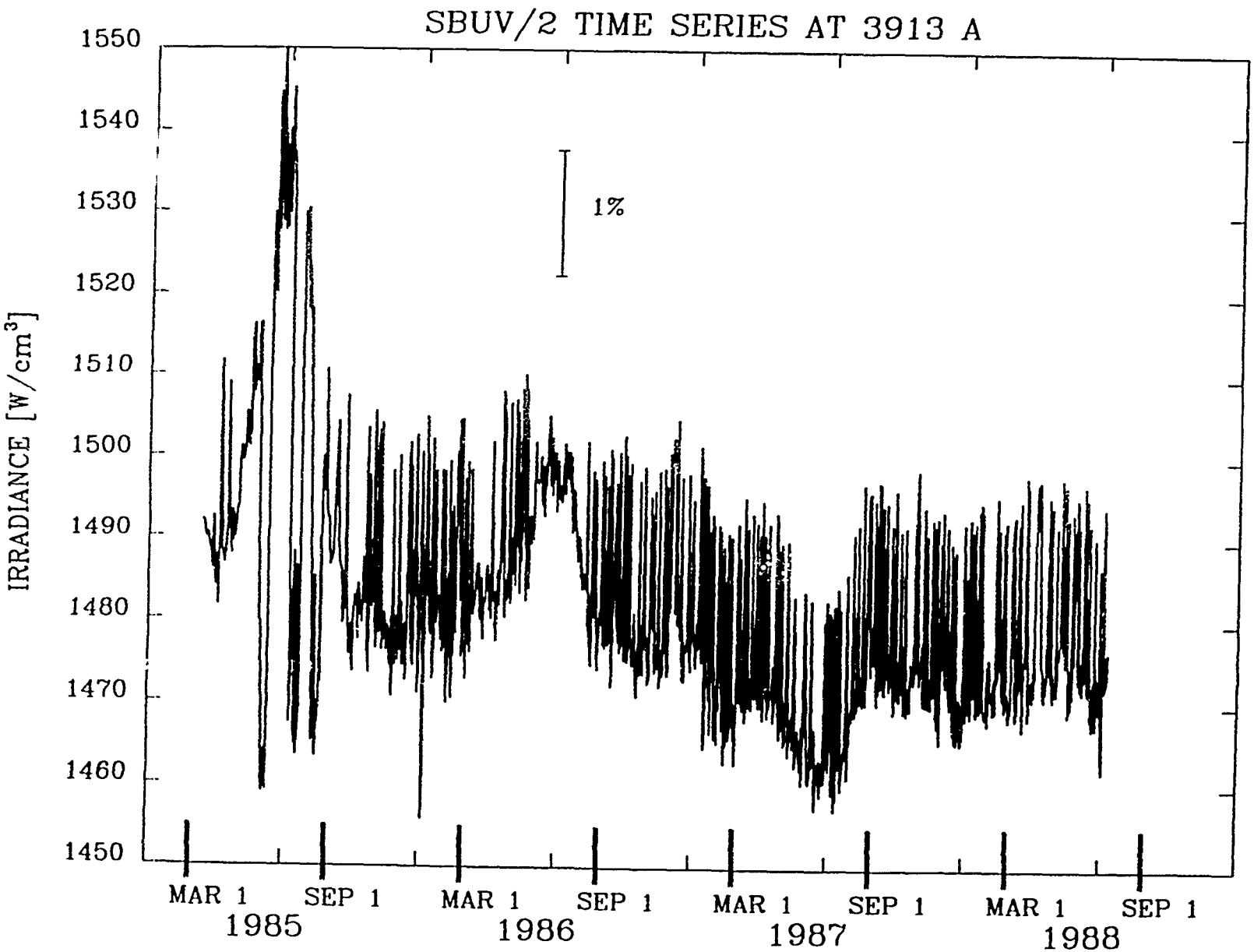
SBUV/2 TIME SERIES AT 3913 A
IRRADIANCE [W/cm³]
1550
1540
1530
1520
1510
1500
1490
1480
1470
1460
1450
1%
MAR 1
SEP 1
MAR 1
SEP 1
MAR 1
SEP 1
MAR 1
SEP 1
1985
1986
1987
1988

FIGURE 8

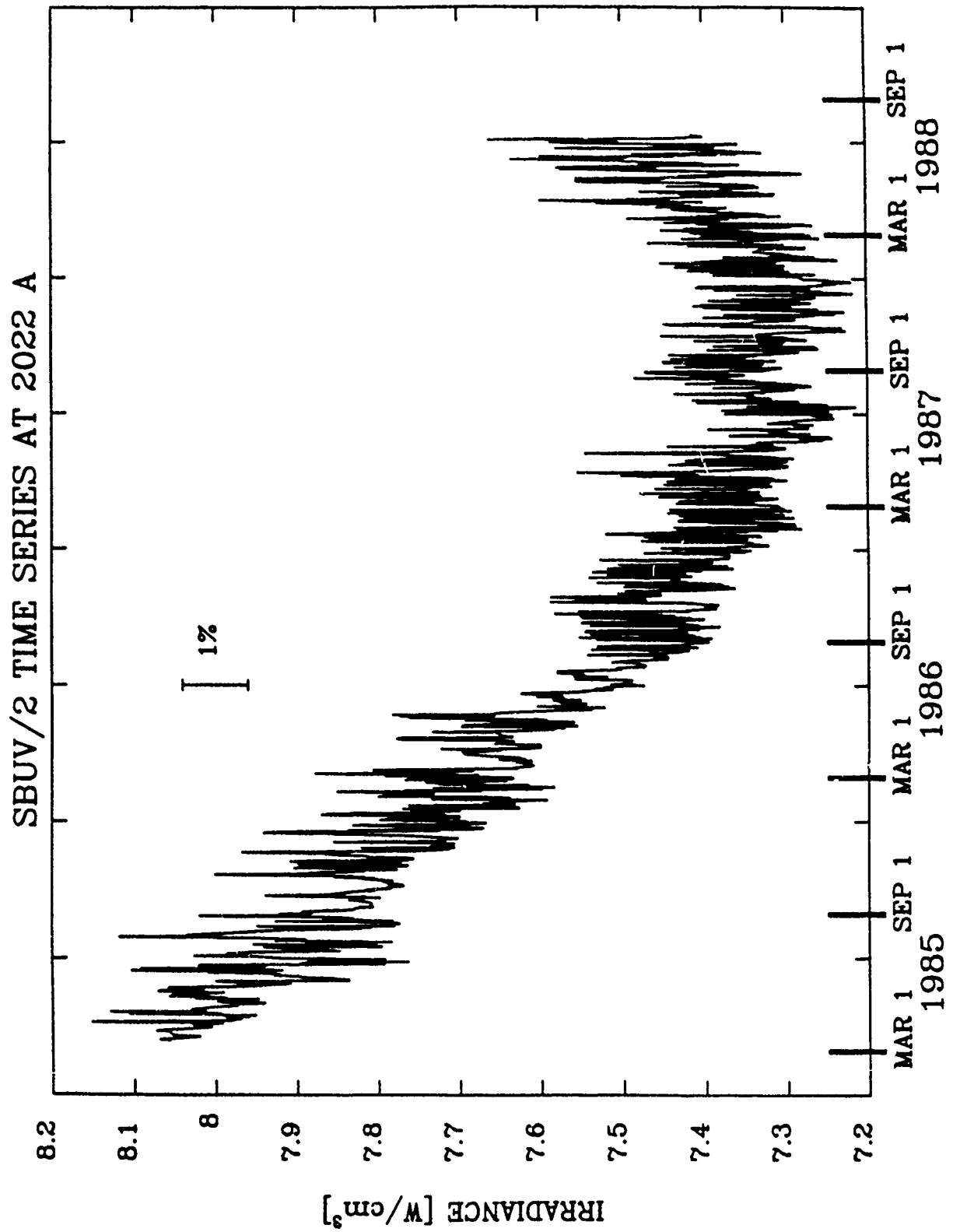
SBUV/2 TIME SERIES AT 2022 A
1%
IRRADIANCE [W/cm²]
8.2
8.1
8
7.9
7.8
7.7
7.6
7.5
7.4
7.3
7.2
MAR 1
1985
SEP 1
MAR 1
1986
SEP 1
MAR 1
1987
SEP 1
MAR 1
1988
SEP 1

FIGURE 9

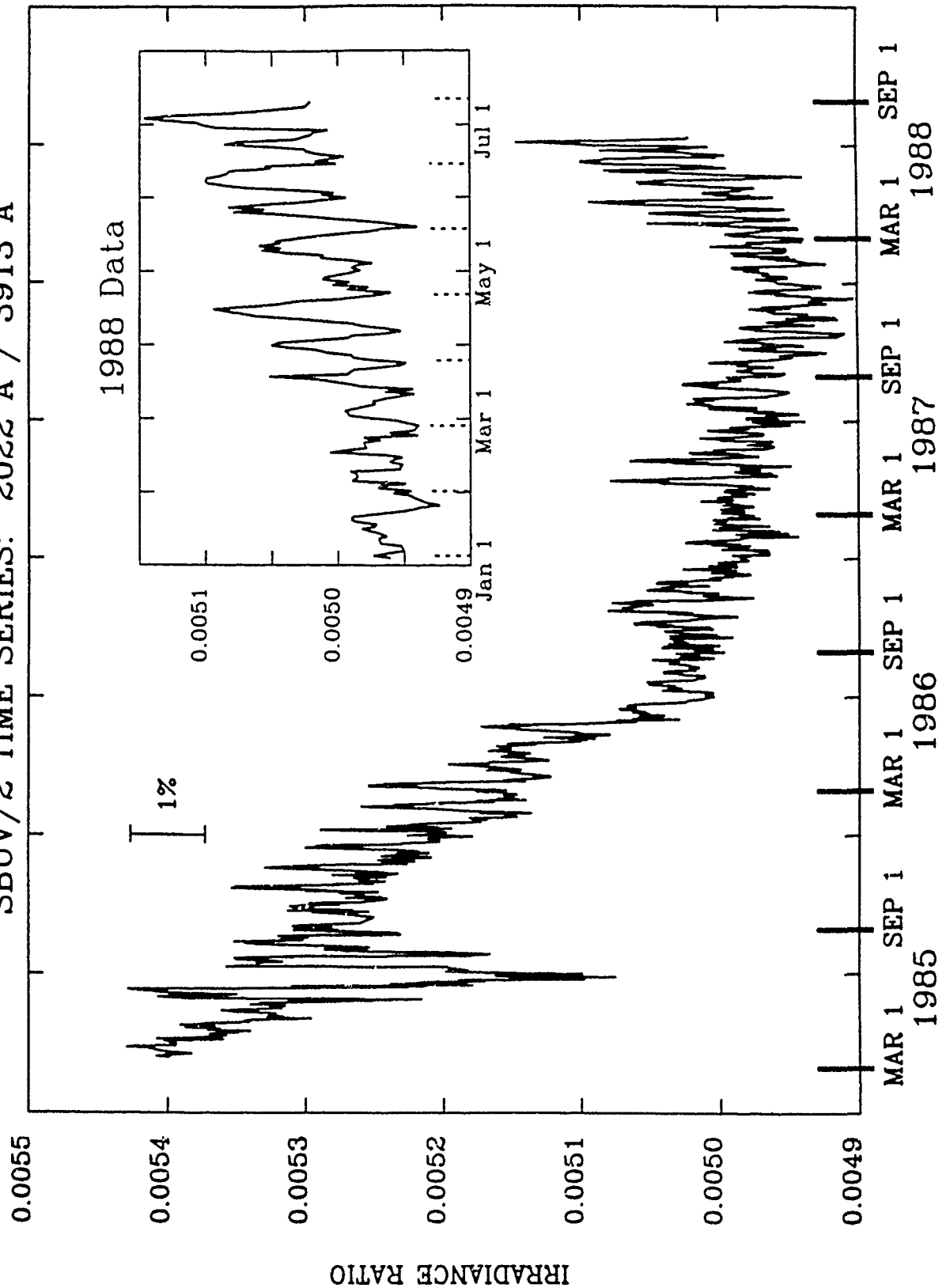
SBUV/2 TIME SERIES: 2022 A / 3913 A
IRRADIANCE RATIO
0.0055
0.0054
0.0053
0.0052
0.0051
0.0050
0.0049
1%
MAR 1 1985
SEP 1
MAR 1 1986
SEP 1
MAR 1 1987
SEP 1
MAR 1 1988
SEP 1
1988 Data
0.0051
0.0050
0.0049
Jan 1
Mar 1
May 1
Jul 1

FIGURE 10

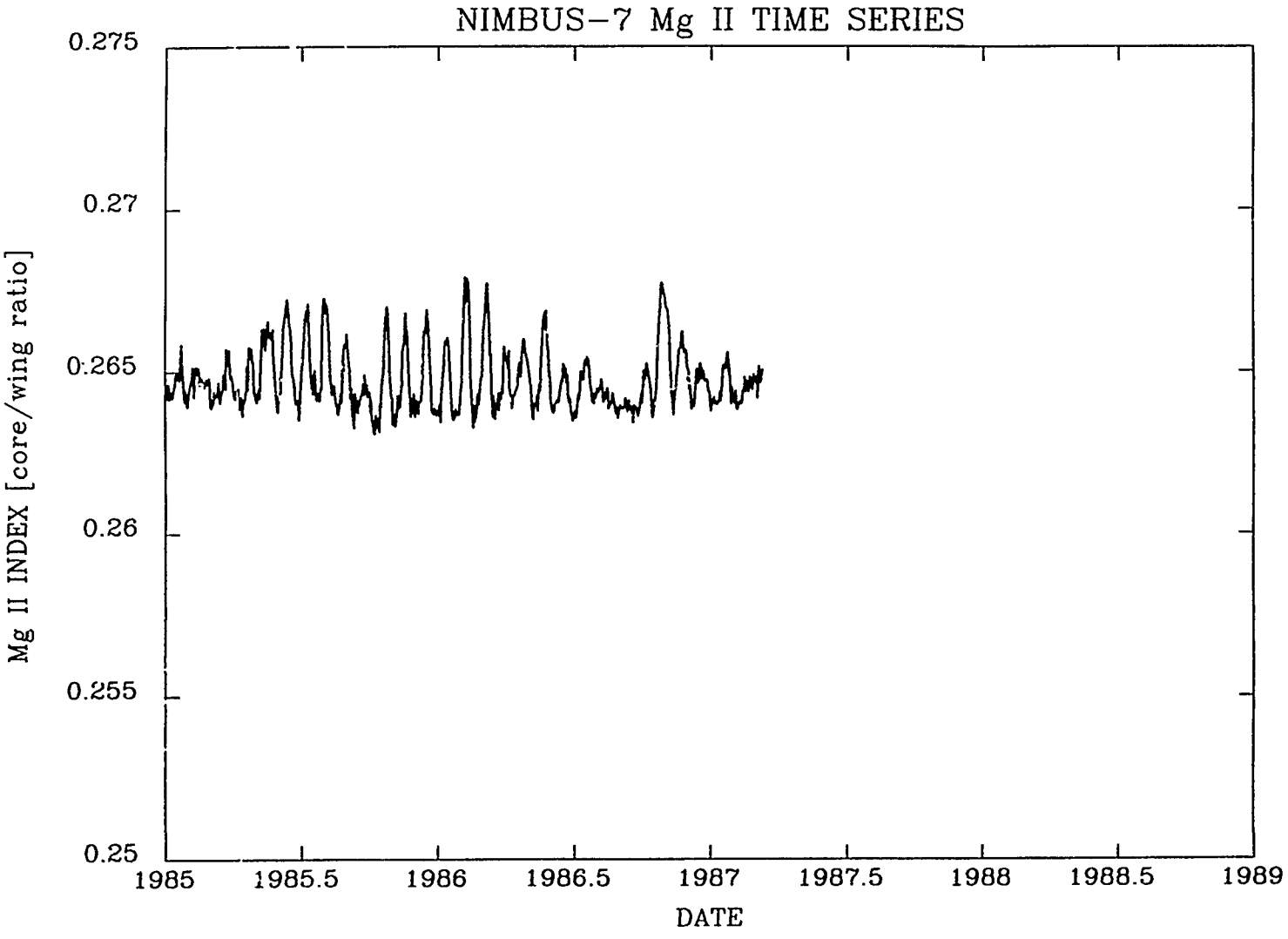
NIMBUS–7 Mg II TIME SERIES
0.275
0.27
0.265
0.26
0.255
0.25
Mg II INDEX [core/wing ratio]
1985
1985.5
1986
1986.5
1987
1987.5
1988
1988.5
1989
DATE

FIGURE 11

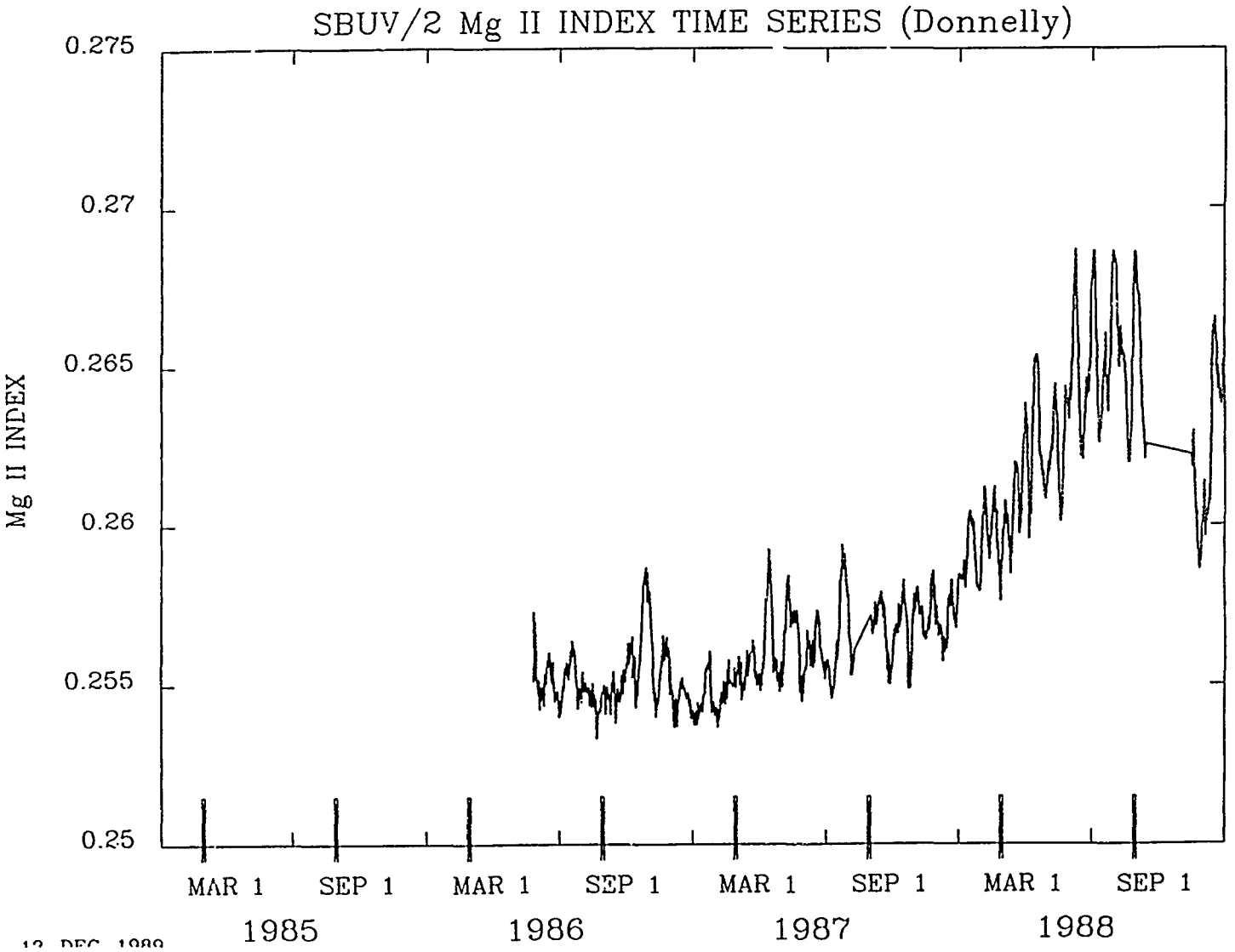
SBUV/2 Mg II INDEX TIME SERIES (Donnelly)
0.275
0.27
0.265
0.26
0.255
0.25
Mg II INDEX
MAR 1
SEP 1
MAR 1
SEP 1
MAR 1
SEP 1
MAR 1
SEP 1
1985
1986
1987
1988

FIGURE 12

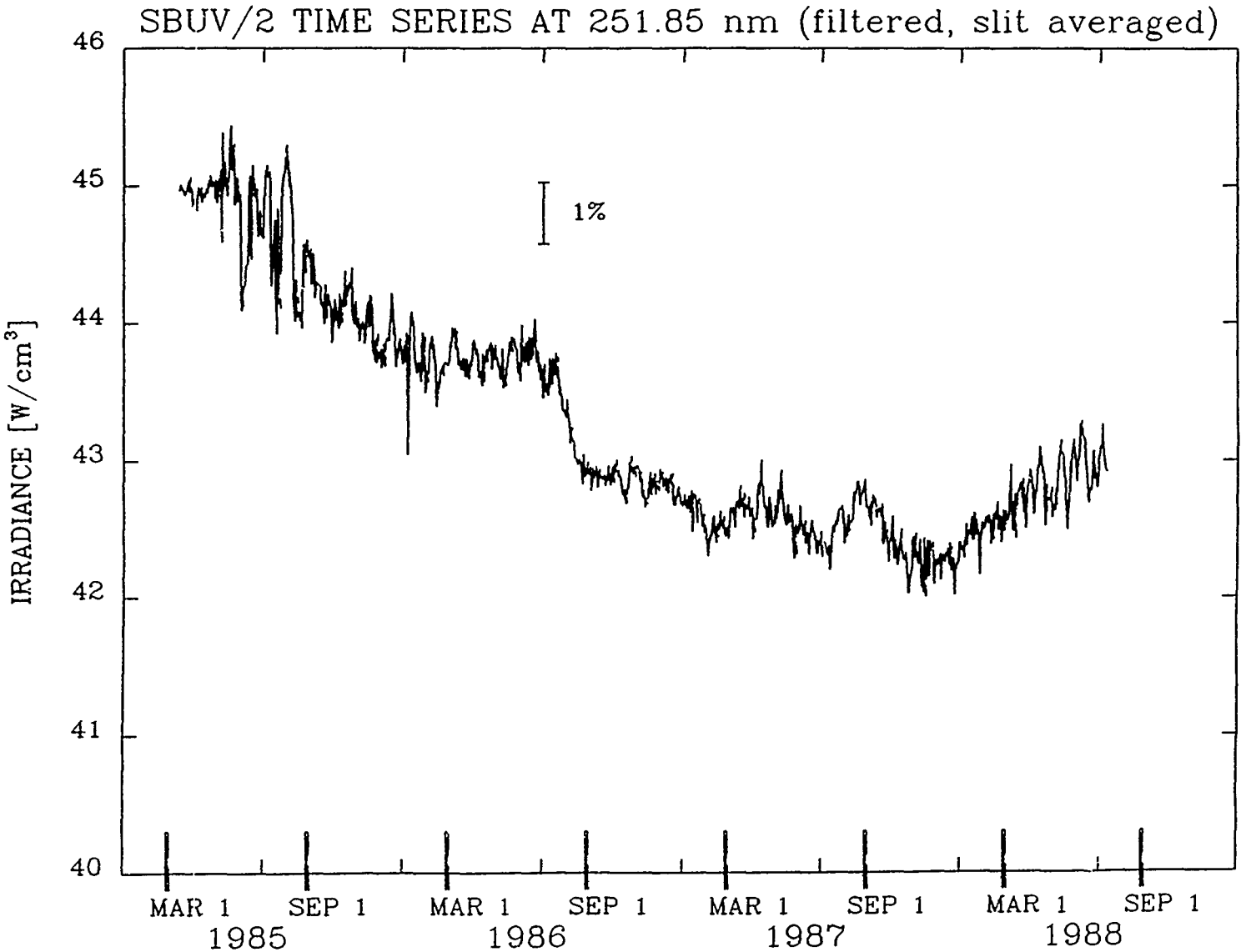

23 - JAN - 1990

FIGURE 13

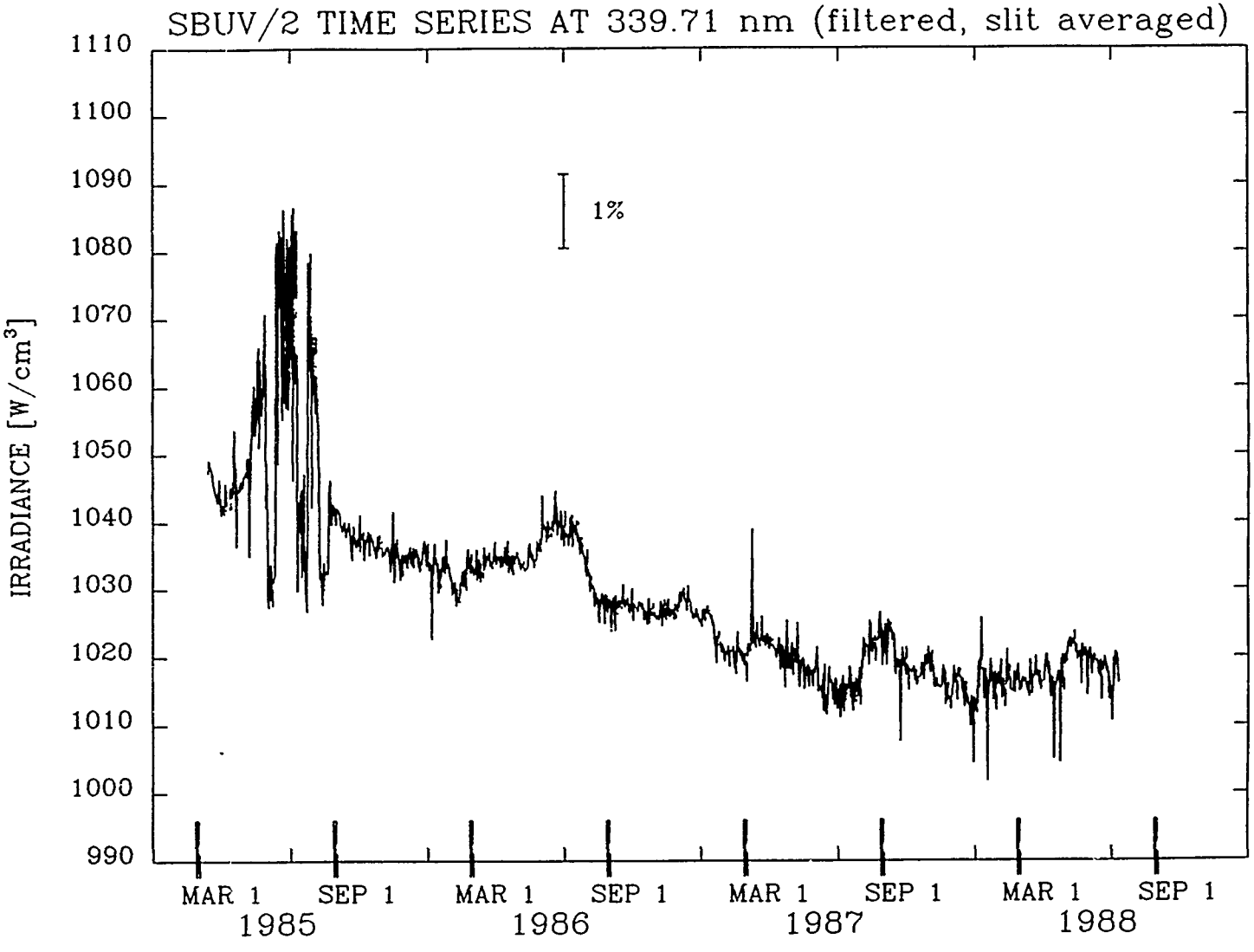

23-AUG 1990

FIGURE 14

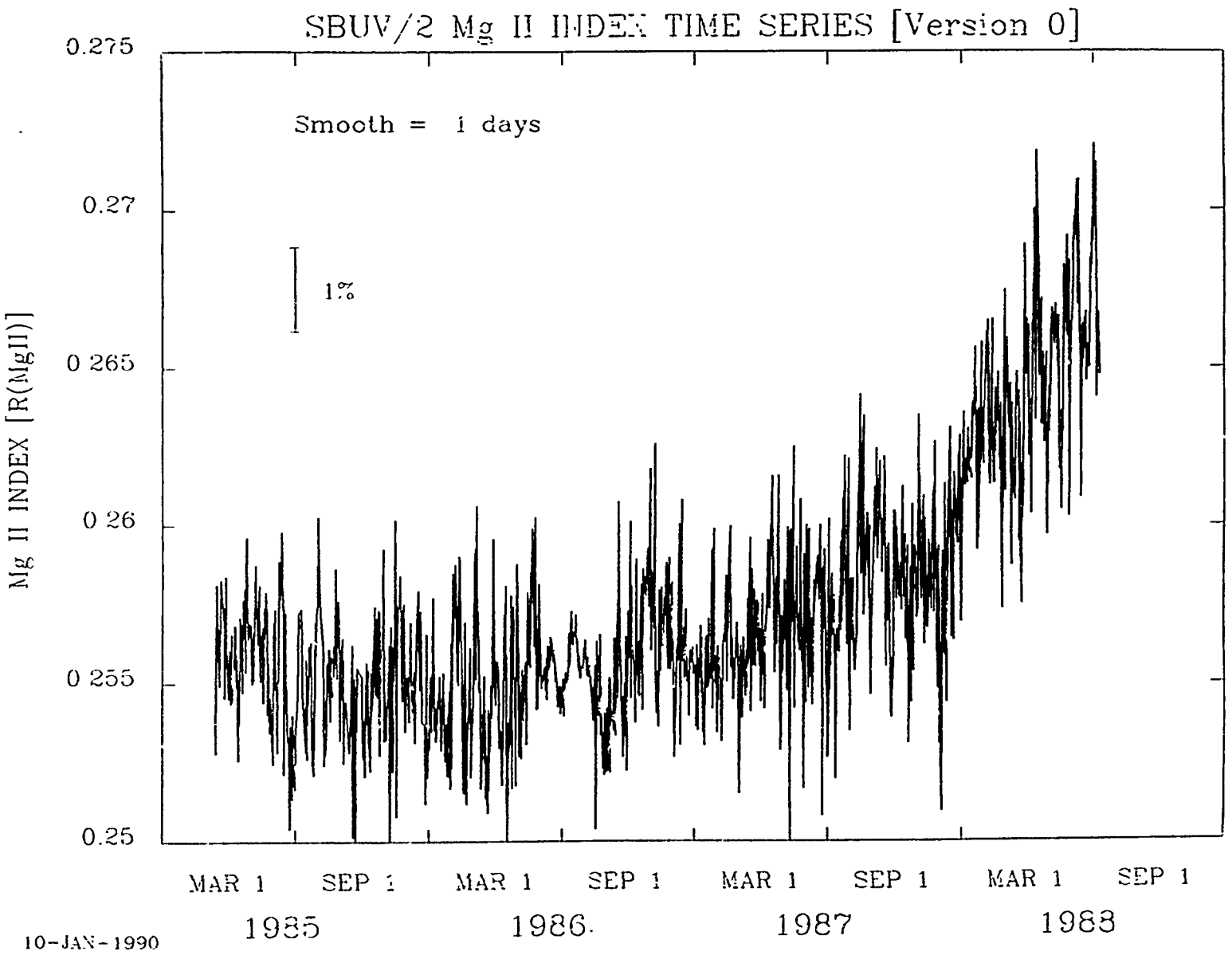
SBUV/2 Mg II INDEX TIME SERIES [Version 0]
Smooth = 1 days
1%
Mg II INDEX [R(MgII)]
0.275
0.27
0 265
0 26
0 255
0.25
MAR 1
SEP 1
MAR 1
SEP 1
MAR 1
SEP 1
MAR 1
SEP 1
1985
1986
1987
1988
10-JAN-1990

FIGURE 15

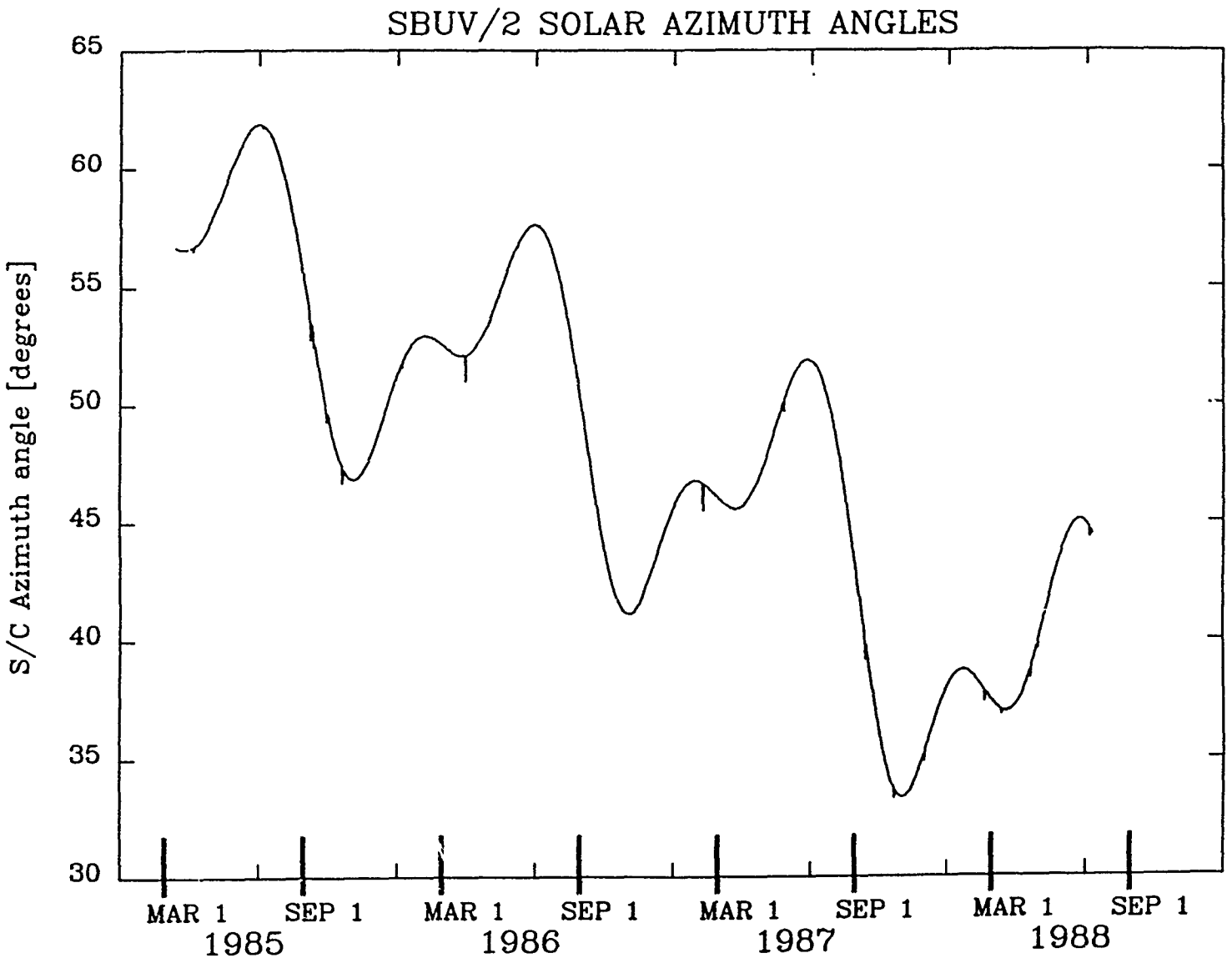
SBUV/2 SOLAR AZIMUTH ANGLES
S/C Azimuth angle [degrees]
65
60
55
50
45
40
35
30
MAR 1
SEP 1
MAR 1
SEP 1
MAR 1
SEP 1
MAR 1
SEP 1
1985
1986
1987
1988
4-JAN-1990

Attachment 5
NOAA-9 SBUV/2 Ozone Sounding Accuracy
H. Weiss
S.T. Systems Corporation

STX
ST SYSTEMS CORPORATION
4400 FORBES BLVD., LANHAM, MARYLAND 20706-9008 • (301) 794-5000 • TELEX 317630

1 February 1990

NOAA-9 SBUV/2 Ozone Sounding Accuracy: Presentation Summary

By Howard Weiss presented on 29 January 1990
at the NOAA World Weather Building

Three and a half years of radiance measurements by the NOAA-9 SBUV/2 at the wavelengths used for total ozone monitoring were analyzed and presented. It was found that the variability in the radiances is dominated by scene related events. The noise to signal was about 4% and decreased in the latter part of the period investigated. Instrumental effects accounted for about 0.5% in noise to signal and was fairly constant during this period. There was a fundamental change in the annual signature of the signal possibly due to a solar zenith angle effect.

1577 Spring Hill Road
Suite 500
Vienna, VA 22180
(703) 827-6600

9701 J. Philadelphia Way
Lanham, MD 20706
(301) 306-1100

28 Research Drive
Hampton, VA 23666
(804) 865-0214

109 Massachusetts Ave.
Lexington, MA 02173
(617) 862-0405

1900 Garden Road
Suite 130
Monterey, CA 93940
(408) 373-7292

NOAA-9 SBUV/2 Ozone Sounding Accuracy

Howard Weiss STX

I. Objective

NOAA-9 SBUV/2 ozone measurements are routinely compared to similar measurements, both ground-based and satellite-based. Each measurement system has inaccuracies associated with it based on many factors. These factors include sampling problems (time and space), inherent instrumental limitations (noise and sensitivity), time-dependent limitations (instrumental component variability), and scene variability (cloud cover). The purpose of this report is to summarize an evaluation and estimate of the sources and magnitude of the uncertainties inherent in the NOAA-9 SBUV/2 ozone products. Special emphasis will be placed on the SBUV/2 measurements without reference to other independent measurements.

II. Approach

The SBUV/2 total ozone measurements are computed using a duel wavelength pair method. In particular, a quality call the N-value, is computed to reduce the dynamic range of the ozone measurements:

$$(1)\quad N_\lambda \equiv -100 * \log(I/F)_\lambda$$

Here I is the measured backscattered radiance off the earth's atmosphere and F is the solar irradiance as measured by the SBUV/2. Two wavelength pairs N-values, the A-pair and B-pair, are used to reduce absolute uncertainties in the SBUV/2 calibration:

$$(2)\quad N_l \equiv N_{\lambda 1} - N_{\lambda 2} \qquad l = (\text{----A----}, \text{----B----})$$

$$= (3125/3312,\ 3175/3398) \text{ in Å}$$

The SBUV/2 instrument was designed to measure both the backscattered earth radiance and the solar irradiance. The solar irradiance measurement was made by deploying a diffuser plate in the instrument's field of view to reflect the solar radiation. Unfortunately, the reflecting properties of the diffuser plate changed dramatically with time. Since the degradation of the diffuser efficiency adds a complication, the determination of the uncertainties in the N_l calculations were separated into a earth intensity, N_{Il}, and solar flux, N_{Fl}, part:

$$(3) \quad N_l = N_{Il} - N_{Fl} \qquad N_{Il} = -100 \log(I_{\lambda 1}/I_{\lambda 2})_l$$

$$N_{Fl} = -100 \log(F_{\lambda 1}/F_{\lambda 2})_l$$

As in (2), l= (A,B) is the pair designation. N_{Il} does not have diffuser effects but does have scene effects (clouds, ozone). N_{Fl} does have diffuser effects (goniometry, reflectivity degradation) but does not have scene effects. They both have instrumental effects. Since the diffuser degradation has been investigated in detail elsewhere, this study will concentrate on the analysis of N_{Il}.

III. Method

Time series and spectral analysis techniques were employed to establish a base or 'noise' level period for the quantities defined in (1) - (3). This baseline period separates the long term atmospheric tends (ie ozone variations) from the short term changes associated with instrument performance or scene character changes (non-ozone related) and was used in constructing simple running statistics (averages, standard deviations). The data was restricted to the tropical equatorial region (5°N to 5°S latitude) to minimize scene variability effects and high solar zenith angles. Daily averages of the N_l were constructed from the Product Master File (PMF) data

tapes and the daily averages of I_λ and N_{Il} were calculated directly form the 1b data tapes.

IV. Analysis

The span of data analyzed was from 14 March 1985 to 31 August 1988; over 1200 days. Gaps in the data (no data or low coverage) were filled using a cubic spline interpolation scheme. This amounted to about 3% of the data coverage and no longer than one day of interpolation. Figure 1 is a plot of $N_{3125Å}$ along with a correction for the solar zenith angle (S_{za}; see figure 2). This correction reduces to the solar flux measurements (F) to overhead (S_{za}=0) incidence (F_0):

$$(4)\quad F_0 = F \,/\, \mathrm{Cos}(\, S_{za}\,)$$

Some of the long term trends are removed by this first order correction. Figure 3 show all four wavelengths corrected using equation (4). The long term variation on the order of a year can be seen at the shorter wavelengths and a fundamental change in the yearly trend is clearly evident in the third year of operation at the ozone-sensitive wavelengths (N_{3125} and N_{3175}).

In an attempt to eliminate any effects due to the diffuser's deterioration, direct radiance measurements were constructed from the 1b data tapes. Figure 4 shows plots of the equatorial radiances for the four wavelengths uncorrected for S_{za}. Besides the yearly trends due to S_{za} variations, the change in the yearly trend in year 3 (as seen in figure 4) is evident in all radiance measurements. Power spectra of these radiances (figures 5 and 6) reveal peaks periods of 180, 90, and 45 days consistent with either the ozone or S_{za} variations. There is a wavelength dependence on the power levels with $P_{3398Å} \approx P_{3312Å} > P_{3175Å} > P_{3125Å}$ although all spectra follow each other in form.

The spectra level off for periods less than 10 days. This 10 day period is the baseline for which variations in the radiances are fairly stationary and 10 day moving statistics were calculated for the radiances. The plots in figure 7 show these 10 day statistics for I_{3125} and I_{3312}. The standard deviation (σ) show a wavelength dependence as seen in the power spectra with $\sigma_{3312} > \sigma_{3125}$. Also, the σ's decrease with time although the decrease is only a few percent. The noise to signal ratio ($\sigma/\langle I \rangle$) shows a decrease with time of a few percent but for the most part remains constant over the 3½ year period.

The significant differences between the σ's at the longer wavelengths to the shorter wavelengths can be explained as a difference in the contribution function with altitude at these wavelengths (figure 8) or as a reflection of the differences in signal magnitudes. In the former situation, the longer wavelengths are more affected by short term scene variations (such as cloud cover) since they sample lower into the atmosphere. The shorter wavelengths are not as affected by the lower atmospheric turbulence and remain steady for periods less than 10 days. The variations apparent decrease with time and subsequent change in year 3 maybe associated with the NOAA-9 orbit precession to a local time with a more stable atmosphere at these wavelengths.

N_{IA} and N_{IB} were constructed from the I_λ using equation (3) (see figure 9). The first two years show a similar trend but the third year displays a fundamentally different pattern increasing the N_{Il} value till its offset by the fourth year by about 10%. This is similar N_l behavior indicating the third year change is not associated with the diffuser changes.Also the power spectra (figure 10) do show a similar peaks at 180, 90 and 45 day periods but are more level at periods > 30 days. The 10 day statistics (figure 11) reveal the A-pair variability lower than the B-pair. This is due to the higher σ in the B-pair wavelengths especially at 3398 Å.

V. Summary

After looking at the variation in I_λ and N_{Il} over the 3½ years worth of NOAA-9 SBUV/2 total ozone measurements, the major contribution to any uncertainty in the derived ozone can be associated with scene variability at the longer wavelengths. The instrument noise to signal performance remains steady throughout this period. This is evident in figure 12 which is the 10 day statistics for I_{2922} which is well above any lower atmospheric influences (see figure 8). The radiance does not show any year three effects and the noise to signal remains highly variable but level at about 0.5%.

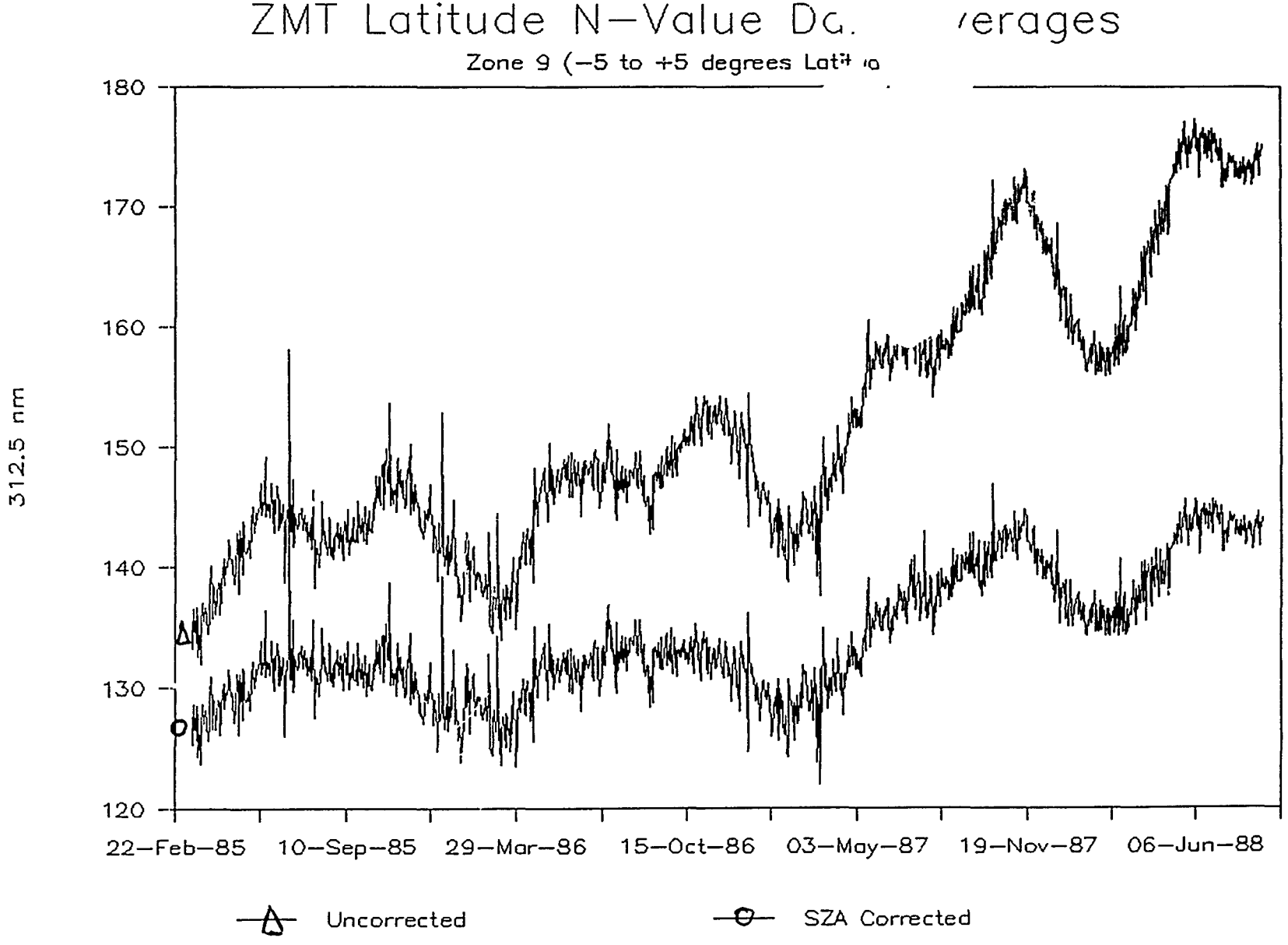
ZMT Latitude N-Value Da. erages
Zone 9 (-5 to +5 degrees Lat
312.5 nm
180
170
160
150
140
130
120
22-Feb-85
10-Sep-85
29-Mar-86
15-Oct-86
03-May-87
19-Nov-87
06-Jun-88
Uncorrected
SZA Corrected

Figure 1

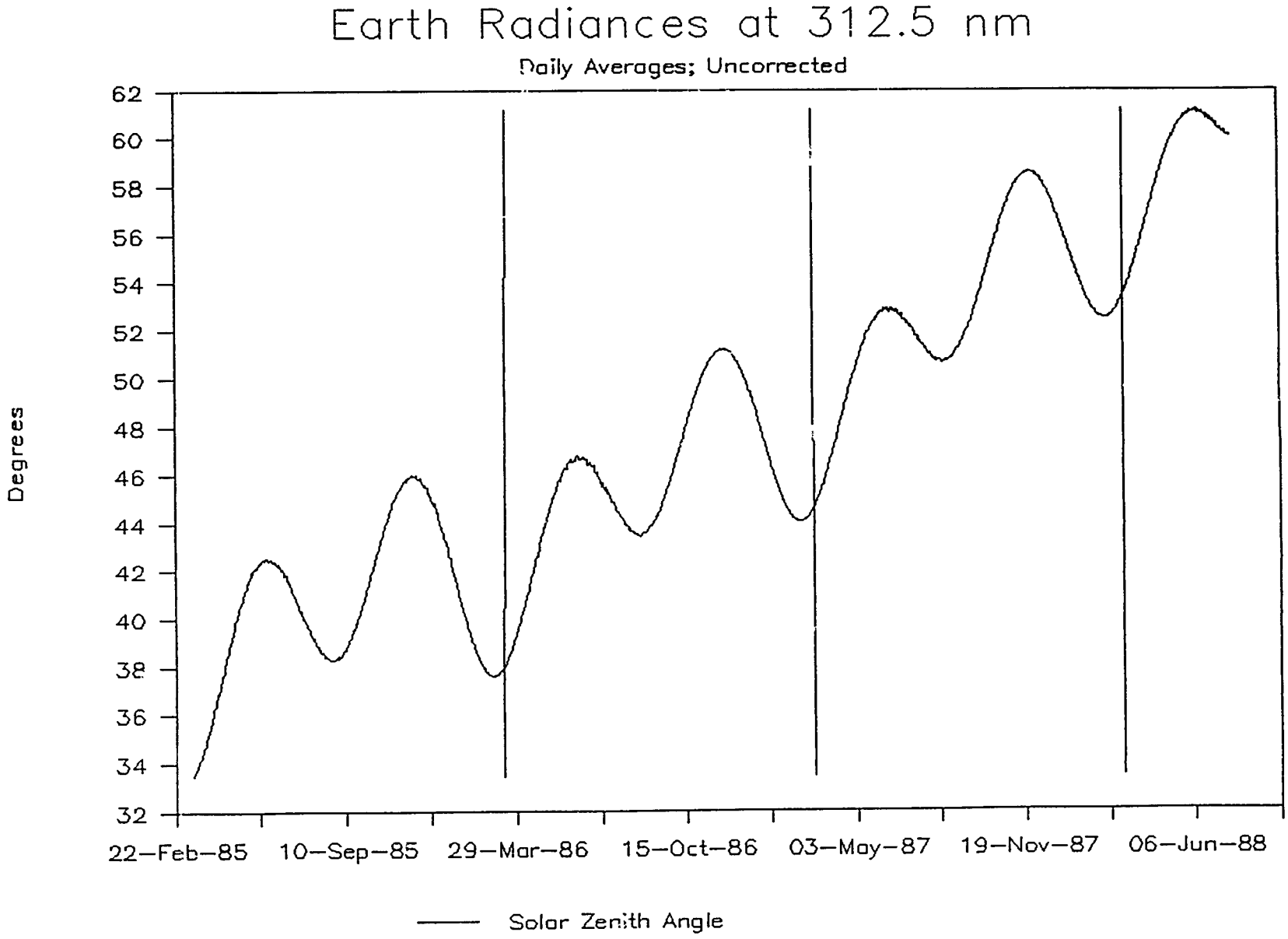
Earth Radiances at 312.5 nm
Daily Averages; Uncorrected
Degrees
62
60
58
56
54
52
50
48
46
44
42
40
38
36
34
32
22–Feb–85
10–Sep–85
29–Mar–86
15–Oct–86
03–May–87
19–Nov–87
06–Jun–88
Solar Zenith Angle

Figure 2

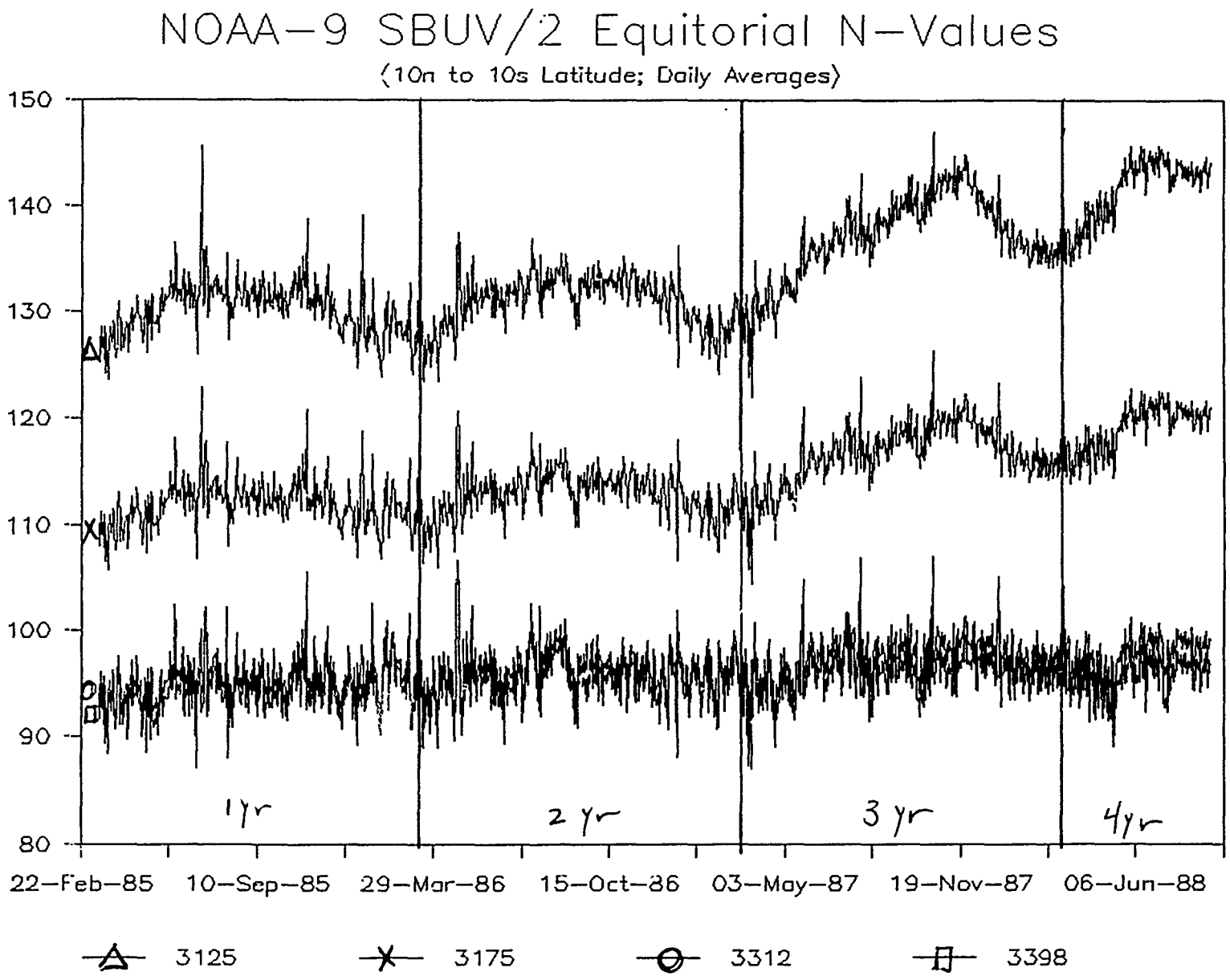
NOAA–9 SBUV/2 Equitorial N–Values
⟨10n to 10s Latitude; Daily Averages⟩
150
140
130
120
110
100
90
80
1yr
2 yr
3 yr
4yr
22–Feb–85
10–Sep–85
29–Mar–86
15–Oct–86
03–May–87
19–Nov–87
06–Jun–88
3125
3175
3312
3398

Figure 3

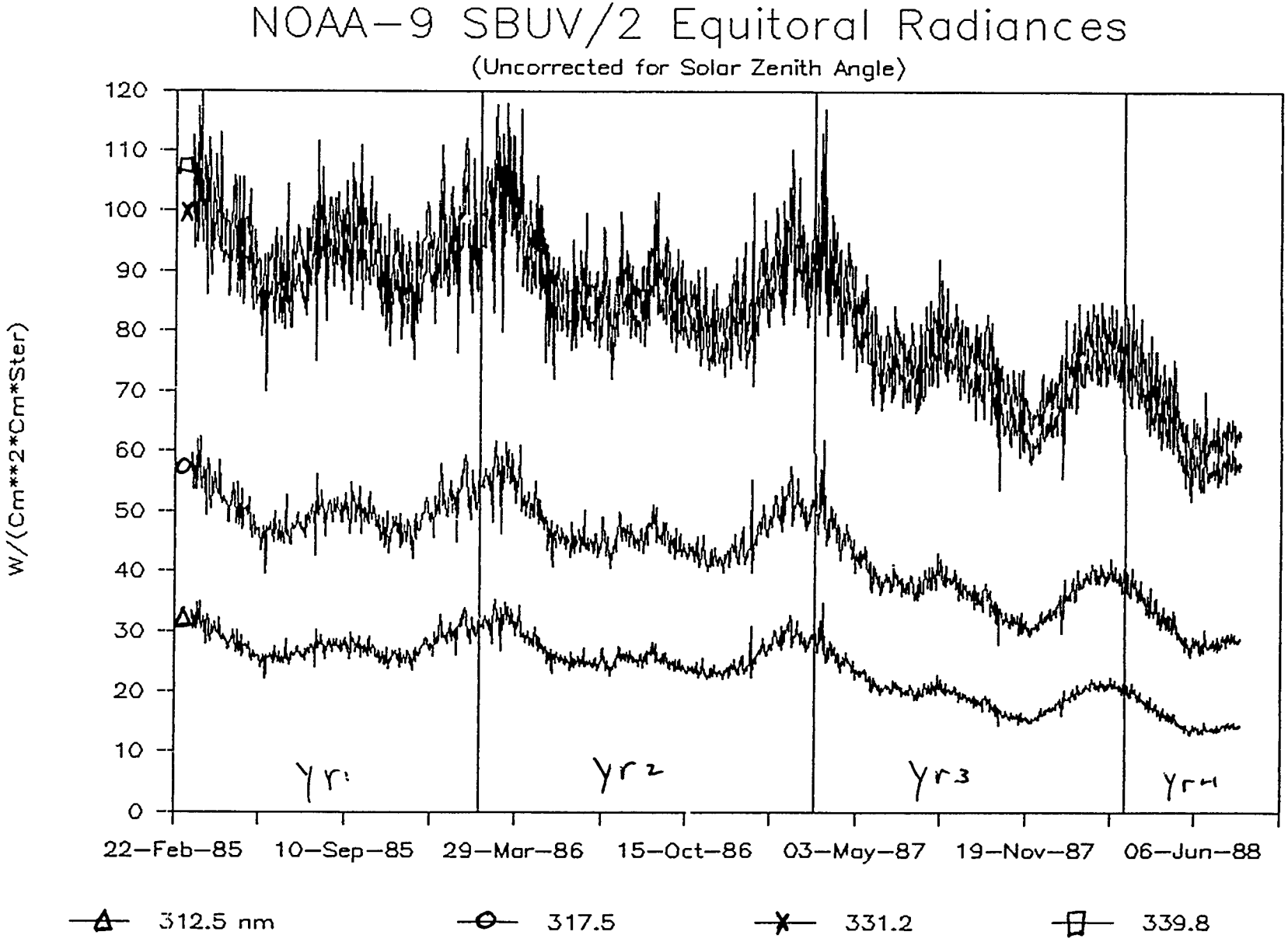
NOAA-9 SBUV/2 Equitoral Radiances
(Uncorrected for Solar Zenith Angle)
W/(Cm**2*Cm*Ster)
120
110
100
90
80
70
60
50
40
30
20
10
0
Yr1
Yr2
Yr3
Yr4
22-Feb-85
10-Sep-85
29-Mar-86
15-Oct-86
03-May-87
19-Nov-87
06-Jun-88
312.5 nm
317.5
331.2
339.8

Figure 4

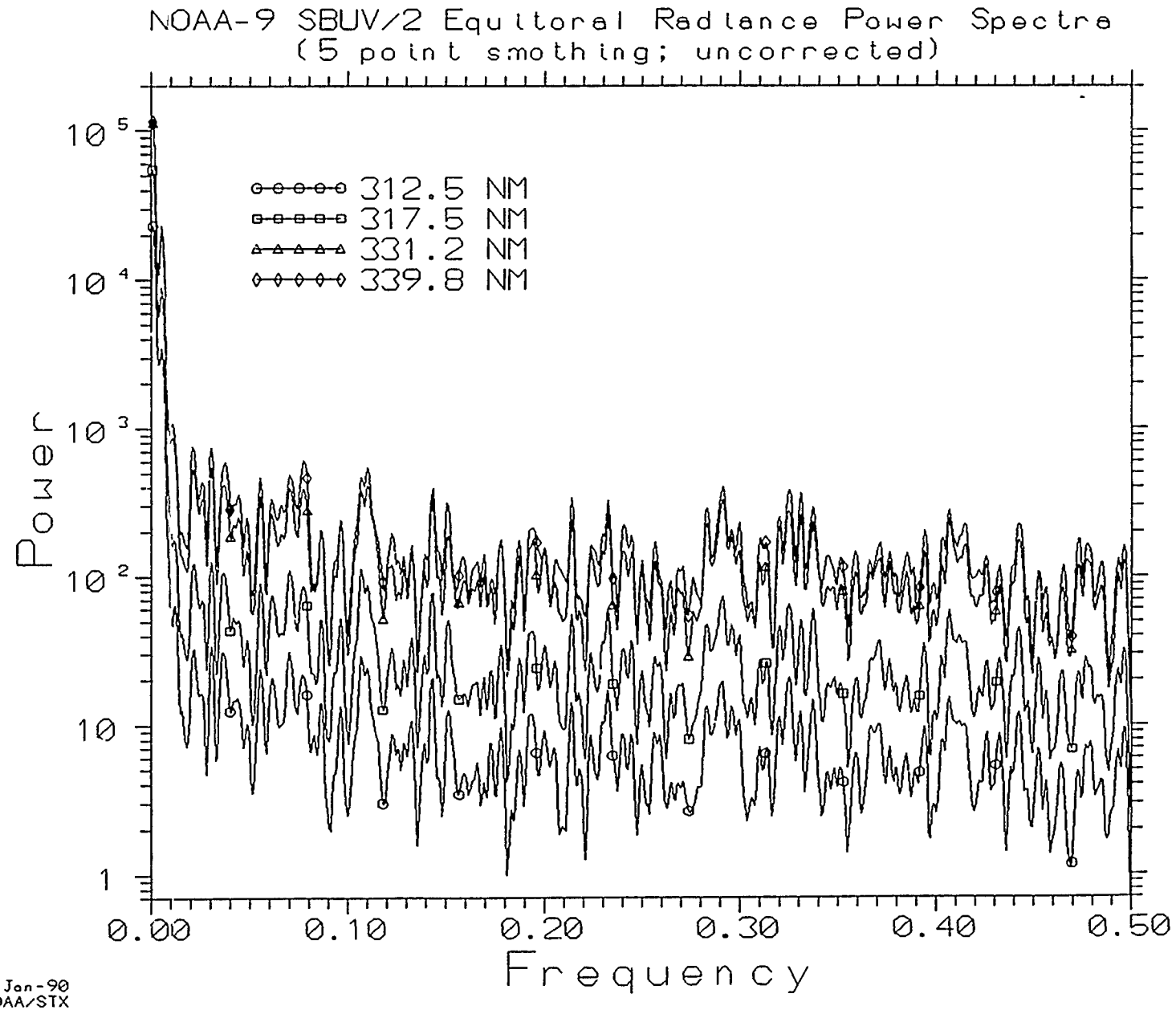
NOAA-9 SBUV/2 Equitoral Radiance Power Spectra
(5 point smothing; uncorrected)
312.5 NM
317.5 NM
331.2 NM
339.8 NM
Power
10 5
10 4
10 3
10 2
10
1
0.00
0.10
0.20
0.30
0.40
0.50
Frequency
3-Jan-90
NOAA/STX

Figure 5

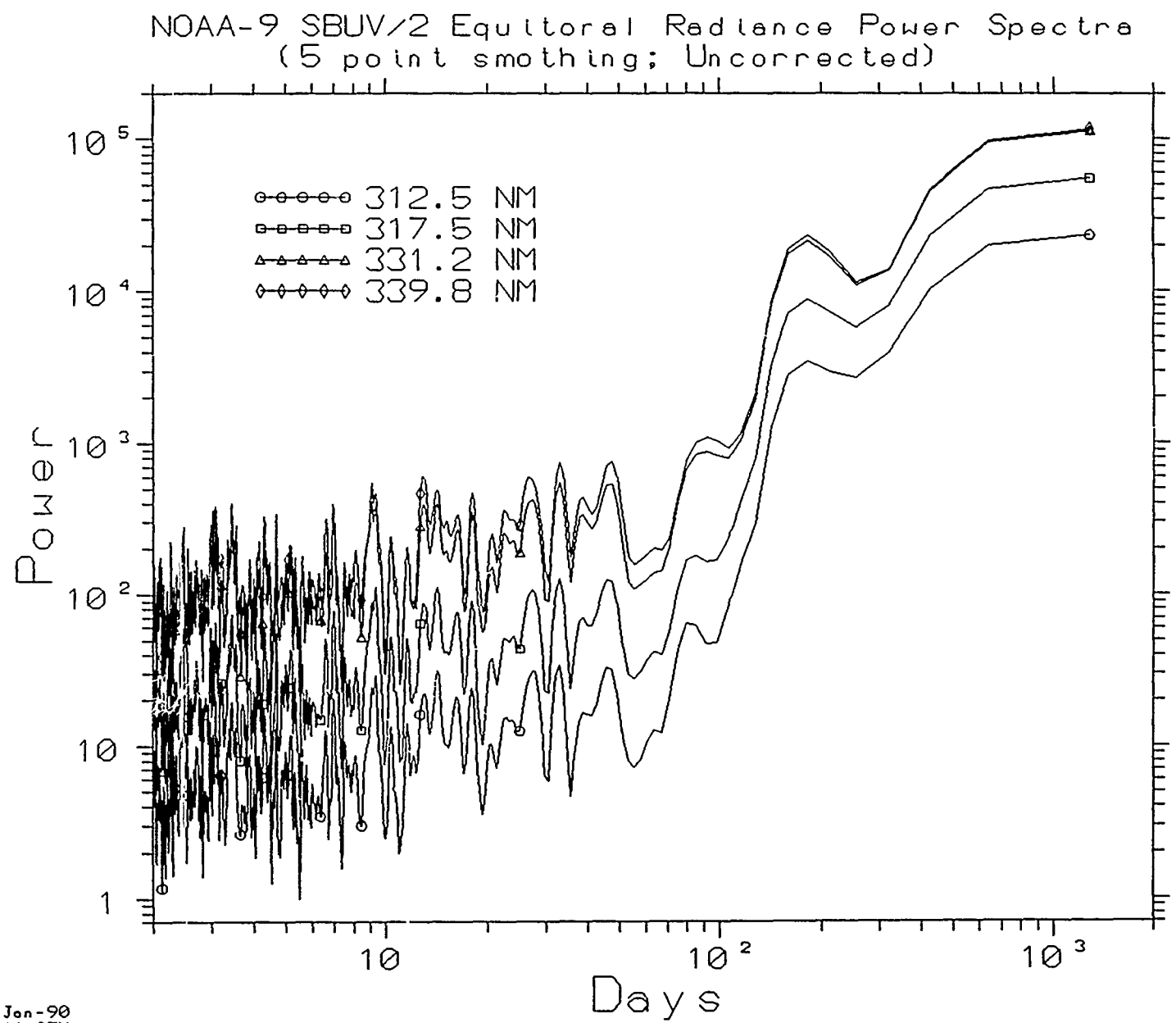

3-Jan-90
NOAA/STX

Figure 6

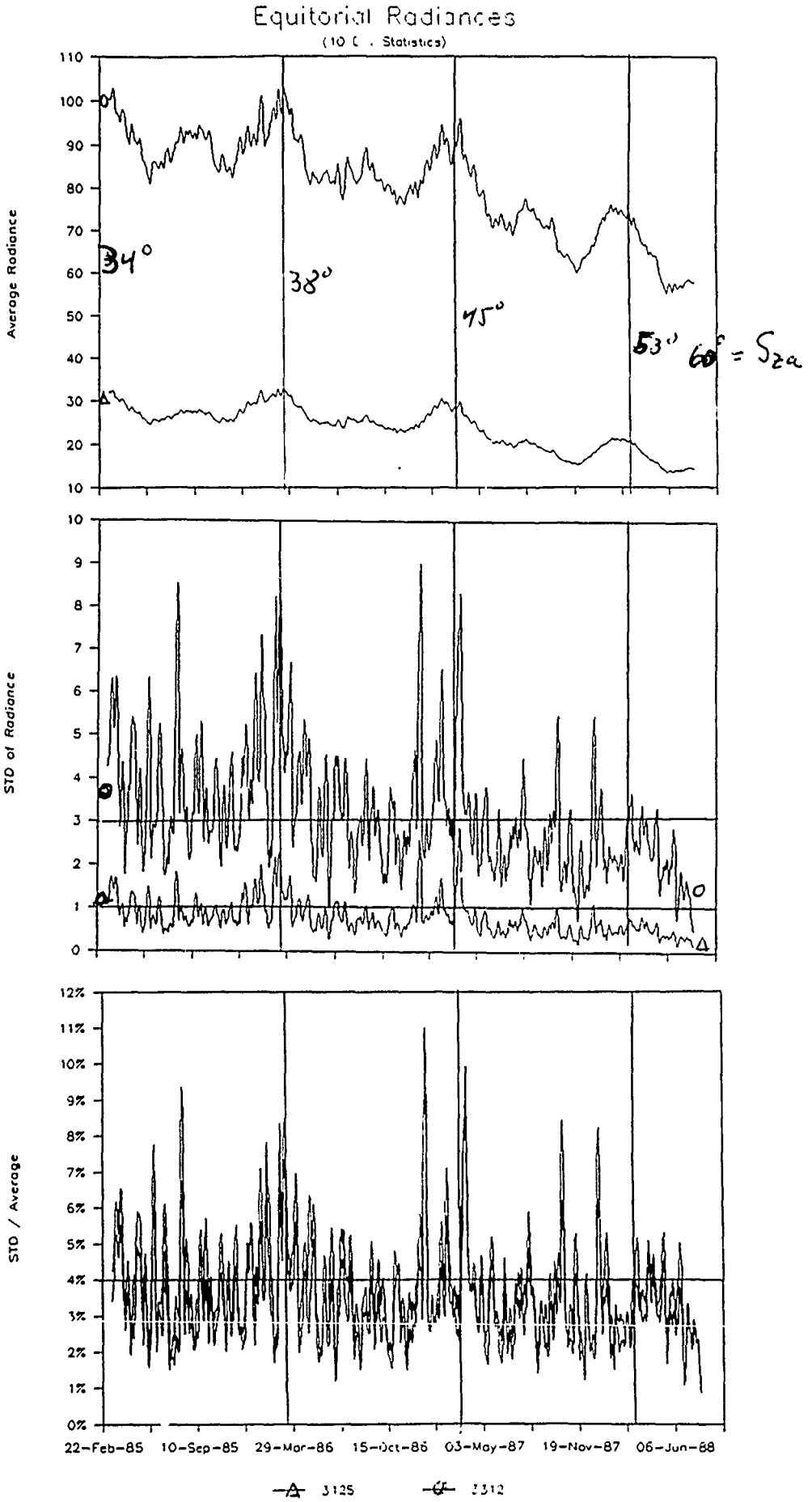
Equitorial Radiances
(10 C . Statistics)
Average Radiance
34°
38°
45°
53°
60°
STD of Radiance
STD / Average
12%
11%
10%
9%
8%
7%
6%
5%
4%
3%
2%
1%
0%
22-Feb-85
10-Sep-85
29-Mar-86
15-Oct-86
03-May-87
19-Nov-87
06-Jun-88
3125
3312

5-13 **Figure 7**

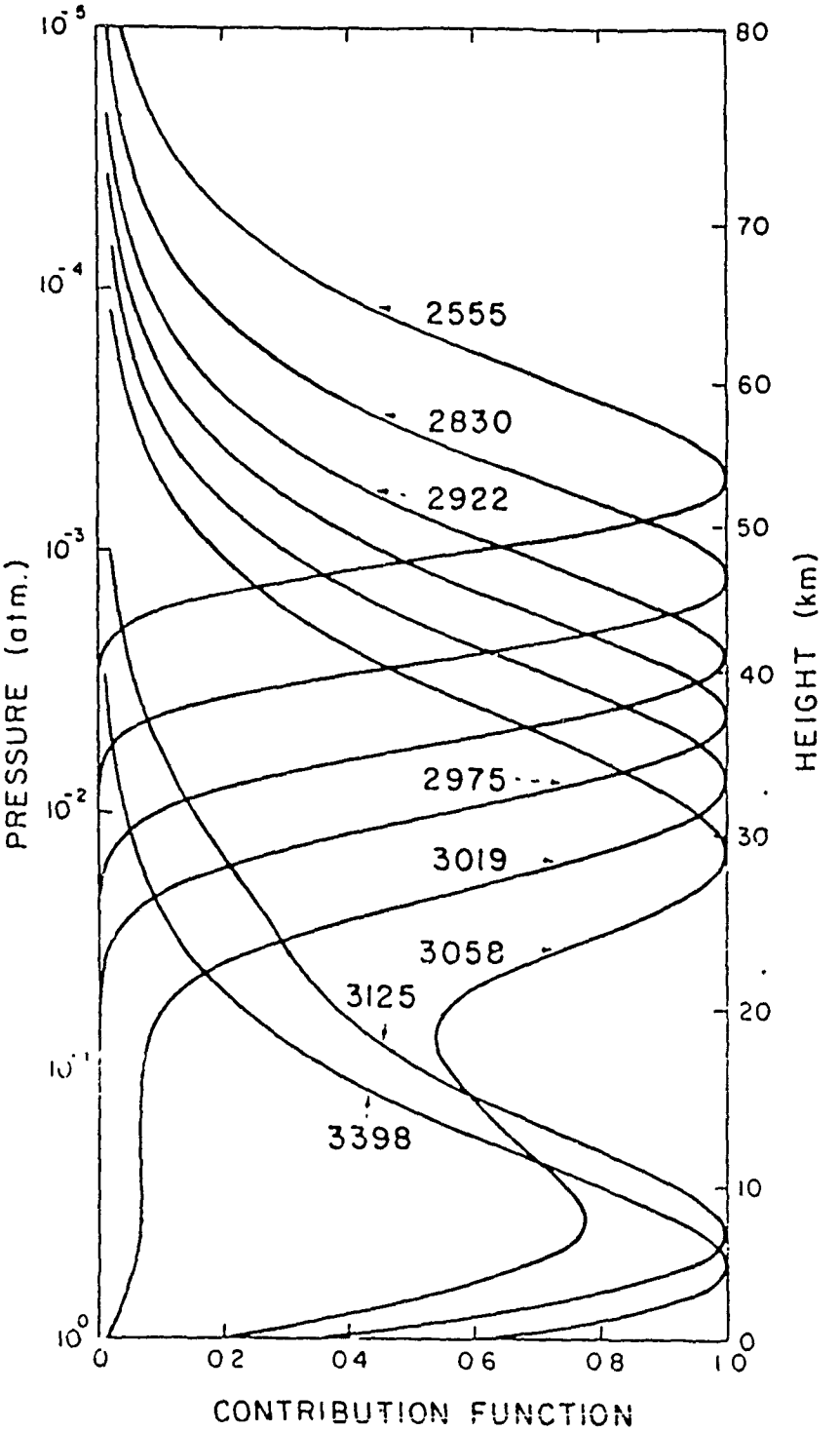

Figure 8

Contribution to the upward radiation from various levels in the atmosphere. Curves are normalized to unity at level of maximum. ($R = 0$, $\theta_0 = 60^\circ$, $\theta = 0^\circ$).

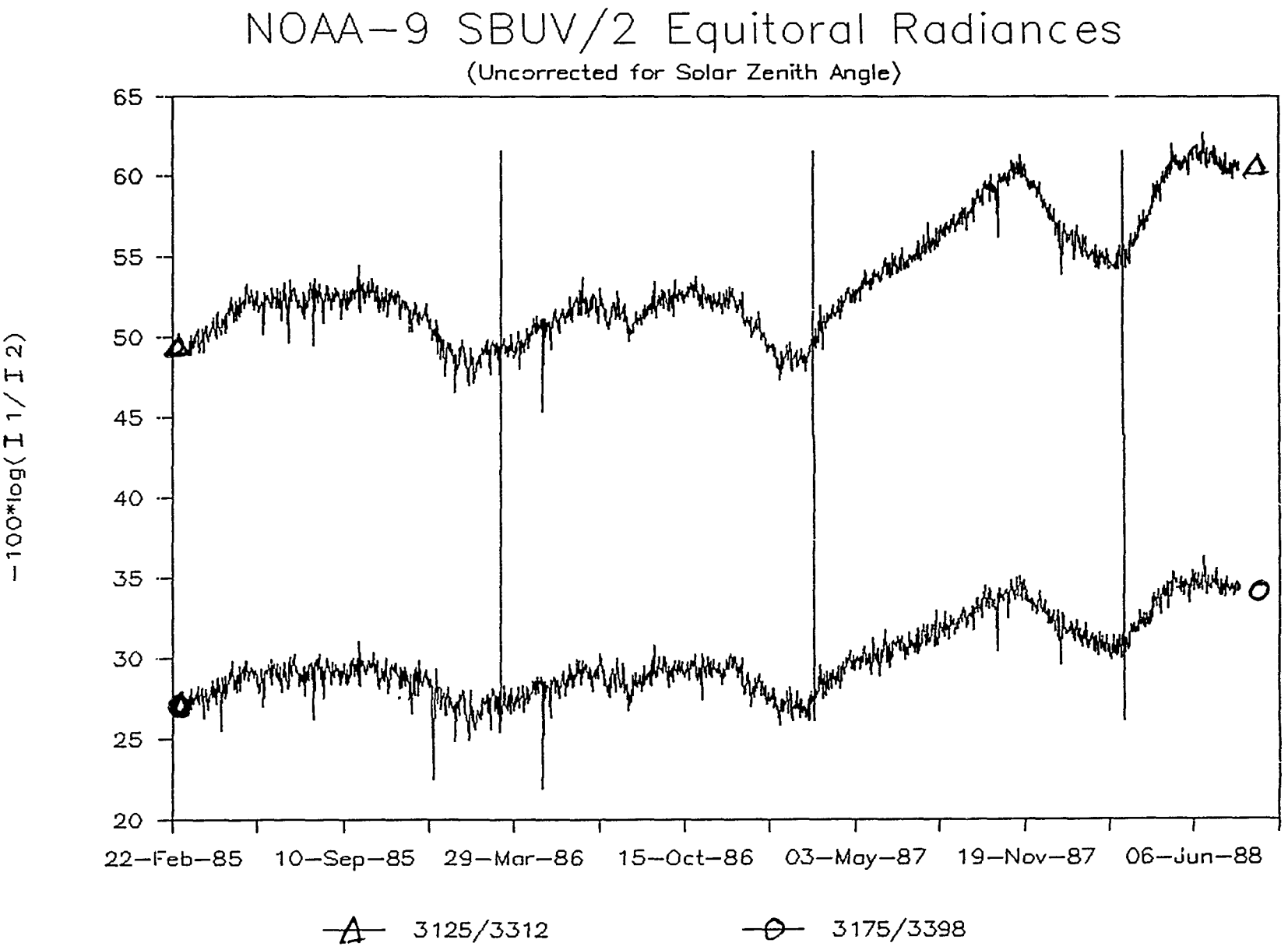
NOAA-9 SBUV/2 Equitoral Radiances
(Uncorrected for Solar Zenith Angle)
-100*log(I1/I2)
65
60
55
50
45
40
35
30
25
20
22-Feb-85
10-Sep-85
29-Mar-86
15-Oct-86
03-May-87
19-Nov-87
06-Jun-88
3125/3312
3175/3398

Figure 9

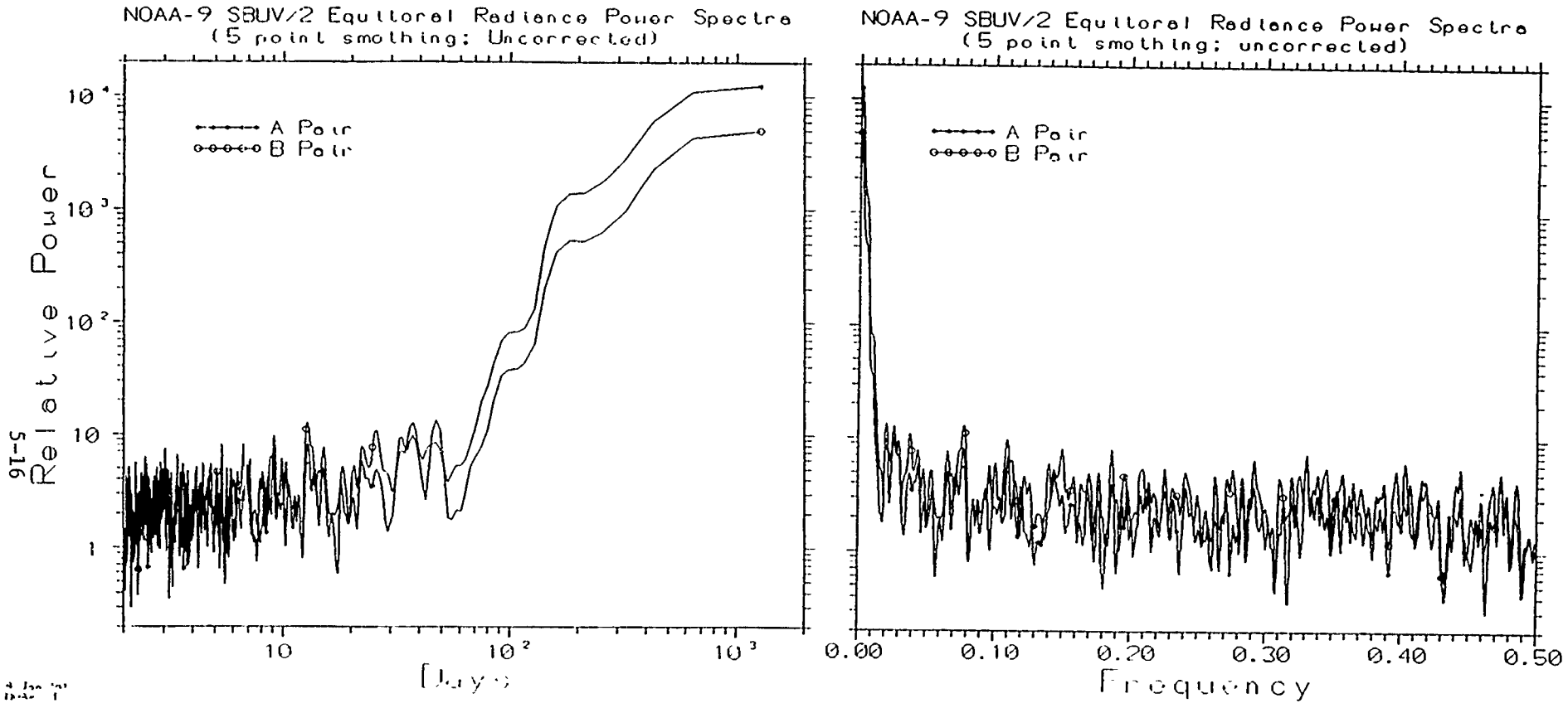
NOAA-9 SBUV/2 Equitoral Radiance Power Spectra
(5 point smoothing; Uncorrected)
A Pair
B Pair
Relative Power
10⁴
10³
10²
10
1
10
10²
10³
Days
NOAA-9 SBUV/2 Equitoral Radiance Power Spectra
(5 point smoothing; uncorrected)
A Pair
B Pair
0.00
0.10
0.20
0.30
0.40
0.50
Frequency

Figure 10

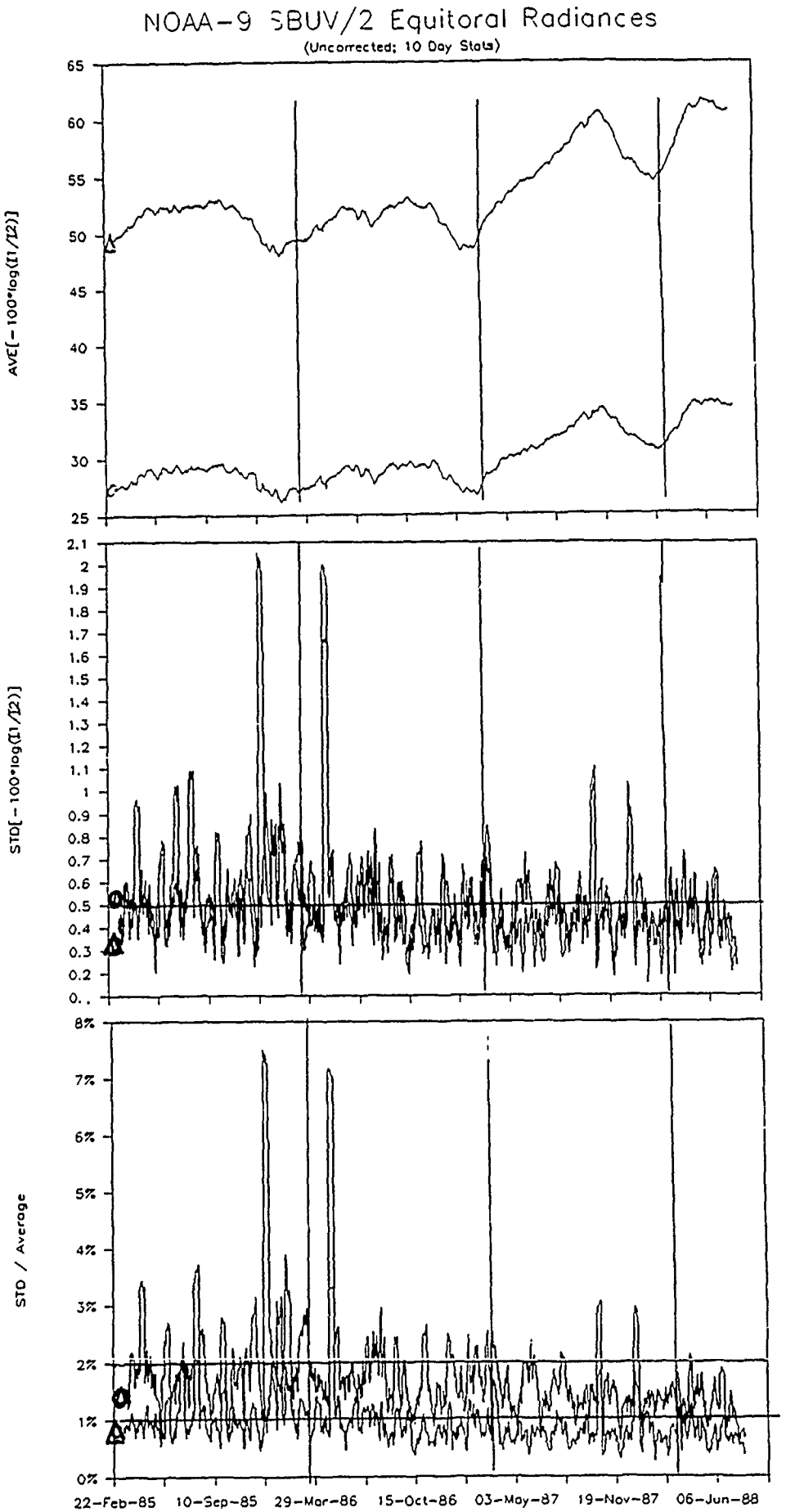
NOAA-9 SBUV/2 Equitoral Radiances
(Uncorrected; 10 Day Stats)
AVE[-100*log(I1/I2)]
STD[-100*log(I1/I2)]
STD / Average
22-Feb-85
10-Sep-85
29-Mar-86
15-Oct-86
03-May-87
19-Nov-87
06-Jun-88
3125/3312
3175/3398

Figure 11

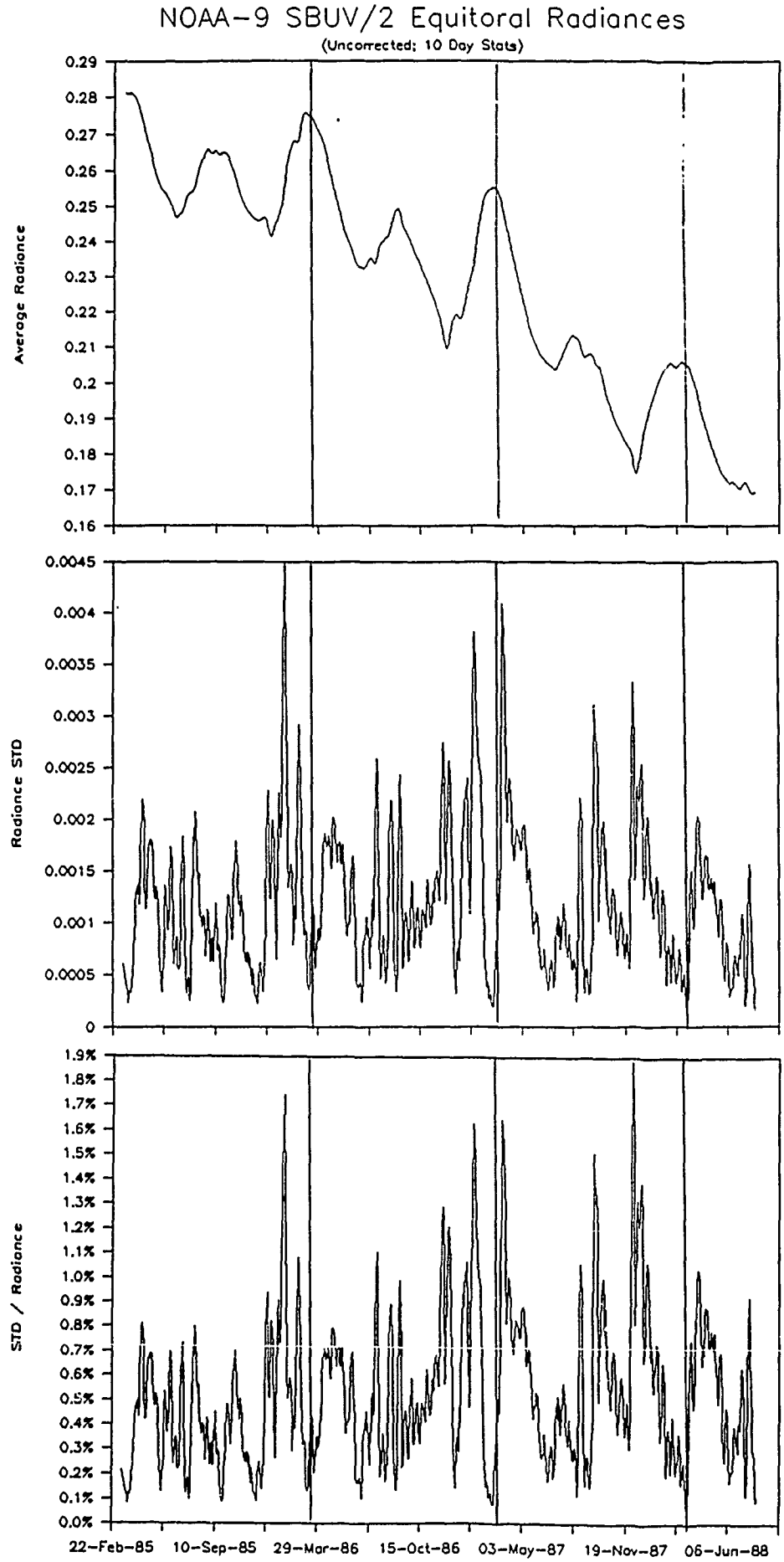
NOAA-9 SBUV/2 Equitoral Radiances
(Uncorrected; 10 Day Stats)
Average Radiance
0.29
0.28
0.27
0.26
0.25
0.24
0.23
0.22
0.21
0.2
0.19
0.18
0.17
0.16
Radiance STD
0.0045
0.004
0.0035
0.003
0.0025
0.002
0.0015
0.001
0.0005
0
STD / Radiance
1.9%
1.8%
1.7%
1.6%
1.5%
1.4%
1.3%
1.2%
1.1%
1.0%
0.9%
0.8%
0.7%
0.6%
0.5%
0.4%
0.3%
0.2%
0.1%
0.0%
22-Feb-85
10-Sep-85
29-Mar-86
15-Oct-86
03-May-87
19-Nov-87
06-Jun-88
292.2 nm

Figure 12

Attachment 6

A Technique for Directly Comparing Radiances from Two Satellites

R.D. McPeters
NASA/GSFC

A Technique for Directly Comparing Radiances From Two Satellites

Richard D McPeters
Laboratory for Atmospheres
NASA/Goddard Space Flight Center
(in cooperation with NOAA/NESDIS)

The SBUV instrument on Nimbus 7 and the SBUV-2 instrument on NOAA-9 are almost identical, each measuring the ultraviolet atmospheric albedo at wavelengths from 2500-3400 Å to infer total ozone and ozone profiles. While derived ozone has been compared for the two instruments, understanding the calibration differences between the two instruments requires that the measured radiances be compared. The problem is that SBUV is in a noon sun synchronous orbit while SBUV-2 is in an afternoon orbit (Figure 1). Radiances cannot be compared directly because the solar zenith angles of the observations are different (Figure 2).

Comparison of ozone values avoids this problem because solar zenith angle effects are implicitly taken into account in the retrieval algorithm. Figure 3 is a plot of the weekly average differences between SBUV and SBUV-2 of total ozone and of Umkehr layer ozone amounts. Initial biases between the two instruments, 5% in total ozone in March of 1985, are probably due to degradation of the SBUV diffuser plate, which had been in use for six years when NOAA-9 was launched. The relative change between 1985 and 1987 was significant for total ozone but was especially striking for ozone in the upper stratosphere, layers 7-10. This change was likely due to SBUV-2 orbit drift since SBUV degradation was fairly well known and much less rapid. In order to understand this change in ozone, it would be very useful to know the changes in the radiances.

A technique to compare radiances has been developed in which the measured albedo at each wavelength is put onto a common solar zenith angle scale. A forward calculation for each wavelength is done using the derived ozone profile, then repeated for the common solar zenith angle to predict what each instrument would have measured had it been at the standard solar zenith angle. This technique is accurate provided neither the zenith angle nor the zenith angle correction is large. Direct comparisons of the instrument measurements (Q values) are then possible. The Q value is the ratio of the backscattered radiance to the extraterrestrial solar irradiance scaled by the Rayleigh scattering phase function.

Such radiance comparisons for March of 1986 are shown in Figures 4 and 5. Differences traceable to calibration should be independent of latitude; ie., the difference curves should be flat. Significant deviations occur at large solar zenith angles (high latitudes) and at wavelengths for which multiple scattering is important (2975-3058 Å), indicating the limits for the

technique.

The time dependence of the relative change between the two instruments is shown in Figure 6, normalized to day 1. Between March 1985 and August 1987 there was almost a 14% relative change at 2975 Å, the longest wavelength shown, and a 20% relative change at the shortest wavelength, 2735 Å. During this period the SBUV-2 orbit drifted from 2 PM local time to approximately 5 PM local time. The increasing incidence angle on the diffuser plate during solar flux measurements is being examined as the possible cause of the apparent SBUV-2 calibration change. To first order, such goniometric errors would be expected to be wavelength independent.

The explicit wavelength dependence is shown in Figure 7. The most striking conclusion is that the differences between SBUV and SBUV-2 are almost wavelength independent for wavelengths 2735 Å through 2922 Å. The results for wavelengths 2975-3058 Å are less reliable because multiple scattering is important for these wavelengths but was not included in the forward calculation. But the fact that total ozone changes relative to the Dobson network are observed indicates that there is <u>some</u> wavelength dependent error for wavelengths greater than 3000 Å. The wavelength dependence that is seen at the shorter wavelengths is consistent with the long term degradation of the SBUV diffuser plate, which is know to greater at shorter wavelengths.

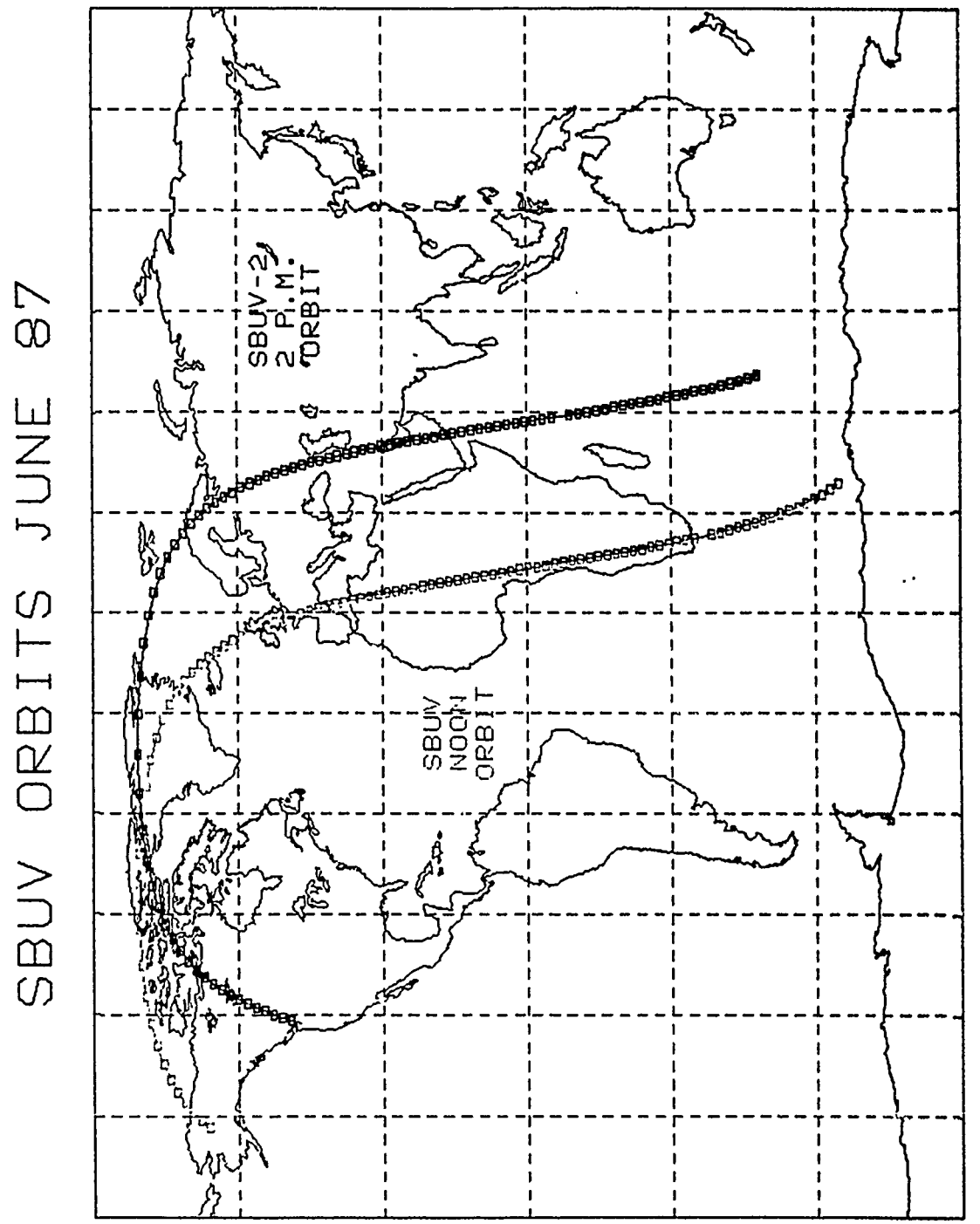
SBUV ORBITS JUNE 87
SBUV-2
2 P.M.
ORBIT
SBUV
NOON
ORBIT

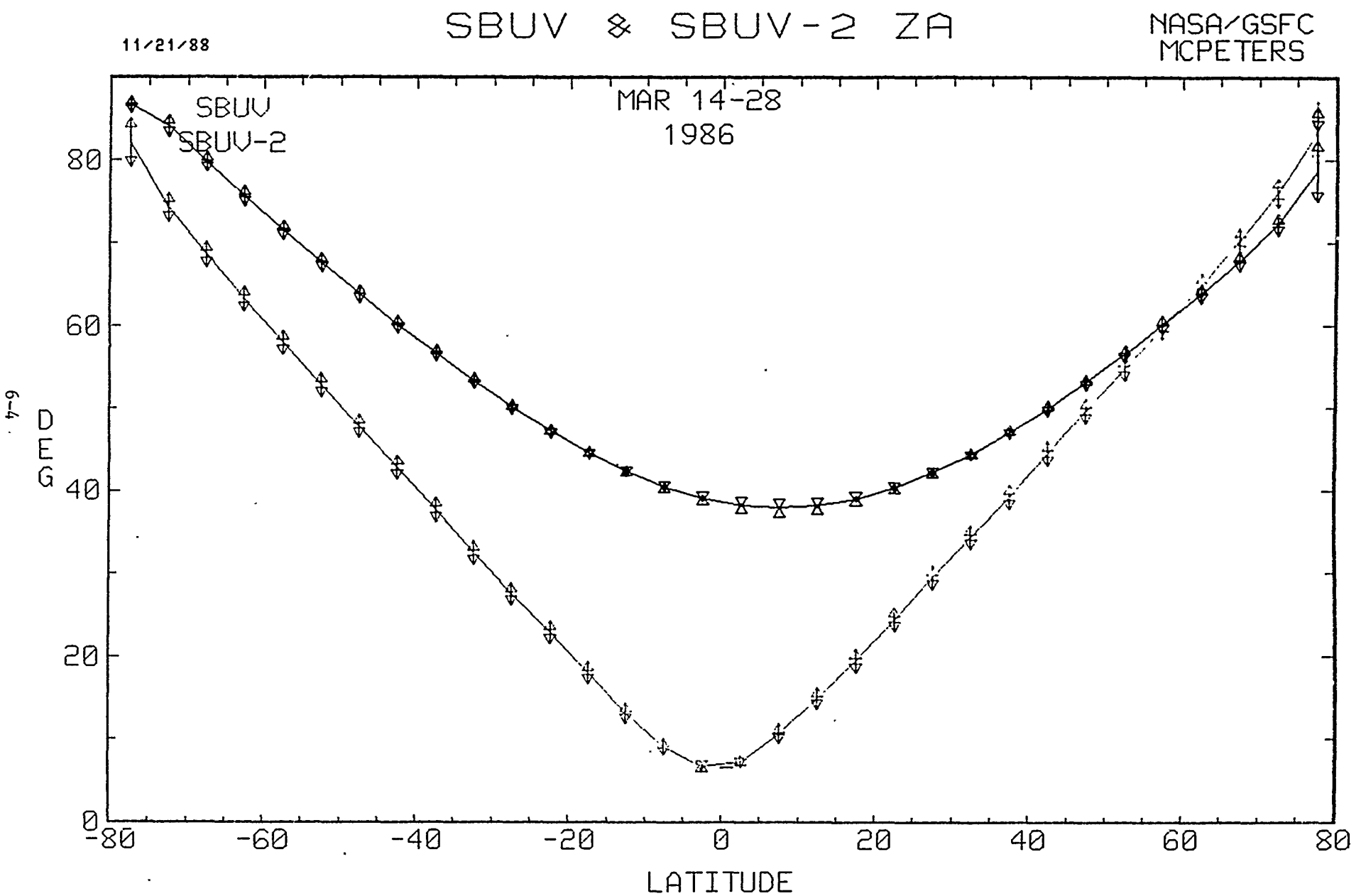
SBUV & SBUV-2 ZA
11/21/88
NASA/GSFC
MCPETERS
SBUV
SBUV-2
MAR 14-28
1986
DEG
80
60
40
20
0
-80
-60
-40
-20
0
20
40
60
80
LATITUDE

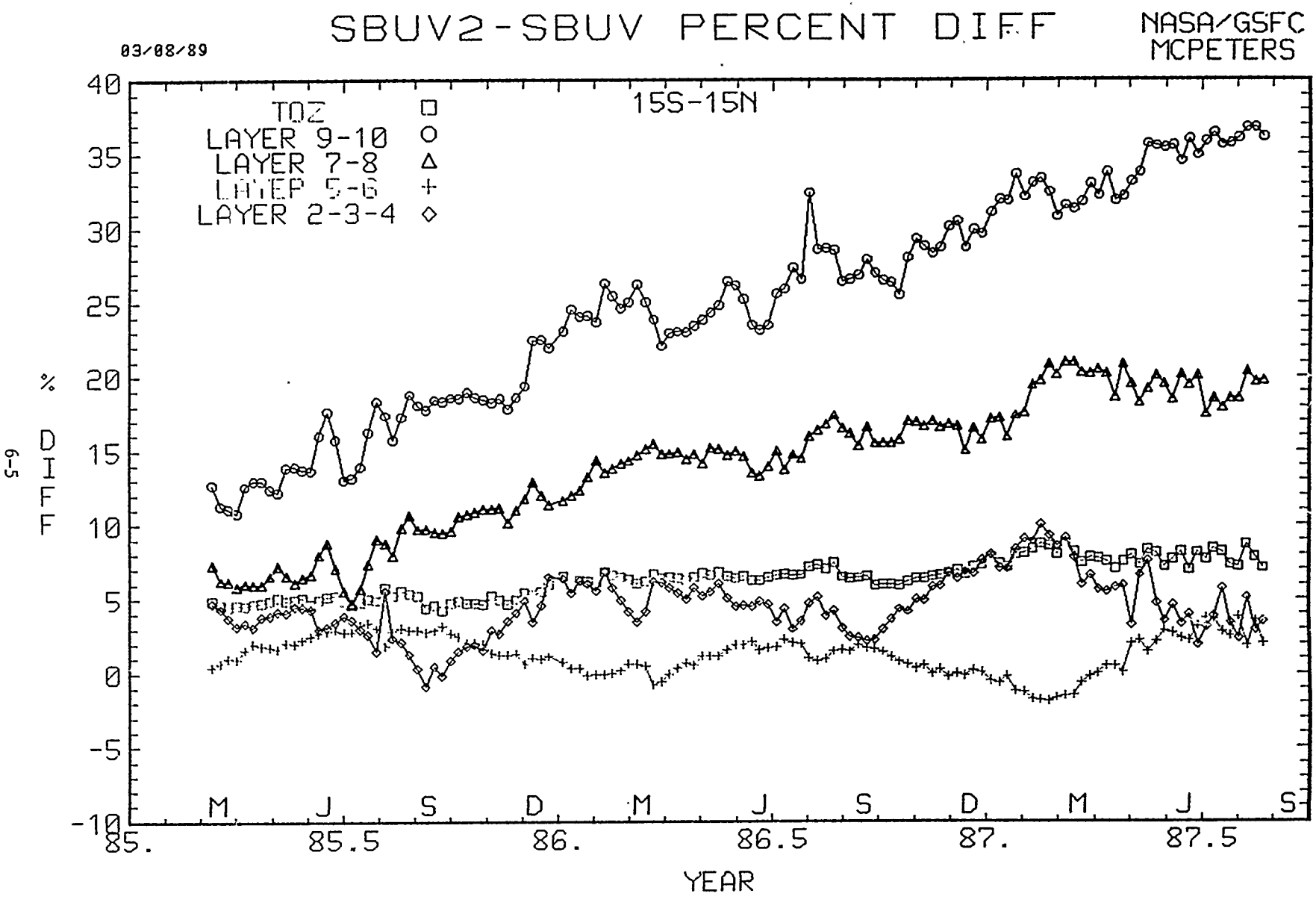
SBUV2-SBUV PERCENT DIFF
NASA/GSFC
MCPETERS
03/08/89
15S-15N
TOZ
LAYER 9-10
LAYER 7-8
LAYER 5-6
LAYER 2-3-4
% DIFF
YEAR
40
35
30
25
20
15
10
5
0
-5
-10
85.
85.5
86.
86.5
87.
87.5
M
J
S
D
M
J
S
D
M
J
S

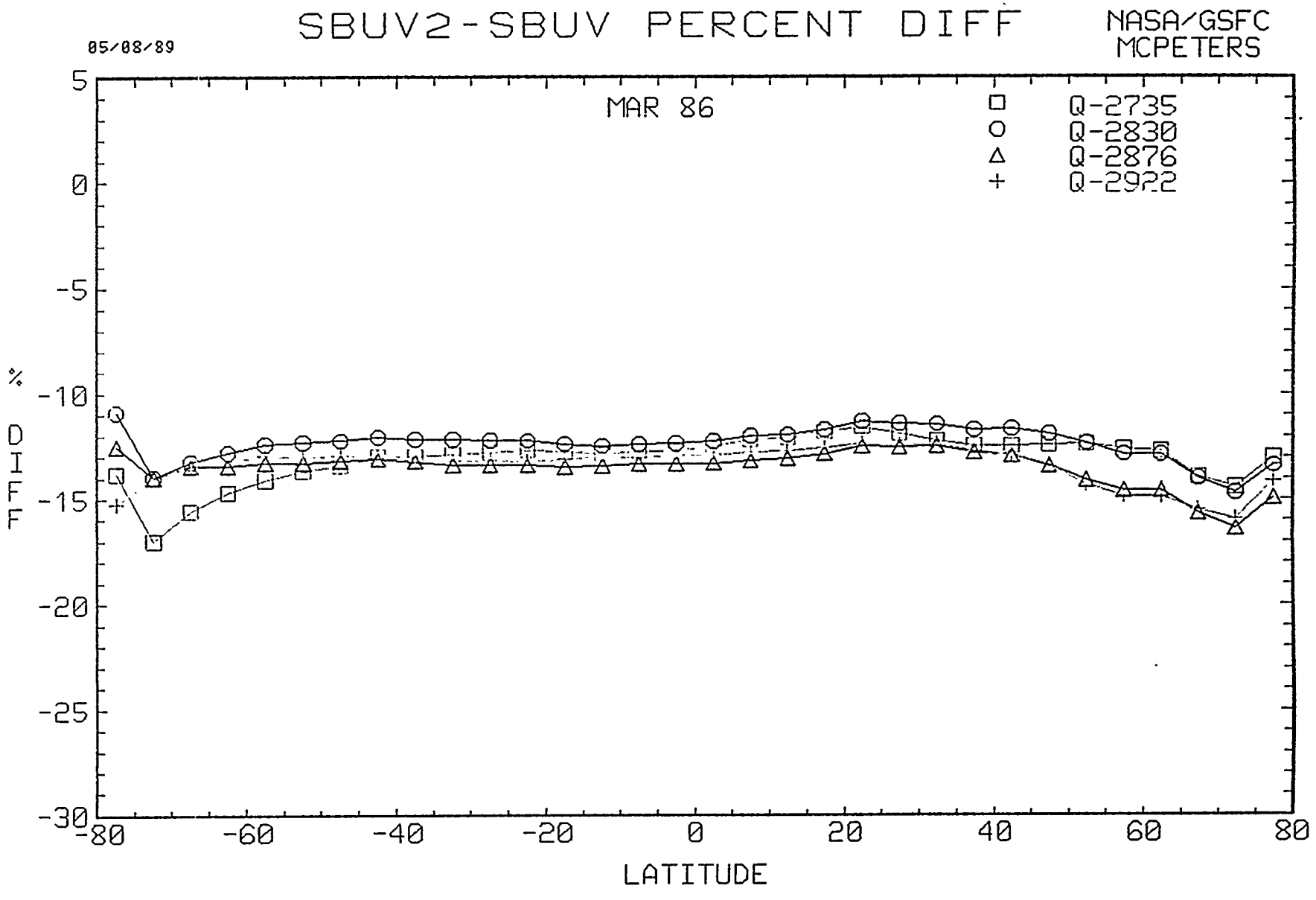
SBUV2-SBUV PERCENT DIFF
NASA/GSFC
MCPETERS
05/08/89
MAR 86
Q-2735
Q-2830
Q-2876
Q-2922
% DIFF
LATITUDE
5
0
-5
-10
-15
-20
-25
-30
-80
-60
-40
-20
0
20
40
60
80

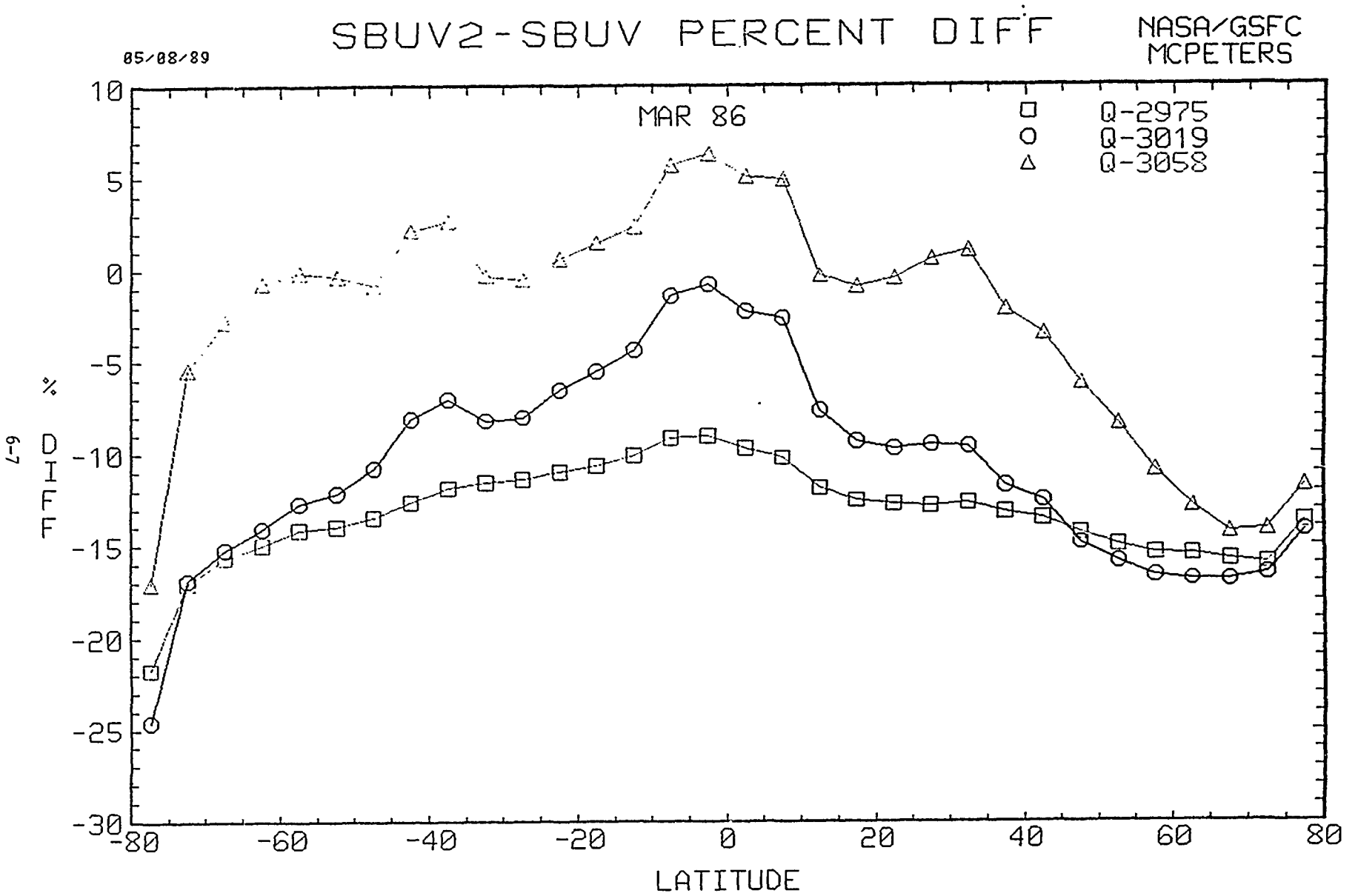
SBUV2-SBUV PERCENT DIFF
NASA/GSFC
MCPETERS
05/08/89
MAR 86
Q-2975
Q-3019
Q-3058
% DIFF
LATITUDE
10
5
0
-5
-10
-15
-20
-25
-30
-80
-60
-40
-20
0
20
40
60
80

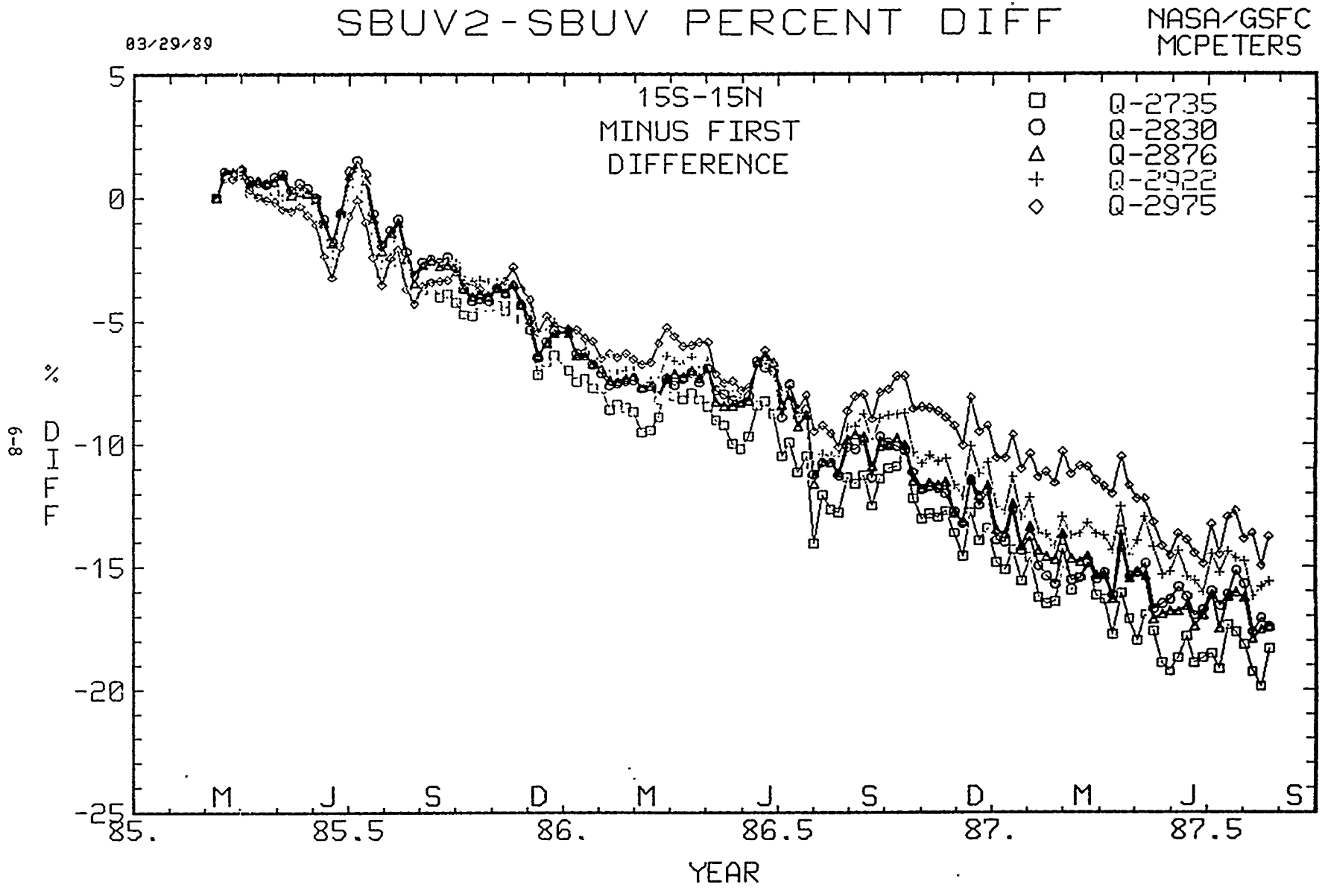
SBUV2-SBUV PERCENT DIFF
03/29/89
NASA/GSFC
MCPETERS
15S-15N
MINUS FIRST
DIFFERENCE
Q-2735
Q-2830
Q-2876
Q-2922
Q-2975
5
0
-5
-10
-15
-20
-25
% DIFF
M
J
S
D
M
J
S
D
M
J
S
85.
85.5
86.
86.5
87.
87.5
YEAR

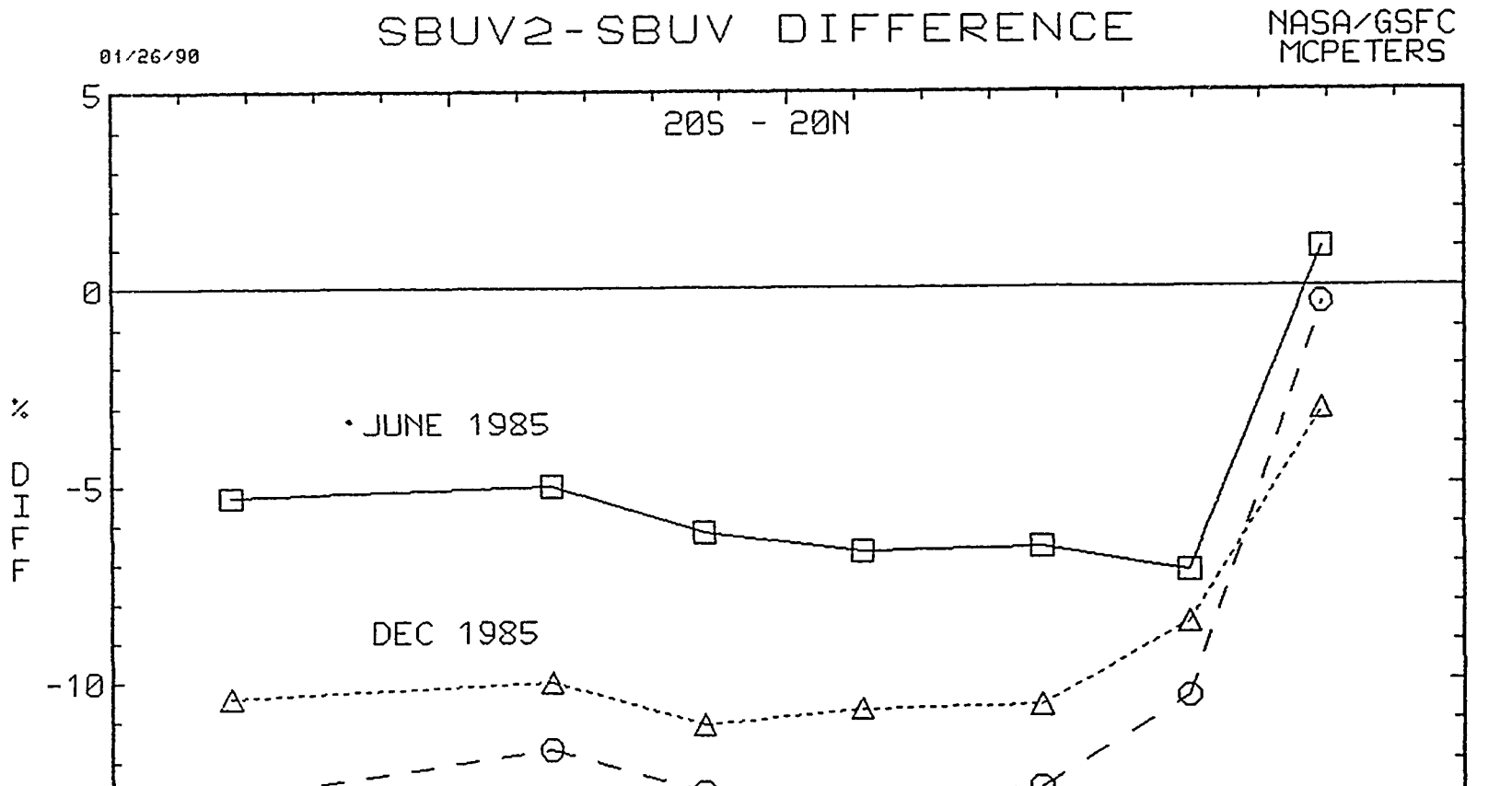
SBUV2-SBUV DIFFERENCE
01/26/90
NASA/GSFC
MCPETERS
20S - 20N
5
0
-5
-10
-15
% DIFF
JUNE 1985
DEC 1985
JUNE 1986
2700
2800
2900
3000
3100
WAVELENGTH

Attachment 7
SBUV/2 Comparisons
A.J. Miller and R. Nagatani
NOAA/NWS-CAC

SBUV/2 Comparisons with Ground-Based and SBUV Spacecraft Data

by

NOAA/NWS/NMC/CAC/Analysis and Information Branch

SBUV/2 Total Ozone versus Latitude/Solar Zenith Angle

Within Figures 1 and 2 are presented the April and December '85 monthly average results for SBUV/2 minus Dobson plotted by station as a function of latitude along with their 95% confidence limits. We see that although there is some indication of a decrease with latitude in December, overall, any pattern to the differences is swamped by the station-to-station biases.

As a consequence of the above, in an attempt to diminish the noise of the comparisons, we compared SBUV/2 with SBUV and the results for the monthly zonal average with the 95% confidence limits are shown in Figure 3 for December '85. In this case a clear bias with latitude is indicated with the maximum in the region of minimum solar zenith angle. Bhartia has suggested that the shape of this difference is to be expected in that the SBUV and SBUV/2 algorithm pass through an error in albedo as an error in ozone as a function of solar zenith angle (Figure 4). To test this hypothesis, we tested a numerical model of the differences (Figure 4) for the months of April and December '85 and the results are plotted in Figures 5 and 6. Overall, the statistical fit of the model to the observations is significant at the 95% confidence limit supporting the hypothesis and establishing this as a basic

error in the ozone retrievals.

Following this assessment, it was suggested that a similar effect should be seen in the summertime high latitude regions where SBUV/2 observations are made over portions of both the ascending and descending orbits. The zonal averages for July 1985 are depicted in Figure 7 over the common latitudes of the orbits. We note that in the SBUV/2 algorithm, the weights for the A and B pair wavelengths dominate the best ozone values until the last 4 values of the descending orbit where C pair is given major weight. This is of importance as the C pair coefficients appear to be in error by about 7% during this version whereas the A and B pair coefficients are within 1.5%.

In Figure 8, the functional model results for the ascending minus descending data are presented along with the actual data. Fit 1 represents the model calculations at all data points, Fit 2 the points where C pair has not been included. For both cases, although better for Fit 2, the model fit is significant at the 95% confidence level.

In summary, then, the hypothesized relationship of an error in SBUV/2 derived total ozone decreasing with increasing solar zenith angle as $1/(1+\sec\theta)$ seems borne out by the statistics. This, in turn, suggests that this error may be "correctable" if we can prove the results are consistent in time.

SBUV/2 Total Ozone versus Time

Examining next the SBUV/2 Dobson comparisons with time, in Figure 9 we present the difference (percent) by month for the period March '85 to May

'89. Within this plot each month may contain a variable number of stations and some of the increased variability toward the latter part of the record is due to this effect in that all stations have not reported their data. Overall, though, an increase in the bias with time is clearly observed of about 0.5% per year.

One suggestion offered is that such a plot contains many stations that may be of lesser quality than others, biasing the result. Therefore, we examined the data further by considering the analysis in a very different manner, one more suitable to culling. First we examined the linear trend by station for all reporting stations and culled the results by the following criteria: All stations that reported at least 20 of the 51 possible months (All 20), all stations with at least 30 months comparisons (All 30), those stations considered by Bojkov (28) in a recent analysis (BOJ 20 and BOJ 30) and, finally, the Bojkov stations that have been recalibrated since 1985 (BST 20 and BST 30). The results and the 95% confidence limits are presented in Figure 10 and we see that while each category is statistically significant from zero, there is virtually no statistically significant difference between groups. It is concluded, therefore, that the SBUV/2 is increasing with respect to the ground-based stations.

Examination of the data in this form provides an additional benefit in that various subsets of stations can be examined for consistency. In particular, we are concerned with a 5 station subset consisting of the stations; Boulder, Belsk, Arosa, Tateno and Lisbon as these are the Umkehr stations DeLuisi has adjusted for aerosol effect. Examination of this 5 station grouping resulted in an average trend value of about - 0.1% per year, a value distinctly different from the others. Further examination of the data

indicated this to be due to the results at Lisbon (Figure 11) where we see a large gap in the record and a distinct shift as the data resume. This suggests that Lisbon data changed calibration during the gap period, and, furthermore, we can not specify when it occurred.

SBUV/2 Profile Data versus Time

As suggested, above, the major data base for these comparisons is the 5 station Umkehr data, adjusted for aerosol effect, provided by John DeLuisi. However, as Lisbon data appear to exhibit an inconsistent record with time, these data must be considered differently, and, therein lies the problem as the Umkehr data were provided as a block of data without the possibility of deleting Lisbon. Fortunately, the records indicate that no Lisbon Umkehr data were considered within the block after February 1987. This means that if we examine the 5 station Umkehr results with time, the Lisbon data up to July '86 appear consistent within themselves, after February '87 are not included, and, therefore, if a calibration shift occurred between these dates it would influence the results.

In Figure 12, we show that SBUV/2 minus Umkehr values as a function of time within the Umkehr levels. We see that a positive bias with time appears in layer 9 with the difference increasing from about +5% to +20% through the period. Layers 8, 7 and 6 each show a positive bias, but with a reduced increase in time. Layer 5 shows, virtually, no change, but a large seasonal effect.

This pattern of SBUV/2 change with time is further examined in Figure 13 where we compare SBUV/2 against SBUV over the 60N-60S domain to reduce random

noise and seasonal effects. Although SBUV can not be considered a stationery standard, we note an overall pattern of change with time similar to that found in Figure 12 except Layer 5 does not exhibit the seasonal effect.

Finally, in Figure 14, we present a comparison of SBUV/2 profiles with SAGE II for April 5, 1985 at 1^{o}N. This is meant to be indicative of further comparisons to be accomplished. We see that below about 5mb the SBUV/2 is lower than SAGE II, but is higher in the region 5-1mb with another cross-over point at 1mb. As SAGE II is considered to be an instrument that suffers less from long-term calibration problems than SBUV/2, it will be interesting to compare these data in time as well as at other latitudes.

Summary

In summary, several points seem clearly evident:

1. The SBUV/2 total ozone values contain a solar zenith angle dependent bias that appears to behave with the anticipated form of $1/(1+\sec\theta)$.

2. The SBUV/2 total ozone values are increasing with respect to the ground-based Dobson stations at the rate of about 0.4-0.5 % per year. This rate is statistically significant from zero.

3. As the solar zenith angle of the SBUV/2 increases with time due to the precession of the orbit, this would lead to a decrease in time of total ozone from effect

(1) above. That the total ozone is observed to increase against the Dobson data means that an additional effect is operative. Also, if we "adjust" the total ozone data for solar zenith angle this would serve to increase the difference against the Dobson data.

4. Although the Umkehr data base has inherently more uncertainty, the SBUV/2 data appear to increase in time with respect to the Umkehr data. This increase is altitude dependent with the largest increases at the highest level and essentially no increase in layer 5.

5. An additional data base to aid evaluation of the SBUV/2 profile data is that from SAGE II and these comparisons should be incorporated within the overall effort.

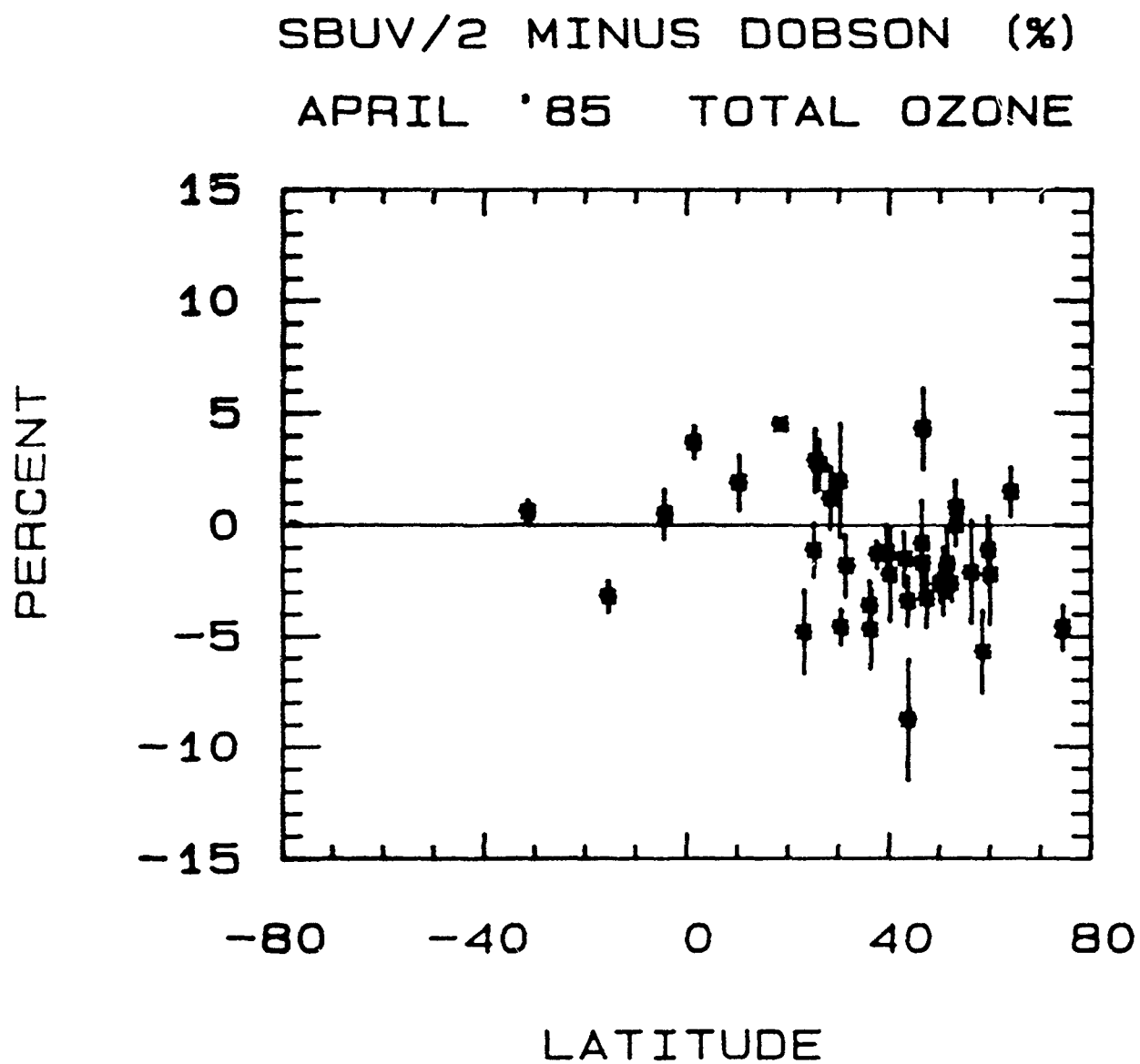
SBUV/2 MINUS DOBSON (%)
APRIL '85 TOTAL OZONE
PERCENT
15
10
5
0
-5
-10
-15
-80
-40
0
40
80
LATITUDE

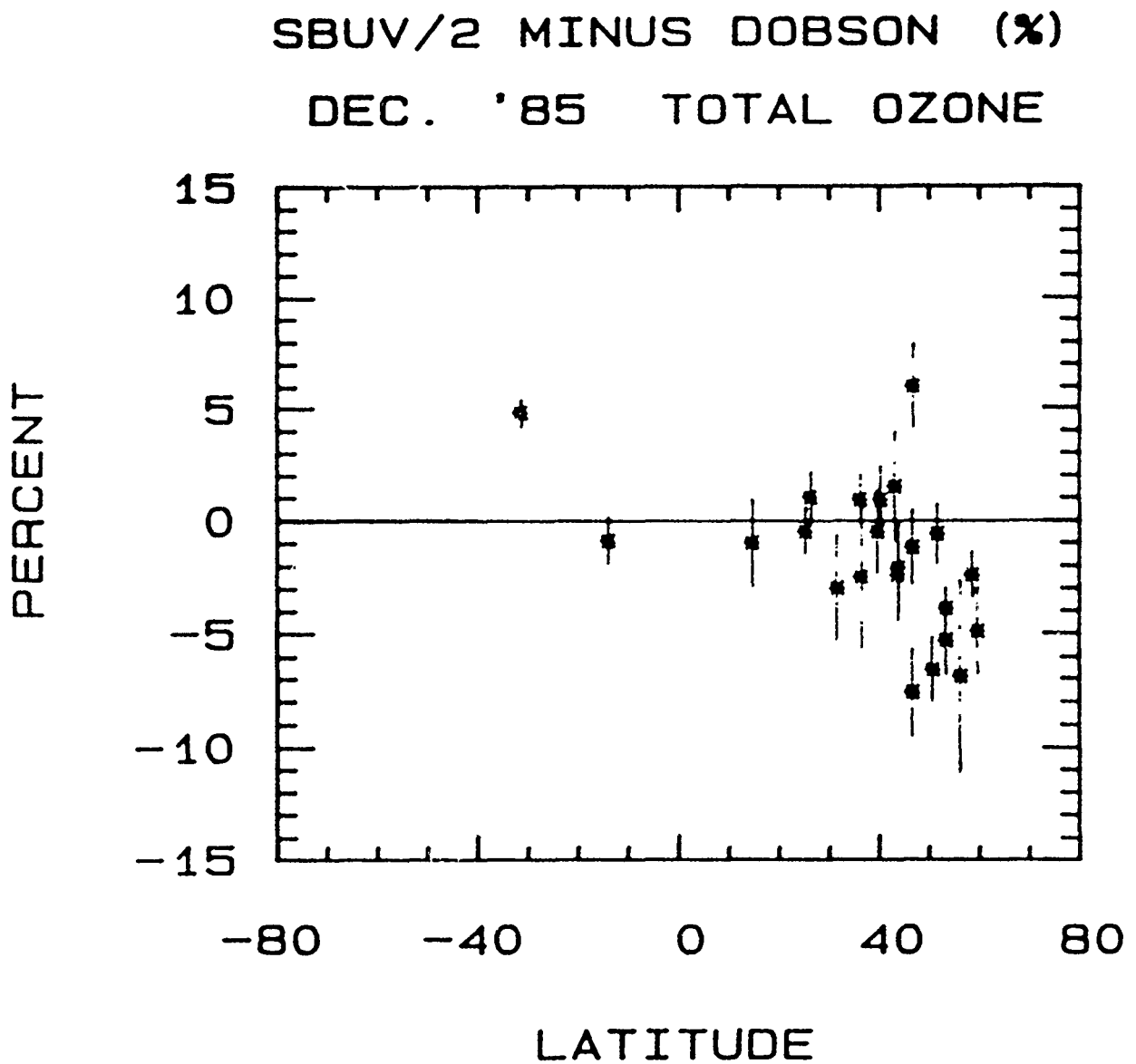
SBUV/2 MINUS DOBSON (%)
DEC. '85 TOTAL OZONE
PERCENT
15
10
5
0
-5
-10
-15
-80
-40
0
40
80
LATITUDE

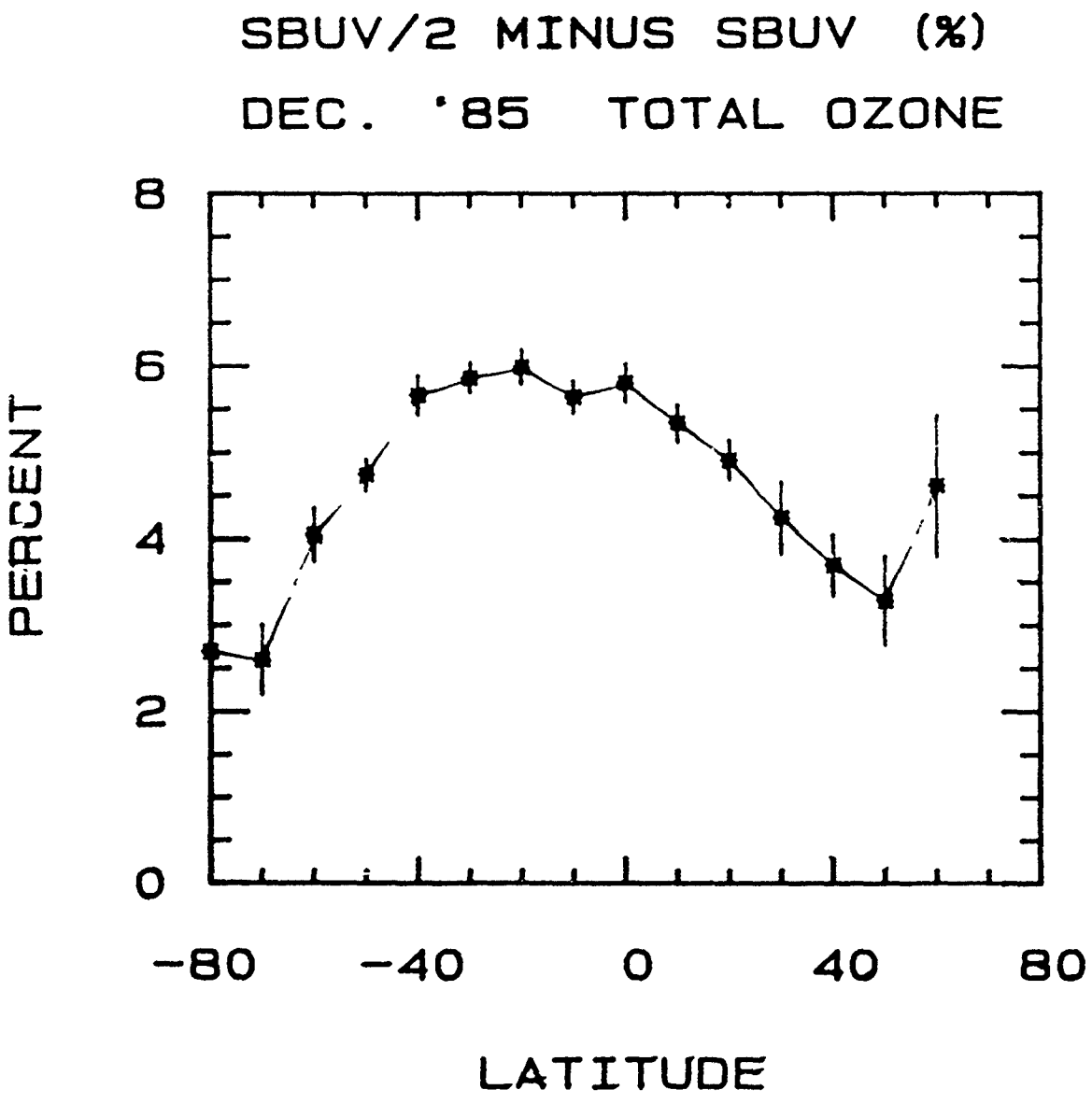
SBUV/2 MINUS SBUV (%)
DEC. '85 TOTAL OZONE
PERCENT
8
6
4
2
0
-80
-40
0
40
80
LATITUDE

TOTAL OZONE MODEL

$$\Delta O3 \sim \Delta \frac{(I/I0)}{1+SEC(\theta)}$$

$$FCT = 1/1+SEC(\theta)$$

$$\delta O3(2-1) = A+B*FCT1+C*FCT2$$

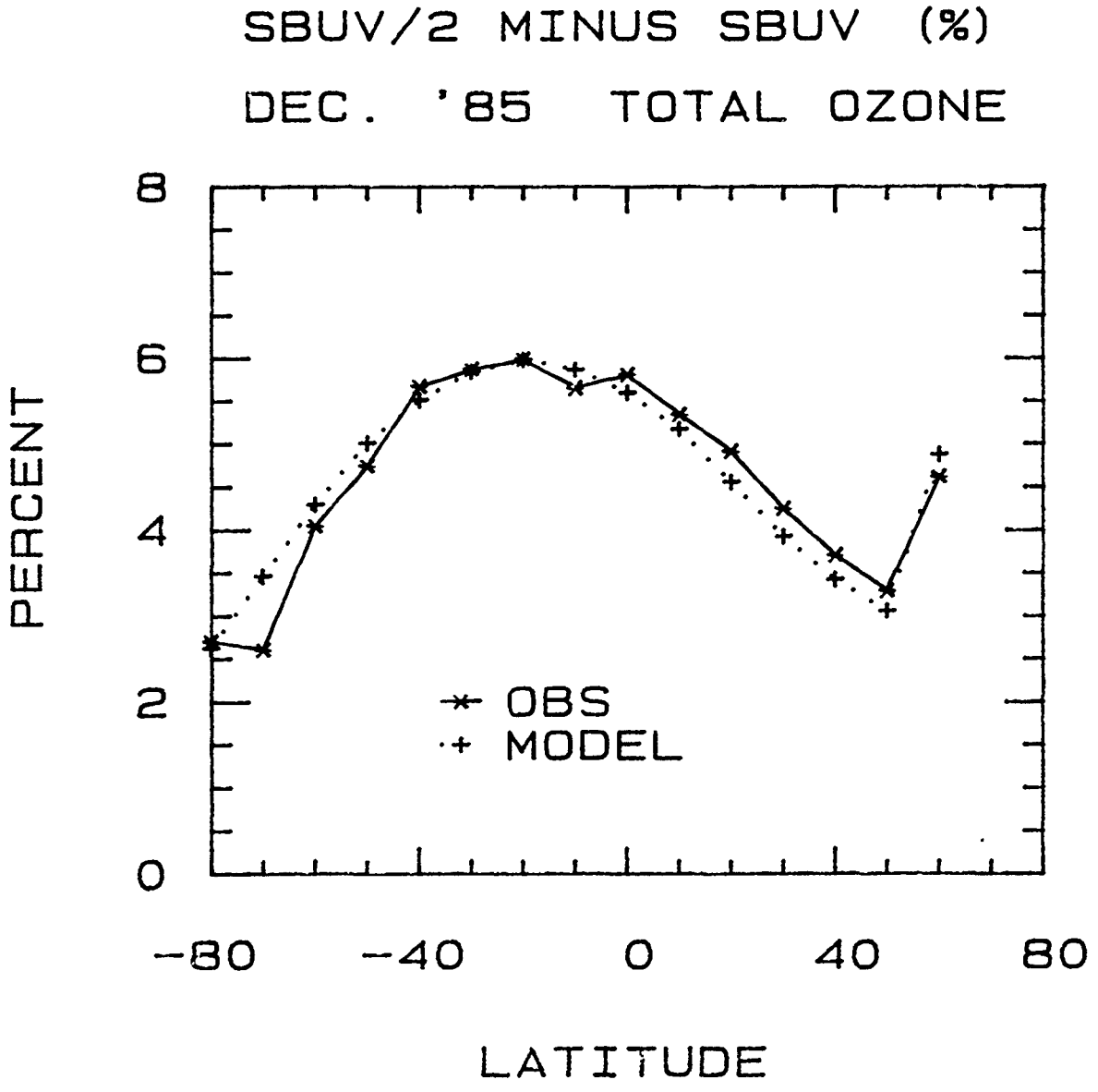
SBUV/2 MINUS SBUV (%)
DEC. '85 TOTAL OZONE
PERCENT
8
6
4
2
0
OBS
MODEL
-80
-40
0
40
80
LATITUDE

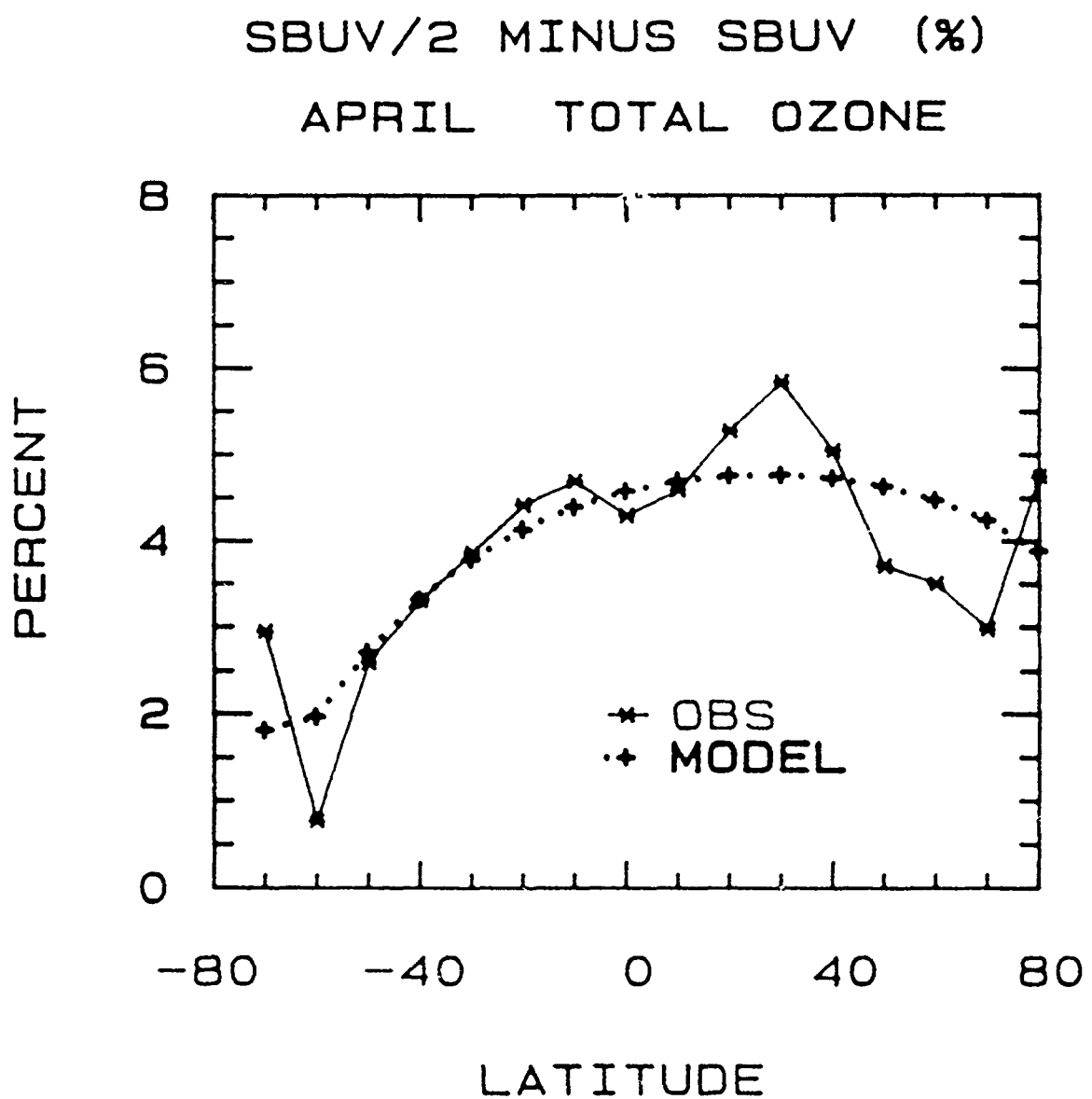
SBUV/2 MINUS SBUV (%)
APRIL TOTAL OZONE
PERCENT
8
6
4
2
0
OBS
MODEL
-80
-40
0
40
80
LATITUDE

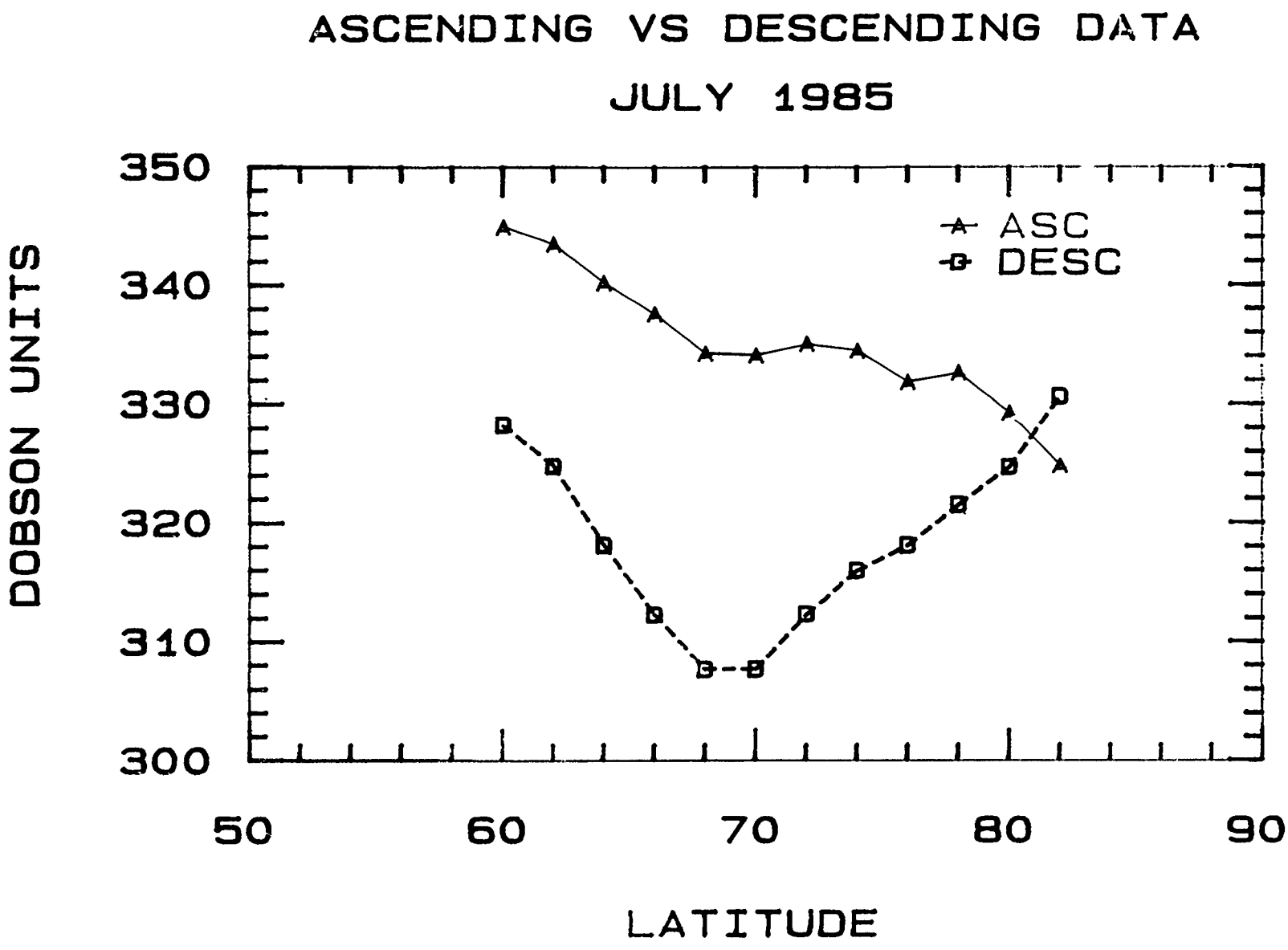
ASCENDING VS DESCENDING DATA
JULY 1985
DOBSON UNITS
350
340
330
320
310
300
50
60
70
80
90
LATITUDE
ASC
DESC

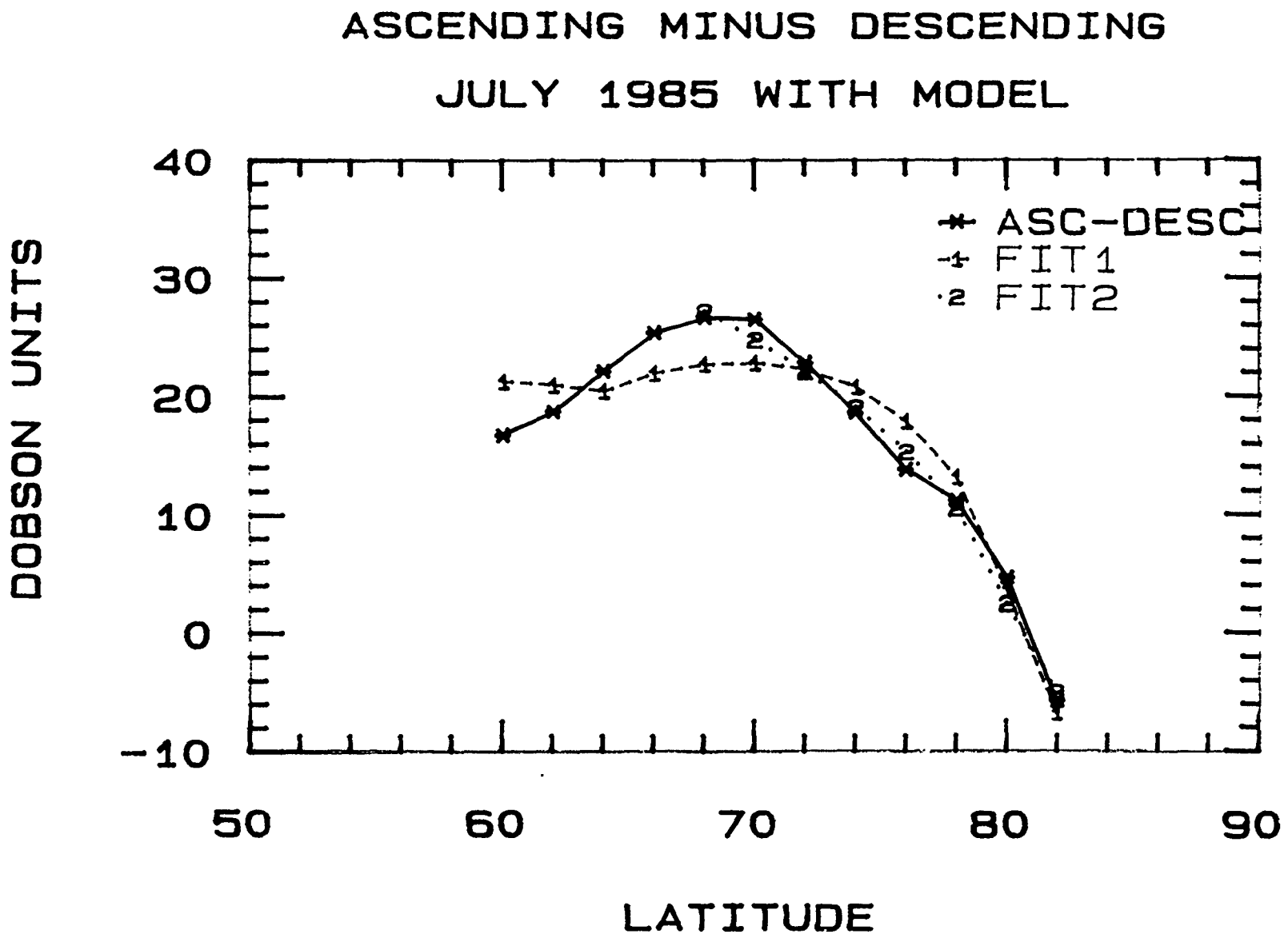
ASCENDING MINUS DESCENDING
JULY 1985 WITH MODEL
DOBSON UNITS
40
30
20
10
0
-10
50
60
70
80
90
LATITUDE
ASC-DESC
FIT1
FIT2

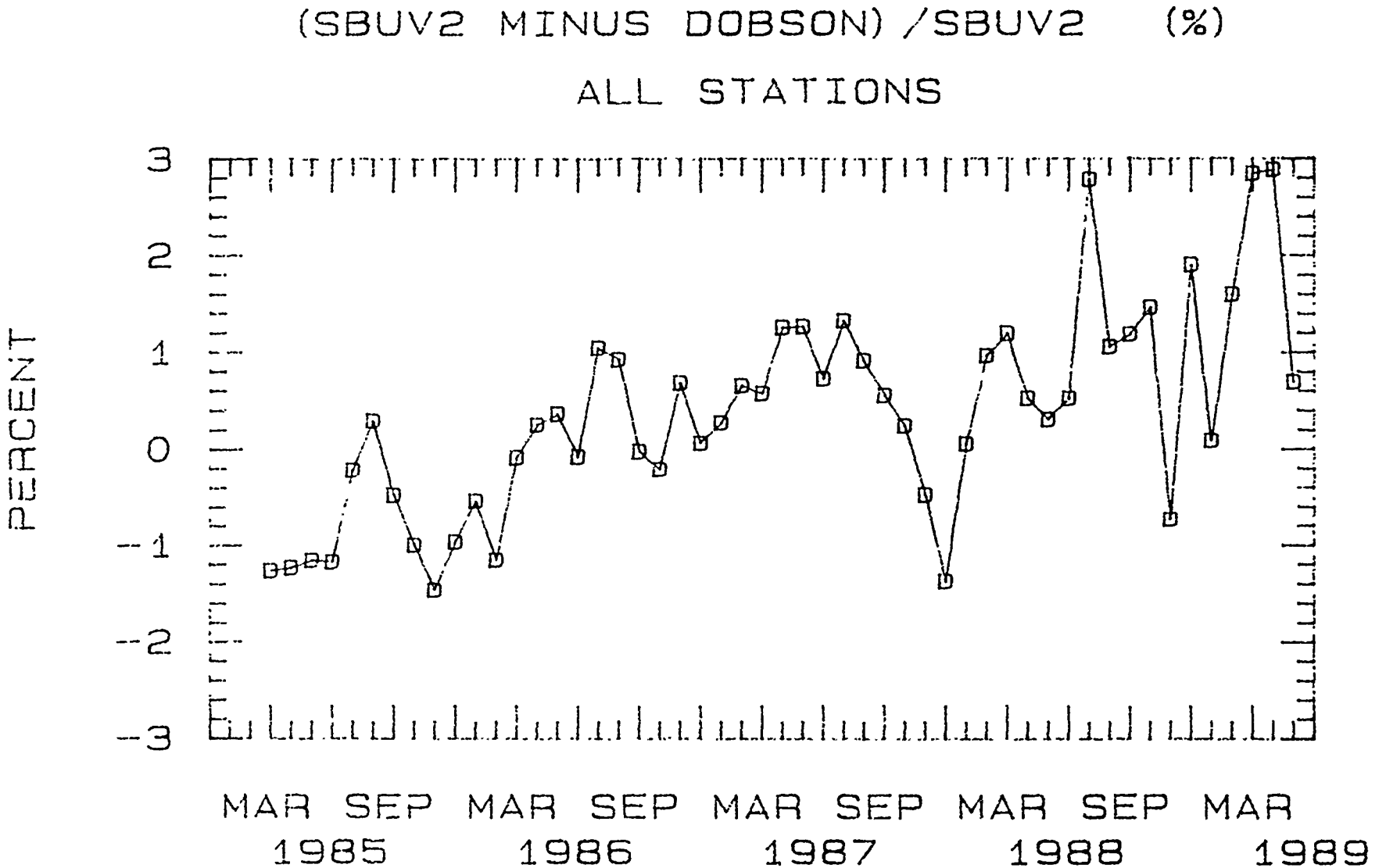
(SBUV2 MINUS DOBSON)/SBUV2 (%)
ALL STATIONS
PERCENT
3
2
1
0
-1
-2
-3
MAR SEP MAR SEP MAR SEP MAR SEP MAR
1985 1986 1987 1988 1989

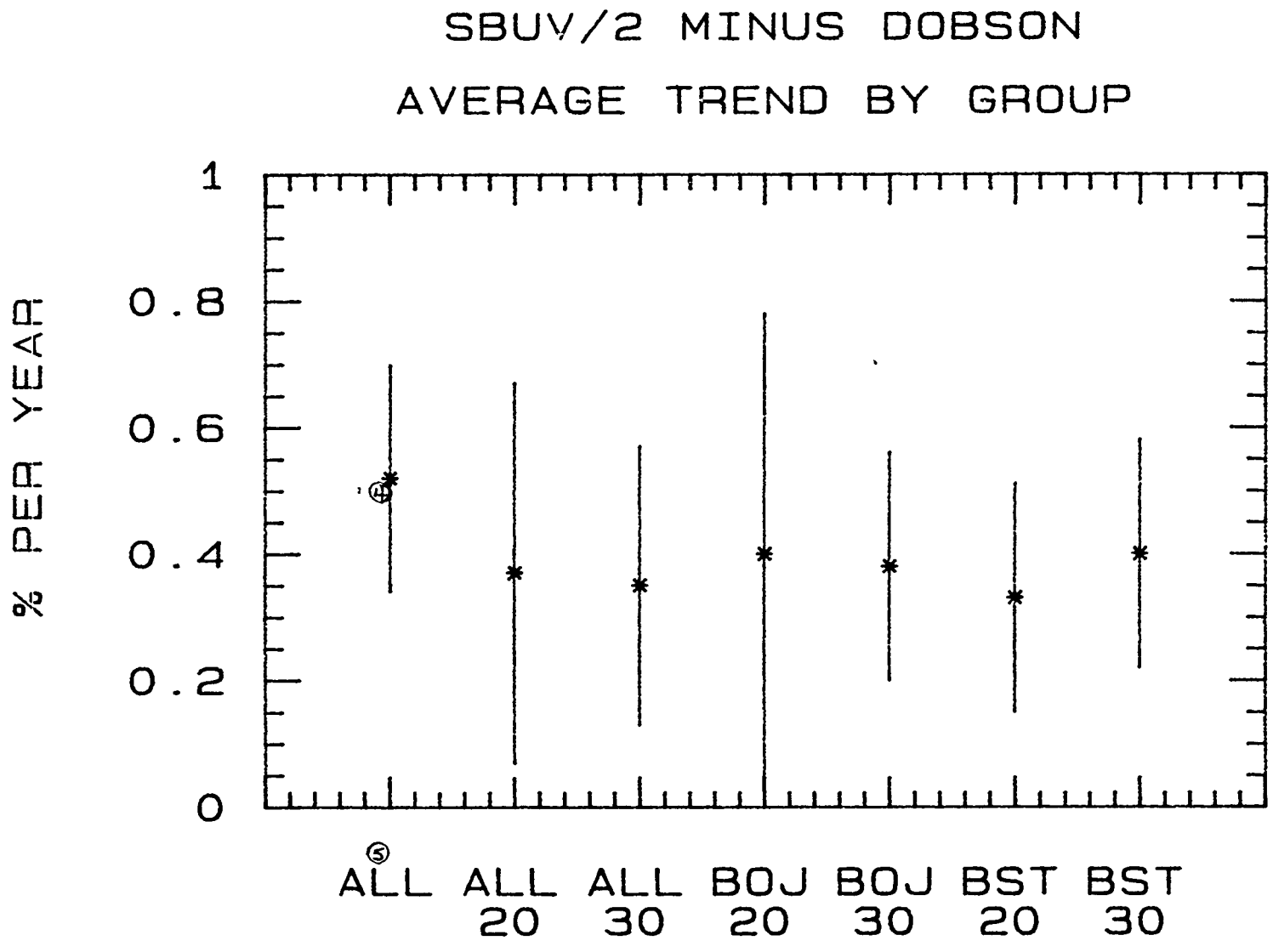
SBUV/2 MINUS DOBSON
AVERAGE TREND BY GROUP
% PER YEAR
1
0.8
0.6
0.4
0.2
0
ALL
ALL 20
ALL 30
BOJ 20
BOJ 30
BST 20
BST 30

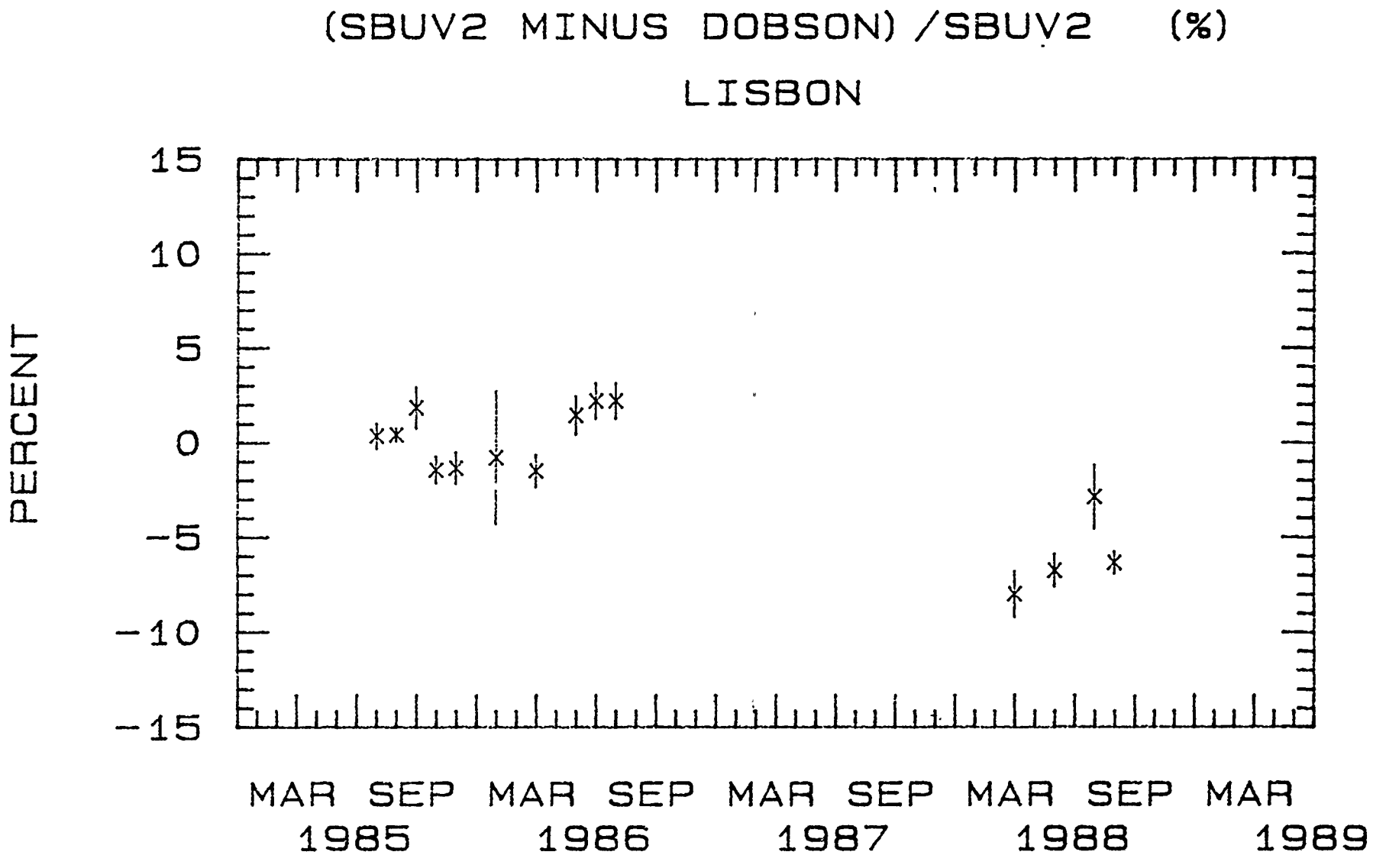
(SBUV2 MINUS DOBSON) /SBUV2 (%)
LISBON
PERCENT
15
10
5
0
-5
-10
-15
MAR SEP MAR SEP MAR SEP MAR SEP MAR
1985 1986 1987 1988 1989

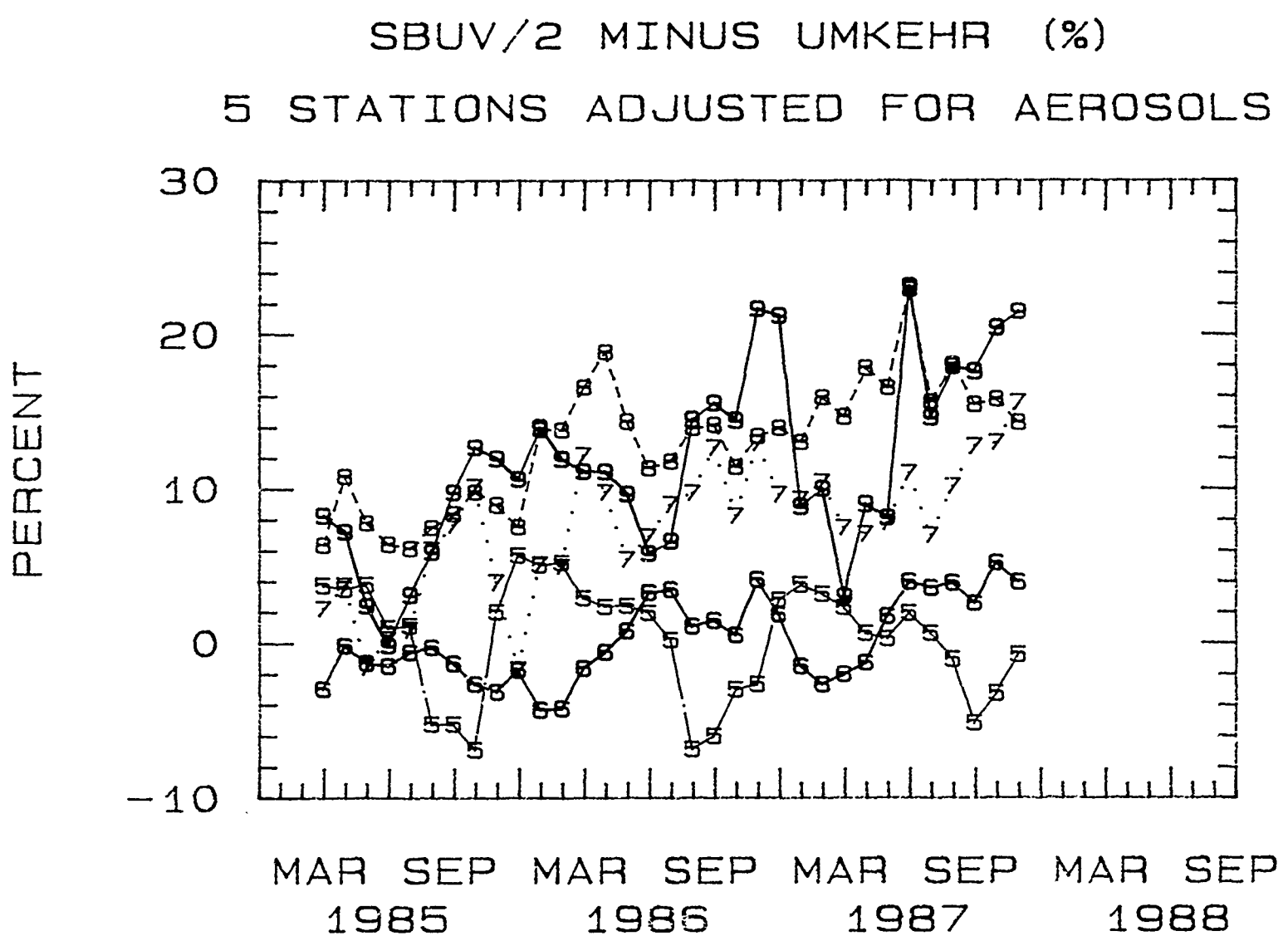
SBUV/2 MINUS UMKEHR (%)
5 STATIONS ADJUSTED FOR AEROSOLS
PERCENT
30
20
10
0
−10
MAR SEP MAR SEP MAR SEP MAR SEP
1985 1986 1987 1988

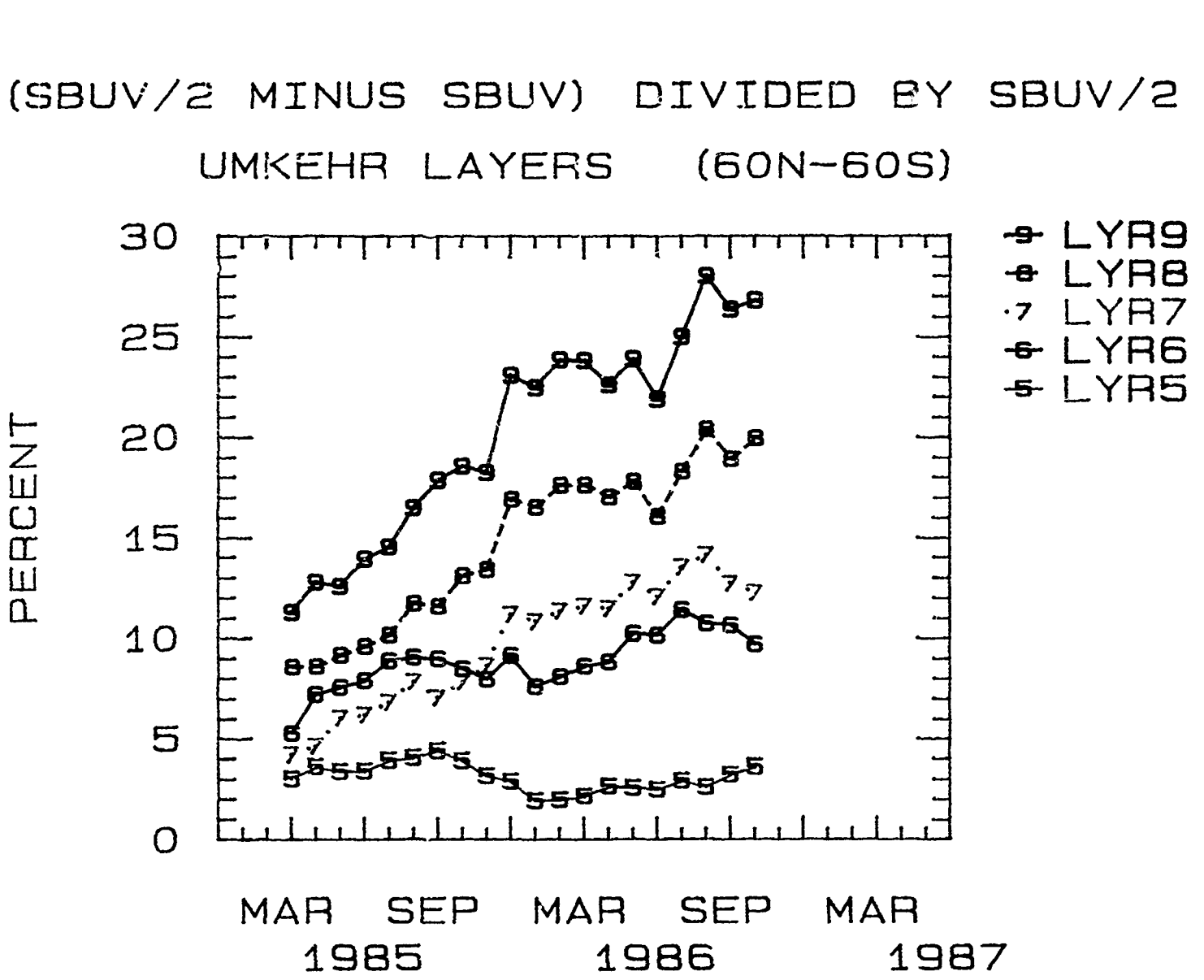
(SBUV/2 MINUS SBUV) DIVIDED BY SBUV/2
UMKEHR LAYERS (60N-60S)
PERCENT
30
25
20
15
10
5
0
MAR
SEP
MAR
SEP
MAR
1985
1986
1987
LYR9
LYR8
LYR7
LYR6
LYR5

Attachment 8
Umkehr Work
J. DeLuisi
NOAA/ERL-CMDL

UMKEHR WORK

J. DeLuisi

INTRODUCTION

The primary focus of our Umkehr work is to produce an Umkehr measurement record of the highest quality for validation of satellite determinations of ozone profile and for determining trends in stratospheric ozone profile as an independent validation of satellite results. To produce Umkehr ozone profiles of the highest quality it is necessary to account for every factor that affects the measurement. To do this, our work involved the following set of tasks:

* corrections for stratospheric aerosol
* qualifying the character of the zenith sky during an observation
* turbidity observations for tropospheric aerosol information
* algorithm performance evaluation and development of updated versions
* comparisons of Umkehr ozone profiles with other types of ozone profiles

By far the greatest effort thusfar is corrections for stratospheric aerosols because of their tendency to introduce characteristic errors in the upper stratospheric ozone concentrations. The correction effort can be separated into two parts:

1) development of the theory for corrections
2) acquisition of stratospheric aerosol information

A schematic diagram of the correction procedure is shown in Fig. 1, taken from DeLuisi, et al., 1989.

This report briefly describes the accomplishments of the past work, which includes special efforts to acquire stratospheric aerosol information.

CORRECTION FOR STRATOSPHERIC AEROSOL ERROR

During the El Chichon episode we had to resort to lidar observations of stratospheric aerosol profiles as our primary data source. We organized a World Lidar Network and approached the WMO for endorsement of the network. The lidar data we acquired from the network permitted us to make corrections for the years 1979-1986. The method of calculation follows that of DeLuisi (1969) and Dave et al. (1979). For stratospheric aerosol optical properties we used the NASA U2 aerosol size distribution to calculate aerosol extinction and phase function. The calculated optical properties were consistent with measured spectral extinction, giving greater credibility to the calculated values. We have provided additional stratospheric aerosol corrections to NESDIS up to and including 1988. The latter set of corrections are based on mid-latitude lidar measurements made at Boulder. Comparisons of Boulder lidar measurements with Mauna Loa lidar measurements indicate little difference in stratospheric aerosol concentrations.

We have now acquired the SAGE II comprehensive data set that begins in late 1984. This data set, consisting of pressure, temperature, ozone profile and aerosol profile, is ideal for calculating aerosol errors. We have edited the data set for cirrus cloud interference (usually below 15 km) and have begun to calculate monthly average stratospheric aerosol error corrections for 10° latitude bands. The results will be forwarded to NESDIS and as they become available (within a few weeks) will be archived in a NOAA data report.

The precision of the SAGE calculations will be much improved over the lidar data set because we have a greater amount of data and more specific information on spectral extinction. An additional benefit derived from the SAGE II data is that we were able to validate the accuracy of the lidar data, which requires two assumptions in the reduction process to obtain optical thickness. The results of this comparison were quite gratifying. Figure 2 shows a comparison between lidar data obtained at Mauna Loa Observatory and SAGE II data for a 10° latitude band centered at 20°N latitude. Figure 3 shows a similar comparison, but for the Boulder lidar located at 40°N. This plot shows an apparent annual variation between the two measurements which we attribute to the problem of normalizing the lidar measurement at the minimum backscattering level, and the use of a standard atmospheric air density profile that does not account for annual variations. We believe the first problem may be the

most important. Regarding the second problem, we are working on an annually varying air density profile for the data reduction procedure. Despite the annual cycle differences seen in the Boulder lidar data the magnitude agrees quite well with the SAGE II data. One must keep in mind that these stratospheric aerosol levels are near background level (defined by the 1979 lidar results) which is extremely low ~0.003. Such low levels are very difficult to measure because we are approaching the lower limits of measurement sensitivity.

The SAGE II data were used to compare our Umkehr aerosol corrections using ground-based data with corrections calculated from the independent satellite data. An example of a comparison is shown in Fig. 4 for Mauna Loa. This exercise helped to provide us with an estimate of our uncertainties on the monthly time scale and the longitudinal representativeness of data obtained at a single site within a latitude band.

A source of stratospheric aerosol optical property information is from Mie calculations using in situ measured size distributions. Approximately 2 years ago we were given reason to believe that in situ measurements might cease entirely. This information stimulated us to write to the chairman of the International Radiation Commission expressing our concern. As a result, a subgroup for stratospheric aerosols was eventually formed as a part of the International Aerosol Climatology Project. The subgroup has been quite active under the leadership of R. Pueschel of NASA Ames.

COMPARISON OF UMKEHR PROFILES

As a part of our attempts to understand and quantify the quality of Umkehr profile data we have compared data with ozonesondes, SAGE, and SBUV. Such comparisons provide us with information which is useful for understanding the performance of the inversion algorithms used for the Umkehr and SBUV. We undertook a cooperative theoretical investigation to compare the performances of the Umkehr algorithm with the SBUV algorithm. Table 1, taken from DeLuisi et al. (1988) shows the results of the comparison. This work was the first of its kind. A similar comparison will be performed with a modernized version of the Umkehr algorithm when it is completed. Work is presently underway on the development of the algorithm which we are attempting to make a closer relative to the SBUV. It is extremely important to understand the mutual performance of the algorithms,

because their differences will appear in the comparisons of operationally retrieved profiles. Such comparisons and algorithm improvements will ultimately lead to a firmer-based ozone profile observation system methodology, leading to a significant reduction in errors.

We plan to make greater use of the SAGE data for comparisons with our aerosol and ozone profile data as well as to use it as a possible source of a priori information for algorithm development and performance evaluation.

SKY QUALITY FOR UMKEHR OBSERVATIONS

Several years ago we developed a highly sensitive zenith-sky cloud detector to observe possible cloud interference while an automated Dobson was making an Umkehr measurement. This detector has become a regular part of the 7-station automated Dobson network. We have now acquired a sufficient amount of simultaneous zenith sky and Umkehr data to begin a study leading to an objective method to define the quality of an Umkehr measurement. Figure 5 shows a plot of an Umkehr and zenith-sky cloud signals, typical of the data sets now being acquired. This work represents our efforts to improve our observational capabilities leading to further reduction in data errors.

REMOTE SENSING IMPROVEMENTS

As a part of the ERL mission to acquire the highest quality ozone profile measurements for trend determinations we have moved ahead with the development of an inversion algorithm to directly infer the expected SBUV albedo measurements from the ground-based Umkehr measurement. Actually, other types of zenith-sky spectral uv measurements can be used instead of the Umkehr; however, the Umkehr data set is the most abundant so we have chosen to use this set. The algorithm uses SAGE II ozone profile data for a priori information.

We finished a preliminary theoretical feasibility study last summer and plan to further explore the potential of the method. As an ultimate goal, we are proposing to develop a four-component remote sensing system with existing measurement. The existing measurements are the SBUV, SAGE II, Umkehr, and the existing Robertson-Berger (RB) uv network (which

we recently acquired in GMCC). It is hoped that the RB instruments will eventually be replaced with higher quality instruments, as being planned by the various agencies such as EPA and DOA. We have already explored the use of the SBUV measurements to estimate the spectral uv flux at the earth's surface by use of an algorithm that is essentially an upside-down version of the Umkehr algorithms used to estimate SBUV albedo measurements.

The value of tying the four measurements is obvious. We have a potentially improved method for monitoring stratospheric ozone trends and a means to obtain a global climatology of uv fluxes at the surface and trends as well. This arrangement is directed towards answering questions concerning ozone trends, calibration, and the impact on the uv climatology at the earth's surface.

REFERENCES

DeLuisi, J. J., A study of the effect of haze upon Umkehr measurements, Q. J. R. Meteorol. Soc., 95, 181-187, 1969.

Dave, J. V. J. J. DeLuisi, and C. L. Mateer, 1979, Results of a comprehensive theoretical examination of the optical effects of aerosols on the Umkehr measurements, Spec. Environ. Rep. 14, pp. 15-22, World Meteorol. Organ., Geneva, 1979.

DeLuisi, J. J., D. U. Longenecker, C. L. Mateer, and D. J. Wuebbles, 1989, An analysis of northern middle latitude Umkehr measurements corrected for stratospheric aerosols for 1979-1986, J. Geophys. Res., 94, 9837-9846, 1989.

DeLuisi, J. J., D. U. Longenecker, P. K. Bhartia, C. L. Mateer, and C. G. Wellemeyer, Ozone profiles by Umkehr, SBUV, and ozonesonde: A comparison including the inversion algorithms for Umkehr and SBUV, Atmospheric Ozone, Quadren. Ozone Symposium, 8-13 August, Gottingen, F.R.G., 1988.

TABLE 1. COMPARISON OF SBUV INVERSION RESULTS WITH UMKEHR INVERSION RESULTS USING SYNTHETIC DATA COMPUTED FROM TEST SAGE II AND OZONESONDE DATA*

a. Bias

Layer No.	Test Profile (annual average) (D.U.)	SBUV-Test (annual average) Difference (%)	Umkehr-Test (annual average) Difference (%)	SBUV-Umkehr (annual average) Difference (%)	SBUV-Umkehr (temp. effect) %
9	2.78	0	-11	12	7.5 ± 2.5
8	8.84	-2	-5	4	4.9 ± 0.9
7	20.4	0	-4	4	3.1 ± 0.8
6	38.7	1	12	-10	0.35 ± 1.1
5	63.0	5	10	-5	-0.75 ± 1.5
4	76.8	8	-8	17	-2.0 ± 1.1
3	57.4	-15	-9	-7	-3.5 ± 1.1
2	25.4	-7	48	-37	-4.0 ± 1.5
1	25.1	9	-27	49	-13.6 ± 9.9

b. Standard deviation

Layer no.	SBUV-Test (%)	Umkehr-Test (%)	SBUV-Umkehr (%)
9	2.9	3.6	4.3
8	1.1	3.7	3.9
7	1.0	3.5	3.9
6	1.5	4.1	5.2
5	2.3	3.5	3.3
4	2.9	3.9	5.7
3	7.0	4.7	6.7
2	6.9	9.2	14.4
1	12.8	3.6	11.3

c. Correlation

Layer no.	SBUV-Test	Umkehr-Test	SBUV-Umkehr
9	0.99	0.95	0.98
8	0.99	0.87	0.83
7	0.99	0.90	0.87
6	1.00	0.97	0.96
5	0.80	0.47	0.35
4	0.97	0.92	0.85
3	0.92	0.98	0.92
2	0.99	0.97	0.95
1	0.36	0.97	0.36

*Number of data points is 11.

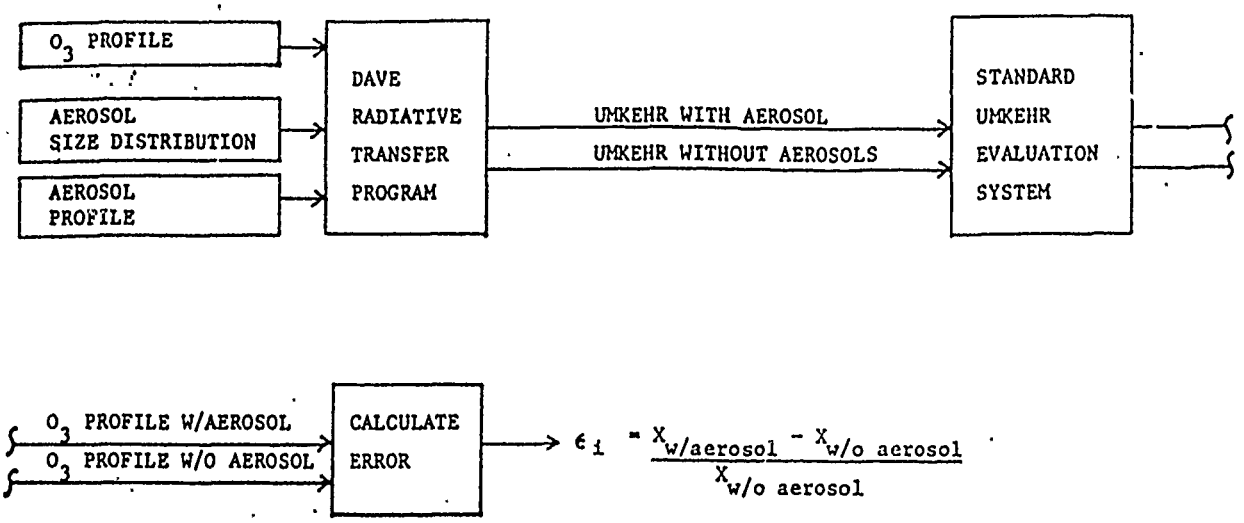

Fig. 1. Scheme of the steps taken to calculate the aerosol error to the Umkehr ozone profile.

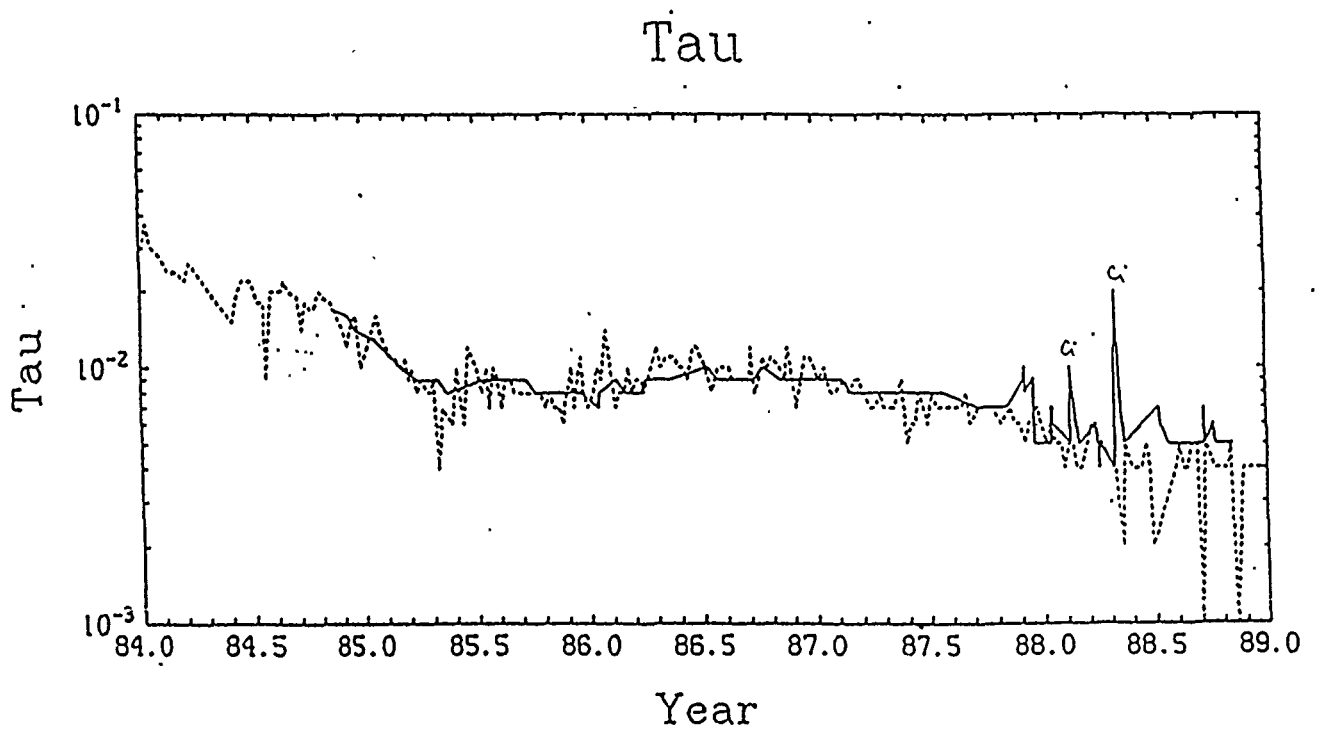

Fig. 2. Comparison between Mauna Loa lidar and SAGE II integrated aerosol optical thickness above 15 km. The SAGE II data are an average over a 10° latitude band centered at 20°N.

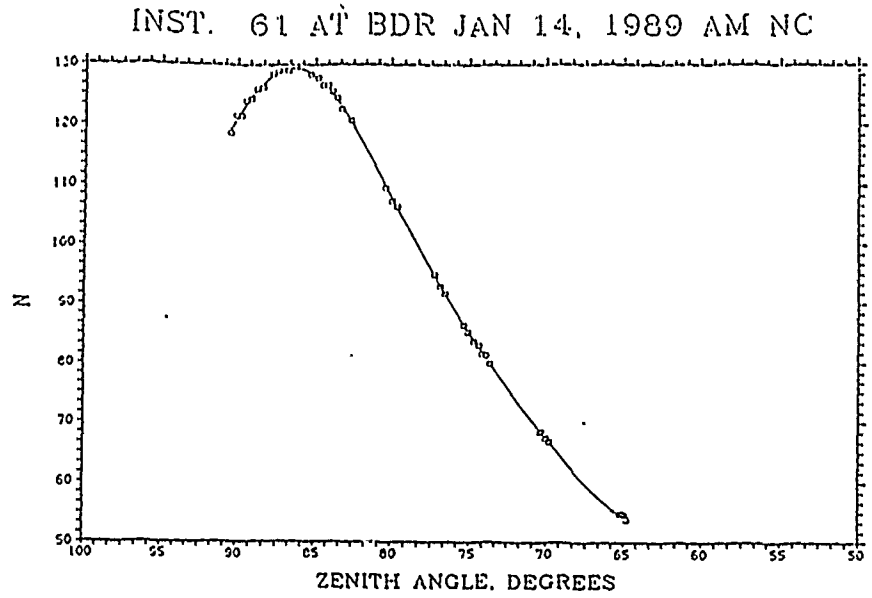

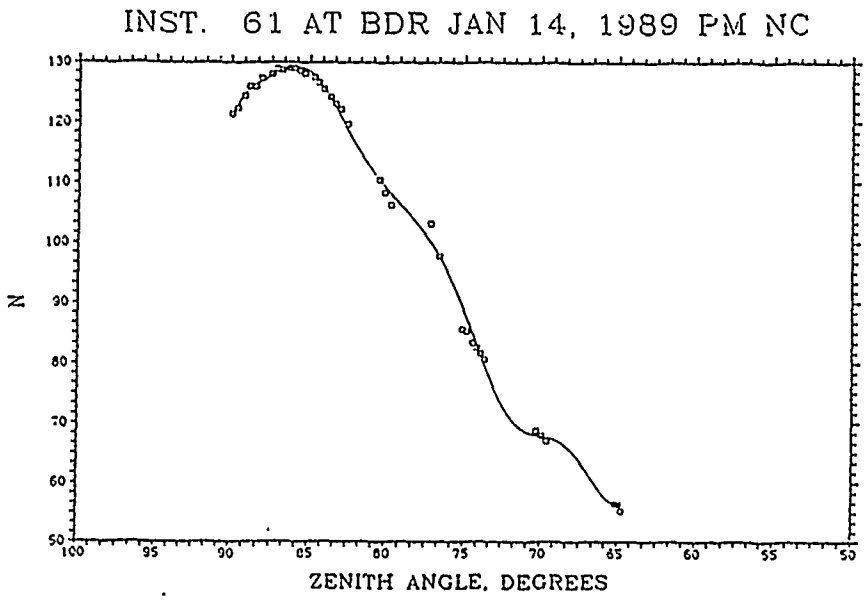

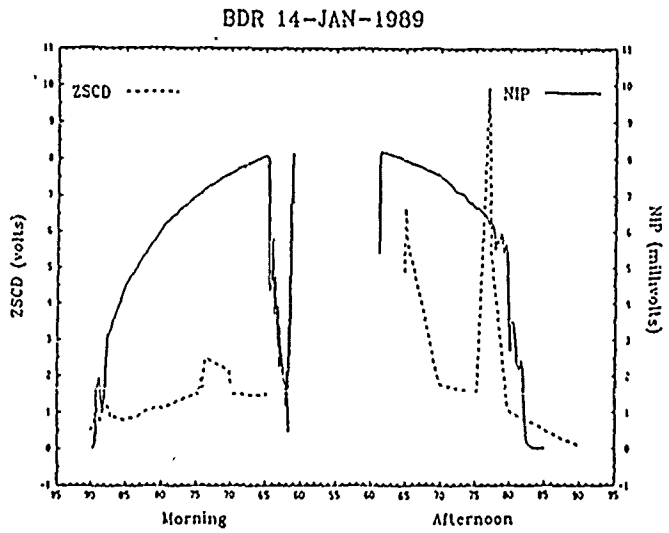

Fig. 5. Plot of an Umkehr measurement and simultaneous signals from the zenith-sky cloud detector.

Attachment 9

Initial Estimate of NOAA-9 SBUV/2 Total Ozone Drift: Based on Comparison with Re-Calibrated TOMS Measurements and Pair Justification of SBUV/2

C.G. Wellemeyer, S.L. Taylor, and X.U. Gu
ST Systems Corp.
R.D. McPeters and R.D. Hudson
NASA/GSFC

Initial Estimate of NOAA-9 SBUV/2 Total Ozone Drift: Based on Comparison with Re-calibrated TOMS Measurements and Pair Justification of SBUV/2

C.G. Wellemeyer, S.L. Taylor, and X.U.Gu
ST Systems Corp., Lanham Maryland

R.D. McPeters and R.D. Hudson
Laboratory for Atmospheres
NASA/GSFC Greenbelt, Maryland

Abstract-Newly recalibrated Version 6 TOMS data are used as a reference measurement in a comparison of monthly means of total ozone in 10 degree latitude zones from SBUV/2 and the nadir measurements from TOMS. These comparisons indicate a roughly linear long-term drift in SBUV/2 total ozone relative to TOMS of about 2.5 Dobson units per year at the equator over the first three years of SBUV/2. The pair justification technique is also applied to the SBUV/2 measurements in a manner similar to that used for SBUV and TOMS. The higher solar zenith angles associated with the afternoon orbit of NOAA-9 and the large changes in solar zenith angle associated with its changing equator crossing time degrade the accuracy of the pair justification method relative to its application to SBUV and TOMS, but the results are consistent with the SBUV/2 - TOMS comparisons, and show a roughly linear drift in SBUV/2 of 2.5 - 4.5 Dobson units per year in equatorial ozone.

SBUV/2 - TOMS Comparisons

The first ten years of data (11/78 - 10/88) from the Total Ozone Mapping Spectrometer (TOMS) have been reprocessed using an improved long-term calibration. The calibration adjustment was derived using the pair justification technique. The nadir samples of these data have been averaged to provide cross-track spacial resolution comparable with the SBUV/2 field of view, and then averaged monthly in 10 degree latitude bands centered at the equator. A little over three years (3/85-8/88) of reprocessed SBUV/2 total ozone data have been averaged monthly in the same latitude bands. Figure 1 shows the difference of these monthly zonal means in the equatorial band over the period of the SBUV/2 data set. The standard error of the monthly means contain a lot of seasonal and day-to-day variance. The standard errors of daily means of SBUV/2 and TOMS should be considered later in this study to provide a statistical estimate of the noise in this comparison. For now, it is noted that an apparent seasonal cycle in the differences is resolved to some extent. A mechanism for such a cycle is not well understood at this time, but correlation between this cycle and the variation in the SBUV/2 solar azimuth angle should be studied further. Note that a smaller seasonal cycle of about 1% amplitude is present in the TOMS total ozone relative to SBUV (Wellemeyer et al, 1988), which also correlates with this effect. A least-squares linear fit to the data in Figure 1 gives a drift in SBUV/2 relative to the preliminary V6 TOMS of about 2.4 D.U./Yr. Figure 2 shows changes in SBUV/2 equatorial reflectivity relative to V6 TOMS. Figures 1 and 2 provide somewhat different impressions of the time signature of SBUV/2 -V6 TOMS differences.

Figures 3 and 4 show differences between the monthly zonal means of the A-pair (312.5-331.2 nm) and B-pair (317.5-331.2 nm) total ozone from SBUV/2 and the corresponding pairs from TOMS. These comparisons indicate that the B-pair from SBUV/2 drifts about twice as much relative to V6 TOMS as does the SBUV/2 A-pair. Note that the V6 TOMS data have been pair justified so that the B'-pair (317.5-339.8 nm) actually used in the TOMS retrieval gives the same long-term change in total ozone as does the V6 TOMS A-pair. The difference in drift between the pair results from SBUV/2 are symptomatic of a wavelength dependent calibration error in the albedo measured by SBUV/2. This is because different pairs of total ozone wavelengths have different sensitivities to this type of calibration error. The two major factors in these differences are the sensitivity of the pair to the presence of ozone, and the wavelength separation the pair. The diagram below illustrates that the B-pair is about twice as sensitive to a given error in the N-value than the B-pair.

Basic Total Ozone Retrieval and Impact of Pair Sensitivity on Error Budget

Measure Quantity: N = -100 log [I/F]

Pair N values: $N_A = N_{313} - N_{331}$ $N_B = N_{318} - N_{331}$

For a given set of viewing conditions:

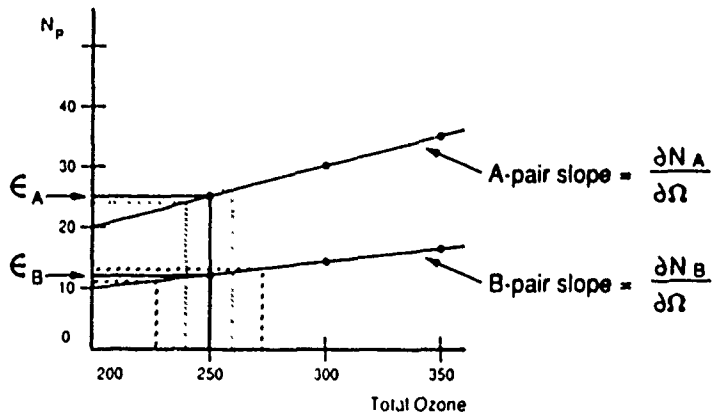

Secondly, if a wavelength dependent error in calibration is present, it would be expected that the size of the error across a given pair would be proportional to its wavelength separation. The table below shows the wavelength separation and the ozone sensitivity of several pairs of total ozone wavelengths. Also shown is the ratio of wavelength separation to ozone sensitivity which provides a sensitivity factor for each pair of wavelengths to the presence of wavelength dependent calibration errors that are proportional to wavelength separation.

Different pairs have different sensitivities to wavelength-dependent calibration errors.

This sensitivity depends on:

1) The separation of the wavelengths used
2) The differential ozone absorption across the pair (ozone sensitivity)

Pair Name	Wavelength (nm)	$\Delta\lambda$ (nm)	Sensitivity (N-value/D.U.)	$\frac{\Delta\lambda}{\text{Sensitivity}}$
B'	318 - 340	22.3	0.073	306
B	318 - 331	13.7	0.063	218
A	313 - 331	18.7	0.125	150
A'	313 - 318	5.0	0.062	81
D	306 - 313	6.7	0.190	35

The D-pair retains high ozone sensitivity at a small wavelength separation because it lies on a steeper portion of the Hartley absorption peak than the other pairs. Because of the higher absorption, however, this pair only provides sufficient penetration to measure total ozone at near overhead sun conditions. This pair was used to good advantage in pair justification of the SBUV and TOMS data sets, but cannot be used for SBUV/2 because of the higher solar zenith angles associated with the afternoon equator crossing of NOAA-9. Pair justification can still be applied to SBUV/2, however by coupling other pairs with contrasting sensitivities to wavelength dependent calibration errors and insisting that they give the same measurement of long-term changes in total ozone.

The diagram below illustrates the fundamental formula used in the application of pair justification. For identical viewing conditions at time t=0 and time t, a change in the measured pair N-value is the sum of two terms: the change in N-value due to real changes in ozone, and the change due to drift in instrument calibration. A difficulty in applying this formula to the SBUV/2 data is that viewing conditions are generally quite different at t=0 and t. Figure 5 shows the monthly zonal mean of the solar zenith angles associated with the SBUV/2 total ozone measurements as a function of time. Because of this, a large adjustment (about 11 N-value units for A-pair) must be made to the measured N-values in 8/88 to normalize them to initial conditions. A test of the accuracy of this correction is discussed below.

Basic Formula for Pair Justification

For identical viewing conditions at t = 0 and t:

$$\Delta N_p(t) = \frac{\partial N_p}{\partial \Omega} \Delta \Omega_{true}(t) + \epsilon_p(t)$$

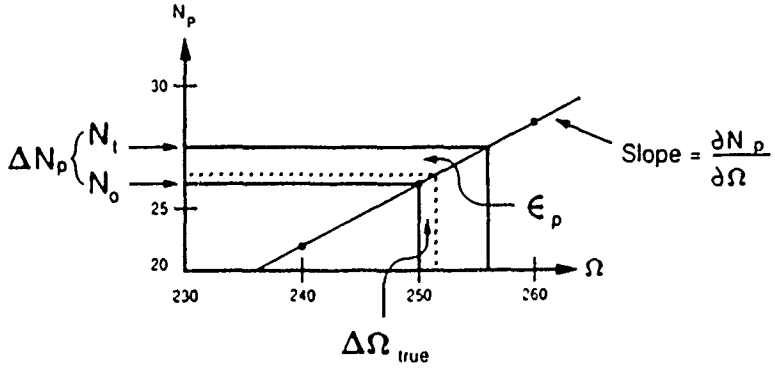

The application of this basic formula consists of writing it for a pair of wavelengths. An assumption about the wavelength dependence of the calibration is required, however to relate the errors of the pairs used. As shown below, this is accomplished by assuming (first order) that the pair error is proportional to the wavelength separation of the pair. This results in a set of three equations with three unknowns (true ozone change, and the errors across the coupled pairs). The solution for true ozone change can be used to compute pair calibration errors across the coupled pairs, and any other total ozone pairs.

Pair Justification Formulation

Write basic formula for pair of pairs:

$$\Delta N_A(t) = \frac{\partial N_A}{\partial \Omega} \Delta \Omega_{true}(t) + \epsilon_A(t)$$

$$\Delta N_{B'}(t) = \frac{\partial N_B}{\partial \Omega} \Delta \Omega_{true}(t) + \epsilon_{B'}(t)$$

Assume pair error proportional to $\Delta\lambda$:

$$\epsilon_A / \epsilon_{B'} = \Delta\lambda_A / \Delta\lambda_{B'}$$

Solve for $\Delta\Omega_{true}(t)$, $\epsilon_A(t)$, $\epsilon_{B'}(t)$, etc.

In general, this solution can be applied to individual scans. In practice, monthly zonal means of the measured N-values have been used, and monthly solutions to the above equations provide estimates of pair calibration errors. Additionally, the averaged N-values have been deseasonalized using the three year mean annual cycle as part of the effort to normalize the measured N-values to standard viewing conditions. In such a procedure, the linearity of operations performed in a convenient order come into question. The linearity test described below provides a test of the accuracy of the basic pair justification applied to mean N-values, and of the large solar zenith correction necessitated by precession of the NOAA-9 satellite.

Linearity Test of Basic Equation

Compute measured ozone change using averaged, deseasonalized, adjusted N-value changes:

$$\Delta\Omega_{meas}(t) = \Delta N_p(t) / \frac{\partial N_p}{\partial \Omega}$$

Compare with averaged, deseasonalized ozone from individual retrievals.

This test checks the linearity assumed in computing ozone from averaged deseasonalized N-values and the accuracy of adjustments.

The results of such a test applied to the first ten years of TOMS data are illustrated in Figure 6. The measured ozone changes derived from the individual V5 TOMS total ozone retrievals (averaged and de-seasonalized), and those derived from the averaged, de-seasonalized V5 TOMS N-values are shown as well as their difference. This result indicates that the basic pair justification equation is quite accurate as applied to the TOMS data set. Figure 2 illustrates the results of the same test applied to the SBUV/2 data set. Here, the measured change in equatorial ozone has no systematic long-term changes as seen in the case of TOMS. The difference between the two computations shows both larger variations and a systematic difference that is not present in the TOMS case.

Another possible error source in the pair justification method is related to the assumption of a linear dependence with wavelength of the calibration error. How sensitive are the pair justification results to the possible presence of curvature in the actual wavelength dependence the calibration error? Simulation studies have been performed in an effort to answer this question. The pair justification formulation is applied to simulated N-values that are computed assuming zero "true" ozone change and contain errors of arbitrary wavelength dependence. Figure 8 shows the results of pair justification applied to simulated N-value changes containing error that is linear wavelength. In this case, the simulated errors are consistent with the assumed wavelength dependence, and each alternate coupling of pairs does a perfect job of retrieving that dependence. For the results in Figure 9, however, a second order dependence has been included in the simulated N-value changes. Here, different couplings of pairs exhibit different sensitivities to the presence of curvature in the actual wavelength dependence. This sensitivity depends on the ozone sensitivities of the coupled pairs, and the wavelength range of the combined pairs. Because of the differing sensitivities of alternate couplings of pairs, the divergence of pair justification results from different couplings might be used to diagnose curvature. Because of the high solar zenith angles and associated errors in the basic equation, the applicability of this technique to the SBUV/2 data is limited.

The pair justification has been applied to the monthly averaged, deseasonalized, adjusted N-values measured by the SBUV/2 in the 10 degree equatorial zone using A-B' and A-A' couplings. The A-pair calibration errors derived using this method are shown in Figure 10. The equivalent error in equatorial ozone for the two couplings is shown in Figure 11. Least squares linear regressions applied to these results give slopes (standard errors) of 2.7 (0.2) D.U./Yr. for A-B' and 4.3 (0.4) D.U./Yr. for A-A'. Though the difference in these results appear to be statistically significant, and might indicate the presence of some curvature in the actual wavelength dependence of the calibration error, these differences might also be due to uncertainty in N-value adjustments for increasing solar zenith angles or non-linearities in the averaging process as described above.

Conclusions

The non-local noon equator crossing time and drift in equator crossing time of the NOAA-9 orbit limit the accuracy of the pair justification technique when applied to SBUV/2 data. This is largely due to the fact that the D-pair wavelengths (305.8-312.5 nm) cannot be used at solar zenith angles much larger than 30 degrees. When applied to the SBUV/2 data set, the pair justification method indicates that the drift in equatorial total ozone is between 2.5 and 4.5 D.U./Yr. This estimate is somewhat higher than estimates based on SBUV/2 - V6 TOMS comparisons presented here or SBUV/2 - Dobson comparisons performed elsewhere.

Continued Analysis

Some further work is planned in understanding the uncertainties in the pair justification technique as applied to the NOAA-9 SBUV/2 data set. In particular, the sources of non-linearities and possible errors in the solar zenith angle correction to the measured N-values will be considered. The pair justification technique, however appears to be of limited value when applied to this data set, and alternate means to the correction of the long-term calibration of the NOAA-9 SBUV/2 should be sought.

Further analysis of the SBUV/2 - V6 TOMS total ozone comparisons is planned. The latitude dependence of the long-term drift and the seasonal variation in the bias should provide additional insight to the character of the calibration error in the SBUV/2.

Reference

Wellemeyer, C.G., A.J. Fleig, and P.K. Bhartia; Internal Comparisons of SBUV and TOMS Total Ozone Measurements, Proceedings of the Quadrennial Ozone Symposium 1988, R.D. Bojkov, editor (1989).

Figure 1. Difference of monthly zonal means of total ozone (SBUV/2 - TOMS)

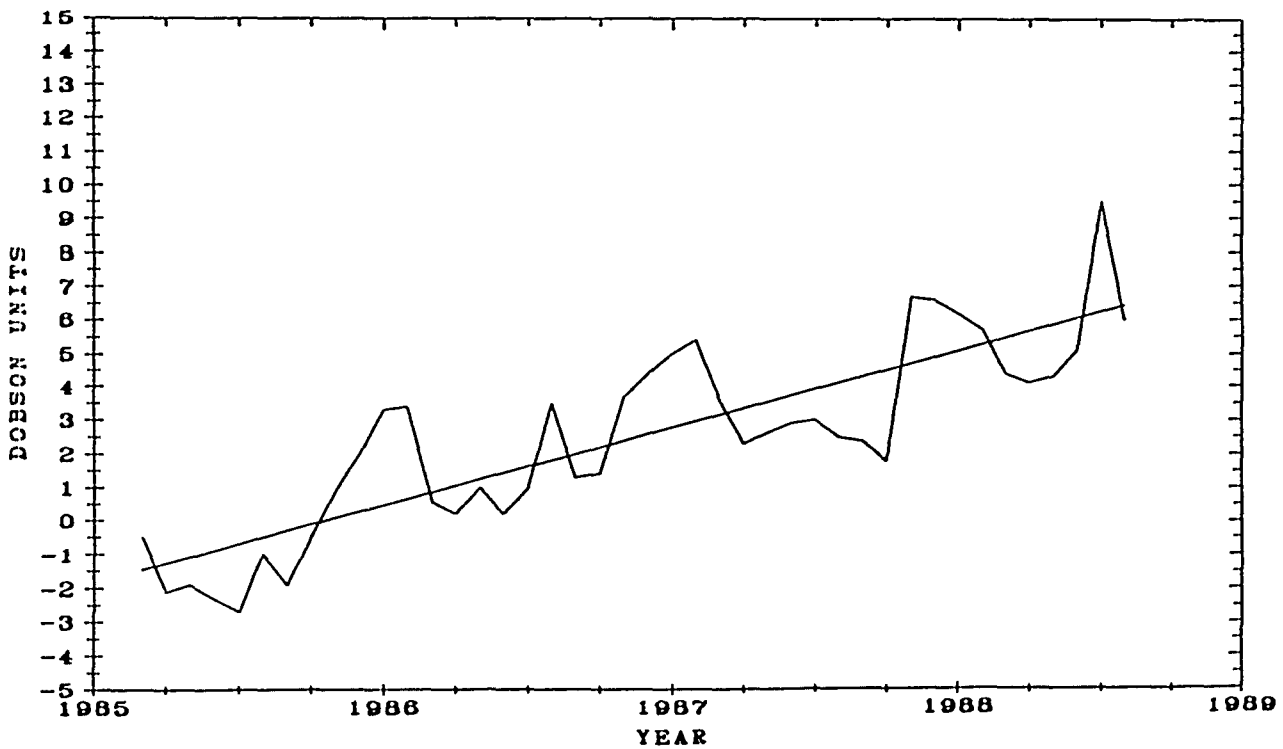

Figure 2. Difference of monthly zonal means of reflectivity (SBUV/2 - TOMS)

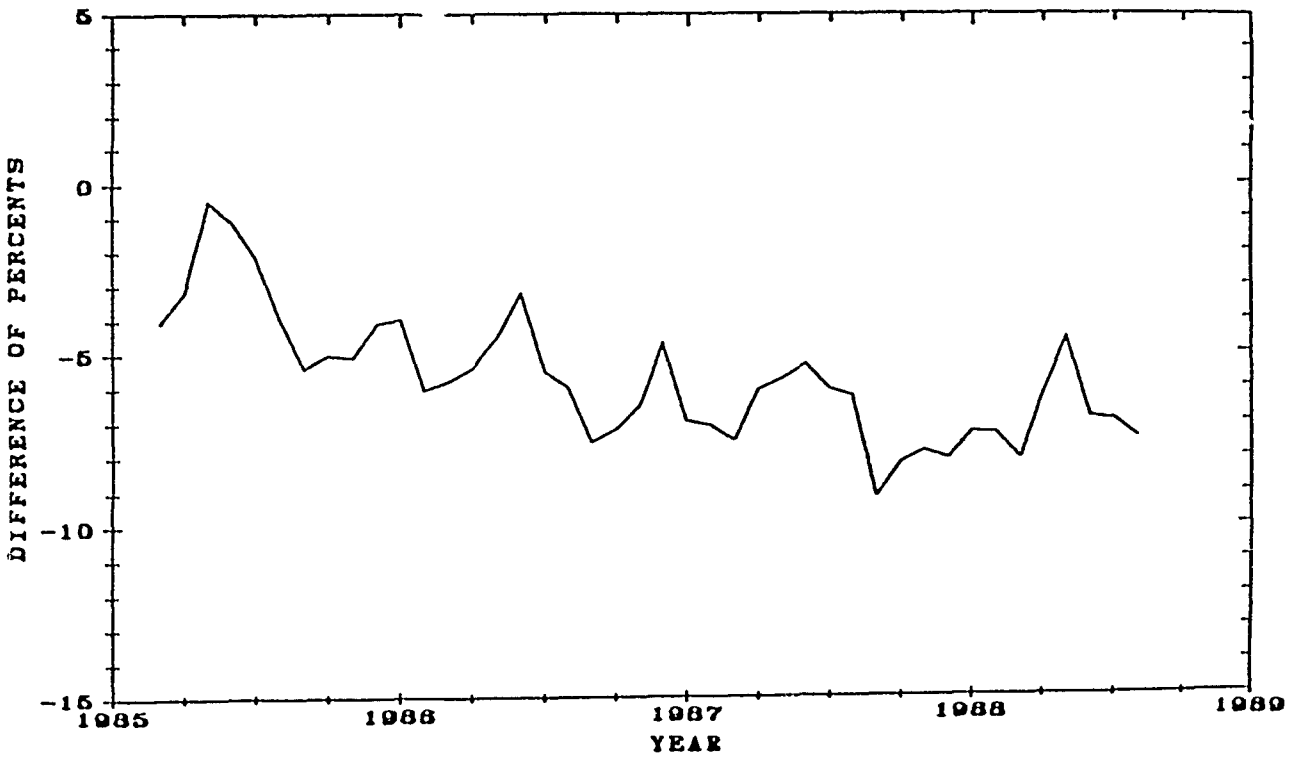

Figure 3. Difference of monthly zonal means of A-pair ozone (SBUV/2 - TOMS)

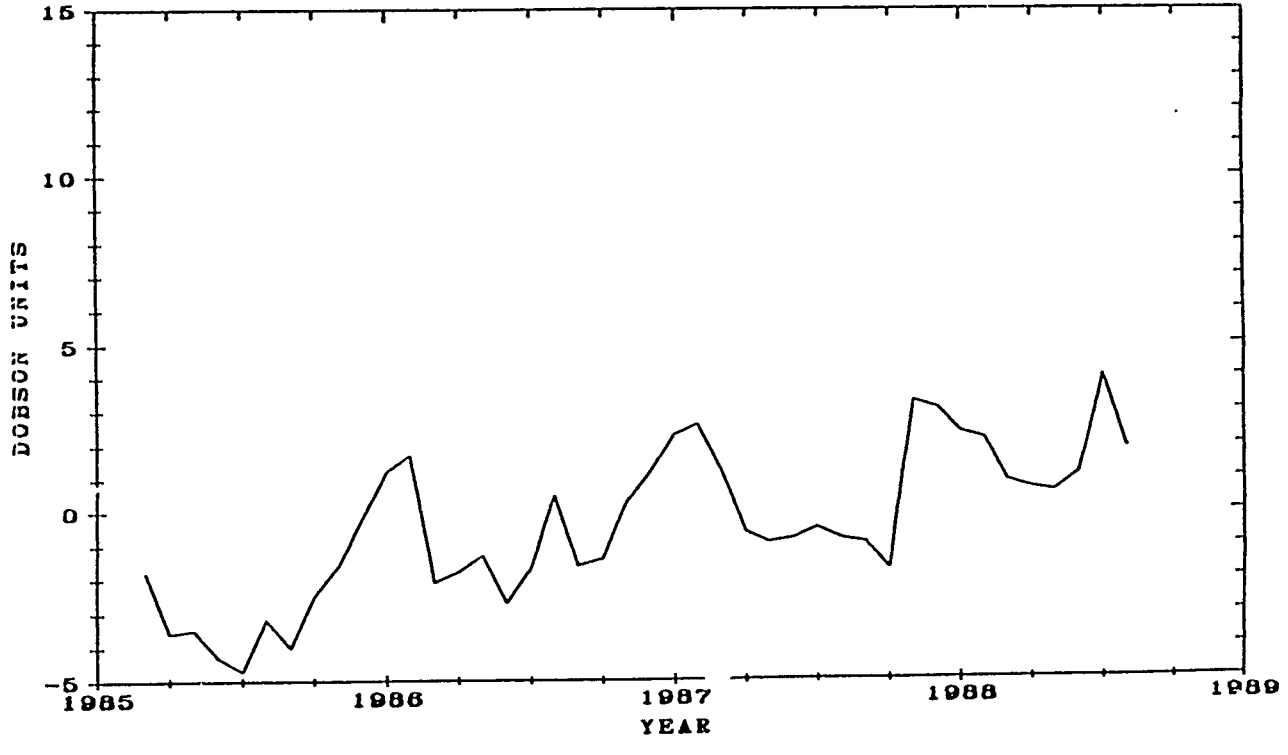

Figure 4. Difference of monthly zonal means of B-pair ozone (SBUV/2 - TOMS)

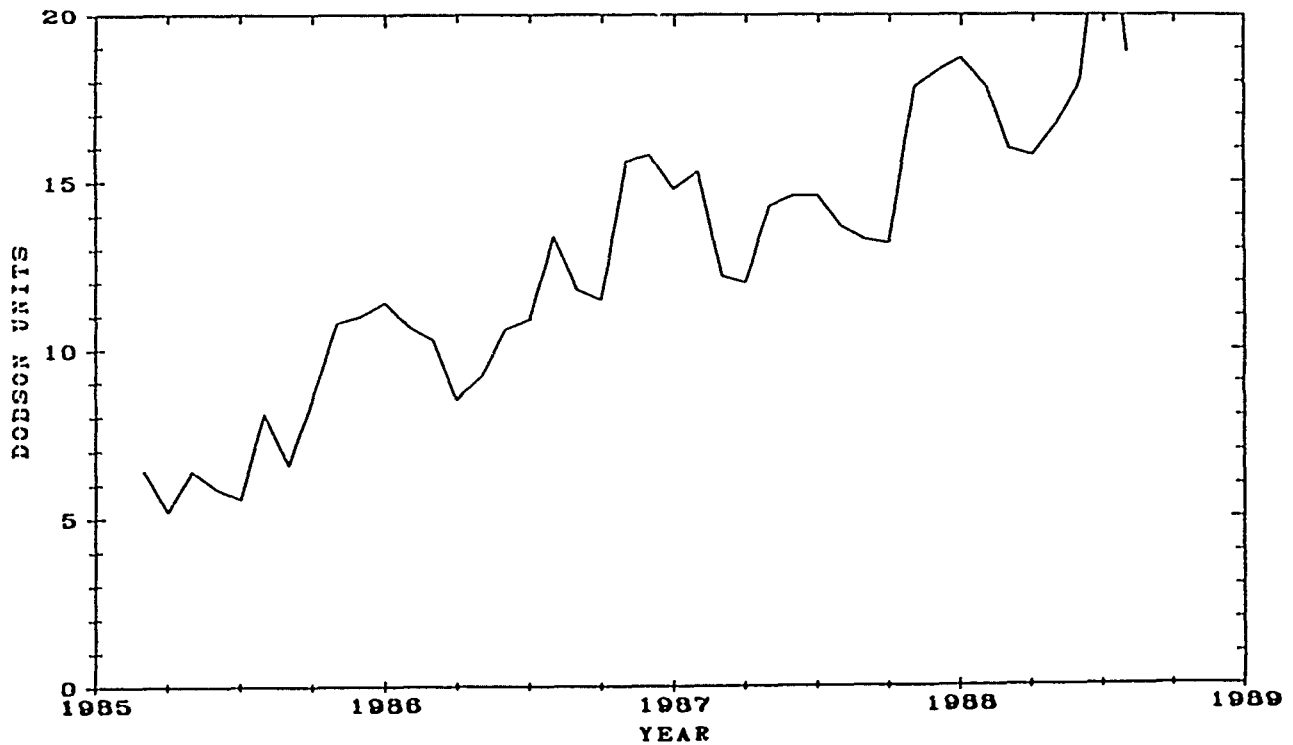

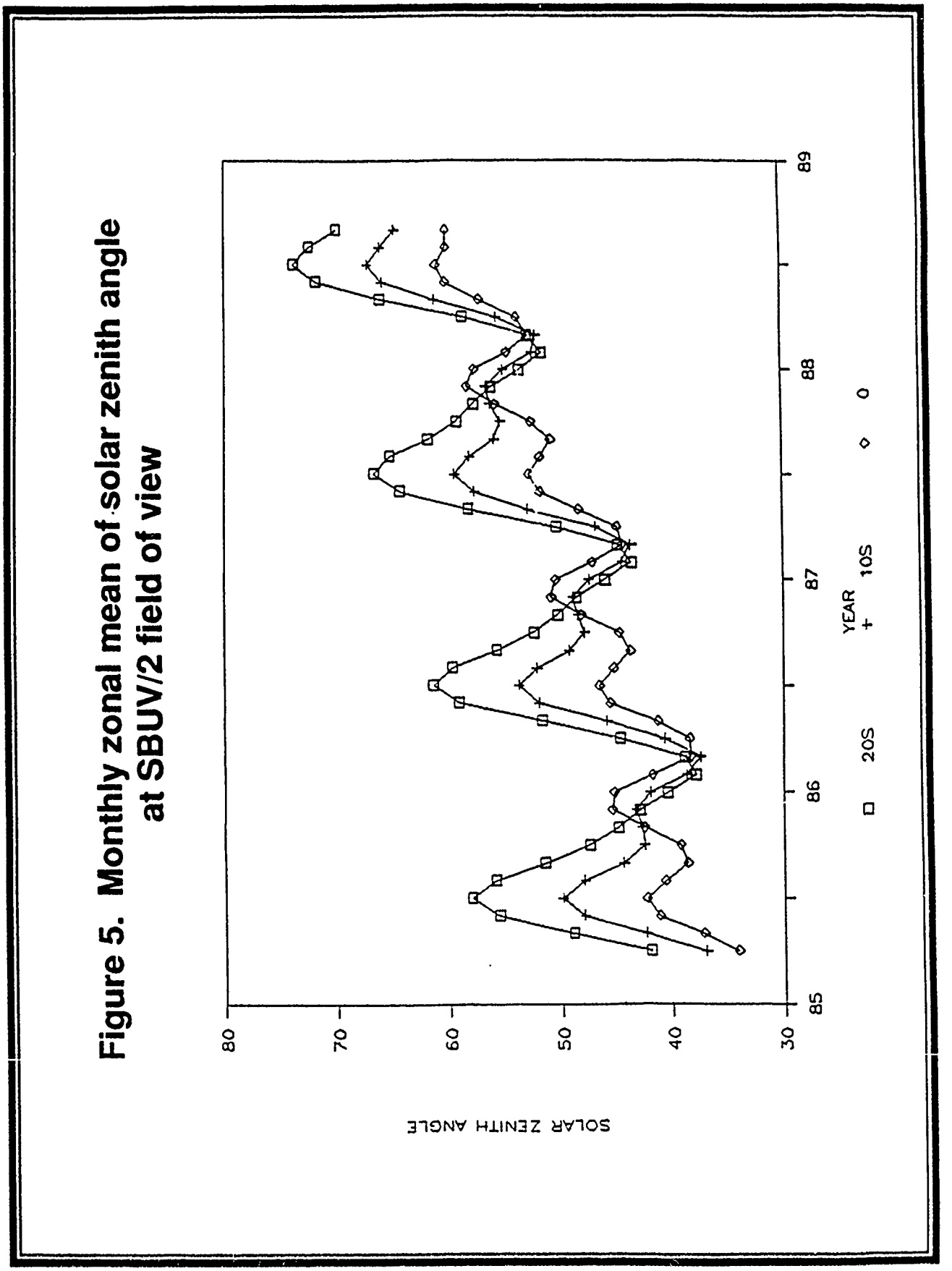

Figure 5. Monthly zonal mean of solar zenith angle at SBUV/2 field of view

Figure 6. Results of linearity test applied to TOMS averaged, deseasonalized, adjusted N-value changes. (Indicates success in deriving ozone from adjusted mean N-value changes.)

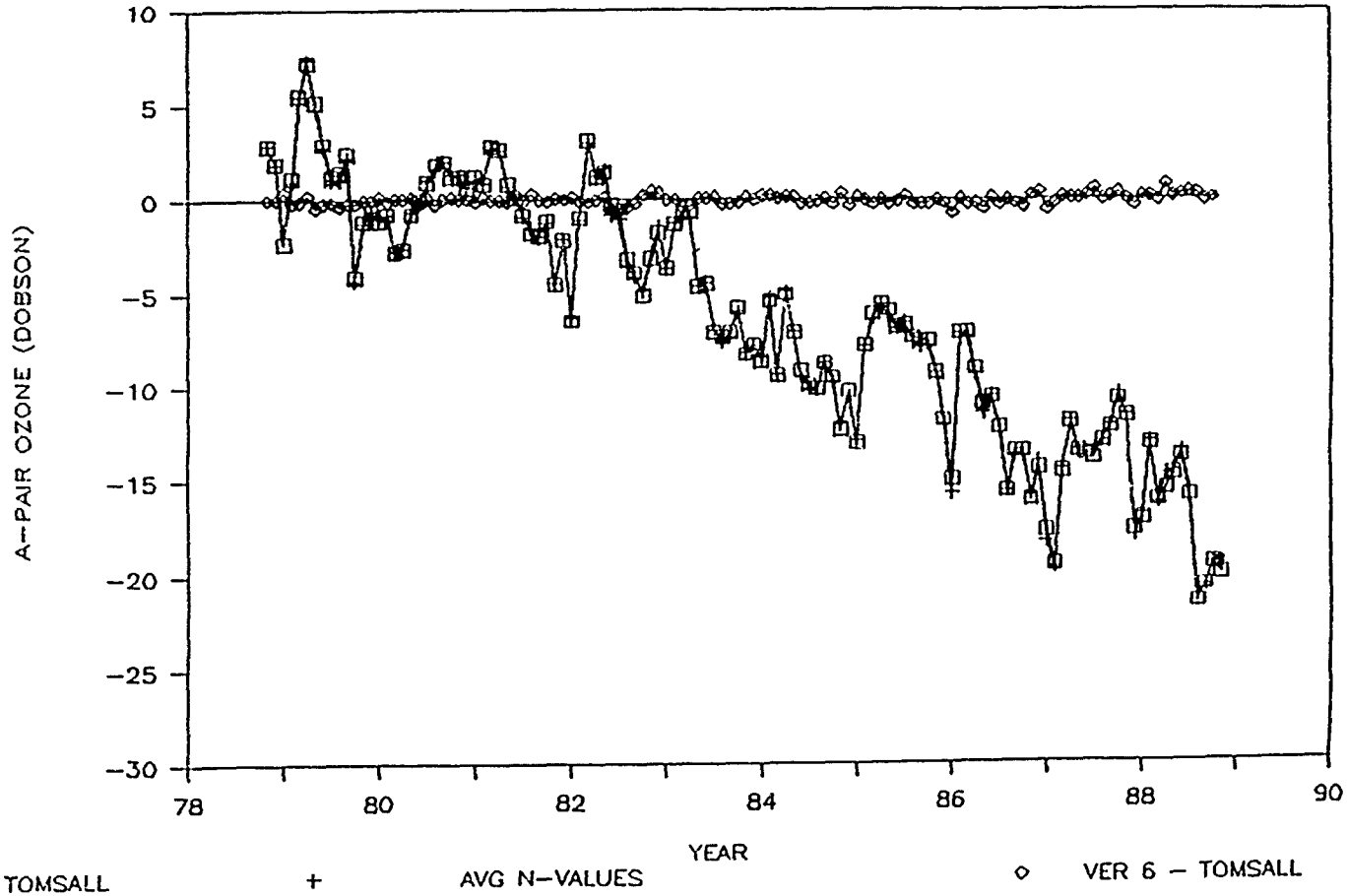

Figure 7. Results of linearity test applied to SBUV/2 averaged, deseasonalized, adjusted N-value changes. (Indicates limited success in deriving ozone from adjusted mean N-value changes.)

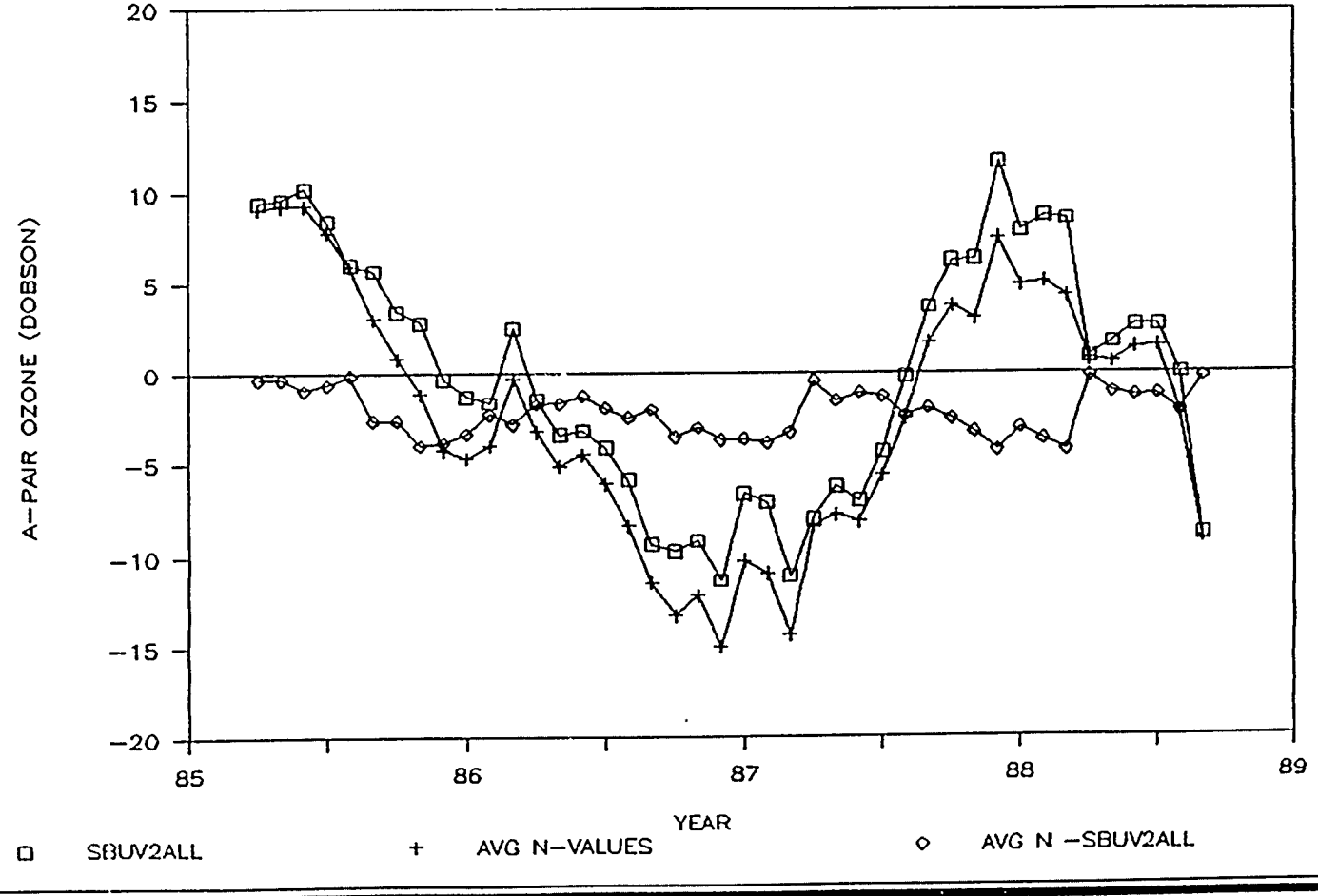

Figure 8. Results of pair justification technique applied to simulated N-value changes containing error that is linear in wavelength.

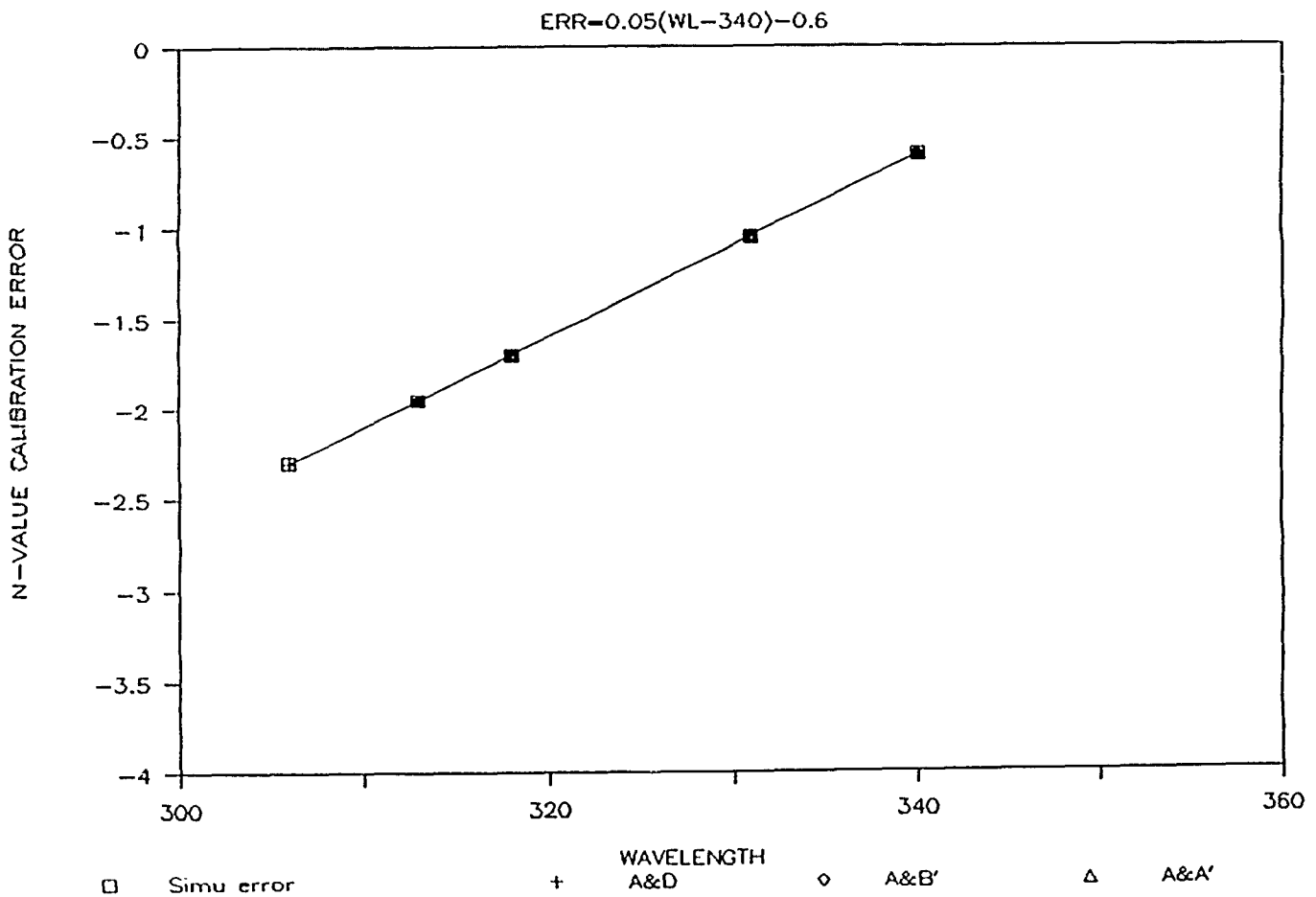

Figure 9. Results of pair justification technique applied to simulated N-value changes containing error that has second order wavelength dependence.

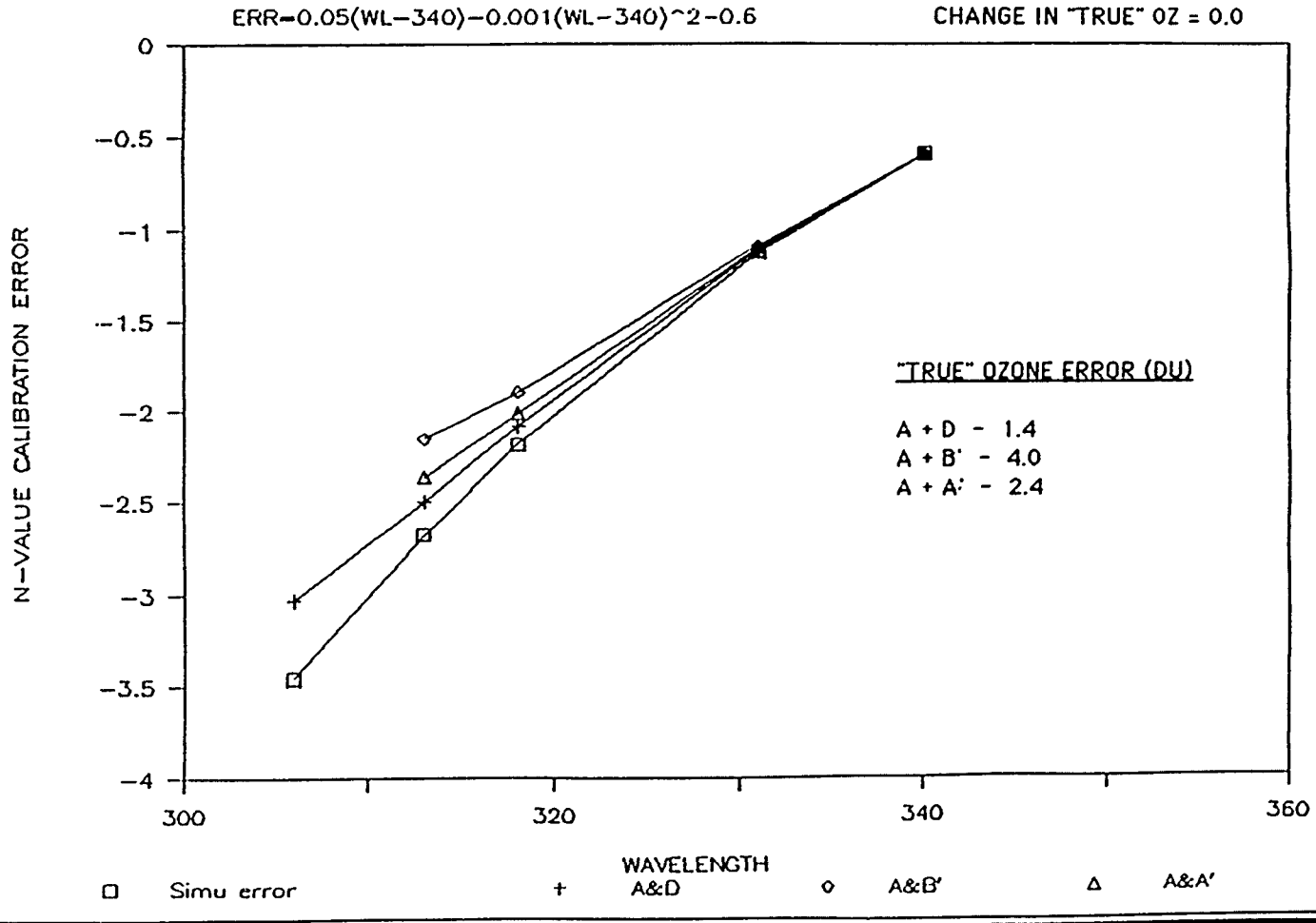

Figure 10. SBUV/2 A-pair calibration error derived using the pair justification technique

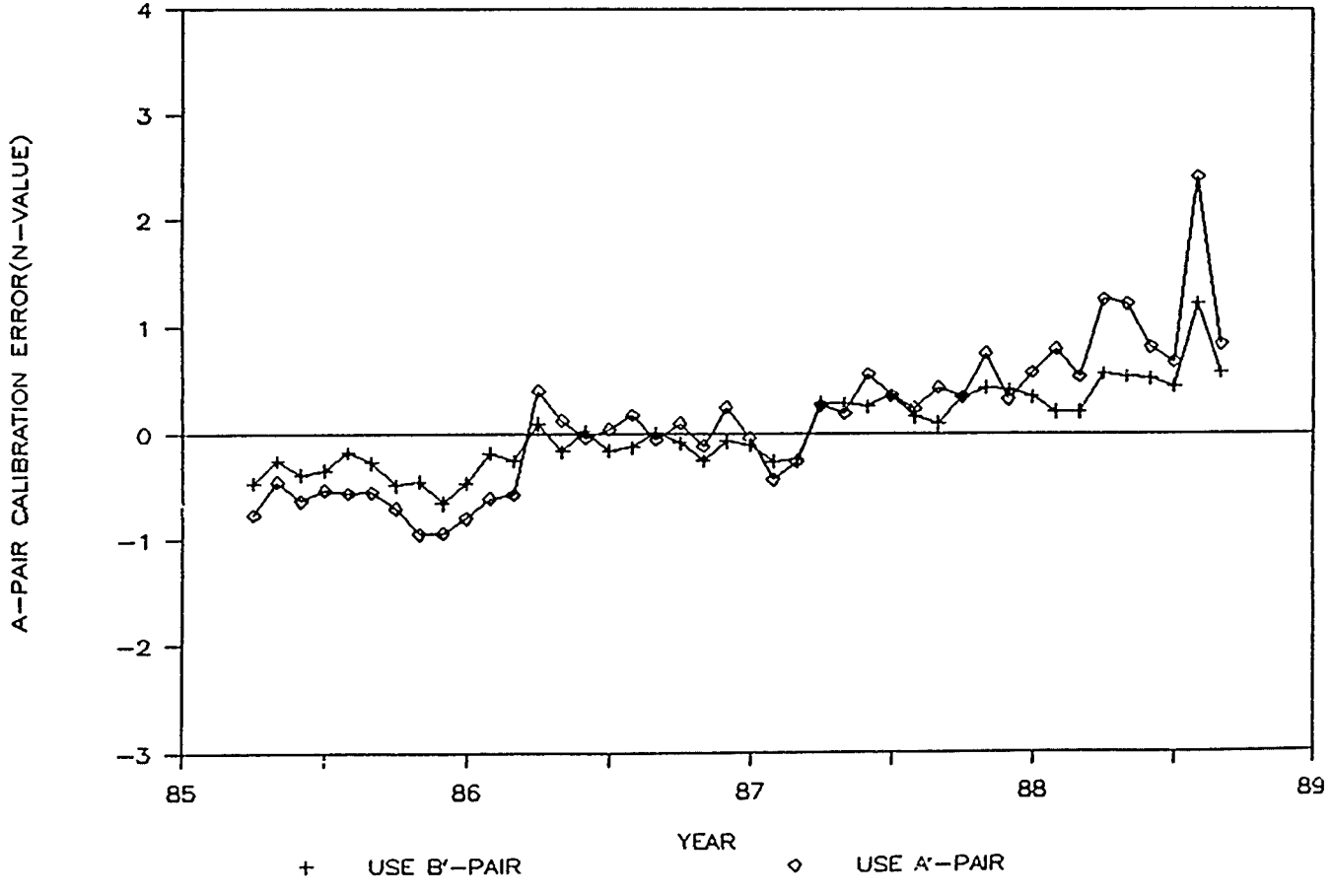

Figure 11. Error in SBUV/2 equatorial ozone derived using the pair justification technique

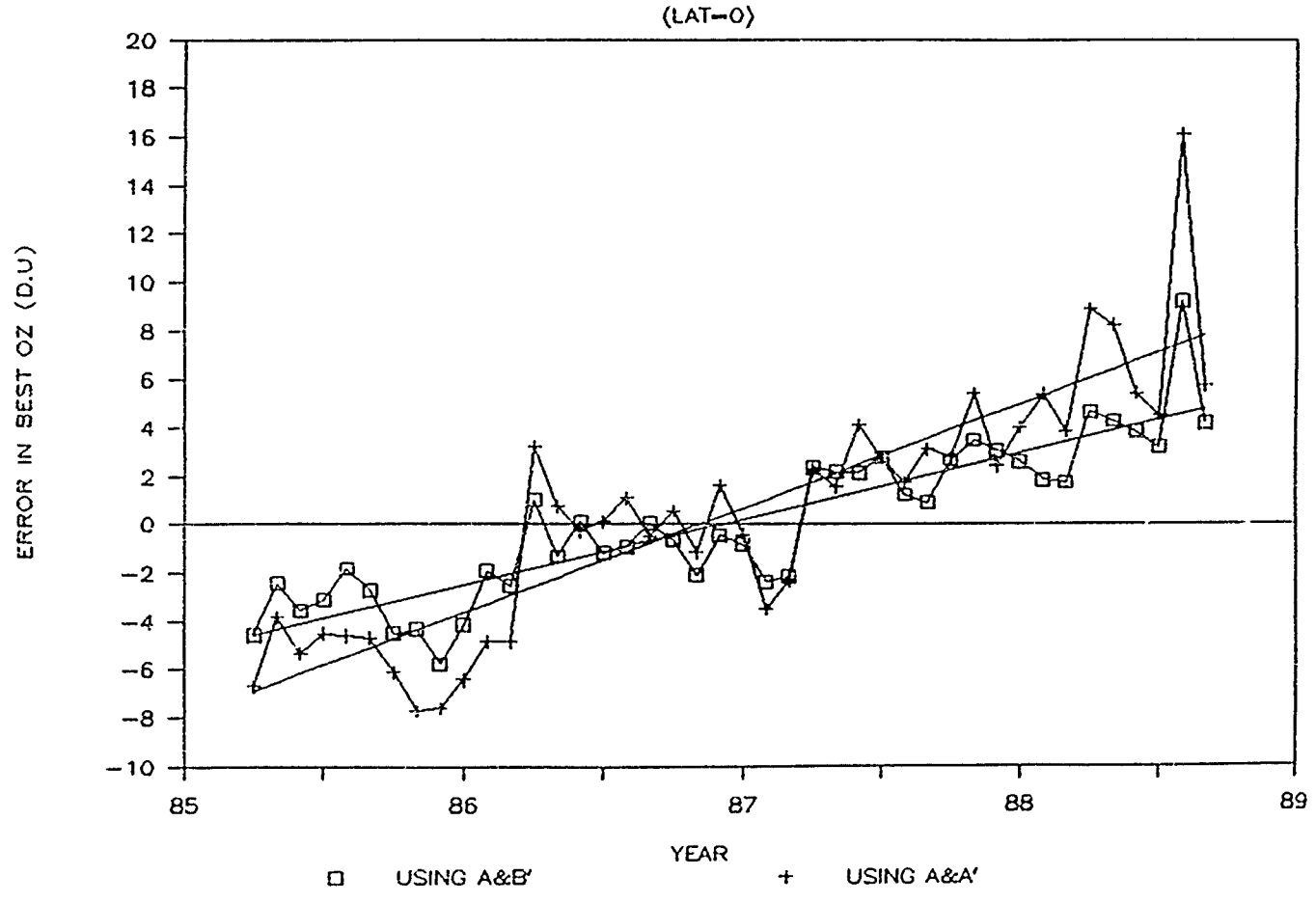

Attachment 10

Calibration of Long Term Satellite Ozone Data Sets Using the Space Shuttle

E. Hilsenrath
NASA/GSFC

Calibration of Long Term Satellite Ozone Data Sets Using the Space Shuttle

Ernest Hilsenrath

NASA Goddard Space Flight Center
Greenbelt, MD 20771
January, 1990

1. Introduction

Trends in atmospheric ozone continue to be an environmental concern. Drifts in satellite observations are the major obstacle in the detection of changes in global ozone over the long term. Careful re-analysis of satellite ozone data along with groundbased observations have more or less corroborated photochemical models which predict ozone depletion [1]. However there remains margin of error in the observations that is as large as the trend itself.

The National Plan for Stratospheric Monitoring [2] calls for monitoring global ozone for at least the next ten years employing the NOAA polar orbiting satellites. Ozone observations will be made with the Solar Backscatter Ultraviolet Spectral Radiometer Mod 2 (SBUV/2) which is a refinement of the SBUV instrument flying on NASA's Nimbus-7 satellite [3]. The first instrument in the operational series began taking data from the NOAA-9 spacecraft in February 1985. A second instrument was launched on NOAA-11 in September 1988. Both continue to operate.

Earlier attempts to calibrate satellite data relied on comparisons with ground based observations. However, differences in instrumental techniques severely complicated these efforts. This problem will be over come by regular flights, about once per year, of the Shuttle Solar Backscatter Ultraviolet radiometer (SSBUV). The data from the SSBUV instrument will be compared with nearly coincident data taken by the NOAA satellite instruments. This procedure will permit a direct calibration transfer in space [4] since the two instruments observe the same quantities thereby bypassing the inversion algorithm which converts the observations to ozone amounts.

2. Flight Instrumentation

The SSBUV payload consists of a SBUV/2 instrument that has been modified for Shuttle flight [4]. The payload is packaged into two Getaway Special canisters as shown in figure 1. One canister contains the instrument, and supporting optical systems. The second canister contains batteries and the data recording system. This stand-alone capability allows easy access to the Shuttle which affords some assurance of regular flights. The SSBUV Instrument is the engineering model to the series of SBUV/2 instruments now flying the NOAA satellites. The Nimbus and NOAA instruments employ a reflective diffuser to bring sunlight into the monochromator as the spacecraft traveled over the pole. For the solar irradiance measurement, the SSBUV employs a transmission diffuser, consisting of two ground crystalline quartz plates, which is deployed in front of the instrument entrance aperture. Therefore the solar irradiance measurement is made normal to the diffuser. SSBUV also contains a unique inflight calibration system which tracks instrument radiometric sensitivity and wavelength stability during flight.

3. Instrument Calibration

Maintaining accurate and precise instrument calibration over the long term is a major objective of the SSBUV program. Procedures have been developed to maintain calibrations with a precision of 1 percent over the long term [4]. This precision is essential in deriving a long term ozone data set. Calibration accuracy relies on the accuracy of the radiometric standards provided by the National Institutes of Standards and Technology (NIST). The accuracy of the radiometric standards will be tracked by a laboratory reference standard spectrometer with radiometric characteristics similar to the flight instrument. A laboratory comparison program involving several other satellite and Shuttle solar irradiance experiments is now underway. This comparison program is being coordinated by NIST. Figure 2 depicts the overall elements of the SSBUV calibration program.

To date the calibration efforts have demonstrated excellent results [5,6]. Calibration repeatability tests indicate that irradiance and radiance calibration constants can be maintained to the order of 0.5 percent (1 sigma). Several other important instrument characteristics such as, linearity and gain wavelength dependence have been measured to a precision of a few tenths of a percent. These results were acquired through a series of laboratory calibrations and environmental testing. This suggests that, with careful attention to all phases of the calibration process, that a 1 percent long-term radiometric calibration precision for SSBUV is a realistic goal.

4. Overall Mission Requirements

The goal of the SSBUV is to remove the uncertainty in the SBUV/2 data set from the NOAA satellite series to value less than the expected ozone trend. The statistical uncertainty (at the 2 sigma level) remaining in the corrected data is the factor which ultimately limits the ability to detect long term ozone changes. Variables determining this uncertainty include: a) the magnitude of the ozone trend, b) the duration of the ozone monitoring period, c) the frequency of SSBUV flights, d) the number of coincident measurements between SSBUV and SBUV/2 for a given shuttle mission, e) atmospheric variability, f) instrument and measurement precision, and g) long term SSBUV calibration precision. Maintaining instrument calibration to within 1 percent is the most critical factor in performing the in orbit long term calibration [7].

Each one of these variables have been treated objectively [4] and can be combined to compute the Shuttle flight frequency needed to correct the satellite data set for a given ozone monitoring period. The results of this computation is given in figure 3. The curves correspond to heights where SSBUV observes ozone which are a function of wavelength. The dashed line helps to illustrate; for example, if the SSBUV flies every 8 months, a monitoring period of 8 years is required to correct the SBUV/2 data set at 40 km to the necessary precision. At 47 km, where the ozone trend is less, 10 years of observations are required at the 8 month flight schedule.

5. Calibration of the Satellite Data Set

Procedures for combining the SSBUV an SBUV/2 data sets are under development. Existing ozone satellite data has been used as model data sets to test these procedures [8]. The average factor, C(i,j), for correcting the SBUV/2 data set can be calculated from SSBUV and SBUV/2 coincident observations of the atmospheric albedo, A(i,j,k) where i=wavelength, j=the SSBUV flight number, and k=number of coincidences per flight.

$$C(i,j) = (1/N) \sum_{k=1}^{N} [A_S(i,j,k)/A_2(i,j,k)] \qquad (1)$$

Where $A_S(i,j,k)$ and $A_2(i,j,k)$ are the coincident observations from SSBUV and SBUV/2 respectively. One flight of the SSBUV produces one value of C(i,j) at each wavelength, i. Interpolation in time between the derived C(i,j) yields correction factors for all times during the SBUV/2 program.

6. SSBUV First Flight

The first flight of SSBUV occurred on October 19, 1989 on the Shuttle Atlantis. During that period coincident observations were taken with the SBUV on Nimbus-7 and the SBUV/2's on NOAA-9 and NOAA-11. Thirty one orbits of earth observations were obtained resulting in over 30 matchups with each of the satellite observations where a one hour window was the matchup criteria. Solar observations and in flight calibration checks were conducted at the beginning, near the middle, and at the end of the observing period. Figure 4 illustrates the one hour window matchup locations for the three satellites during the SSBUV observing period.

An initial and preliminary comparison has been performed between the solar irradiances observed by the SSBUV and the day 1 solar irradiance (March, 1985) observed by the NOAA-9 SBUV/2. For the ozone observing channels agreement was about +/- 2%.

7. Summary

Detecting an ozone trend is a formidable task since our observing systems drift at a rate that is comparable to the trend itself. Satellite observations must be carefully checked to accurately reveal an ozone trend. A program is now underway in which an instrument similar to the ozone sounders on the NOAA operational satellites is flown regularly on the Space Shuttle to perform in orbit calibration checks by comparing observables. It is essential that the calibration of the Shuttle instrument be known to 1% over the long term. Tests to date demonstrate that this is an achievable goal.

8. References

[1] Watson, R. T., M. J. Prather, and M. J. Kurylo, Present State of Knowledge of the Upper Atmosphere, 1988: An Assessment Report, NASA Reference Publication 1208, 1988

[2] National Plan for Stratospheric Monitoring and Early Detection of Change, 1988-1997, U. S. Dept of Commerce/NOAA, FCM-P17-1989, July, 1989.

[3] Heath, D. F., A. J. Krueger, H. R. Roeder, B. D. Henderson, The Solar Backscatter Ultraviolet and Total Ozone Mapping Spectrometer (SBUV/TOMS) for Nimbus G, Optical Engineering, Vol. 14, pp. 323-331, 1975.

[4] Hilsenrath, E., D. Williams, and J. Frederick, Calibration of Long Term Data Sets from Operational Satellites Using the Space Shuttle, SPIE Proc., 924, 215-222, 1988.

[5] Cebula, R. P., E. Hilsenrath, B. Guenther, Calibration of the Shuttle Borne Solar Backscatter Ultraviolet Spectrometer, SPIE Proc., 1109, 205-218, 1989

[6] Cebula, R. P., E. Hilsenrath, Prelaunch Calibration of the Shuttle Solar Backscatter Ultraviolet (SSBUV) Spectrometer for STS-34, Proceedings of OSA., Feb, 1990.

[7] Frederick, J. E., X. Niu, E. Hilsenrath, The Detection and Interpretation of Long-Term Changes in Ozone from Space, Adv. Space Res., 9 (7) 317- (7) 321, 1989.

[8] Frederick, J.E., X. Nir, E. Hilsenrath, An Approach to the Detection of Long Term Trends in Stratospheric Ozone from Space, submitted to Journ. Oceanic and Atmos. Tech.

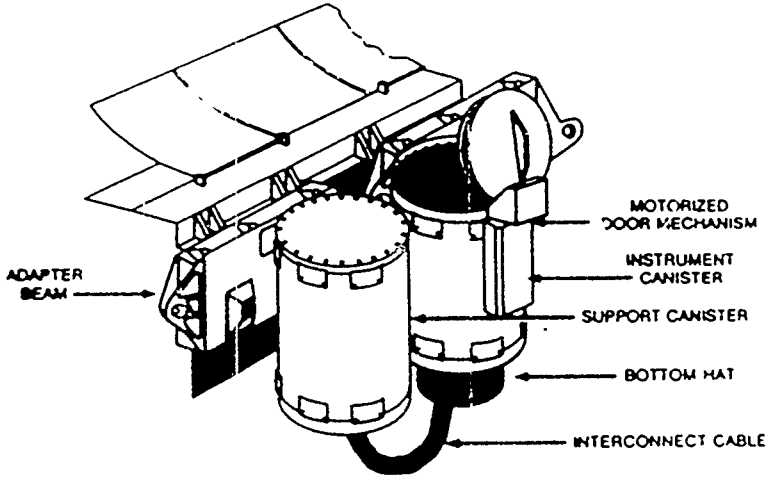

Figure 1. SSBUV Flight Configuration

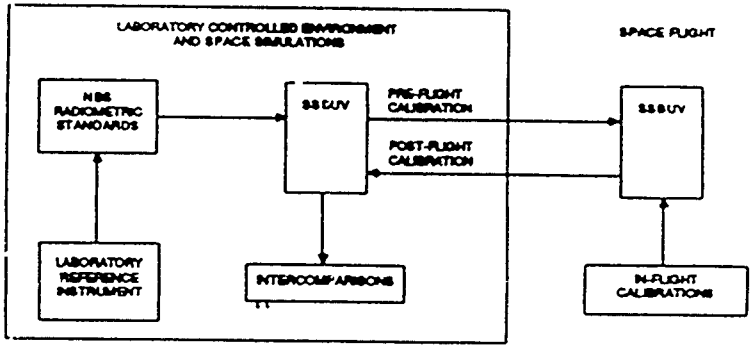

Figure 2. SSBUV Calibration Program

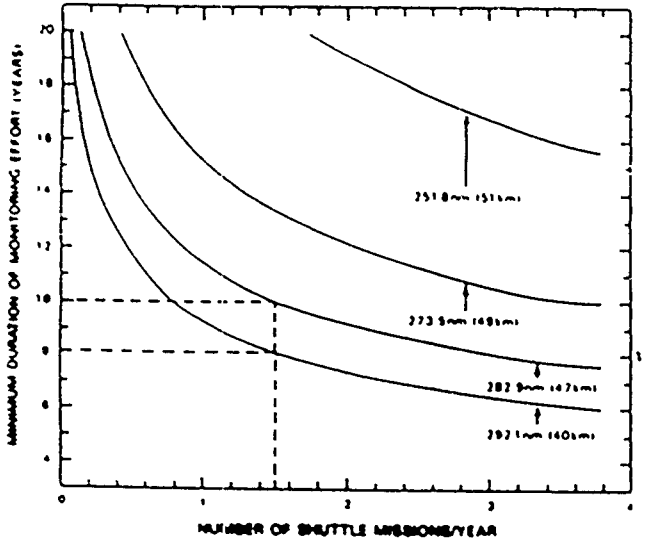

Figure 3. SSBUV Flight Requirements

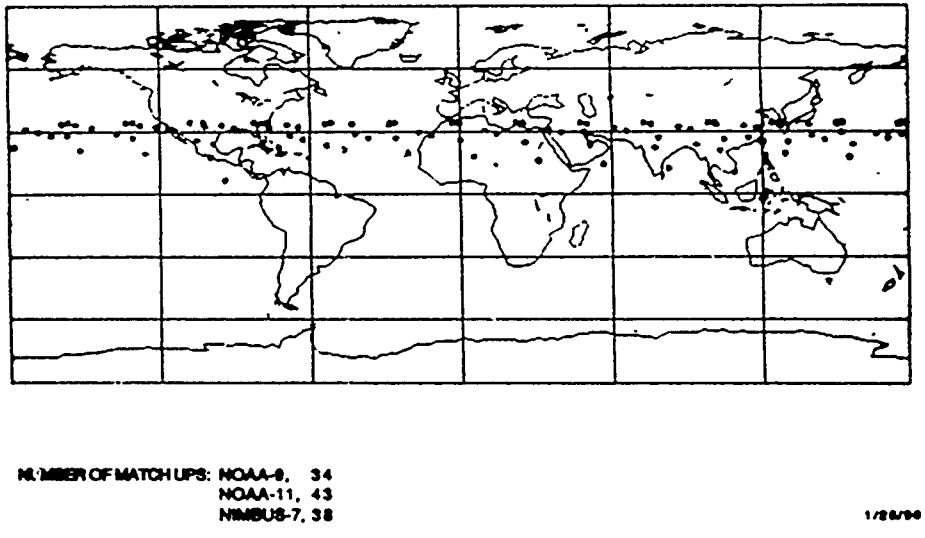

Figure 4. Orbit Intersections for STS-34

SHUTTLE SOLAR BACKSCATTER ULTRAVIOLET (SSBUV)

NOAA-9 SBUV/2 SUMMARY MEETING
JANUARY 28, 1990

SSBUV IN ORBIT CALIBRATION

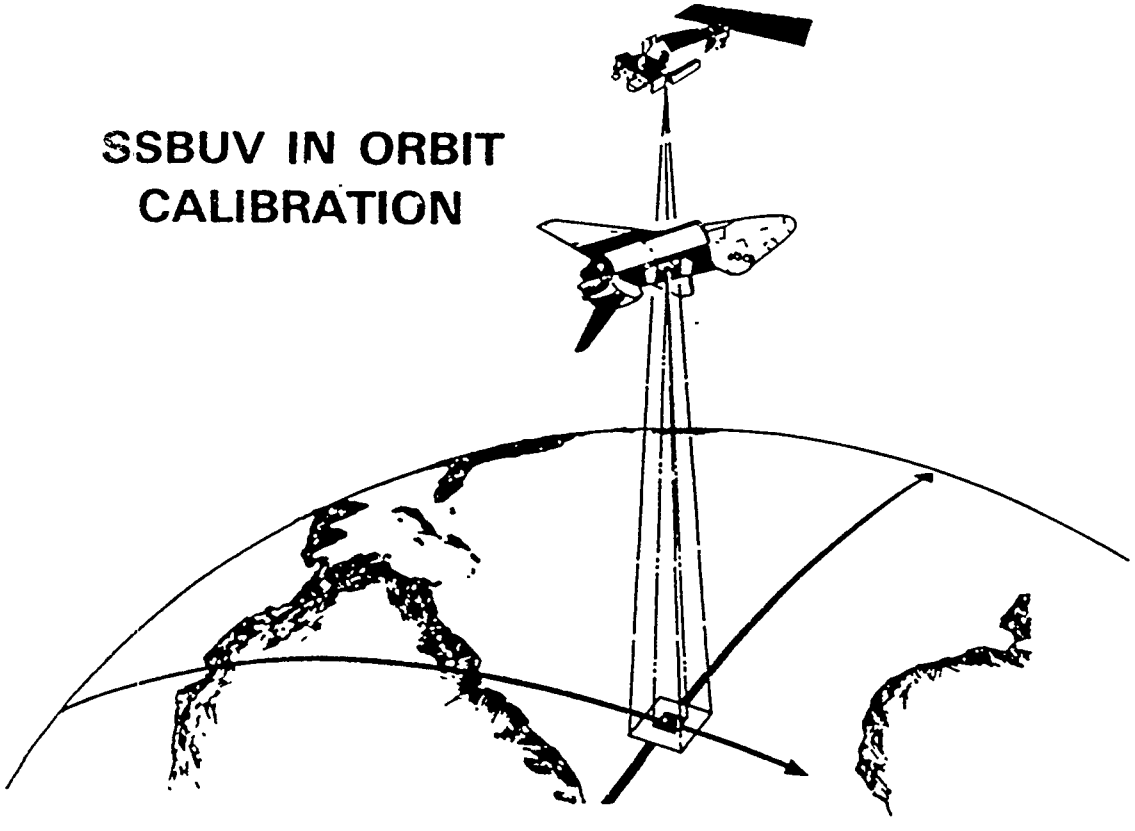

SHUTTLE SOLAR BACKSCATTER ULTRAVIOLET SPECTROMETER (SSBUV)

SHUTTLE ATTACHED, SELF-CONTAINED PAYLOAD TO MEASURE TOTAL AMOUNT AND HEIGHT DISTRIBUTION OF OZONE IN UPPER ATMOSPHERE

PROVIDE HIGHLY ACCURATE AND RELIABLE OZONE MEASUREMENTS TO AID CALIBRATION OF OPERATIONAL OZONE INSTRUMENTS ON NOAA SATELLITES

PERIODIC SAMPLING, LONG-TERM DATA SET FOR TREND ANALYSIS

COMPARE OBSERVABLES, BYPASSING ALGORITHM

UNIQUE CHARACTERISTIC: CALIBRATION CONCEPT - PRE & POST LAUNCH AND ON-ORBIT

FLIGHTS: AT LEAST ONCE PER YEAR, THROUGH 1990'S
FIRST FLIGHT IN OCTOBER 1989

PRINCIPAL INVESTIGATOR: E. HILSENRATH
NASA/GODDARD SPACE FLIGHT CENTER

CO-INVESTIGATORS: NASA AND NOAA

EXPERIMENT MANAGER: D. E. WILLIAMS
NASA/GODDARD SPACE FLIGHT CENTER

1/25/90

U.S. DEPARTMENT OF COMMERCE / National Oceanic and Atmospheric Administration

OFCM

OFFICE OF THE FEDERAL COORDINATOR FOR
METEOROLOGICAL SERVICES AND SUPPORTING RESEARCH

National Plan for Stratospheric Monitoring, 1988 - 1997

FCM-P17-1989

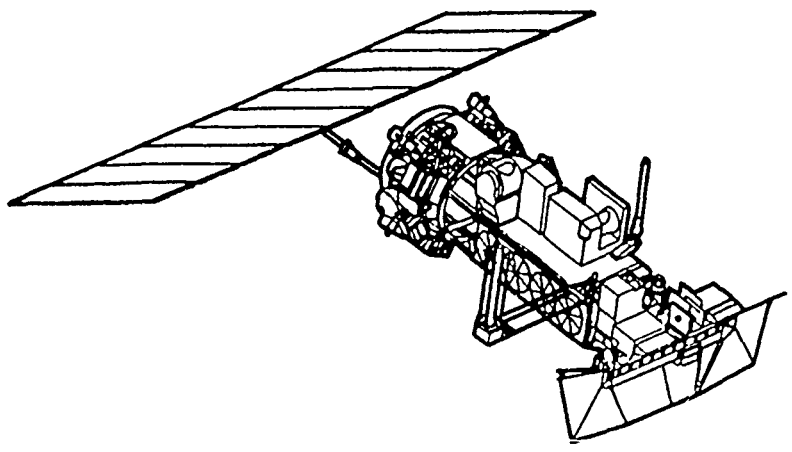

Washington, D.C.
July 1989

NATIONAL PLAN FOR OZONE MONITORING

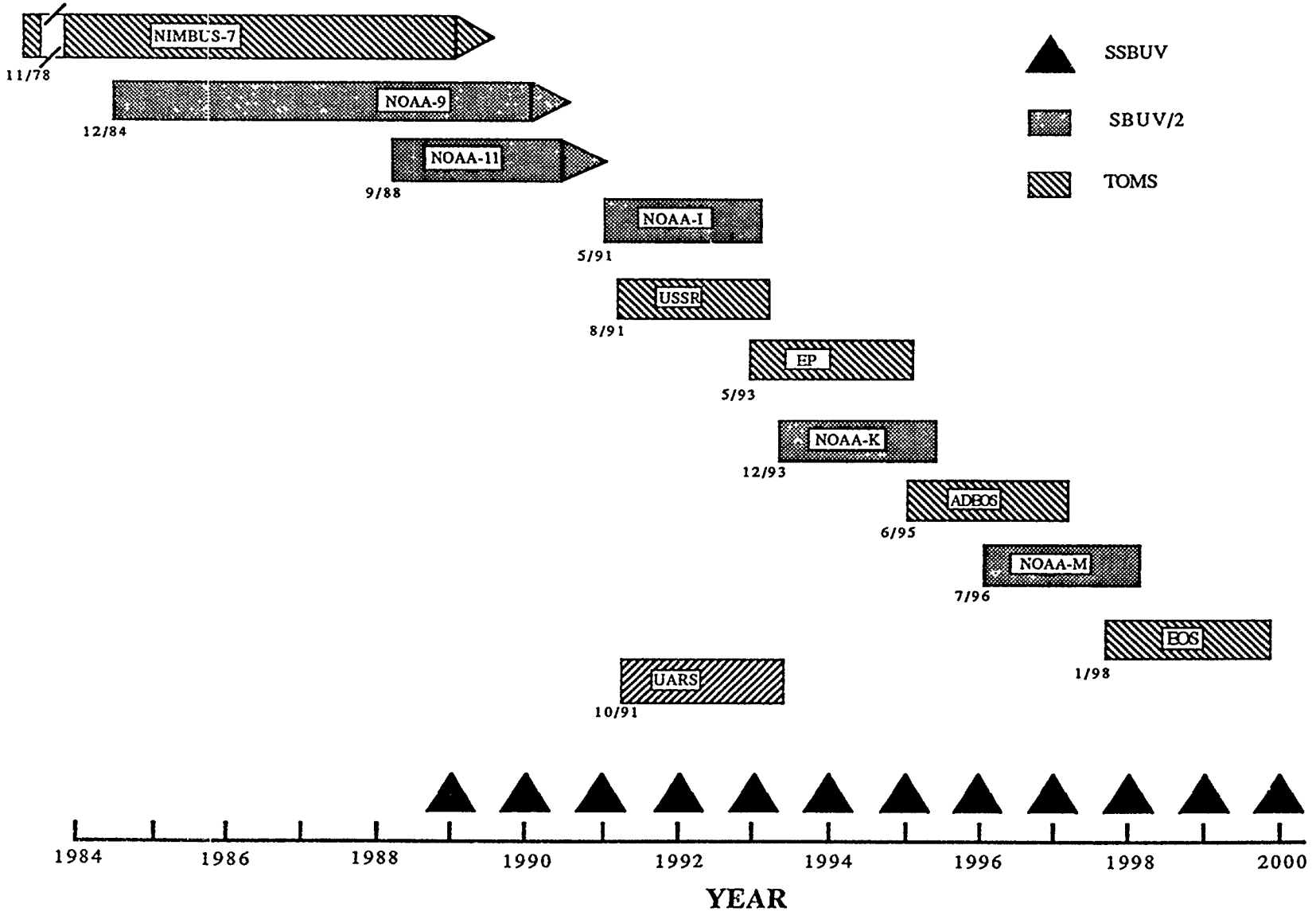

APPLICATION OF SSBUV DATA TO SATELLITE OBSERVATIONS

PROBLEM

THE STATISTICAL UNCERTAINTY REMAINING IN THE TREND DERIVED FROM A CORRECTED DATA SET IS THE FACTOR WHICH ULTIMATELY LIMITS OUR ABILITY TO DETECT A TREND.

REQUIREMENT

ACHIEVE AN UNCERTAINTY IN THE SATELLITE DATA DRIFT THAT IS SMALLER, AT THE 2 SIGMA LEVEL, THAN THE PREDICTED OZONE (ALBEDO) TREND

VARIABLES

MAGNITUDE OF OZONE TREND

ATMOSPHERIC "NOISE"

MEASUREMENT PRECISION

REPEATABILITY (CONSTANCY) OF CALIBRATION

NUMBER OF COINCIDENCES PER MISSION

FREQUENCY OF SHUTTLE MISSIONS

DURATION OF MONITORING PERIOD

CALIBRATION - 1% (1 SIGMA) LONG TERM REPEATABILITY REQUIRED

RADIOMETRIC STANDARDS AND CALIBRATIONS ARE PROVIDED BY THE NATIONAL INSTITUTE OF STANDARDS AND TECHNOLOGY (FORMALLY NBS)

LINEARITY - PRINCIPAL OF SUPERPOSITION

WAVELENGTH AND BANDPASS - 3 LINE SOURCES

IRRADIANCE - QUARTZ HALOGEN (FEL) AND DEUTERIUM LAMPS

RADIANCE - ABOVE LAMPS AND $BaSO_4$ DIFFUSER PLATES

DATES:

OCTOBER 1988, FEBRUARY 1989, APRIL 1989

RESULTS (1 SIGMA):

LINEARITY	- 1% OVER ENTIRE DYNAMIC RANGE AND CHARACTERIZED TO 0.1%
WAVELENGTH	- ABSOLUTE ACCURACY, 0.014NM PRECISION, 0.013NM
IRRADIANCE	- ESTIMATED ABSOLUTE ACCURACY, 2-3% PRECISION, 0.2% REPEATABILITY, 0.3%
RADIANCE	- ESTIMATED ABSOLUTE ACCURACY, 3-5% PRECISION, 0.1% REPEATABILITY, 0.2%
ALBEDO	- < 0.3%

SSBUV MISSION FREQUENCY REQUIREMENTS

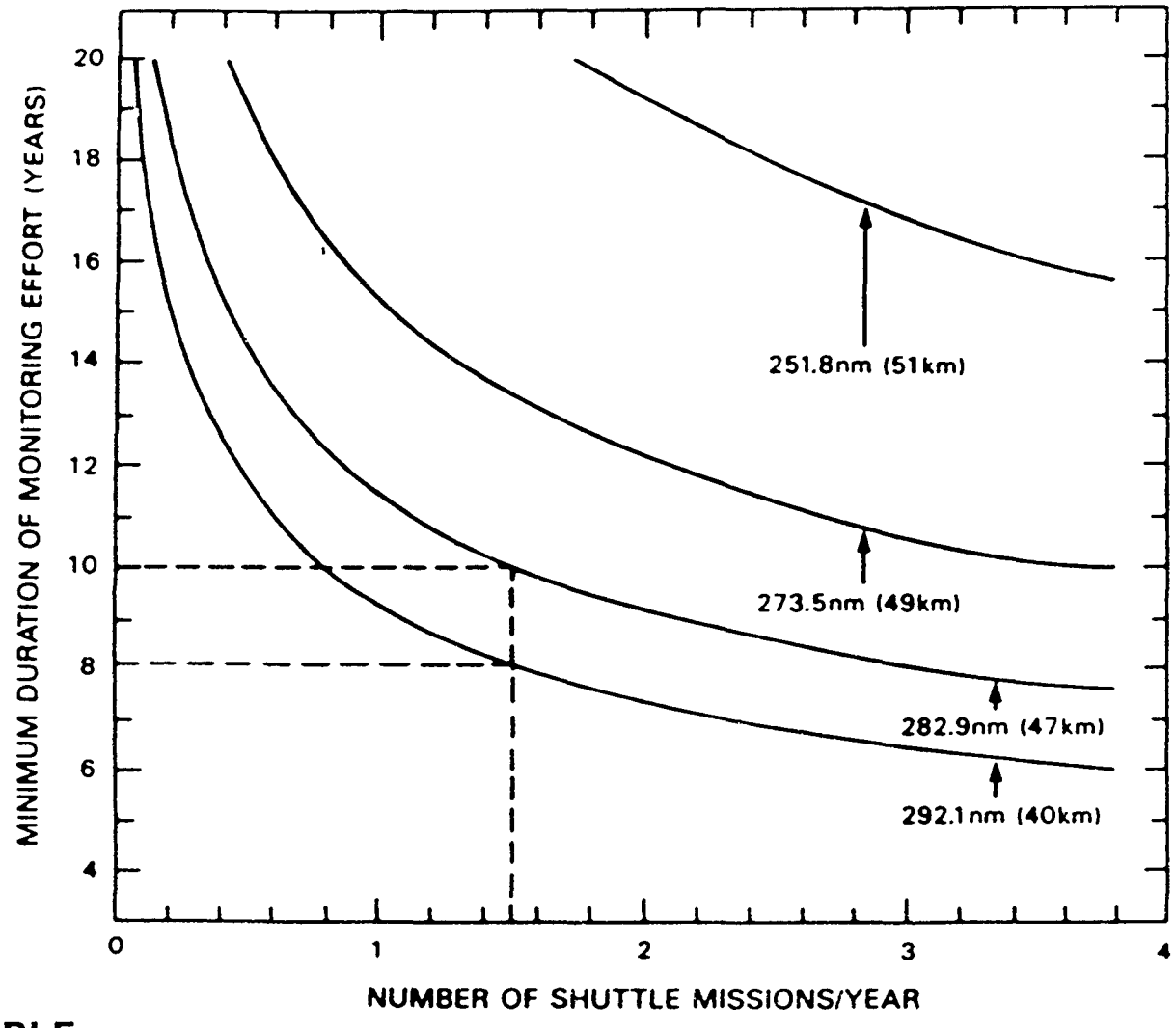

EXAMPLE

REQUIRES A MONITORING PERIOD OF:

8 YEARS FOR THE TREND AT 40km

10 YEARS FOR THE TREND AT 47km

Correction factor which normalizes the SBUV/2 albedos to the SSBUV albedos.

$$C(\lambda, j) = \frac{1}{N} \sum_{k=1}^{N} \frac{A_2(\lambda, j, k)}{A_s(\lambda, j, k)}$$

λ= wavelength
j = shuttle mission
k = number of coincidences

Correcting actual SBUV data with a given trend with simulated SSBUV data results in a long term data set that is less than ($\pm$2 sigma) the expected trend due to anthropogenic by-products.

Paper submitted JOAT, Frederick and Hilsenrath

SSBUV SHUTTLE MANIFEST - JUNE 1989

	STS #	DATE	PAYLOAD
SSBUV-1	34	10/89	GALILEO
SSBUV-2	37	11/90	GRO
SSBUV-3	43	1/91	TDRSS-E
SSBUV-4	51	1/92	SPACEHAB
SSBUV-5	57	7/92	ATLAS-2
SSBUV-6	62	12/92	TDRSS-F
SSBUV-7	70	5/93	ATLAS-3
SSBUV-8	81	4/94	ATLAS-4
SSBUV-9	87	10/94	TDRSS-H
SSBUV-10	99	9/95	ATLAS-5

STS-34 GALILEO/SSBUV

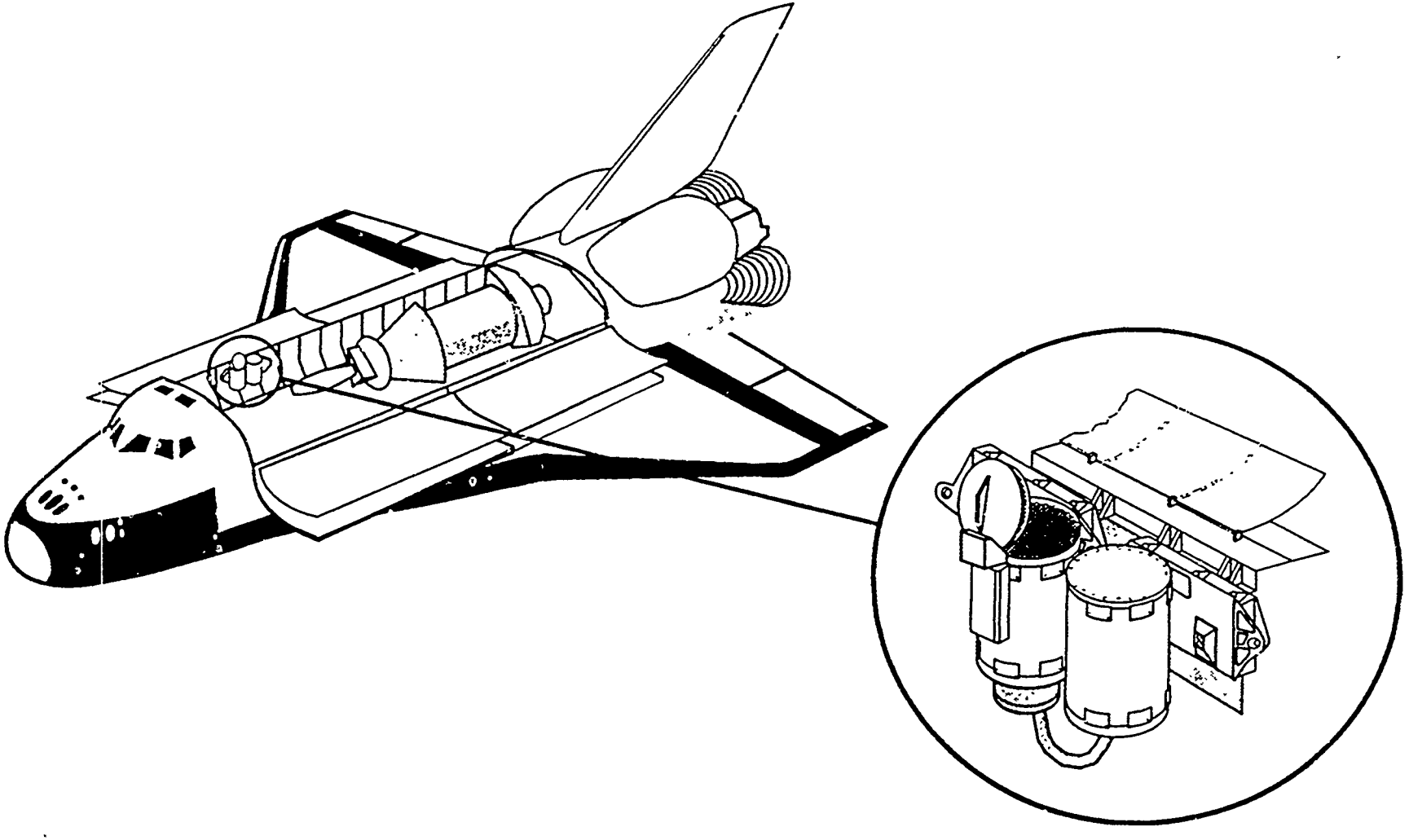

G66.001

ORBIT INTERSECTIONS FOR PROBLEM SET STS-34
SYSTEM: SBUV/2

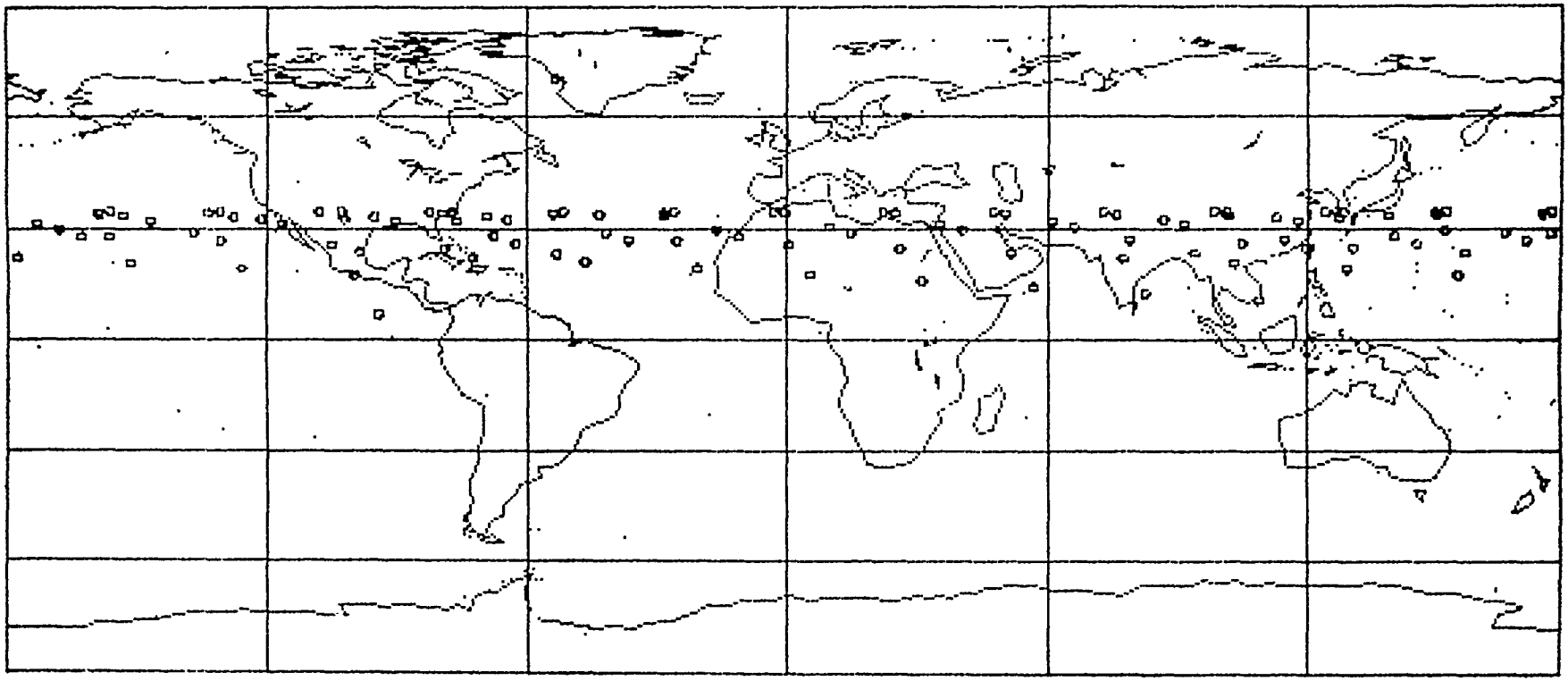

NUMBER OF MATCH UPS: NOAA-9, 34
NOAA-11, 43
NIMBUS-7, 38

1/26/90

SSBUV DATA PROCESSING

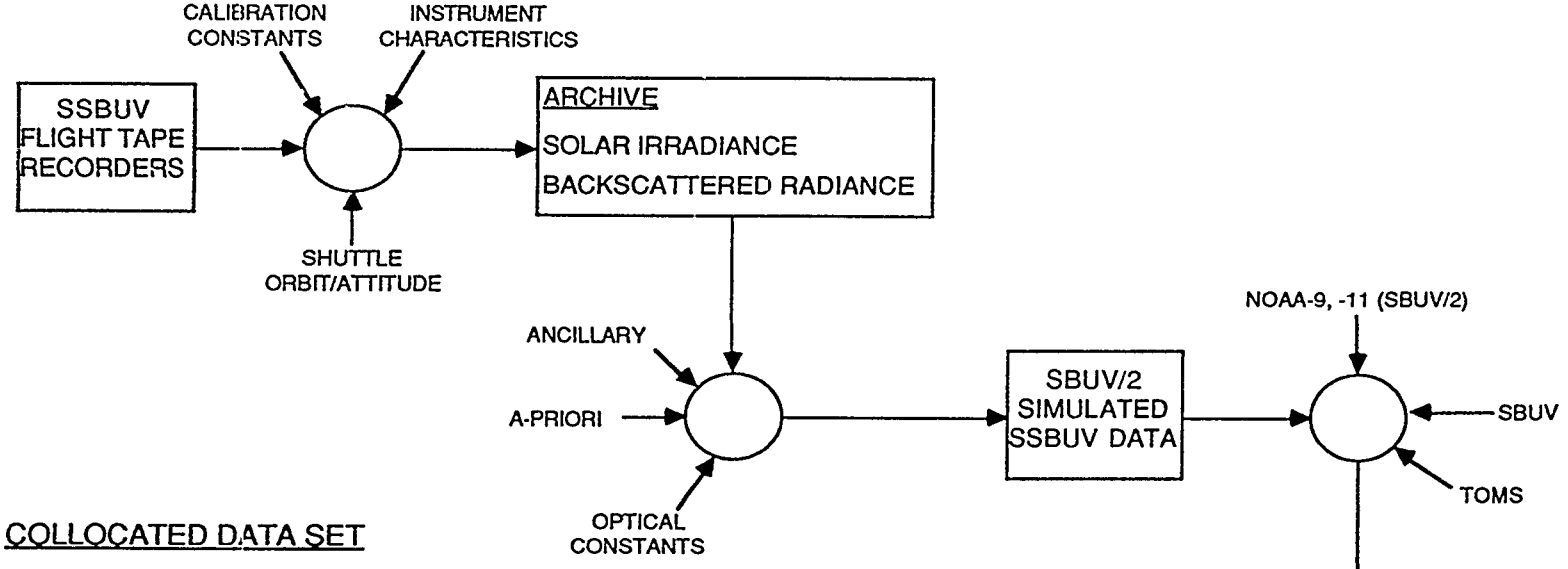

COLLOCATED DATA SET

3 DAYS SSBUV, SBUV/2, AND TOMS
DATA MATCHED TO WITHIN 2 1/2 HOURS

RADIANCES & ALBEDOS

TOTAL OZONE

OZONE PROFILES 25-55 km

SOLAR IRRADIANCE, 180 - 400 nm, 1.1 nm RESOLUTION

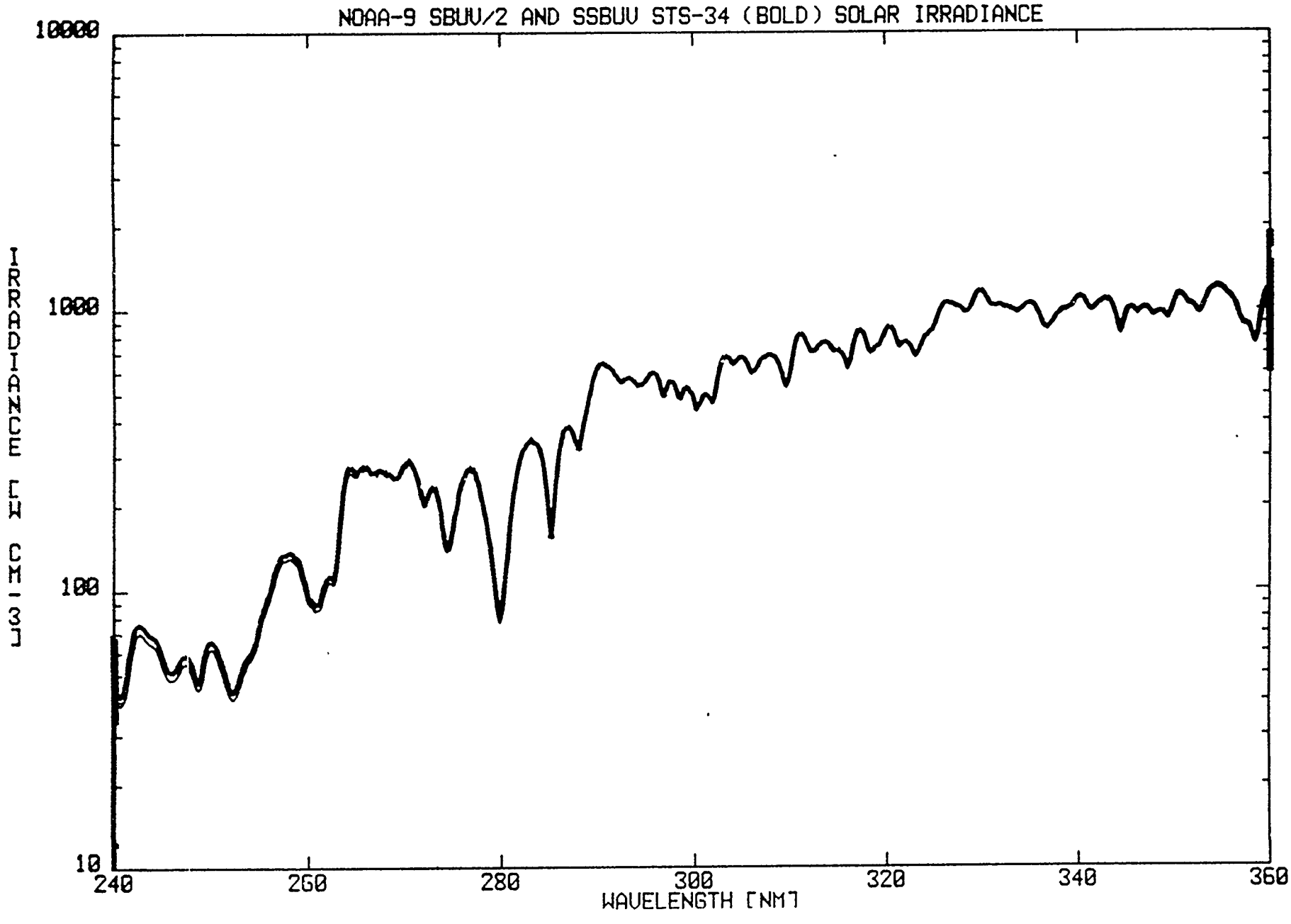
NOAA-9 SBUV/2 AND SSBUV STS-34 (BOLD) SOLAR IRRADIANCE
10000
1000
100
10
IRRADIANCE [W CM-2 NM-1]
240
260
280
300
320
340
360
WAVELENGTH [NM]

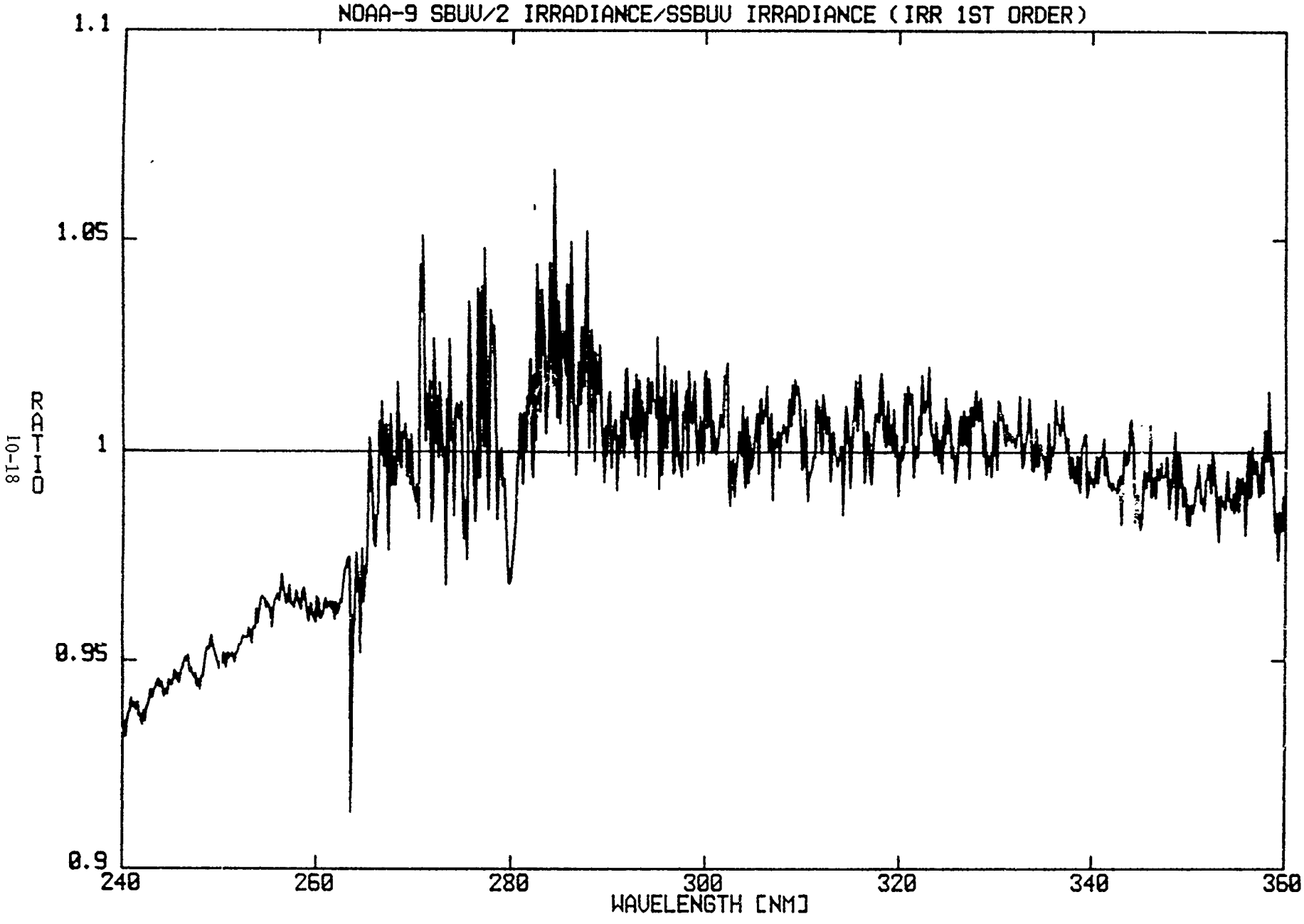
NOAA-9 SBUV/2 IRRADIANCE/SSBUV IRRADIANCE (IRR 1ST ORDER)
1.1
1.05
1
0.95
0.9
RATIO
240
260
280
300
320
340
360
WAVELENGTH [NM]

Attachment 11

Total Ozone Ozonesonde and Umkehr Observations for Satellite Ozone Data Validation

W.O. Komhyr, R.D. Grass, and G.L. Koenig
NOAA/ERL-CMDL
R.D. Evans, P. Franchois, and R.L. Leonard
University of Colorado, CIRES

Total Ozone, Ozonesonde, and Umkehr Observations for Satellite Ozone Data Validation

W. D. Komhyr, R. D. Grass, and G. L. Koenig
NOAA Climate Monitoring and Diagnostics Laboratory
Boulder, Colorado 80303-3328

R. D. Evans, P. Franchois, and R. K. Leonard
Cooperative Institute for Research in Environmental Sciences
University of Colorado, Boulder 80309

1. Introduction

The NOAA Air Resources Laboratory, Geophysical Monitoring for Climatic Change (GMCC) Division* has been providing total ozone, ozonesonde, and Umkehr data to the National Environmental Satellite Data and Information Service (NESDIS) for NOAA-9 solar backscattered ultraviolet (SBUV-2) satellite ozone data validation since 1984. This report describes the data and provides information on ozone measurement precision and accuracy.

2. Total Ozone Observations with Dobson Spectrophotometers

2.1. A Primary Standard for Total Ozone Observations: Dobson Spectrophometer No. 83

Dobson spectrophotometer 83 was established in 1962 as a standard for total ozone measurements in the United States. In 1980, the instrument was designated by the World Meteorological Organization (WMO) as the Primary Standard Dobson spectrophotometer for the world. Since the early 1970's, instrument 83 has been used extensively to calibrate instruments of the global Dobson total ozone station network. Calibrations of the instrument [on the Vigroux (1953) ozone absorption coefficient scale for AD wavelengths] were performed by the Langley slope method (Dobson and Normand, 1962) at Sterling, Virginia, in 1962, and at Mauna Loa, Hawaii (MLO), in 1972, 1976, 1978, 1979, 1980, 1981, 1984, and 1986-1989. Additionally, calibration checks on the instrument have been performed routinely since 1962 with a set of standard lamps. Results of the calibrations through 1987 were described in detail by Komhyr et al. (1989*a*).

Calibration of a Dobson spectrophotometer on an absolute scale by the Langley slope method entails obtaining a series of one-half-day total ozone measurements on AD wavelengths of the rising or setting sun, and deducing corrections S_{AD} to the instrument N_{AD}^* values, defined as follows by the fundamental Dobson instrument relation:

$$\frac{N_{AD}^* - [(\beta-\beta')_A - (\beta-\beta')_D]\, mp/p_0}{\mu} + S_{AD}\left(\frac{1}{\mu}\right) = [(\alpha-\alpha')_A - (\alpha-\alpha')_D]\, x + \frac{[(\delta-\delta')_A - (\delta-\delta')_D]\sec Z}{\mu} \quad (1)$$

where

$$N_A = \log \frac{I_\lambda}{I_{\lambda'}} - \log \frac{I_{0\lambda}}{I_{0\lambda'}} + k, \text{ for } A \text{ wavelengths;}$$

$$N_D = \log \frac{I_\lambda}{I_{\lambda'}} - \log \frac{I_{o\lambda}}{I_{o\lambda'}} + k, \text{ for } D \text{ wavelengths;}$$

*The GMCC Division of the Air Resources Laboratory was incorporated into the NOAA Climate Monitoring and Diagnostics Laboratory (CMDL) on December 3, 1989.

$N_{AD}^* = N_A^* - N_D^*$;

$N_A^* \sim N_A = N_A^* + S_A$;

$N_D^* \sim N_D = N_D^* + S_D$;

$S_{AD} = S_A - S_D$;

I_λ = intensity of the shorter wavelength of the A or D wavelength pair;

$I_{\lambda'}$ = intensity of the longer wavelength of the A or D wavelength pair;

$I_{0\lambda}$ = extraterrestrial value of I_λ;

$I_{0\lambda'}$ = extraterrestrial value of $I_{\lambda'}$;

k = the instrument constant;

β,β' = molecular scattering coefficients for the wavelengths λ and λ';

m = air mass, the ratio of the actual and vertical path lengths of the solar beam through the atmosphere;

p = mean station pressure;

p_0 = sea level pressure;

δ, δ' = particle scattering coefficients for the wavelengths λ and λ';

Z = solar zenith angle;

α,α' = ozone absorption coefficients for the wavelengths λ and λ';

μ = ratio of the actual and vertical path lengths of the solar beam through the ozone layer;

x = total ozone amount in a vertical column of the atmosphere.

For observations made during clear-sky conditions, the last term of (1) becomes negligible, and if the ozone amount is assumed to be constant during the one-half-day's observations, then from (1), a plot of

$$\frac{N_{AD}^* - [(\beta - \beta')_A - (\beta - \beta)_D]\, mp/p_0}{\mu} \text{ vs. } \frac{1}{\mu}$$

yields S_{AD}, the correction needed to the provisional N_{AD}^* values of the Dobson instrument.

The most comprehensive calibration of instrument 83 was performed in 1976 at MLO when ozone observations were made during 90 one-half days. The standard error associated with the determination of the mean S_{AD} correction to the instrument N_{AD}^* values at that time was 0.0006, which corresponds to an uncertainty in the measurement of ozone of 0.07% for x = 300 Dobson units (D.U.) and μ = 2. This calibration of instrument 83 resulted in establishment of an August 26, 1976, Calibration Scale for the instrument that was used through 1987 in calibrating all domestic and foreign Dobson spectrophotometers.

The August 26, 1976, Calibration Scale was used to establish N values in 1976 for Dobson instrument 83 standard lamps 83A, 83B, W, X, Y, Z, 83Q1, and 83Q2, some of which had been run on the instrument since 1962. The lamp data were then used to establish a 1962-1987 Standard Lamp Calibration Scale for instrument 83, which, except for the 1976 tie in, is independent of the Langley slope calibrations of the instrument.

Table 1 compares ozone values, x_1, determined with instrument 83 during 1962-1987 using the August 26, 1976, Calibration Scale, with similar values, x_2, incorporating Langley slope calibration corrections; with x_3 values measured on the 1976 Standard Lamp Scale; and with x_4 values determined on the 1976 Standard Lamp Scale with Langley slope calibration corrections applied. We conclude from the results that the August 26, 1976, Calibration Scale for Dobson instrument 83, and its equivalent scale dated July 10, 1987, have remained unchanged to within an uncertainty of ±0.5% during 1962-1989.

TABLE 1. Stability of the August 26, 1976, Calibration Scale for Dobson Instrument 83*

Year	$\frac{100(x_1-x_2)}{x_2}$ (%)	$\frac{100(x_1-x_3)}{x_3}$ (%)	$\frac{100(x_1-x_4)}{x_4}$ (%)
1962	--	-0.7	-1.0
1972	-0.1	-0.3	-0.1
1976	0.0	0.0	0.1
1978	0.0	0.0	0.0
1979	-0.2	-0.1	-0.2
1980	0.2	0.0	-0.4
1981	-0.3	-0.1	-0.7
1984	0.5	-0.1	0.1
1986	0.2	-0.5	-0.5
1987	0.2	-0.2	-0.1
1988*	0.0	--	--
1989*	-0.4	--	--

*Ozone values x_1, x_2, x_3, and x_4 are defined in the text. Data for 1988 and 1989 are presented relative to the July 10, 1987, calibration scale for instrument 83, which differs from the August 26, 1976, Calibration Scale by 0.1%.

2.2. Dobson Instrument 83 Absolute Calibration Scale

As indicated in section 2, Dobson spectrophotometer 83 is operated on the Vigroux (1953) ozone absorption coefficient scale. Several corrections must be applied to the data obtained to express ozone values on an absolute scale.

Bass and Paur (1985) redetermined the ozone absorption coefficients over the spectral range 230-350 nm that encompasses the Dobson instrument wavelengths. Although these new data have not been officially adopted by the International Ozone Commission, their use by a number of researchers is increasing. Using the Bass and Paur data, and slit function data for Dobson spectrophotometer 83 obtained by W. D. Komhyr (NOAA, Air Resources Laboratory, Boulder, Colorado, unpublished data, 1985), C. L. Mateer (Canadian Atmospheric Environment Service, Downsview, Canada, private communication, 1986) calculated effective ozone absorption coefficients for the Dobson instrument at -44°C. For observations on AD wavelengths, the new absorption coefficient is 1.430, which yields total ozone amounts 3.0% smaller than those obtained using the standard 1.388 ozone absorption coefficient for AD wavelengths.

Because the effective temperature of ozone over MLO during June-July months is near -44°C, no adjustment of the MLO total ozone data is needed to account for the dependence (0.13%/°C) of the AD wavelength ozone absorption coefficient on temperature. The -44°C effective temperature was derived from convolution of 33 ozone and air temperature profiles obtained with ECC ozonesondes at Hilo, Hawaii, during June-August months of 1985-1987. In the analysis, tropical model ozone and temperature values of McClatchey (1980) were used at pressure altitudes above about 5 mb.

Two other corrections are needed to Dobson instrument ozone values obtained during 1962-1989 to reduce them to absolute values. The first arises from use at MLO throughout the years of 24 km as the effective height of the ozone layer above sea level. Elecrochemical concentration cell (ECC) ozonesonde soundings in recent years have shown the effective height to be 26 km. Use of the 26 km value in processing the Dobson instrument data causes ozone values to increase by 0.2% at $\mu = 2$. Finally, the computer program that has been used to compute μ throughout the years in processing the Dobson data has had a minor glitch in it related to computation of the Julian calendar day. Corrected μ values yield higher ozone values by 0.1% at $\mu = 2$.

With the above corrections applied, instrument 83 ozone values are probably accurate on an absolute scale to ±2%. About 1% of this uncertainty stems from the uncertainty in the AD wavelength ozone absorption coefficient. It is of interest to note that preliminary analyses of ozone observations made with Dobson instrument 65, established independently at MLO as a secondary standard during the summer of 1989, yielded ozone values that agreed with instrument 83 values to within ±0.5%.

2.3. Check on the Calibration of the TOMS and SBUV Satellite Total Ozone Sensors

The Dobson instrument 83 instrument calibration observations made at MLO on AD wavelengths during 1979-1989 have yielded a unique, highly accurate total ozone data set, suitable for use in checking the calibration of satellite total ozone measurement instrumentation. A comparison of Dobson instrument 83 data with the Total Ozone Mapping Spectrometer (TOMS) satellite near-noon overpass data for 1979-1987 was described by McPeters and Komhyr (1989). Updated comparison results including comparison with the Solar Backscatter Ultraviolet (SBUV) spectrometer aboard the satellite, are shown in Figure 1 where Dobson instrument 83 values are shown on an absolute scale as described in section 2.2.

The TOMS and SBUV satellite data were obtained using the version 5 data processing program. Additionally, the satellite observations, applicable to sea level, were adjusted to the altitude of MLO (3.4 km) by subtracting from the satellite values the amount of ozone between sea level and MLO. Amounts to be subtracted were derived from 158 ECC ozone soundings made at Hilo, Hawaii, during the summers of 1983-1987.

Figure 1 indicates that, relative to Dobson instrument 83 ozone values, the TOMS data have drifted non-linearly downward by 7% since 1979. A similar downward drift has occurred for the SBUV instrument. On an absolute scale, the SBUV instrument, originally calibrated, gave ozone values higher than instrument 83 values by nearly 2%. TOMS values were higher initially than instrument 83 values by 4.5%.

2.4. Dobson Spectrophotometer Calibrations With Primary Standard Dobson Instrument 83

Appendix A summarizes data for instruments of the global Dobson spectrophotometer station network that were calibrated by direct comparison with Primary Standard instrument 83 since January 1, 1980. The calibrated instruments include the set of Regional Secondary Standard spectrophotometers established by the WMO in 1977 for the purpose of conducting calibrations within their respective regions. They are

Inst. No.	Country	Inst. No.	Country
41	U.K.	105	Australia
71	G.D.R.	108	U.S.S.R.
77	Canada	112	India
96	Egypt	116	Japan

Use of the regional standards throughout the years has increased the number of Dobson instruments of the global network having calibrations traceable to Primary Standard instrument 83.

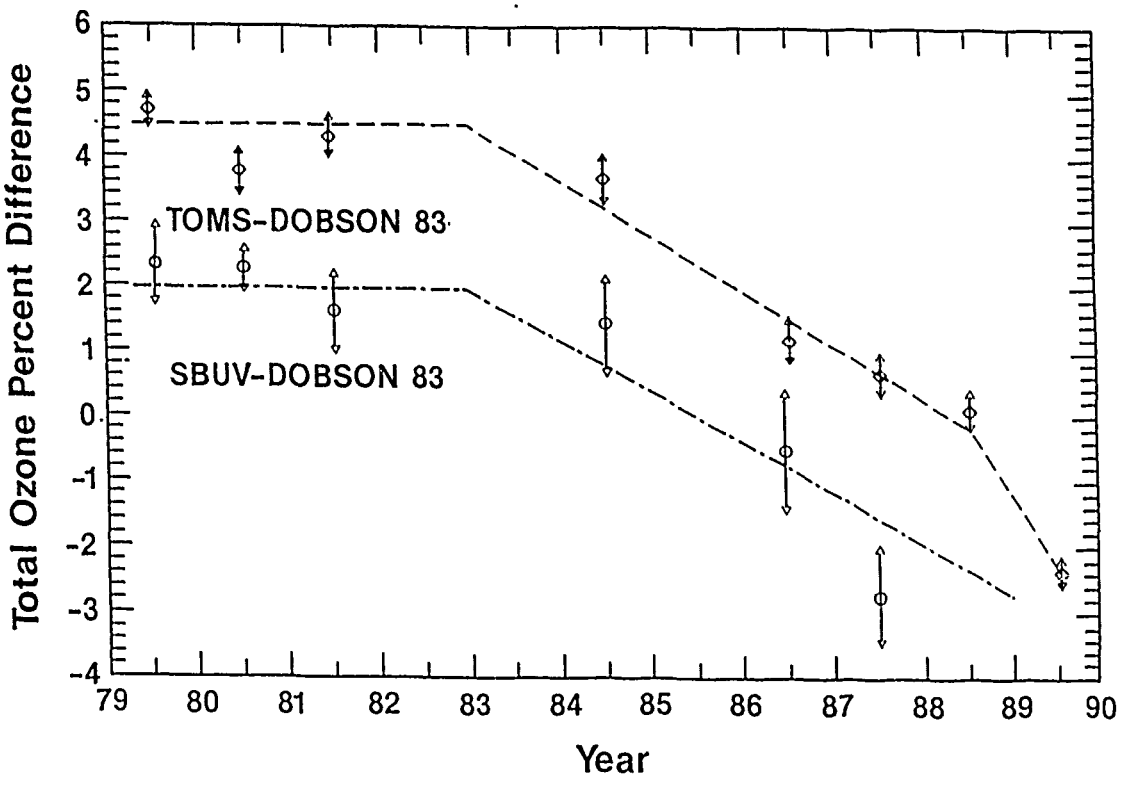

Figure 1. Total ozone data obtained at MLO during 1979-1989 with Dobson spectrophotometer 83 compared with data obtained with and TOMS and SBUV satellite instrumentation.

The calibrated instruments of Appendix A also include those from the set of select Dobson stations designated by NESDIS for use in satellite SBUV-2 ozone data validation. The instruments and stations are

Inst. No.	Station	Inst. No.	Station
15	Arosa	105	Melbourne
61	Boulder	112	New Delhi
102	Edmonton	81	Perth
62	Goose Bay	63	Poker Flat
87	Huancayo	89	Pretoria
85	Haute Provence	5702	Sapporo
72	Lauder	226	Tateno
76	Mauna Loa	55	Varanasi

Some comments about calibrations at these sites follow.

NOAA/GMCC calibrates the Dobson instruments at Boulder, Haute Provence, Huancayo, Mauna Loa, Perth, Lauder, and Poker Flat, and processes the ozone data from these sites.

Arosa Dobson instrument 15 was calibrated by GMCC in August 1986. At that time it measured ozone values 2.45% lower on average than did instrument 83. The next calibration of Arosa instrument 15 will be performed in July 1990. We do not know what calibration scale is used for processing Arosa data that are archived at the World Ozone Data Centre in Canada.

The Canadians calibrate the Edmonton and Goose Bay instruments. Calibrations are performed relative to Dobson instrument 77, calibrated with Primary Standard Dobson instrument 83 in 1977, and relative to Brewer spectrophotometer 017 calibrated with instrument 83 in 1986.

Huancayo Dobson instrument 87 has not been calibrated since 1985, and prospects for recalibration in the immediate future are poor because of political problems in Peru. Communications with Huancayo are scant, and travel to Huancayo is dangerous.

Pretoria Dobson instrument 89 was modernized and calibrated in our laboratory at GMCC in 1989, and observations began in Pretoria in 1989.

Except for calibration of Indian regional Secondary Standard Dobson instrument 112 in late 1984, we have not been able to perform any additional calibrations of the India instruments. Our attempts to arrange such calibrations with the Indian Meteorological Service have been unsuccessful. Neither have our attempts been fruitful in enlisting the help of the WMO in this matter. Therefore, we do not know the calibration status of the New Delhi and Varanasi instruments at present.

The Japanese regional standard Dobson instrument 116, operated at Tateno, was calibrated by GMCC in 1984 and 1989. Presumably, the Japanese keep their Sapporo instrument well calibrated.

2.5. Dobson Spectrophotometer Calibration Checks with Traveling Standard Lamps

At the 1977 International Comparison of Dobson Ozone Spectrophotometers held in Boulder, Colorado, a standard lamp method was devised (Komhyr et al., 1981) for identifying Dobson instruments that have gross calibration errors. To upgrade the calibration of Dobson instruments throughout the world, seven standard lamp units, each consisting of two calibrated lamps and a stable power supply, were fabricated in 1981. The global Dobson instrument network was then divided into seven areas, each containing from 5 to 17 instruments, and a lamp unit was shipped to each area for checking the calibrations of the Dobson instruments in each area. Results of the calibration checks performed during 1981-1983 (Grass and Komhyr, 1985) are shown in Appendix B. A similar program of Dobson instrument calibration checks was carried out during 1985-1987 (Grass and Komhyr, 1989). Results are summarized in Appendix C.

In 1981-1983, lamp calibrations were performed on 78 instruments. Of these, 27 exhibited errors exceeding 2%, and several instruments had errors in the 6-10% range. During 1985-1987, calibration checks were made on 81 instruments. Errors larger than 2% were obtained for only 13 instruments, the largest error being 4.6%.

3. ECC Ozonesonde Observations for Satellite Ozone Data Validation

In 1985, NOAA/GMCC began flying ECC ozonesondes at Boulder, Colorado, and Hilo, Hawaii, and cooperatively at Edmonton, Canada with scientists from the Canadian Atmospheric Environment Service, for the purpose of obtaining ozone profile data to 40 km altitude for

comparison with SBUV-2 satellite ozone profile data. Results obtained at the three sites, combined with ECC sonde data from six other stations with locations ranging from the Arctic to Antarctica, have yielded a self-consistent ozone data base from which the latitudinal ozone distribution to 35 km altitude has been derived (Komhyr et al., 1989*b*). We reproduce here the derived mean seasonal and annual ozonesonde profiles for the nine stations (including numerical data), and present new information on the accuracy of the measurements. The data should be useful for comparison with model calculations of the global distribution of atmospheric ozone, for serving as a priori statistical information in deriving ozone vertical distributions from satellite and Umkehr observations, for improving the satellite and Umkehr ozone inversion algorithms, and for improving the quality of satellite total ozone data.

The mean seasonal and annual ozone vertical distribution data are presented for Resolute, Canada (RES, 74°N, 95°W); Point Barrow, Alaska (BRW, 71°N, 156°W); Edmonton, Canada EDM, 53°N, 114°W); Boulder, Colorado (BDR, 40°N, 105°W); Hilo, Hawaii (HIL, 19°N, 155°W); American Samoa, South Pacific (SMO, 14°S, 170°W); Lauder, New Zealand (LDR, 45°S, 170°E); Syowa, Antarctica (SYO, 69°S, 39°E); and South Pole, Antarctica (SPO, 90°S, 24°W). Most of the observational data used in the analysis were obtained during 1985-1987. Table 2 shows the actual period of record for each station from which the mean data were derived, and the number of soundings made at each station. NESDIS funding support for observations at Edmonton, Boulder and Hilo were terminated, respectively, in 1987, 1988 and 1989.

Figure 2 depicts average seasonal and annual ozone profiles derived at the nine stations. The data base used in forming the plots is listed in Table 3. Recently, a new improved method was devised for measuring ECC ozonesonde pump efficiencies at reduced ambient pressures (Komhyr, manuscript of NOAA/GMCC, 1989). The method yields pump efficiency data obtained under simulated ozonesonde flight conditions. On the basis of the preliminary new results, estimated correction factors required for 10, 7, 5, 4, 3.5, and 3 mb data of Table 3 are 1.001, 1.012, 1.026, 1.041, 1.059, and 1.087. The data in Table 3 are, furthermore, expressed on the Vigroux (1953) ozone absorption coefficient scale. To express results on the Bass and Paur (1985) ozone absorption coefficient scale, all values in Table 3 should be multipled by 0.9706 -- the ratio of the Bass and Paur to the Vigroux ozone absorption coefficients. With the data corrected as indicated above, we estimate the accuracy of ozone measurements with the ECC ozonesondes to be ±10% in the troposphere, ±5% in the stratosphere to 10 mb, and ±5 to ±15% at altitudes of 10-3 mb.

TABLE 2. Periods of Record and Number of ECC Ozonesonde Soundings Used in Deriving Average Seasonal and Annual Ozone Profiles at Nine Stations

Station	Period of Record	Number of Soundings				
		DJF	MAM	JJA	SON	ANN
RES	Jan. 1982 - April 1986	27	33	37	27	124
BRW	Feb. 1986 - April 1988	16	35	14	27	82
EDM	Jan. 985 - Nov. 1987	19	22	21	17	79
BDR	Jan. 1985 - Dec. 1987	37	43	34	42	156
HIL	Jan. 1985 - Dec. 1987	33	34	33	35	135
SMO	April 1986 - May 1988	16	25	25	19	85
LDR	Aug. 1986 - May 1988	24	22	25	39	110
SYO	Jan. 1982 - Dec. 1986	15	6	4	29	54
SPO	Jan. 1986 - Dec. 1987	22	29	23	58	122

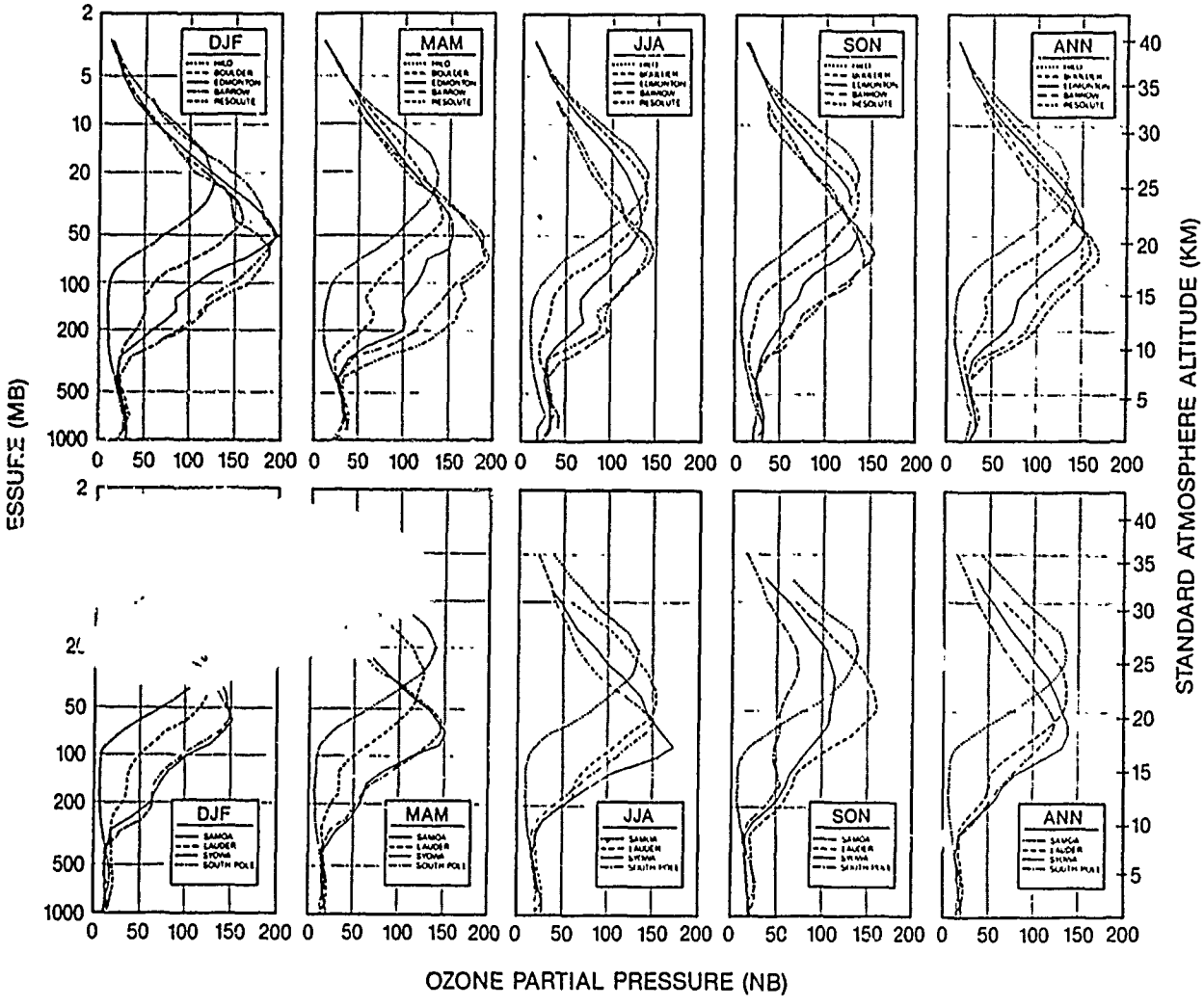

Figure 2. Average seasonal and annual ozone profiles derived at nine stations, from observations made with ECC ozonesondes during time periods indicated in Table 1.

Apart from use of the ECC ozonesonde data of Figure 2 and Table 3 for comparison with SBUV-2 satellite ozone profile data, the ozonesonde data can be used to improve the accuracy of satellite total ozone measurements. Ozone measurements with satellite instruments are relatively insensitive to tropospheric ozone. Ozonesonde observations offer the only means of measuring tropospheric ozone in vertical profile at a relatively large number of stations and under all weather conditions. Note from Figure 2 that the Southern Hemisphere troposphere contains only about one-half the ozone present in the Northern Hemisphere. The seasonal variations in tropospheric ozone are large in both hemispheres. The tropical tropopause can contain up to 17% of the total ozone, and it can have factor of 2 variations over time intervals of several days. Such information should be taken into account in processing TOMS and SBUV satellite data to improve data quality.

TABLE 3. AVERAGE SEASONAL AND ANNUAL OZONE PARTIAL PRESSURES (NB) FROM ECC OZONESONDE SOUNDINGS AT 78°N AND 90°S LATITUDE*

Pressure (mb)	DJF	MAM	JJA	SON	ANN	DJF	MAM	JJA	SON	ANN	DJF	MAM	JJA	SON	ANN
	Resolute					Point Barrow					Edmonton				
Surface	30.4	21.2	24.8	32.2	27.1	25.4	20.5	22.7	27.7	23.8	24.8	35.5	29.9	26.5	29.2
1000	30.7	22.0	25.9	31.6	27.3	29.2	25.1	24.5	29.9	26.9	-	-	-	-	-
700	30.5	34.0	36.6	30.3	32.8	29.6	36.7	36.8	30.5	33.7	23.3	30.1	29.4	26.4	27.3
500	24.3	31.3	33.0	24.7	28.4	23.3	30.1	33.0	25.5	28.2	22.8	39.6	29.1	28.6	29.9
300	34.4	77.7	46.8	34.1	47.8	37.8	44.8	31.0	30.9	34.8	59.0	99.6	58.0	46.2	64.3
200	87.7	142.4	98.5	65.2	97.4	95.4	116.3	86.4	66.4	88.6	86.3	98.7	66.1	55.2	76.5
150	113.2	160.2	94.4	88.8	112.4	118.6	133.1	84.9	78.4	100.4	108.2	115.3	81.4	75.6	94.8
100	167.3	164.3	116.8	128.6	142.9	149.1	159.4	117.3	120.8	125.7	161.4	126.9	105.8	112.5	127.0
70	186.5	196.3	144.7	152.4	169.1	178.3	192.2	139.6	144.9	156.5	197.8	153.9	128.0	134.8	153.0
50	176.1	183.8	141.0	142.0	160.5	195.1	189.6	131.2	135.3	156.5	164.9	137.5	129.8	126.8	140.2
30	146.3	141.6	98.9	110.7	121.7	175.9	147.9	110.2	114.6	131.4	124.8	109.8	115.4	112.1	115.7
20	106.0	103.6	76.9	83.5	90.6	148.0	107.6	83.2	86.8	98.9	97.1	91.2	100.4	88.3	94.1
15	88.4	82.6	66.2	64.8	74.4	114.5	87.2	70.0	71.1	80.7	60.6	67.2	71.2	62.0	64.3
10	-	57.9	49.8	38.1	49.7	76.8	57.4	53.7	51.3	56.5	38.4	48.2	49.3	42.5	43.8
7	-	43.9	37.2	35.0	39.4	57.7	36.6	37.5	35.8	39.8	25.0	32.7	29.8	29.6	28.6
5	-	-	-	-	-	-	-	-	-	-	20.3	22.9	25.0	22.7	22.5
4	-	-	-	-	-	-	-	-	-	-	13.9	9.0	13.0	13.7	12.5
	Boulder					Hilo					Samoa				
Surface	28.9	39.1	42.5	28.6	34.5	18.0	30.7	20.3	19.4	21.7	11.0	14.5	21.2	18.4	16.5
1000	-	-	-	-	-	22.9	32.1	19.3	20.7	23.5	11.4	15.2	21.2	18.5	16.7
700	32.7	40.8	42.8	32.6	37.3	29.5	37.1	28.5	24.9	29.9	16.7	18.3	22.0	25.9	20.3
500	24.9	30.1	31.1	25.2	27.8	21.8	28.9	20.6	19.8	22.7	15.3	15.6	18.5	22.8	17.9
300	22.9	23.7	20.2	14.6	20.4	13.4	16.7	12.7	11.6	13.5	9.3	8.9	11.7	12.1	10.5
200	41.1	54.3	25.6	18.6	34.9	10.5	11.7	10.1	7.6	9.9	5.9	6.7	8.8	7.4	7.1
150	51.4	67.9	32.7	23.5	44.0	9.4	13.1	12.0	8.8	10.7	5.6	6.3	8.0	6.8	6.7
100	61.1	70.2	46.2	43.7	55.4	11.8	20.8	24.2	15.9	17.9	7.2	8.9	11.0	10.2	9.2
70	106.2	98.2	84.8	84.0	93.7	34.4	55.3	50.1	44.3	45.8	33.5	26.8	36.6	36.8	33.4
50	144.1	128.0	116.0	111.8	125.9	73.3	91.8	88.6	75.4	82.1	72.6	68.0	80.6	77.5	74.5
30	152.0	138.5	138.9	136.6	141.9	120.1	128.4	131.4	127.3	126.7	126.9	125.0	125.2	127.3	126.0
20	116.6	118.2	131.6	125.8	122.9	124.2	137.1	140.9	137.6	134.7	140.3	140.0	133.6	139.3	138.3
15	88.0	101.3	112.7	101.6	100.7	116.5	126.9	125.8	123.4	123.1	134.7	130.7	118.3	131.2	128.4
10	61.6	76.1	80.9	71.3	72.3	83.3	89.9	90.3	86.2	87.4	105.9	96.8	81.5	92.1	94.6
7	42.9	50.7	52.3	48.0	48.5	53.2	54.2	58.3	54.4	55.0	72.3	65.2	57.3	65.3	66.5
5	28.4	31.1	33.0	31.0	30.9	32.3	30.8	34.6	31.3	32.1	55.0	39.3	37.6	-	43.9
4	19.8	20.8	21.8	22.3	21.2	21.3	20.7	24.4	20.7	21.6	-	-	-	-	-
3	10.8	10.2	13.1	14.9	12.1	11.4	10.3	13.0	10.0	11.0	-	-	-	-	-
	Lauder					Syowa					South Pole				
Surface	14.0	15.3	17.8	19.7	16.9	14.3	20.7	26.8	20.9	20.7	14.7	17.1	21.1	18.9	17.8
1000	-	-	-	-	-	11.6	16.5	24.3	18.1	18.3					
700	20.5	20.1	26.9	26.0	23.3	12.1	17.0	19.5	16.2	17.4	29.7	22.8	15.1	13.4	20.6
500	18.2	17.5	22.1	23.8	20.2	18.2	30.0	20.3	16.3	18.5	64.3	52.9	41.3	37.5	48.9
300	18.0	15.3	18.6	20.2	17.3	62.1	57.3	49.8	43.5	50.5	66.3	67.6	67.3	53.9	64.0
200	33.2	24.3	50.3	55.1	39.7	71.9	63.7	81.0	59.2	66.4	98.6	116.0	111.0	47.1	94.3
150	35.5	33.5	61.6	66.0	49.4	103.1	115.3	153.5	77.3	111.4	140.7	146.9	145.1	53.4	121.7
100	50.7	49.8	91.5	90.0	69.6	143.7	151.7	161.0	99.9	139.4	148.2	133.9	140.6	52.6	118.6
70	81.5	86.3	124.4	135.2	106.9	146.4	131.8	143.0	108.2	132.3	125.0	83.3	89.7	72.4	91.2
50	115.5	114.9	152.4	160.2	134.4	134.3	87.8	116.0	113.9	116.7	84.3	52.5	65.3	71.8	67.2
30	124.0	128.3	146.5	147.6	135.9	104.6	60.6	86.5	104.0	92.3	61.3	37.6	56.3	59.6	53.0
20	117.4	114.4	121.3	126.8	119.4	85.2	52.3	70.2	85.8	75.0	40.5	27.1	41.7	42.5	37.4
15	101.5	92.1	99.9	103.5	98.5	59.0	42.2	47.5	62.9	54.7	22.5	17.5	32.0	28.4	25.7
10	73.9	61.1	55.8	70.3	67.1	40.2	34.8	-	36.0	36.5	17.0	10.5	21.0	16.1	15.4

*See text for corrections needed to the data.

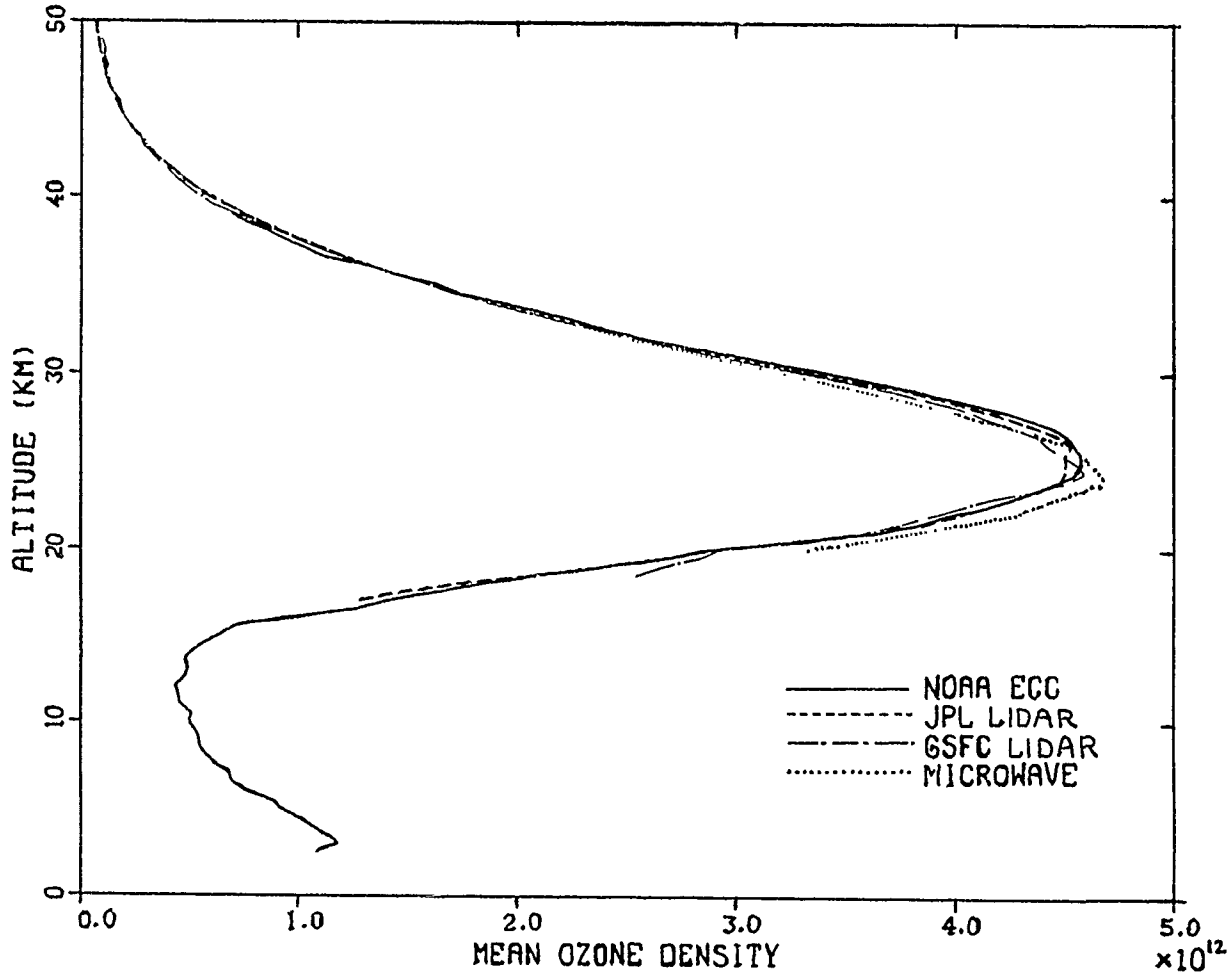

Figure 3. Comparison of mean ECC ozonesonde, JPL lidar, GSFC lidar, and Millitec Corporation microwave ozone data obtained at Table Mountain, California, July 21-August 1, 1989.

Performance characteristics of ECC ozonesondes, the Jet Propulsion Laboratory (JPL) ozone lidar, the Goddard Space Flight Center (GSFC) lidar, and the Millitec Corporation microwave ozone instrument were intercompared during the Stratospheric Ozone Intercomparison Campaign (STOIC) conducted at Table Mountain, California, during July 21-August 2, 1989 (Komhyr et al., 1990). Figure 3 shows the intercomparison results. The plots of Figure 3 are mean data obtained from 10 ozone soundings, 10 each lidar soundings, and 9 microwave instrument ozone soundings. Of the 10 ECC ozonesonde releases, two flights attained maximum altitudes of 30.8 ±1.0 km, six 34.3 ± 1.0 km, and two 38.8 ± 0.3 km.

4. Umkehr Observations with Automated Dobson Spectrophotometers

Funding was obtained in 1982 from the U.S. Environmental Protection Agency, the Chemical Manufacturers' Association, the WMO (Voluntary Cooperation Program), and NOAA for automating seven Dobson spectrophotometers and deploying them at a number of stations for long term ozone trend monitoring in the stratosphere, and for validation of satellite ozone measurements. Automation of the Dobson instruments, and results of initial instrument intercalibrations were described by Komhyr et al. (1985). The automated Dobson stations are

Boulder, Colorado; Haute Provence, France; Mauna Loa, Hawaii; Poker Flat, Alaska; Huancayo, Peru; Lauder, New Zealand, and Perth, Australia. Since 1984, funding for routine operations and data processing have been provided by NESDIS.

Table 4 shows the time intervals during which observations were at the various stations, and lists the number of observations made per year through June 1989. Automatic operation of Huancayo, Peru, Dobson instrument 87 failed in 1986, and all attempts at repair have been unsuccessful. Umkehr observations at Huancayo, with instrument 87 operated manually, were resumed in 1988.

During STOIC 1989 referred to previously, an effort was made to assess the quality of Umkehr data obtained at Table Mountain, California, with Dobson spectrophotometer 91 relative to ECC ozonesonde, lidar, and microwave instrument ozone data. Ozonesonde releases were generally made near 2200 local standard time. Comparison Umkehr data were obtained from observations made earlier each evening, and the following morning.

TABLE 4. Record of Umkehr Observations at the Automated Dobson Spectrophotometer Stations

Year	bs. Quality	Boulder	Haute Provence	Mauna Loa	Poker Flat	Perth	Huancayo	Lauder
1982	Attempts	88						
	Useful	75						
	Good	62						
1983	Attempts	209	166					
	Useful	103	83					
	Good	86	83					
1984	Attempts	465	517	353	319	250		
	Useful	206	305	260	98	132		
	Good	132	103	216	60	107		
1985	Attempts	417	459	557	299	520	59	
	Useful	197	210	354	81	318	19	
	Good	141	74	301	45	248	14	
1986	Attempts	484	432	604	296	504	96	
	Useful	188	231	371	61	259	21	
	Good	100	147	327	43	197	14	
1987	Attempts	523	420	603	425	563	-	451
	Useful	238	235	408	95	302	-	102
	Good	204	278	387	77	263	-	76
1988	Attempts	546	447	554	390	476	39	599
	Useful	240	256	372	89	263	?	188
	Good	188	219	355	73	246	?	144
1989*	Attempts	286	266	274	165	295	62+	344
	Useful	77	162	138	40	143		94
	Good	61	139	125	32	133		80

*The record of observations for 1989, is from January through June, only.

Figure 4 compares data from six ECC ozonesonde soundings and six morning conventional (C-wavelength) Umkehr observations; results are expressed on the Bass and Paur (1985) ozone absorption coefficient scale. In general, Umkehr ozone values are not considered reliable in layers 1-4 (below the layer of ozone maximum). The agreement in results in layers 5-7 is excellent, with differences in the sonde and Umkehr data ranging only from 2-4%.

Figure 5 compares data from six ECC ozonesonde soundings and six evening Umkehr observations. While the agreement in the two kinds of data in layers 6 and 7 is highly satisfactory (3-4%), the difference in layer 5 is greater (9.4%), with the ozonesonde measurements giving the higher value.

The lower atmosphere at Table Mountain was highly polluted in the late afternoons, and afternoon total ozone amounts were higher on average than morning values by 2.8%. Thus, the morning Umkehr data are probably more representative of the true stratospheric ozone vertical distribution than are the evening Umkehr data. From the limited data sets, we infer that ECC ozonesonde observations and conventional Umkehr observations made at Table Mountain, California, in clean air yield ozone data in layers 5-7 (24-38 km) that agree to within 2 -4%, and that pollution in the lower atmosphere degraded the Umkehr observations in layers 1-5.

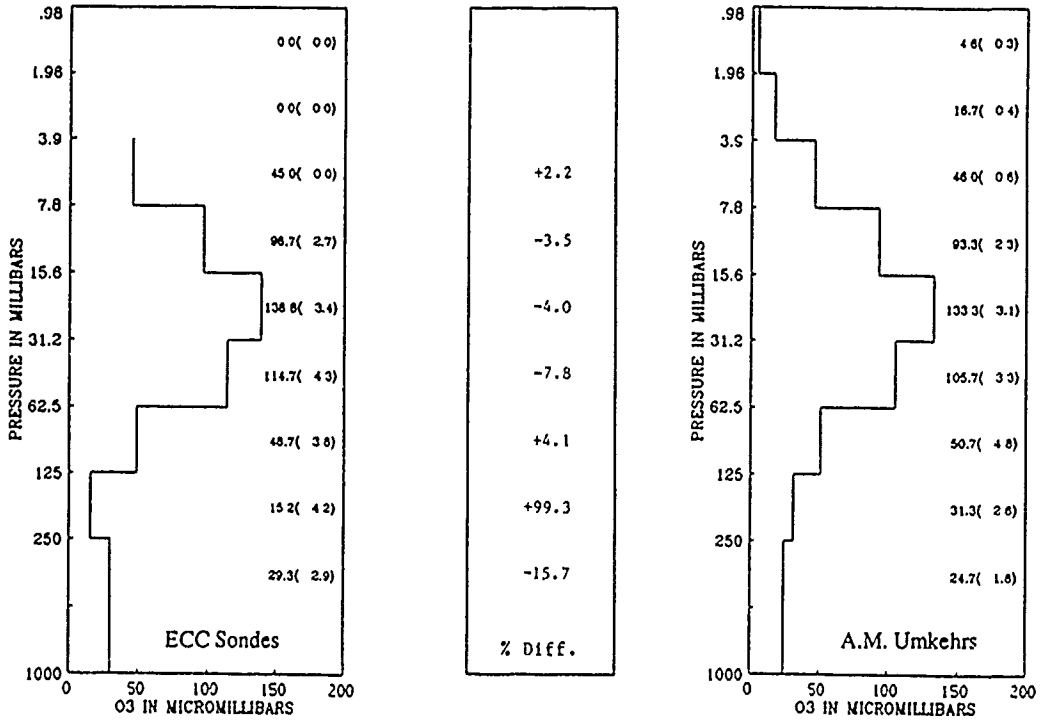

Figure 4. Comparison of morning mean conventional Umkehr data from Table Mountain, California, with corresponding mean ECC sonde data reduced to Umkehr layers. Numerical values shown between the pair data plots are layer ozone differences in percent. The number of measurements in each layer is 6, except 5 in layer 6, and 1 in layer 7 for the ECC sondes. Also shown in the figures are layer mean ozone partial pressures with standard deviations (bracketed values).

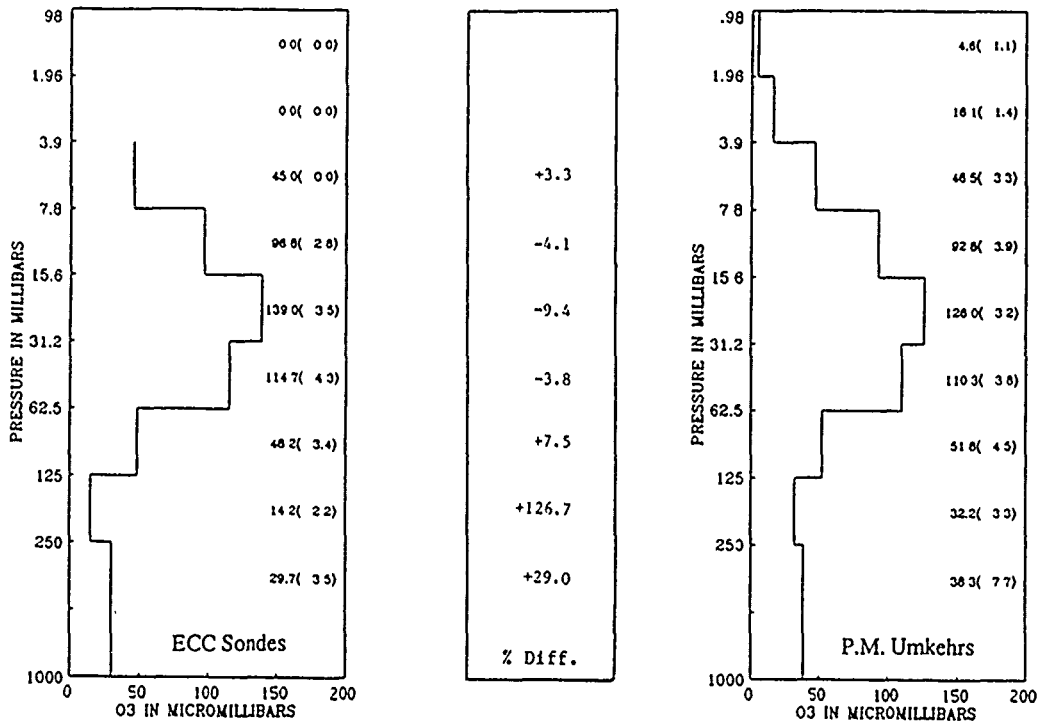

Figure 5. Comparison of evening mean conventional Umkehr data from Table Mountain, California, with corresponding mean ECC sonde data reduced to Umkehr layers. Numerical values shown between the pair data plots are layer ozone differences in percent. The number of measurements in each layer is 6, except 5 in layer 6, and 1 in layer 7 for the ECC sondes. Also shown in the figures are layer mean ozone partial pressures with standard deviations (bracketed values).

References

Bass, A.M., and R.J. Paur, The ultraviolet cross-sections of ozone, I, The measurements, in *Atmospheric Ozone, Proc. Quadrennial Ozone Symposium*, Halkidiki, Greece, 3-7 September 1984, pp. 606-610, D. Reidel, Dordrecht, Holland, 1985.

Dobson, G.M.B., and C.W.B. Normand, Determination of the constants etc. used in the calculation of the amount of ozone from spectrophotometer measurements and of the accuracy of the results, *Ann. Int. Geophys. Year, 16, part 2*, 161-191, 1962.

Grass, R.D., and W.D. Komhyr, Traveling standard lamp calibration checks on Dobson ozone spectrophotometers during, 1981-83, in *Atmospheric Ozone, Proc. Quadrennial Ozone Symposium,* Halkidiki, Greece, 3-7 September 1984, pp. 376-380, Reidel, Dordrecht, Holland, 1985.

Grass, R.D., and W.D. Komhyr, Traveling standard lamp calibration checks of Dobson ozone spectrophotometers during 1985-1987, *Proc. 1988 Quadrennial Ozone Symposium,* Göttingen, Federal Republic of Germany, A. Deepak, Hampton, Va., in press, 1989.

Komhyr, W.D., R.D. Grass, and R.K. Leonard, WMO 1977 International Comparison of Dobson Spectrophotometers, *Proc. Quadrennial International Ozone Symposium*, Boulder, Colorado, 4-9 August 1980, pp. 25-32, National Center for Atmospheric Research, Boulder, Colo., 1981.

Komhyr, W.D., R.D. Grass, R.D. Evans, R.K. Leonard, and G.M. Semeniuk, Umkehr observations with automated Dobson spectrophotometers, *Atmospheric Ozone, Proc. Quadrennial Ozone Symposium*, Halkidiki, Greece, 3-7 September 1984, D. Reidel, Dordrecht, Holland, 371-375, 1985.

Komhyr, W.D., R.D. Grass, and R.K. Leonard, Dobson spectrophotometer 83: A standard for total ozone measurement, 1962-1987, *J. Geophys. Res., 94 (D7)*, 9847-9861, 1989*a*.

Komhyr, W.D., S.J. Oltmans, P.R. Franchois, W.F. Evans, and W.A. Matthews, The latitudinal distribution of ozone to 35 km altitude from ECC ozonesonde observations, *Proc. 1988 Quadrennial Ozone Symposium*, Göttingen, Federal Republic of Germany, A. Deepak, Hampton, Va., in press, 1989*b*.

Komhyr, W.D., J.A. Lathrop, and D.P. Opperman, ECC ozonesonde and Dobson Umkehr observations during STOIC 1989, *Digest of Topical Meeting on Optical Remote Sensing of the Atmoshere, 1990*, Vol. 4, 441-444, Optical Society of America, Washington, D.C., 1990

McPeters, R.D., and W.D. Komhyr, Long-term changes in SBUV/TOMS relative to the World Standard Dobson Ozone Spectrophotometer, *Proc. 1988 Quadrenniel Ozone Symposium*, Göttingen, Federal Republic of Germany, A. Deepak, Hampton, Va., in press, 1989.

Vigroux, E., Contribution à l'étude expérimentale de l'absorption de l'ozone, *Ann. Phys., 8*, 709-762, 1953.

APPENDIX A

Instruments of the Global Dobson Spectrophotometer Network Calibrated Relative to Primary Standard Dobson Instrument 83 Since January 1, 1980

Calibration Date	Instrument Number	Station	% Error in Ozone*	Notes
2-28-80	76	Pt. Barrow	1.02	
5-20-80	76	Pt. Barrow	-	
5-20-80	72	Wallops Island	-1.42	
5-20-80	82	Boulder	0.44	
5-20-80	82	Boulder	-	
5-20-80	33	Bismarck	-0.73	
5-20-80	33	Bismarck	-	
6-11-80	63	Mauna Loa	0.64	
6-18-80	63	Mauna Loa	-	
9-03-80	91	Boulder	-1.73	
4-10-81	58	Tallahassee	2.62	
4-10-81	65	Boulder	-	
4-23-81	58	Tallahassee	-	
8-14-81	79	Nashville	3.33	
8-25-81	79	Nashville	-	
8-25-81	64	Potsdam	-	
8-25-81	41	U.K.	-2.71	
9-08-81	61	Boulder	-	Initial calibration, automated Dobson
9-08-81	41	U.K.	-	
2-20-82	72	Boulder	-	
4-23-82	69	Egypt	-	
5-18-82	91	Boulder	-	
5-18-82	52	Manila	8.88	
5-18-82	94	Fresno	-	
5-26-82	34	Caribou	1.09	
5-26-82	63	Mauna Loa	0.0	
7-13-82	52	Manila	-	
7-20-82	34	Caribou	-	
7-20-82	72	Boulder	-1.45	
7-20-82	72	Boulder	-	
8-20-82	86	Boulder	0.57	
8-20-82	86	Boulder	-	
4-20-83	85	Haute Provence	1.91	
4-25-83	85	Haute Provence	2.49	
4-25-83	76	Pt. Barrow	0.85	
4-25-83	87	Huancayo	4.92	
4-25-83	76	Pt. Barrow	0.85	
5-26-83	63	Poker Flat	-	Automated Dobson
5-26-83	86	Boulder	-	
6-21-83	85	Boulder	-	Initial calibration, automated Dobson
8-17-83	76	Mauna Loa	-	Initial calibration, automated Dobson
8-17-83	87	Huancayo	-	Initial calibration, automated Dobson
8-24-83	82	Boulder	1.88	
8-24-83	90	Bangkok	4.90	
8-24-83	82	Boulder	-	
10-04-83	90	Bangkok	-	
2-23-84	81	Perth	1.98	
5-08-84	81	Perth	-	Initial calibration, automated Dobson
5-08-84	38	Wallops Island	-0.41	
5-08-84	61	Boulder	1.53	

Appendix A - Continued

Calibration Date	Instrument Number	Station	% Error in Ozone*	Notes
5-08-84	61	Boulder	-	Initial calibration after repair of optical wedge
5-31-84	82	Boulder	-1.38	
11-17-84	105	Melbourne	0.09	Regional standard
11-17-84	111	Australia	-	No data
11-17-84	115	Australia	-	No data
11-29-84	105	Melbourne	-	
11-29-84	112	India	+1.50	Regional standard
11-29-84	116	Japan	-	Regional standard, no data
11-29-84	82	Invercargill	-0.57	Temporary loan to Invercargill, N.Z.
12-01-84	112	India	-	
12-01-84	82	Invercargill	-0.75	
12-01-84	82	Invercargill	-	
4-11-85	65	Boulder	0.74	
4-11-85	61	Boulder	0.33	
5-08-85	17	Invercargill	-	Initial calibration after instrument flooded
5-08-85	38	Wallops Island	-	Initial calibration after installing air wedge
5-15-85	87	Huancayo	0.04	Automated Dobson
5-15-85	87	Huancayo	-	
6-19-85	79	Nashville	4.71	
8-06-85	82	South Pole	-	
8-26-85	33	Bismarck	-0.77	
9-12-85	41	U.K.	-0.95	
9-17-85	41	U.K.	-	
4-15-86	33	Bismarck	-	Initial calibration after installing air wedge
4-28-86	79	Nashville	-	
4-28-86	93	Natal	6.33	
5-01-86	72	Boulder	-	Initial calibration, automated Dobson
5-01-86	80	South Pole	0.53	
5-20-86	93	Natal	-	
8-06-86	104	F.R.G.	0.89	
8-15-86	51	Arosa	-1.77	
8-15-86	56	Norway	-1.15	
8-15-86	71	G.D.R.	1.81	
8-15-86	74	Czechoslavakia	-1.68	
8-15-86	92	Denmarck	0.57	
8-15-86	96	Egypt	-0.04	
8-15-86	101	Arosa	-3.17	
8-15-86	40	Belguim	1.13	
8-21-86	84	Poland	1.38	
8-21-86	64	G.D.R.	-0.13	
8-21-86	85	Haute Provence	-0.62	Automated Dobson
8-25-86	120	Spain	-0.89	
8-25-86	13	Portugal	-1.94	
8-25-86	15	Arosa	-2.45	
10-01-86	34	Caribou	0.94	
10-01-86	42	Samoa	4.41	
10-01-86	42	Samoa	-	
4-22-87	34	Caribou	-	
4-22-87	42	Samoa	-	
5-14-87	76	Mauna Loa	-0.01	

Appendix A - Continued

Calibration Date	Instrument Number	Station	% Error in Ozone*	Notes
5-19-87	76	Mauna Loa	-	
9-01-87	61	Boulder	0.77	
9-01-87	61	Boulder	-	
9-01-87	86	Boulder	-0.22	
10-20-87	13	Portugal	-	
5-11-88	33	Bismarck	-1.96	
5-25-86	33	Bismarck	-	
5-26-88	80	South Pole	-	
5-26-88	86	Boulder	-	
6-02-88	107	U.S.S.R.	-4.58	
6-02-88	108	U.S.S.R.	-0.18	Regional standard
6-16-88	108	U.S.S.R.	-	
9-08-88	107	U.S.S.R.	-	
9-08-88	65	Boulder	-0.56	Secondary standard
9-08-88	65	Boulder	-	Secondary standard
11-17-88	105	Melbourne	0.37	Regional standard
11-18-88	81	Perth	-2.66	Optical wedge repaired several months earlier
11-25-88	81	Perth	-	
11-25-88	105	Melourne	-	Regional standard
12-13-88	72	Lauder	0.45	
12-20-88	72	Lauder	-	
3-24-89	91	Pt. Barrow	1.57	
3-24-89	63	Poker Flat	-0.19	
5-19-89	94	Fresno	-1.14	
5-24-89	91	Pt. Barrow	-	
6-02-89	89	South Africa	-	
6-05-89	94	Fresno	-	
6-20-89	116	Japan	-1.21	Regional standard
11-14-89	120	Spain	1.82	
11-14-89	120	Spain	-	

*A positive error means that the instrument measured ozone values too high. Errors are shown for $\mu \sim 2$ and 300 m-atm-cm of ozone.

APPENDIX B

Results of 1981-1983 Calibration Checks on Dobson Spectrophotometers, Using Traveling Standard Lamps

Station	Inst No.	Date of Calib. Check	Inst. Calib. Error (%)*
Area 1-North America			
Toronto, Canada	77	Oct. 15, 1981	-0.15
Resolute, Canada	59	Dec. 11, 1981	-0.74
Churchill, Canada	60	Jan. 1, 1982	+1.62
Goose Bay, Canada	62	May 11, 1981	+0.00
Edmonton, Canada	102	Nov. 30, 1981	+0.08
Reykjavic, Iceland	50	March 23, 1982	+0.44
South Pole, Antarctica	80	Jan. 25, 1982	+1.32
Bismark, N. Dak.	33	July 15, 1982	+0.88
Caribou, Maine.	34	June 2, 1982	-1.25
Wallops Is., Virginia	38	June 17, 1982	-0.96
Tallahassee, Florida	58	Oct. 1, 1982	+0.88
Nashville, Tennesse	79	Sept. 27, 1982	+1.18
Mauna Loa, Hawaii	63	June 2, 1982	-1.25
Am. Samoa, South Pacific	42	Aug. 28, 1982	+0.81
Point Barrow, Alaska	76	April 29, 1982	+1.62
Boulder, Colorado	61	June 2, 1982	-0.37
Boulder, Colorado	82	July 9, 1982	+0.30
Area 2-South America			
Mexico City, Mexico	98	Oct. 30, 1981	+1.32
Huancayo, Peru	87	April 18, 1982	-4.84
Cachoeira Paulista, Brazil	114	Oct. 21, 1982	-3.67
Natal, Brazil	93	Sept. 9, 1982	+0.73
Buenos Aires, Argentina	97	Jan 20, 1983	-0.15
Buenos Aires, Argentina	99	March 14, 1983	-0.07
Area 3-Western Europe (1)			
Bracknell, U.K.	41	June 22, 1982	-0.15
Bracknell, U.K.	2	June 22, 1982	+0.59
Halley Bay, U.K.	31		
Argentine Is., U.K.	73		
Seychelles, Seychelles	57		
St. Helena, U.K.	35		
King Edward Point, U.K.	103		
Lerwick, U.K.	32	July 7, 1982	+2.13
Arosa, Switzerland	15	Nov. 8, 1982	-0.88
Arosa, Switzerland	101	Nov. 8, 1982	-0.08
Hohenpeissenberg, F.R.G.	104	Nov. 30, 1982	-6.10
Cologne, G.F.R.	44		
Oslo, Norway	8	April 8, 1983	-0.96
Oslo, Norway	56	April 11, 1983	-0.29
Tromsø, Norway	14	April 8, 1983	-1.17
Area 4-Western Europe (2)			
Aarhus, Denmark	92	June 10, 1981	+0.74
Uccle, Belgium	40	Oct. 27, 1981	+1.25
Biscarrosse, France	11	1982	-2.42
Magny-Les-Hameaux, France	85	May 2, 1982	+1.98
Lisbon, Portugal	13	April 22, 1982	-0.07
El Arenosillo, Spain	120	1982	+0.66
Vigna D' Valle, Italy	47	Dec. 13, 1982	+0.44
Brindisi, Italy	46	Dec. 27, 1982	+3.30
Sestola, Italy	48	Jan. 10, 1983	-0.08
Cagliari/Elmas, Italy	113	Dec. 21, 1982	-1.25
Casablanca, Morocco	106	June 2, 1983	-
Cairo, Egypt	69	March 9, 1984	-1.47
Cairo, Egypt	96	March 10, 1984	+0.52
Area 5-Eastern Europe, U.S.S.R.			
Leningrad, U.S.S.R.	108	Oct. 22, 1981	+0.29
Belsk, Poland	84	Jan. 7, 1982	+1.32
Hradec Králové, Czechoslovakia	74	Feb. 4, 1982	-3.30
Budapest-Lorinci, Hungary	110	Jan. 3, 1982	-3.52
Bucharest, Romania	121	April 20, 1982	+3.30
Potsdam, G.D.R.	71	May 1982	+0.59
Potsdam, G.D.R.	64	May 1982	-0.44
Area 6-India			
New Delhi, India	36	1982	-0.44
New Delhi, India	112	1982	-1.47
Srinagar, India	10	1982	+1.76
Varanasi, India	55	1982	-1.62
Mt. Abu, India	54	1982	+2.27
Poona, India	39	1982	+0.44
Kodaikanal, India	45	1982	+2.57
Quetta, Pakistan	43		
Quetta, Pakistan	100	April 8, 1983	+1.91
Bangkok, Thailand	90	June 10, 1983	+10.79
Singapore, Singapore (U.K.)	7		
Manila, Philippines	52	Nov, 1, 1983	-1.25
Area 7-Australia, Japan			
Sapporo, Japan	5702	Jan. 5, 1982	-0.44
Kagoshima, Japan	5704	Dec. 10, 1981	+4.55
Tateno, Japan	116	Nov. 20, 1981	+3.08
Naha/Kagamizu, Japan	5705	Dec. 21, 1981	-3.52
Tateno, Japan	122	Nov. 20, 1981	+3.37
Sapporo, Japan	5703	Jan. 6, 1982	-0.44
Tateno, Japan	5706	Nov. 24, 1981	+1.32
Shiangher, China	75	March 30, 1982	+0.15
K'un-ming, China	3	April 13, 1982	-2.05
Aspendale, Australia	105	Sept. 6, 1982	+0.59
Aspendale, Australia	115	June 18, 1982	+0.15
Perth, Australia	111	Aug. 17, 1982	-8.95
Cairns, Australia	81	July 13, 1982	+6.60
Brisbane, Australia	6	July 15, 1982	-4.11
Hobart, Australia	12	July 5, 1982	-8.80
McQuarie Island, Australia	78	Oct. 28, 1982	-0.29
Invercargill, New Zealand	17	March 3, 1983	+0.15

*See text for significance of indicated calibration error. Positive error means that instrument yields ozone values that are too large

APPENDIX C
Results of 1985-1987 Calibration Checks on Dobson Spectrophotometers, Using Traveling Standard Lamps

Station	Inst No.	Date of Calib. Check	Inst. Calib. Error (%)*
Area 1-North America			
Toronto, Canada	77	May 31, 1985	-0.29
Resolute, Canada	59	Dec. 30, 1985	-0.81
Churchill, Canada	60	Feb. 12, 1986	+1.10
Goose Bay, Canada	62	July 13, 1985	+0.08
Edmonton, Canada	102	Nov. 14, 1985	+0.15
Reykjavik, Iceland	50	June 10, 1986	+0.15
SPO	82	Feb. 2, 1988	+0.15
Bismarck, N. Dak.	33	July 28, 1986	-2.35
Caribou, Maine	86	Oct. 6, 1986	-0.15
Wallops Is., Va.	38	Oct. 10, 1986	-0.22
Tallahassee, Fla.	58	Dec. 31, 1986	-0.29
Nashville, Tenn.	79	Jan. 9, 1987	+1.17
Poker Flat, Alaska	63	Jan. 13, 1987	-1.10
MLO	76	May 24,1987	+1.47
SMO	42	July 15, 1987	+1.61
BRW	91	Jan. 29, 1988	+0.30
Fresno, Calif.	94	May 5, 1987	+1.18
Boulder, Colo.	61	April 11, 1985	-1.03
Boulder, Colo.	65	April 11, 1985	-1.25
Boulder, Colo.	34	Jan. 27, 1988	+0.22
Boulder, Colo.	80	Jan. 13, 1988	+1.40
Area 2-South America, Africa			
Mexico City, Mexico	98	May 22, 1985	+1.32
Huancayo, Peru	87	April 1, 1985	-0.37
Cachoeira Paulista, Brazil	114	June 6, 1986	±0.00
Natal, Brazil	93		
Buenos Aires, Argentina	97	Nov. 4, 1985	-0.52
Buenos Aires, Argentina	99	Nov. 6, 1985	+0.15
Nairobi, Kenya	18		
Area 3-Western Europe (1)			
Bracknell, U.K.	41		
Bracknell, U.K.	2	July 25, 1985	-0.52
Halley Bay, U.K.	123	Dec. 28, 1985	+3.67
Argentine Is., U.K.	31	Feb. 19, 1986	+0.37
Seychelles, U.K.	57	Aug. 26, 1985	-2.50
St. Helena, U.K.	35	Sept. 25, 1985	-0.59
King Edward Point, U.K.	103	Oct. 17, 1985	-1.32
Lerwick, U.K.	32	July 31, 1985	-2.28
Arosa, Switzerland	15	March 27, 1985	-2.57
Arosa, Switzerland	101	March 27, 1985	+4.55
Hohenpeissenberg, F.R.G.	104	April 22, 1985	+2.42
Cologne, F.R.G.	44		
Oslo, Norway	56	July 12, 1985	-0.66
Tromsø, Norway	14	July 5, 1985	-1.03
Spitzbergen, Norway	8	July 3, 1985	-0.22
Cambridge, U.K.	73	Sept. 9, 1986	-2.79
Area 4-Western Europe (2)			
Aarhus, Denmark	92	March 19, 1985	+3.60
Uccle, Belgium	40	April 5, 1985	+1.61
Biscarrosse, France	11		
Haute Provence, France	85	June 27, 1985	-1.25
Lisbon, Portugal	13	July 26, 1985	+0.66
El Arenosillo, Spain	120	Oct. 8, 1985	+0.66
Vigna DiValle, Italy	47	Nov. 27, 1985	+1.03
Brindisi, Italy	46	Nov. 23, 1985	+0.88
Sestola, Italy	48	Dec. 6, 1985	+1.10
Calgiari/Elmas, Italy	113	Nov. 16, 1985	-0.59
Casablanca, Morocco	106		
Cairo, Egypt	69	Feb. 6, 1986	-1.25
Cairo, Egypt	96	Feb. 11, 1986	+1.17
Area 5-Eastern Europe, U.S.S.R.			
Leningrad, U.S.S.R.	108	April 2, 1985	+0.08
Belsk, Poland	84	May 23, 1985	+1.24
HradecKrálové, Czechoslovakia	74	June 26, 1985	-4.40
Budapest-Lorinci, Hungary	110	July 31, 1985	-1.54
Bucharest, Romania	121	Sept. 5, 1985	+2.72
Potsdam, G.D.R.	64	Oct. 10, 1985	-0.52
Potsdam, G.D.R.	71	Oct. 10, 1985	+0.66
Area 6-India			
New Delhi, India	36	Aug. 9, 1985	+0.73
New Delhi, India	112	April 22, 1985	-0.52
Srinagar, India	10		
Varanasi, India	55	Aug. 22, 1985	-1.76
Mt. Abu, India	54		
Poona, India	39	Jan. 23, 1986	+1.54
Kodaikanal, India	45	July 5, 1985	+2.42
Quetta, Pakistan	43	July 22, 1986	+1.40
Quetta, Pakistan	100	July 19, 1986	+1.47
Bangkok, Thailand	90	Oct. 9, 1986	-1.17
Singapore	7	Dec. 18, 1986	+3.06
Manila, Philippines	52	June 22, 1987	+1.18
Area 7-Australia, Japan			
Sapporo, Japan	5704	July 15, 1985	-0.88
Kagoshima, Japan	5705	June 18, 1985	-0.22
Tateno, Japan	116	July 25,1985	-0.34
Naha/Kagamizu, Japan	5706	June 29, 1985	-0.44
Tateno, Japan	5703	Oct. 24,1985	-0.49
Sapporo, Japan	5702		
Tateno, Japan	122		
Xianghe, China	75	Feb. 3, 1987	+0.66
Kunming, China	3	June 16, 1987	-0.74
Melbourne, Australia	105	July 9, 1986	+0.52
Perth, Australia	81	June 16, 1986	+0.52
Brisbane, Australia	111	Jan. 5, 1986	+0.22
Hobart, Australia	12	March 16, 1986	+0.73
Macquarie Is., Australia	6		
Invercargill, New Zealand	17	Oct. 17,1986	-1.17
Lauder, New Zealand	72		
Seoul, Korea	124	Nov. 30, 1985	+1.17
Melbourne, Australia	115		
Melbourne, Australia	78		

*See text for significance of indicated calibration error. Positive error means that instrument yields ozone values that are too large.

Attachment 12
Analysis of SBUV/2 Measurements of Solar Irradiance Variations
R.F. Donnelly and J. Barrett
NOAA/ERL-CMDL

Analysis of SBUV2 Measurements of Solar UV Irradiance Variations

Richard F. Donnelly and Joan Barrett
Space Environment Lab., NOAA ERL, Boulder, Colorado 80303

ABSTRACT

The NOAA-9 and NOAA-11 SBUV2 monitoring measurements in the discrete wavelength mode are discussed for the core-to-wing ratio of the solar Mg II h & k lines near 280 nm. A new ratio, similar to Heath and Schlesinger's (1986) ratio for NIMBUS7, has been adopted for NOAA-9 and NOAA-11 to avoid drift problems associated with the low-amplification third intensity range in the photomultiplier cathode circuit. This new ratio provides an excellent ratio of solar signal to instrument noise for NOAA-9 & 11 because of SBUV2's superb wavelength repeatability. Recommendations for the SBUV2 instruments that have not yet flown and for future operation of the SBUV2 monitors are presented based on our experience with NOAA-9 and NOAA-11.

INTRODUCTION

Our goals are to conduct research of the temporal variations of solar ultraviolet irradiance, to study why these variations occur and whether we can predict the variations, and to determine the stratospheric effects of the UV variations and their possible effects on climate. The SBUV2 solar UV flux measurements are not our end product, but are a byproduct of the early stages of our research. When we started to analyze the NOAA-9 measurements, our philosophical outlook was that we expected to encounter instrument radiometric drift problems, because all spectrometers flown in space to measure the solar ultraviolet (UV) flux have had drift problems.

The most important results of studies of solar UV variability in NIMBUS7 measurements were the following: (1) The core-to-wing ratio R(MgIIc/w,t) for the Mg II h & k lines as a function of time (t) provide an excellent measure of solar UV variability that is insensitive to long-term drifts in instrument throughput (Heath and Schlesinger, 1986). The insensitivity to drift in instrument gain is achieved at the expense of an increased sensitivity to the instruments' wavelength repeatability. (2) A wavelength scaling function can be used with R(MgIIc/w,t) to estimate UV fluxes in the 160 - 300 nm range. It has not yet been published but hopefully will be soon (Heath and Schlesinger, 1990). (3) The short-term UV variations are very uniform in relative temporal shape at almost all wavelengths in the 175 - 290 nm range (Donnelly, 1988b). Given these earlier results, we first pursued the Mg II core-to-wing ratio in the NOAA-9 measurements and the results are reported in detail in Donnelly et al. (1990). Here, a brief summary is given, with emphasis on recommendations to NOAA NESDIS for the future flights of SBUV2 monitors.

The solar UV measurements from the SBUV2 monitors involve three types: (1) solar UV measurements made at 12 selected wavelengths as part of the terrestrial ozone monitoring program; (2) measurements as a function of wavelength in the approximate range 160 - 400 nm, typically two scans per day; and (3) discrete-wavelength mode measurements at 12 selected wavelengths in the wings, sides or core of the unresolved Mg II h & k lines near 280 nm. We will mainly discuss the latter type of measurements. Discrete-wavelength mode measurements have the advantage of including the output for all three

intensity ranges rather than having the output from only one range, as in the case of the wavelength-scan mode, where the choice of ranges is made by software on the satellite. Also, about nine sunlit sets of discrete-wavelength measurements are made for NOAA9 each day while typically only two wavelength-scan sets are made.

Although we mainly discuss problems here, please keep in mind that the modified core-to-wing ratio discussed below is excellent and can be converted to values equivalent to the NIMBUS7 values. It is like a vein of gold that should be continued through all the future SBUV2 measurements and be a major source of information on solar UV variations for many years.

CLASSICAL Mg II CORE-TO-WING RATIO

Heath and Schlesinger (1986) derived R(MgIIc/w,t) for each NIMBUS7 wavelength-scan of the solar UV spectrum. Typically three to four wavelength scans were made on most days. Daily average values of R(MgIIc/w,t) are now commonly used. The individual values of R(MgIIc/w,t) were derived from the ratio of an average core flux to an average of the flux in the far wings of the combined absorption lines. The average of flux measurements at the three wavelength steps closest to the center of the core of the unresolved Mg II h & k lines near 280 nm were used to provide a measure with a strong signal of solar UV variability. In this technique, the small amount of signal averaging will reduce noise and provide a slight reduction in sensitivity to jitter in the wavelength settings. They also used the average of the flux at two adjacent wavelengths in the long-wavelength wing and two adjacent wavelengths in the short-wavelength wing. These wing averages provide a measure of instrument output with a weak solar signal having comparable instrument effects as those affecting the core measurement. So the ratio has a strong solar signal while the comparable multiplicative instrument drift effects in both the numerator and denominator cancel out. Their ratio, based on measurements at seven wavelengths, is referred to below as the "classical" R(MgIIc/w,t). The corresponding seven-term ratio for NOAA-9 involves slightly different wavelengths than in the case of NIMBUS7, which causes a slight constant offset and a slight difference in solar signal amplitude; but the NIMBUS7 and NOAA-9 ratios are linearly related. Classical ratio results have been published for NOAA-9 in Solar Geophysical Data for 1986 and 1987, but because of problems discussed below 1988 and later data have not yet been published.

In the case of the NOAA-9 discrete-wavelength mode measurements, the wavelength repeatability is excellent (Donnelly, 1988a), much better than on NIMBUS7, which was quite good. Upon this SBUV2 strength of excellent wavelength repeatability, or low wavelength jitter and long-term drift, we are building our relative photometry analyses of solar UV variability in the SBUV2 data. We find one wavelength step at the core and one in each wing provides as good or better a solar signal, based on a comparison of the 27-day and 13-day peaks in the power spectrum of the temporal variations of R(MgIIc/w,t) with respect to the continuum at periods shorter than 12 days, because of the extremely low jitter in wavelength positions. This simplified three-term ratio allows us to use the other wavelengths normally used in the classical ratio as an independent check for isolated anomalous data.

Ca-K LINE COMPARISONS

The relative temporal variations of the solar Mg II h & k lines are known to

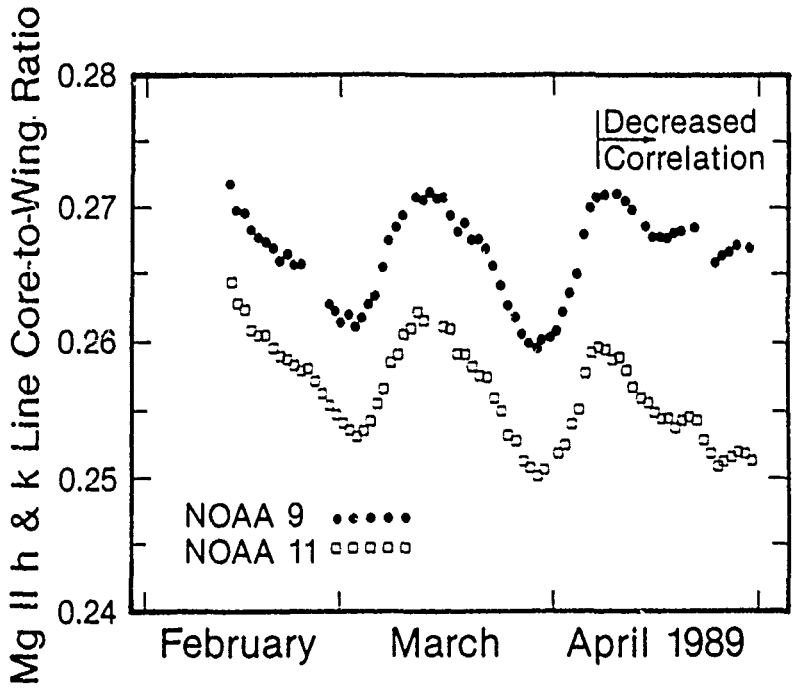

Figure 1. Classical Mg II core-to-wing ratios for NOAA-9 and NOAA-11.

be very nearly the same as those of the ground-based measurements of the solar Ca II K line by White et al. (1987) at the National Solar Observatory on Kitt Peak in Arizona, where measurements are made on about three to four days per month. Comparisons with their data gave good agreement in 1986 and early 1987. However, there was a slight suggestion of differences in the fall of 1987 and larger differences in mid and late 1988. We then realized we had a problem. This problem became more evident when results were compared between NOAA-9 and NOAA-11.

NOAA-9 & NOAA-11 COMPARISONS

Figure 1 shows the first few months of NOAA-11 classical R(MgIIc/w,t) in comparison with NOAA-9 values. There is an offset because the wavelength positions are not identical, which can be corrected by a simple linear relation. The relative shapes of the curves should appear to be nearly identical, with a slight difference from unity caused by small measurement noise and measurements being made at different times of day.

The differences in April are unacceptably large. Our studies showed that drifts in the range 3 output relative to the range 2 output in both NOAA9 and NOAA11 were the cause. R(MgIIc/w,t) is not affected by drifts in instrument gain, including those that are wavelength dependent, as long as relative intensities can be accurately measured. The overlap in dynamic response in ranges 2 and 3 was insufficient to measure both core and wing with the same intensity range. Therefore, the drift in the relation between range 3 output and range 2 output could not be accurately removed from the derived ratio.

MODIFIED Mg II CORE-TO-WING RATIO

To be able to use only range 2 values for either NOAA-9 or NOAA-11 measurements, we used a modified ratio of the range 2 flux at the wavelength nearest

the center of the line to the average of one flux measurement in the short-wavelength steep outer side of the absorption line pair and a second flux measurement in the long-wavelength side. Moving to the steep outer sides of the line lowers the denominator intensities so that range 2 values can be used for both the numerator and denominator. This change makes the modified ratio more susceptible to wavelength jitter and drift, but that has not been a problem so far because of the excellent wavelength repeatability in SBUV2. The wavelength jitter was too large in NIMBUS7 to allow such a ratio to be used. This change also increases significantly the average value of the ratio and reduces the relative amplitude of the solar signal, because the denominator terms have a stronger solar signal than in the case of the wing measurements of the classical ratio, which reduces the solar signal of the core measurement. These differences can be corrected using a simple linear relation to obtain equivalent NIMBUS7 values. One might expect a reduction in signal to noise because of the increased canceling of solar signal in the denominator, but we obtained an improvement in signal to noise as evident from the background continuum relative to the solar 27-day and 13-day lines in the power spectrum. This improvement came partly through avoiding the low signal to noise ratio present near the bottom of intensity range 3. The solar signal relative to the observational noise for the modified ratio appears to be as good or better than in the NIMBUS7 data.

Comparing the modified ratios for NOAA-9 & 11 for February through July 1989, the correlation coefficient is 0.9965; so we are back in business and plan to publish modified ratios for May 1986 through 1988 this fall. Preliminary comparisons with the Ca K measurements similarly show excellent agreement for the modified ratio. For more information about the modified R(MgIIc/w,t), see Donnelly et al. (1990). Comparisons of the modified and classical ratios show that range 3 to range 2 drift problems occur in both NOAA-9 and NOAA-11.

COMMENTS ON PROBLEMS IN SBUV2 SOLAR UV MEASUREMENTS

NOAA-11 uses a different photomultiplier than NOAA-9, and the flux levels corresponding to the bottom of the intensity range 3 or top of the unsaturated linear portion of range 2 in NOAA-11 are lower than in the case of NOAA-9. This was thought to benefit the solar measurements by lowering the lower flux limit for intensity range 3 and improving the signal-to-noise ratio for many range 3 values. This may be helpful for the ozone/sun measurement sets that others are using and it may be helpful for the solar wavelength-scan measurements, where we have not yet formed our final conclusions. We definitely know it is a disadvantage for the modified solar Mg II ratios derived from the discrete-wavelength measurements because only the last couple of each daily group of nine sunlit sets of 12-wavelength measurements have low enough range 2 values in the long-wavelength side to be in the linear range for NOAA-11. For NOAA-9, we are able to use nearly all of the sets and gain more by means of daily averaging.

In the case of the wavelength scan measurements, we often wish we had range 2 values rather than the preprogrammed choice of range 3 values. Our experience with the discrete-mode data, where we have a choice of the outputs for all three ranges as well as the "recommended" values has taught us that we often prefer the range 2 value to the recommended range 3 value. Counter-overflowed range 2 values are not much of a problem and are much preferable than the range 3 values currently available in the scan mode as long as the range 2 value is not saturated.

RECOMMENDATIONS

1. We wholeheartedly recommend that a low sensitivity range be added to the photomultiplier anode circuit to serve as a replacement for the current range 3 in the cathode circuit in the SBUV2 monitors for future flights.

2. Future flights of SBUV2 should include discrete-wavelength mode measurements of the solar Mg II h & k lines near 280 nm from the start of NOAA operations. We can provide a set of guidelines for the choice of the 12 wavelengths based on preliminary tests of solar wavelength-scan measurements that take into account that the wavelength positions are not precisely the same from one instrument to another. Whoever made the wavelength choices for NOAA-9 and NOAA-11 did well.

3. A couple of years ago, there was some debate over how long NOAA-9 and NOAA-11 should both be operated. One month? Several months? Until a third SBUV2 is flown? We recommend that two be operated as long as there are two in space that can operate, with changes occurring only when another SBUV2 monitor is launched. Using hindsight, considering problems we have had comparing NIMBUS7 and NOAA-9 during solar minimum conditions when the solar signal does not vary much for several months, a one-year overlap may not be sufficient. Considering the problems evident through comparisons such as in Figure 1, overlaps of at least a year are very important.

4. We recommend that notes summarizing the informal monthly SBUV2 meetings in the Washington area be typed and distributed to those working on the SBUV2 data. Some of the problems we have encountered in the data probably have been seen earlier by others working on different portions of the data. This technical memorandum will help. We are writing a series of technical memorandums on our work so others will have the benefit of our findings.

REFERENCES

Donnelly, R. F., The solar UV Mg II core-to-wing ratio from the NOAA9 satellite during the rise of solar cycle 22, Adv. Space Res., 8, (7)77-(7)80, 1988a

Donnelly, R. F., Uniformity in solar UV flux variations important to the stratosphere, Annales Geophys., 6, 417-424, 1988b.

Donnelly, R. F., J. Barrett, S. D. Bouwer, J. Pap, L. Puga, and D. Stevens, Solar UV Flux Measurements from the SBUV2 Monitor on the NOAA9 Satellite, Part I. Mg II h & k Line Core-to-Wing Ratio for 1986 - 1987, to be published as a NOAA ERL SEL Tech. Memo., 1990.

Heath, D. F., and B. M. Schlesinger, The Mg 280-nm doublet as a monitor of changes in solar ultraviolet irradiance, J. Geophys. Res. **91**, 8672, 1986.

Heath, D. F., and B. M. Schlesinger, private communication, 1990.

White, O. R., W. C. Livingston and L. Wallace, Variability of chromospheric and photospheric lines in solar cycle 21, J. Geophys. Res., 92, 823 - 827, 1987.

Attachment 13

Intercomparison of Ozone Measured from the NOAA-9 and the Nimbus-7 Satellites on Short and Long Time Scales

S. Chandra, R.D. McPeters, and R.D. Hudson
NASA/GSFC
W. Planet
NOAA/NESDIS

Ozone Measurements from the NOAA-9 and the Nimbus-7 Satellites Implications of Short and Long Term Variabilities

S. Chandra, R. D. McPeters and R. D. Hudson
Laboratory for Atmospheres
NASA Goddard Space Flight Center

and

W. Planet
NOAA/NESDIS, Washington, DC

Abstract This paper gives an overview of the measurements of total ozone and ozone profiles by the SBUV/2 instrument on the NOAA-9 spacecraft relative to similar measurements from the SBUV and TOMS instruments on Nimbus-7. It is shown that during the three year period from March 14, 1985, to February 28, 1988, when these data sets overlap, there have been significant changes in the calibrations of the three instruments which may be attributed to diffuser plate degradation (for SBUV/TOMS) and to the drift of the NOAA-9 orbit to later equator crossing times (for SBUV/2). These changes in instrument characteristics have affected the absolute values of the trends derived from the three instruments, but their geophysical characteristics and response to short term variations are accurate and correlate well among the three instruments. For example, the total column ozone measured by the three instruments shows excellent agreement with respect to its day to day, seasonal, and latitudinal variabilities. At high latitudes, the day to day fluctuations in total ozone show a strong positive correlation with temperature in the lower stratosphere, as one might expect from the dynamical coupling of the two parameters at these latitudes.

Introduction

The SBUV/2 (Solar Backscatter Ultraviolet) spectrometer on NOAA-9 has been providing global measurements of ozone in the stratosphere on a

continuous basis since March 14, 1985. The SBUV/2 ozone data set consisting of total ozone and ozone mixing ratio at pressure levels from 100 to 0.3 mb is currently being archived at the NOAA/NESDIS/NCDC Satellite Data Services Division (Princeton Executive Square, Room 100, Washington DC 20233). This data set, in conjunction with similar data sets obtained from the SBUV and TOMS spectrometers on Nimbus-7 and the BUV spectrometer on Nimbus-4, comprise one of the most comprehensive data sets on stratospheric ozone available, extending over two decades (Hilsenrath and Chandra, 1988). These data sets, if intercalibrated, constitute a valuable resource for monitoring long term changes in the stratosphere and for studying the natural and man made perturbations on time scales varying from a single day to a solar rotation to a solar cycle.

The purpose of this paper is to give an assessment of the SBUV/2 data with respect to their usefulness in studying geophysical and man made perturbations in the stratosphere. This assessment is made by comparing the temporal and spatial characteristics of the SBUV/2 data with those of the TOMS and SBUV data over a three year period (March, 1985 - February, 1988) when these data sets overlap.

Instrument Related Changes in SBUV/2, SBUV, and TOMS

The SBUV/2 instrument on the NOAA-9 satellite and to be flown on a series of future NOAA operational satellites is an improved version of the SBUV instrument flown on Nimbus-7 (Heath et al., 1975). The instrument is a nadir viewing scanning double monochromator designed to measure total ozone and the ozone vertical profile over the pressure (altitude) range 0.7 mb to 30 mb (25 km - 50 km) by accurately measuring the atmospheric albedo, which is defined as the ratio of the radiance backscattered from the terrestrial atmosphere to the extraterrestrial solar irradiance. In its primary mode of operation the monochromator measures the solar UV radiances backscattered by the atmosphere at 12 discrete wavelengths from 255 nm to 340 nm with 1 nm bandpass. Albedos between 255 nm and 306 nm are used in the ozone profile inversion, while albedos between 312 and 340 nm are used to calculate total ozone. TOMS is a variation of the SBUV designed to mea-

sure total ozone only. It consists of a single monochromator that very rapidly scans wavelengths from 312 nm to 380 nm while spatially scanning across the orbital track to produce complete global maps of ozone on a daily basis.

The extraterrestrial solar irradiance needed to calculate an albedo is measured daily by deploying a diffuser plate. Since this diffuser plate is the only optical element not common to both the radiance and irradiance measurements, errors in long term calibration for SBUV type instruments are usually traceable to uncorrected changes in the reflecting properties of the diffuser plate. In comparing the SBUV/2 data with data from SBUV and TOMS, one must recognize that there have been changes in the characteristics of each of the three instruments. Comparisons of total ozone measured by SBUV and TOMS with measurements from a network of 36 Dobson stations showed that total ozone measured by the SBUV/TOMS instruments declined relative to the Dobson network by 3 percent between 1979 and 1988 (Heath, 1988; Reinsel et al.,1988). This calibration drift was most likely caused by undercorrection for the degradation of the diffuser plate (Watson, 1988).

Changes are also occurring in the SBUV/2 spectrometer, but for different reasons than for SBUV/TOMS. For SBUV/2 the changes appear to be associated with the drift of the NOAA-9 orbit. Both Nimbus 7, launched in 1978, and NOAA-9, launched in 1984, are in sun synchronous orbits. But where the equator crossing time for Nimbus-7 is very close to noon and has been stable for more than a decade, the equator crossing time for NOAA-9 was 1420 hours local time at launch and has drifted by about 3 hours over the 5 year period since. By the end of 1987 the time of equatorial crossing was at 1535 hours; and two years later, at the end of 1989, it was 1717 hours. As a result of this change in orbit, the incidence angle of the sun on the diffuser plate has increased with time. While it has not yet been proven, it is likely that error (or change) in the reflective properties of the diffuser plate, its goniometric calibration, has led to the observed apparent *increase* in diffuser plate reflectivity with time. Also, the SBUV/2 measurements of atmospheric radiance at a given latitude are made at continually increasing solar zenith angles which impacts the accuracy of the ozone retrieval algorithm (Klenk et al., 1982).

The "pair justification" technique has recently been developed by the GSFC Ozone Processing Team (McPeters et al., 1989) to stabilize the calibration of backscattered ultraviolet instruments against long term changes in instrument characteristics for the total ozone wavelengths. The total ozone measurement is based on the differential absorption of wavelength pairs, but different pairs have varying sensitivity to calibration change. Time dependent changes in instrument calibration will result in a relative drift between an error sensitive pair and an error insensitive pair. Pair justification uses this relative drift to infer the calibration error itself by requiring that ozone measured by different wavelength pairs be self consistent. The pair justification technique has been used to reprocess the entire TOMS data set. The reprocessed data will be noted as the version 6 (V6) data to distinguish them from the version 5 (V5) data which are currently archived at the National Space Science Data Center (NASA/GSFC, Greenbelt, Md, 20771).

While total ozone from SBUV could be corrected now, the ozone profile data cannot be corrected by pair justification. Other approaches to correct the profile data are currently being explored. Similarly, data from the NOAA-9 SBUV/2 will not be corrected until the physical mechanism for the observed change is better understood.

Comparisons of the SBUV/2, SBUV and TOMS Total Ozone

The data used in this study consist of daily values of total ozone obtained from the SBUV/2, TOMS (versions 5 and 6), and SBUV instruments. The data are zonally averaged in latitude intervals of 10 degrees from 80°S to 80°N and are smoothed with a 5 day running average. Figure 1 shows a comparison of total column ozone measured by different instruments at 50°N . The SBUV and TOMS (V5 and V6) time series start from January 1, 1979 and extend up to February 28, 1988, overlapping with the SBUV/2 time series after March 14, 1985. These plots and similar plots at other latitudes (not shown) suggest that the general characteristics of total ozone measured by the different instruments are remarkably similar both with respect to their seasonal and day to day

changes.

Their absolute values and their long term characteristics are, however, different. This is illustrated in Figure 2 which shows the relative changes in TOMS (V5), SBUV and SBUV/2 with respect to TOMS (V6) at the equator. All the time series in Figure 2 are smoothed with a 30 day running average to emphasize their long term characteristics. If one assumes that TOMS (V6) total ozone is independent of instrument drift, an assumption probably good to within ±1%, one may use Figure 2 to estimate the long term changes in the instrument characteristics of TOMS (V5), SBUV, and SBUV/2. For example, the curve labeled TOMS (V5) suggests that the TOMS total ozone measurements degraded by about 4 percent from 1979 to 1988, with most of this degradation occurring after 1983. During the first five years, the TOMS (V5) measurements appear to have been accurate to within 1 percent. The drift in the SBUV instrument was very similar to that for TOMS (V5) since the curve labeled SBUV is almost parallel to the TOMS (V5) curve. This is consistent with the assumption that the cause of the drift is degradation of the shared diffuser plate. However, these curves also indicate that the absolute value of total ozone measured by the SBUV instrument have been about 4 percent less than that measured by TOMS. This constant offset has been recognized since shortly after launch. The difficulty of deriving an absolute wavelength calibration for the multiple-slit TOMS instrument might be the cause of the offset. The difference in time dependence is due to sampling differences between the high density TOMS data set and the low density SBUV data set. The characteristics of the SBUV/2 curve are very different from those of TOMS and SBUV. During the period when both the SBUV and TOMS measurements are drifting downwards, the SBUV/2 curve shows an upward trend of about 3 percent over the three year time interval after 1985. Such an upward trend is difficult to explain in terms of the diffuser plate degradation, since an *increase* in plate reflectivity would be required. The orbital changes for NOAA-9 mentioned earlier coupled with a small goniometric error could produce the observed time dependence.

In spite of the apparent differences in the long term behavior of the three instruments, there are striking similarities in the latitudinal characteristics of trends inferred from

these measurements. Figure 3 compares the linear trends over the three year period from March 1985 to February 1988. These trends are derived using a regression model consisting of linear and seasonal (annual and semiannual) terms. It shows that the three year trends in total ozone inferred from the four data sets are nearly symmetric with respect to the equator. For TOMS (V6) the trend varies from about -3 percent at the equator to about +2 or +3 percent at higher latitudes (40°) in both the hemispheres. The average trend for these latitude bands is only about +0.31 percent. This curve also shows a transition from a negative to a positive trend at about 20°. These trends are largely manifestations of quasi biennial oscillations (QBO) which are extensively discussed in literature (eg., Oltmans and London, 1982; Hilsenrath and Chandra, 1988). Trends derived from such a short data record, only three years, will be particularly influenced by the QBO. The point here is not so much the trend itself as the similarity of the latitude dependence of the trends derived from the four data sets. They differ only by an offset. The SBUV and SBUV/2 data are respectively about 1.5 percent lower and 2.5 percent higher with respect to the TOMS (V6) trends. The trends derived from the TOMS (V5) are almost the same as those from SBUV.

The long term instrument changes have fortunately not affected most of the geophysical characteristics of the SBUV/2 data including the day to day and short term changes. An example of such changes are shown in Figure 4 which compares the daily fluctuations in total ozone inferred from the SBUV and SBUV/2 instruments with those in temperature at 50 mb at 50°S. All the time series in Figure 4 are deseasonalized and detrended using a linear regression model. Figure 4 shows that the day to day fluctuations in total ozone from the SBUV/2 and SBUV measurements are very similar. They both show oscillations with periods ranging from a few days to a few months and strong positive correlation with temperature at 50 mb. A regression analysis of ozone and temperature time series indicates a regression coefficient of 6.4 DU/°K or about a 2 to 3 percent increase in total ozone for a 1°K increase in temperature. These values are in good agreement with the values derived from the spatial variabilities in ozone and temperature during spring months in the southern hemisphere as re-

ported by Newman and Randall (1988) and are indicative of a strong dynamic coupling between ozone and temperature associated with planetary waves at high latitudes (Tung and Yang, 1988).

Comparisons of Ozone Profiles from SBUV/2 and SBUV

In comparing ozone profiles from the SBUV/2 and SBUV instruments, there is no simple way to account for the instrument effects as in case of total ozone. Therefore, a meaningful comparison of the SBUV and SBUV/2 data can only be made by removing linear trends from both the data sets. Figure 5 shows such a comparison for Umkehr layer 8 (about 40 Km) at the equator (±5°). Both the SBUV and SBUV/2 curves in Figure 5 have been detrended, and the SBUV values have been normalized to the March 14, 1985 value of the SBUV/2 to account for the drift in the SBUV data before 1985. In Figure 5, the temporal characteristics of both the SBUV and SBUV/2 curves are almost identical in all their details. The seasonal characteristics of both the curves are predominantly semiannual in nature and are modulated by shorter term fluctuations. These short term fluctuations are manifestations of winter time planetary waves in both the hemispheres. The comparisons at other latitudes and pressures (Umkehr layers) suggest that the temporal and spatial characteristics of the detrended SBUV/2 data are almost identical to those of SBUV over the three year period where the two data sets overlap.

Concluding Remarks

In this paper we have attempted to give an overview of the measurements of total ozone and ozone profiles by SBUV/2 instrument on NOAA-9 by comparing them to similar measurements from the SBUV and TOMS instruments on Nimbus-7. These comparisons clearly suggest that the SBUV/2 data, like that from SBUV, are not presently useful for studying long term trends. However, the detrended data can be very useful for studying a number of geophysical phenomena including short term changes, the QBO, and interannual variabilities.

During the three year period for which these

data sets overlap, the total ozone measured by the three instruments show excellent agreement with respect to their day to day, seasonal, and latitudinal variabilities. At high latitudes the day to day fluctuations in total ozone show a strong positive correlation with temperature in the lower stratosphere, as one might expect from the dynamical coupling of the two parameters at these latitudes. The linear trends in total ozone inferred from the three instruments show remarkable similarities with respect to their latitudinal characteristics. The trend itself appears to be largely a manifestation of QBO. Relative to TOMS measurements corrected for instrument drift by pair justification, the version 6 data, the SBUV/2 trends appear to be displaced by about 2.5 percent with respect to the corrected TOMS trends at all latitudes between ±50°. In comparison, the uncorrected SBUV and TOMS trends are about 1.5 percent lower in the same latitude region. The TOMS and SBUV trends were affected by the degradation of the common diffuser plates used to measure the extra-terrestrial solar irradiance, while the SBUV/2 instrument appears to have been affected by the drift of the NOAA-9 orbit to higher solar zenith angles (later equator crossing times).

Acknowledgements. We are grateful to D. Bowman and J. Lienisch at NOAA for providing the SBUV/2 data as they were produced and for helping us understand some of the initial problems. We are also grateful to J. Stokes for helping in the analysis of the data sets.

References

Heath, D. F., Non-Seasonal changes in total column ozone from satellite observations, 1970-86, *Nature*, *332*, 219, 1988.

Heath D. F., A. J. Krueger, H. A. Roeder, and B. D. Henderson, The solar backscatter ultraviolet and total ozone mapping spectrometer(SBUV/TOMS) for Nimbus G, *Opt. Eng.*, *14*, 323, 1975.

Hilsenrath, E., and S. Chandra, Satellite total ozone climatology covering 18 years, *Pro-*

ceedings of International Ozone Symposium 1988, ed. R. D. Bojkov & P. Fabian, A. Deepak Publishing, Hampton, Va.

Klenk, K.F., P.K. Bhartia, A.J. Fleig, V.G. Kaveeshwar, R.D. McPeters, and P.M. Smith, Total ozone determination from the backscatter ultraviolet (BUV) experiment, *J. Appl. Meteor.*, *21*, 1072-1684, 1982.

McPeters et al., Pair justification: A technique for achieving one percent accuracy in satellite ozone trend determination, Presented at 28th Liege International Astrophysical Colloquium, 'Our Changing Atmosphere', June 26 - 30, 1989.

Newman, P. A., and W. J. Randel, Coherent ozone-dynamical changes during the Southern Hemisphere Spring, 1979-1986, *J. Geophys. Res.*, *93*, 12585, 1988.

Oltmans, S. J. and J. London, The quasi-biennial oscillation in atmospheric ozone, *J. Geophys. Res.*,*87*, 8981, 1982.

Reinsel et al., An analysis of the 7-year record of SBUV satellite ozone data: Global profile features and trends in total ozone, *J. Geophys. Res.*, *93*, 1689, 1988.

Tung, K. K. and H. Yang, Dynamic variability of column ozone, *J. Geophys. Res.*, *93*, 11,123, 1988.

Watson, R. T. and Ozone Trends Panel, Present State of Knowledge of the upper atmosphere 1988: An assessment report, NASA Reference Publication 1208, 1988 (Available from the National Technical Information Service, Springfield, VA 22161.

S. Chandra, R.D. McPeters and R.D. Hudson, Code 616, NASA Goddard Space Flight Center, Greenbelt Md. 20771

W. Planet, NOAA/NESDIS, Washington, DC 20233

Figure Captions

Fig. 1. Time series representing daily values of total ozone at 50°N based on TOMS version 6, TOMS version 5, SBUV, and SBUV/2 measurements. All the curves begin January 1, 1979 and end on February 28 1988, except for the SBUV/2 curve which begins March 14, 1985.

Fig. 2. Long term changes in total ozone at the equator for TOMS (V5), SBUV, and SBUV/2 relative to the TOMS (V6) data which have been corrected for long term instrument change. All the time series are smoothed with a 30 day running average to accentuate their long term trends.

Fig. 3. The latitudinal characteristics of linear trends in total ozone based on the three years (1985-1988) of data from the SBUV/2, TOMS (V6), SBUV, and TOMS (V5) measurements.

Fig. 4. The correlation of daily fluctuations in total ozone from SBUV and SBUV/2 with 50 mb temperature at 50°S. The values shown in this figure are differences of the daily values from the values based on time series consisting of annual, semiannual and linear trends as explained in the text.

Fig. 5. Comparison of SBUV/2 and SBUV time series for Umkehr layer 8 (approximately 40 km) at the equator showing the high correlation of the short term variations. Both the SBUV and SBUV/2 curves have been detrended. The SBUV values have been normalized to those of SBUV/2 on March 14, 1985 to account for possible drift in the SBUV data prior to that date.

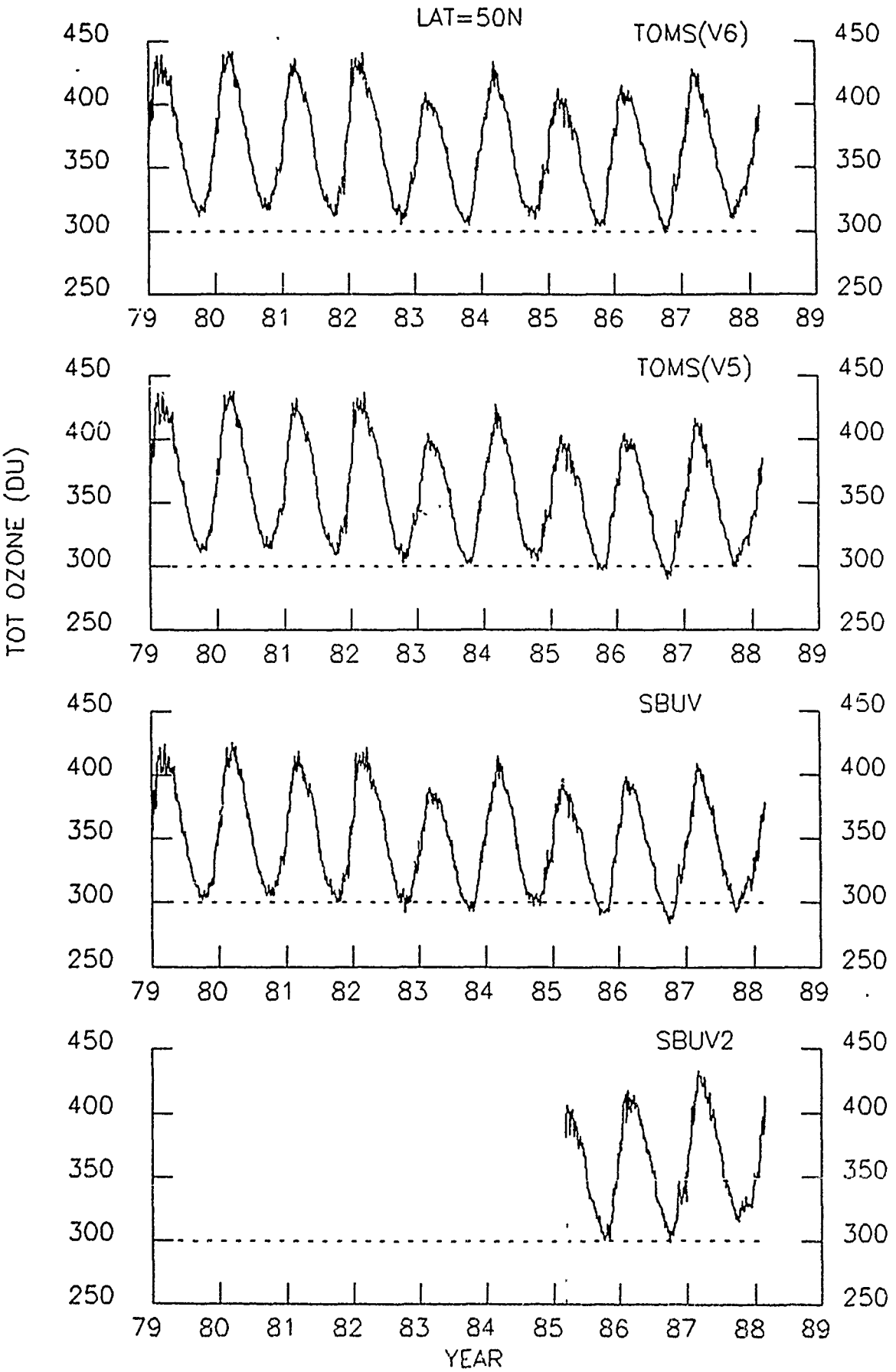
LAT=50N
TOMS(V6)
TOMS(V5)
SBUV
SBUV2
TOT OZONE (DU)
YEAR
450
400
350
300
250
79
80
81
82
83
84
85
86
87
88
89

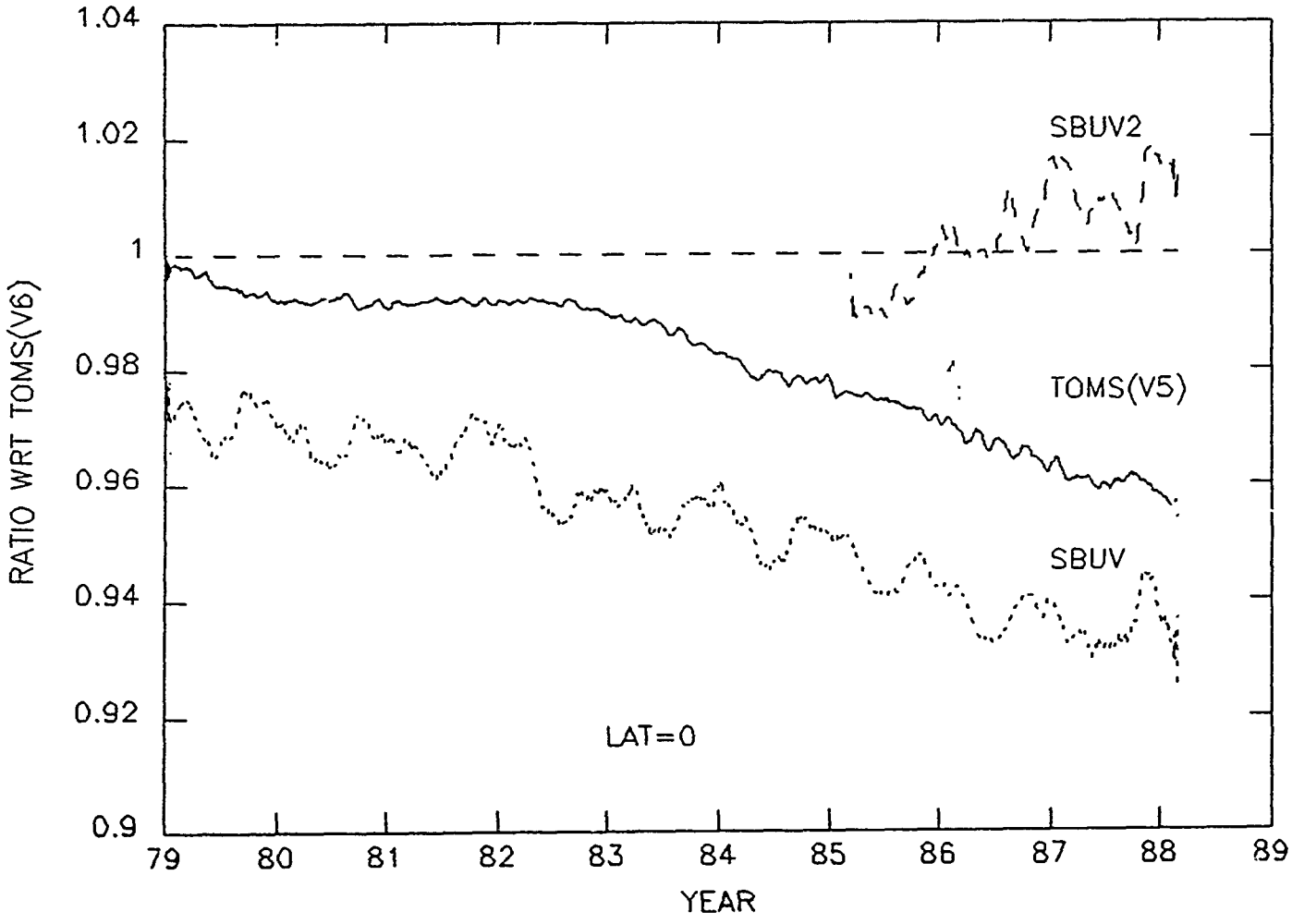
1.04
1.02
1
0.98
0.96
0.94
0.92
0.9
RATIO WRT TOMS(V6)
SBUV2
TOMS(V5)
SBUV
LAT=0
79
80
81
82
83
84
85
86
87
88
89
YEAR

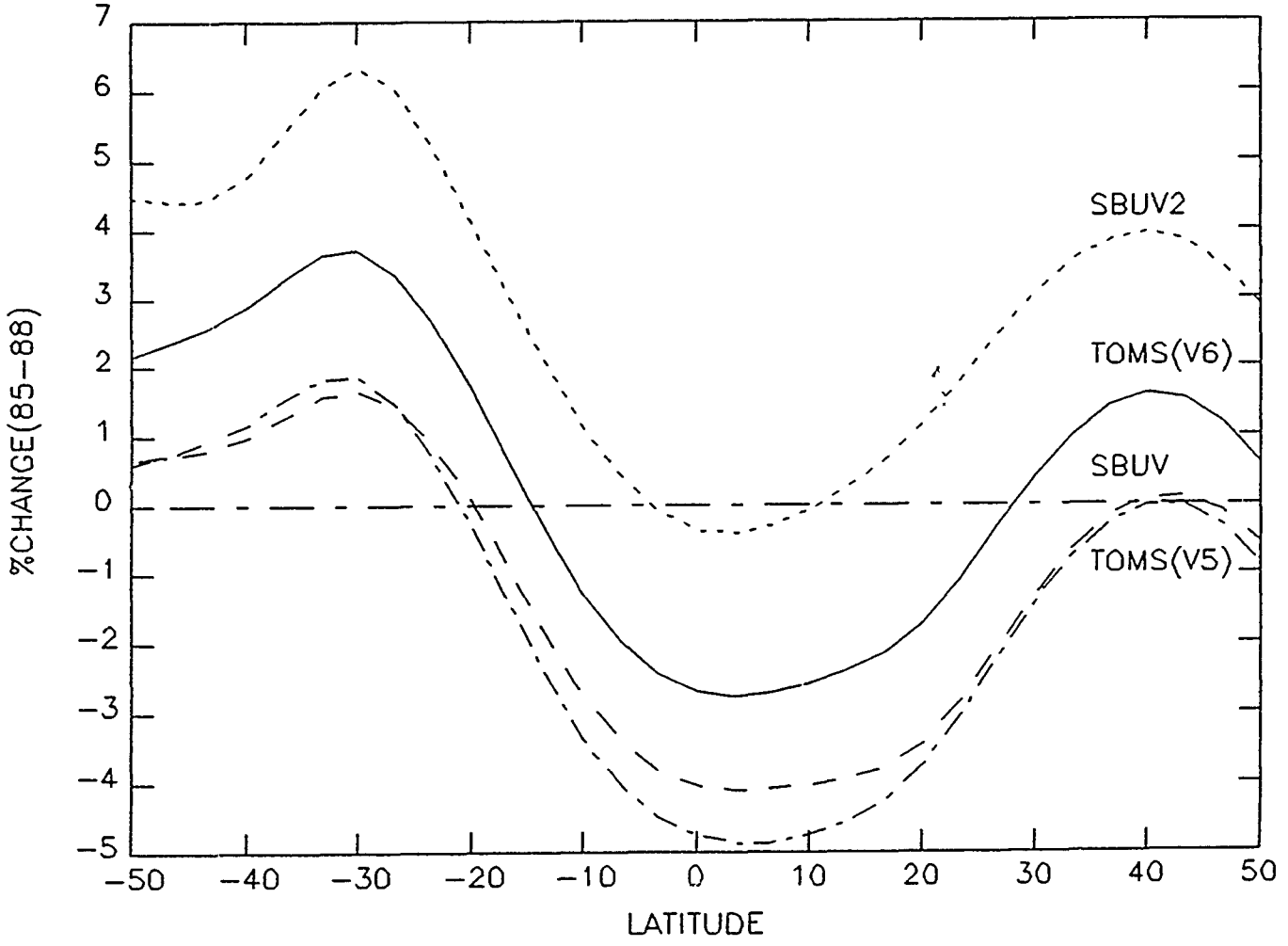
7
6
5
4
3
2
1
0
−1
−2
−3
−4
−5
%CHANGE(85−88)
−50
−40
−30
−20
−10
0
10
20
30
40
50
LATITUDE
SBUV2
TOMS(V6)
SBUV
TOMS(V5)

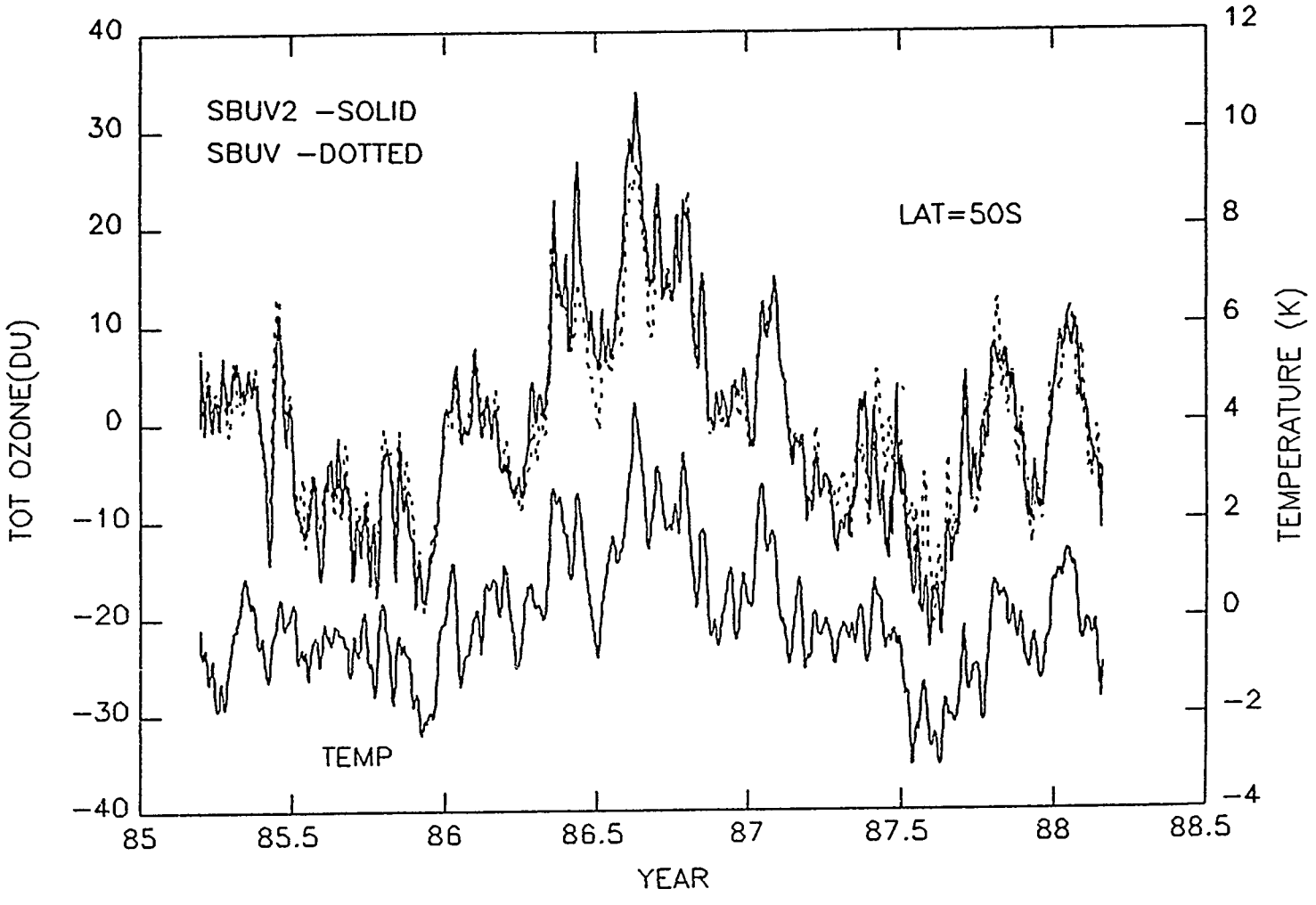
SBUV2 –SOLID
SBUV –DOTTED
LAT=50S
TEMP
TOT OZONE(DU)
TEMPERATURE (K)
YEAR
40
30
20
10
0
−10
−20
−30
−40
12
10
8
6
4
2
0
−2
−4
85
85.5
86
86.5
87
87.5
88
88.5

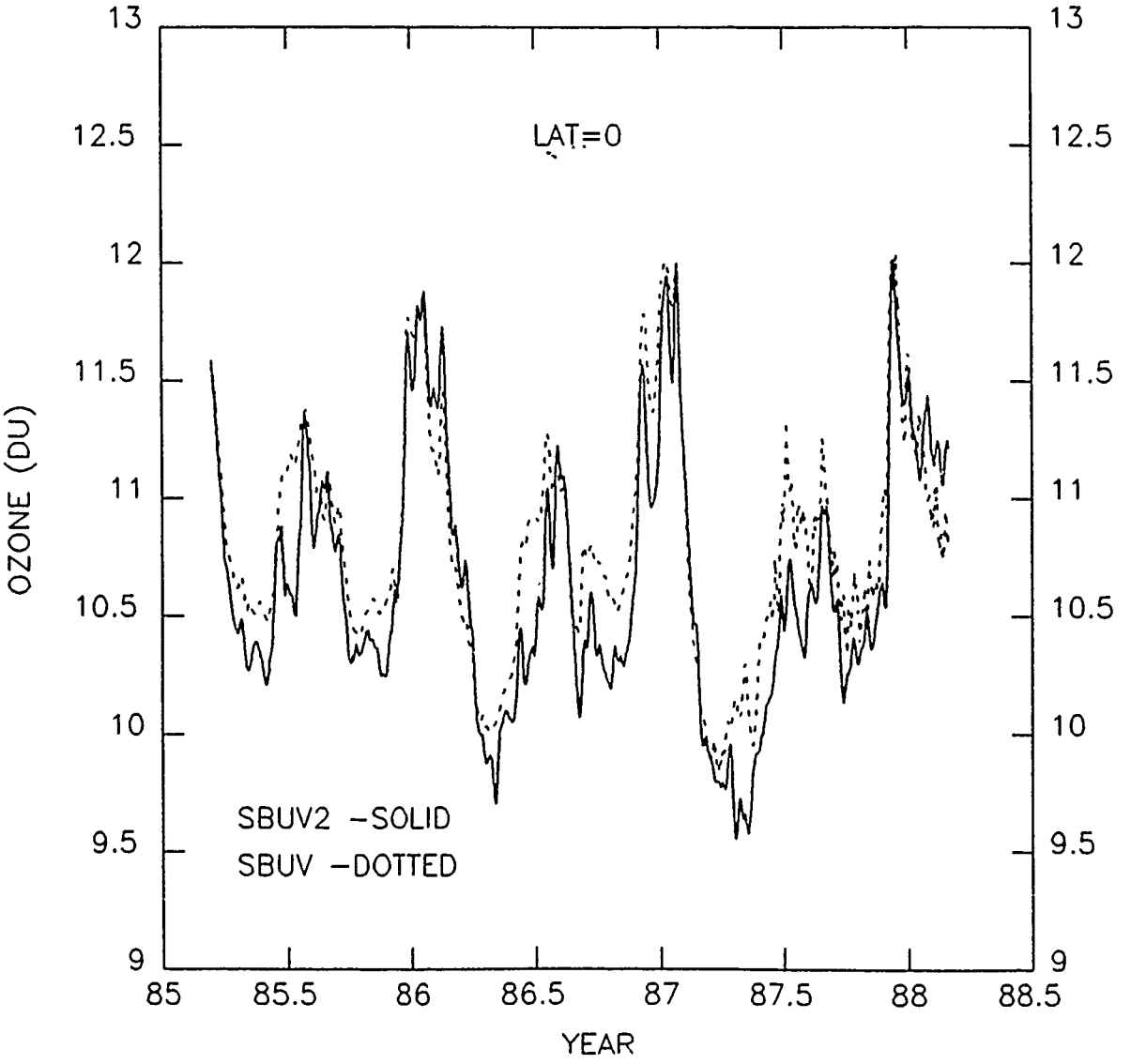

☆ US GOVERNMENT PRINTING OFFICE :(80) - 2 6 1 9 1 5 2 0 6 2 4

(Continued from front inside cover)

NESDIS 22 The Space Station Polar Platform: NOAA Systems Considerations and Requirements. John H. McElroy and Stanley R. Schneider, June 1985. (PB86 6109246/AS)

NESDIS 23 The Use of TOMS Data in Evaluating and Improving the Total Ozone from TOVS Measurements. James H. Lienesch and Prabhat K.K. Pandey, July 1985. (PB86 108412/AS)

NESDIS 24 Satellite-Derived Moisture Profiles. Andrew Timchalk, April 1986. (PB86 232923/AS)

NESDIS 25 reserved

NESDIS 26 Monthly and Seasonal Mean Outgoing Longwave Radiation and Anomalies. Arnold Gruber, Marylin Varnadore, Phillip A. Arkin, and Jay S. Winston, October 1987. (PB87160545/AS)

NESDIS 27 Estimation of Broadband Planetary Albedo from Operational Narrowband Satellite Measurements. James Wydick, April 1987. (PB88-107644/AS)

NESDIS 28 The AVHRR/HIRS Operational Method for Satellite Based Sea Surface Temperature Determination. Charles Walton, March 1987. (PB88-107594/AS)

NESDIS 29 The Complementary Roles of Microwave and Infrared Instruments in Atmospheric Sounding. Larry McMillin, February 1987. (PB87 184917/AS)

NESDIS 30 Planning for Future Generational Sensors and Other Priorities. James C. Fischer, June 1987. (PB87 220802/AS)

NESDIS 31 Data Processing Algorithms for Inferring Stratospheric Gas Concentrations from Balloon-Based Solar Occultation Data. I-Lok Chang (American University) and Michael P. Weinreb, April 1987. (PB87 196424)

NESDIS 32 Precipitation Detection with Satellite Microwave Data. Yang Chenggang and Andrew Timchalk, June 1988. (PB88-240239)

NESDIS 33 An Introduction to the GOES I-M Imager and Sounder Instruments and the GVAR Retransmission Format. Raymond J. Komajda (Mitre Corp) and Keith McKenzie, October 1987. (PB88-132709)

NESDIS 34 Balloon-Based Infrared Solar Occultation Measurements of Stratospheric O3, H2O, HNO3, and CF2C12. Michael P. Weinreb and I-Lok Chang (American University), September 1987. (PB88-132725)

NESDIS 35 Passive Microwave Observing From Environmental Satellites, A Status Report Based on NOAA's June 1-4, 1987, Conference in Williamsburg, Virginia. James C. Fischer, November 1987. (PB88-208236)

NESDIS 36 Pre-Launch Calibration of Channels 1 and 2 of the Advanced Very High Resolution Radiometer. C.R. Nagaraja Rao, October 1987. (PB88-157169 A/S)

NESDIS 39 General Determination of Earth Surface Type and Cloud Amount Using Multispectral AVHRR Data. Irwin Ruff and Arnold Gruber, February 1988. (PB88-199195/AS)

NESDIS 40 The GOES I-M System Functional Description. Carolyn Bradley (Mitre Corp), November 1988.

NESDIS 41 Report of the Earth Radiation Budget Requirements Review - 1987 Rosslyn, Virginia, 30 March - 3 April 1987. L.L. Stowe (Editor), June 1988.

NESDIS 42 Simulation Studies of Improved Sounding Systems. H. Yates, D. Wark, H. Aumann, N. Evans, N. Phillips, J. Sussking, L. McMillin, A. Goldman, M. Chahine, and L. Crone, February 1989.

NESDIS 43 Adjustment of Microwave Spectral Radiances of the Earth to a Fixed Angle of Progagation. D. Q. Wark, December 1988. (PB89-162556/AS)

NESDIS 44 Educator's Guide for Building and Operating Environmental Satellite Receiving Stations. R. Joe Summers, Chambersburg Senior High, February 1989.

NESDIS 45 Final Report on the Modulation and EMC Considerations for the HRPT Transmission System in the Post NOAA-M Polar Orbiting Satellite ERA. James C. Fischer (Editor), June 1989. (PB89-223812/AS)

NESDIS 46 MECCA Program Documentation. Kurt W. Hess, September 1989.

NESDIS 47 A General Method of Using Prior Information in a Simultaneous Equation System. L.J. Crone, D.S. Crosby, and L.M. McMillin, October 1989.

NOAA SCIENTIFIC AND TECHNICAL PUBLICATIONS

The National Oceanic and Atmospheric Administration was established as part of the Department of Commerce on October 3, 1970. The mission responsibilities of NOAA are to assess the socioeconomic impact of natural and technological changes in the environment and to monitor and predict the state of the solid Earth, the oceans and their living resources, the atmosphere, and the space environment of the Earth.

The major components of NOAA regularly produce various types of scientific and technical information in the following kinds of publications:

PROFESSIONAL PAPERS—Important definitive research results, major techniques, and special investigations.

CONTRACT AND GRANT REPORTS—Reports prepared by contractors or grantees under NOAA sponsorship.

ATLAS—Presentation of analyzed data generally in the form of maps showing distribution of rainfall, chemical and physical conditions of oceans and atmosphere, distribution of fishes and marine mammals, ionospheric conditions, etc.

TECHNICAL SERVICE PUBLICATIONS—Reports containing data, observations, instructions, etc. A partial listing includes data serials; prediction and outlook periodicals; technical manuals, training papers, planning reports, and information serials, and miscellaneous technical publications.

TECHNICAL REPORTS—Journal quality with extensive details, mathematical developments, or data listings.

TECHNICAL MEMORANDUMS—Reports of preliminary, partial, or negative research or technology results, interim instructions, and the like.

U.S. DEPARTMENT OF COMMERCE
NATIONAL OCEANIC AND ATMOSPHERIC ADMINISTRATION
NATIONAL ENVIRONMENTAL SATELLITE, DATA, AND INFORMATION SERVICE
Washington, D.C. 20233